A PETROLOGICAL STUDY OF THE TIN- TUNGSTEN DEPOSIT AT RENOSTERKOP, AUGRABIES, NORTHERN CAPE PROVINCE

by
ALLAN EMILE SAAD
BSc Honns.

Submitted in partial fulfilment of the requirements for the degree
Master of Science
in the Departement of Geology
at the
Potchefstroomse Universiteit vir Christelike Hoër Onderwys

Potchefstroom
June 1987

Supervisor: Prof. S.A. de Waal

Abstract

Renosterkop is a large low grade tin- tungsten- zinc deposit located 85km WSW of Upington in the northern Cape Province, South Africa. The mineralization is hosted by a number of shallow- dipping, sheeted greisen bodies that are surrounded by, and partly intercalated with a well foliated granite gneiss country rock. The gneiss is taken to belong to the intrusive Riemvasmaak gneiss of the Namaqualand Metamorphic Complex.

The mineralized host (referred to as TBQ) is a grey, homogeneous, fine to medium grained rock composed predominantly of quartz, biotite and topaz with minor amounts of fluorite and accessory opaque minerals, zircon and secondary chlorite. The unmineralized granite gneiss country rock is medium- to coarse- grained, pinkish in colour and composed primarily of microcline, plagioclase, quartz and biotite, with or without hornblende. Rock types, transitional in mineralogy but with clearly distinguishable contacts, are present between the TBQ and the granite gneiss.

A prominant chemical and mineralogical halo, 20 m to 50 m wide, envelopes the Renosterkop deposit. There is a gradational transition from an unaltered hornblende biotite gneiss, through gneiss containing greenish-brown biotite to an approximately 2 m wide transition zone, characterized by the partial replacement of the greenish- brown biotite by chlorite. The transition zone in turn yields to the TBQ in which reddish- brown biotite forms at the expense of the chlorite, and topaz, quartz and fluorite are formed at the expense of the feldspar. Major and trace element analyses show a spectrum of chemical compositions with coherent trends that support a gradational transition from the hornblende- bearing granite gneiss, through the transitional rock types to the TBQ.

The mineralogical and chemical characteristics of the Renosterkop rock types are consistent with an origin by progressive greisenization of a "within plate" A- type granitoid host rock. A genetic model is proposed which involves the formation of the TBQ greisen during intense metasomatic alteration and replacement of the granite gneiss within a zone

of structural weakness that provided conduits for migrating, F- rich, metal- bearing solutions, and thereby inherited the foliation and structural features present in the original granite gneiss.

Uittreksel

Renosterkop is 'n groot laegraadse tin- wolfram- sinkafsetting geleë 80km WSW vanaf Upington in die noordelike Kaapprovinsie, Suid-Afrika. Die mineralisasie is beperk tot 'n aantal vlak- hellende plaatagtige greisen liggame wat as gasheer optree en wat gedeeltelik tussengelaagd is met, sowel as onder- en oorlê word deur, 'n goedgefolieerde granietgneisnewegesteente wat beskou word as deel van die intrusiewe Riemvasmaakgneis van die Namakwalandse Metamorfekompleks.

Die gemineraliseerde gasheer (waarna verwys word as TBQ) is 'n grys homogene, fyn tot mediumkorrelrige gesteente wat hoofsaaklik uit kwarts, biotiet en topaas bestaan en wat kleiner hoeveelhede fluoriet en bykomstige opaak minerale, sirkoon en sekondêre chloriet bevat. Die newegesteente van granietgneiss, wat nie gemineraliseerd is nie, is 'n pienk medium- tot grofkorrelrige gesteente wat hoofsaaklik uit mikroklien, plagioklaas, kwarts en biotiet, met of sonder horingblende, bestaan. Gesteentetipes wat oorganklik is in mineralogie maar duidelik onderskeibare kontakte het, is teenwoordig tussen die TBQ en die granietgneiss.

'n Prominente veranderingskrans, 20 m tot 50 m wyd, omsluit die Renosterkopafsetting. 'n Graderingsoorgang is teenwoordig wat wissel vanaf die onveranderde horingblendebiotietgneis deur 'n biotietgneis wat 'n groenbruin biotiet bevat, tot by 'n ongeveer 2 m- wye oorgangsone wat gekenmerk word deur die gedeeltelike vervanging van die groenbruin biotiet deur chloriet. Op sy beurt gaan die oorgangsone oor na die TBQ waarin rooibruin biotiet ten koste van chloriet vorm, en topaas, kwarts en fluoriet vorm ten koste van veldspaat. Hoof- en spoorelementontledings wys op 'n spektrum van chemiese samestellings wat koherente neigings toon en wat daarop dui dat 'n graderingsoorgang teenwoordig is vanaf die horingblende- draende gneis, deur die oorgangsgesteentetipes, tot by die TBQ.

Die mineralogiese en chemiese kenmerke van die Renosterkop gesteentetipes is versoenbaar met 'n oorsprong wat spruit uit die

progressiewe greisenisasie van 'n "binne plaatse" A- tipe granitoied. 'n Genetiese model word voorgestel waarin die TBQ greisen vorm gedurende intensiewe metasomatiese verandering en vervanging van 'n granietgneisgasheer in 'n struktureel verswakte sone wat voerkanale beskikbaar gestel het vir migrerende, F- ryke, metaal- draende vloeistowwe, en daardeur die foliasie sowel as die strukturele verskynsels van die oorspronklike granietgneis geërf het.

TABLE OF CONTENTS

I. INTRODUCTION

Renosterkop is a large, low- grade tin- tungsten- zinc deposit located 85 km WSW of Upington in the northern Cape Province, South Africa (Figure 1). The mineralization is present in a topaz biotite quartz host rock (abbreviated TBQ) that is preserved within the Riemvasmaak gneiss which comprises part of the Namaqualand Metamorphic Complex.

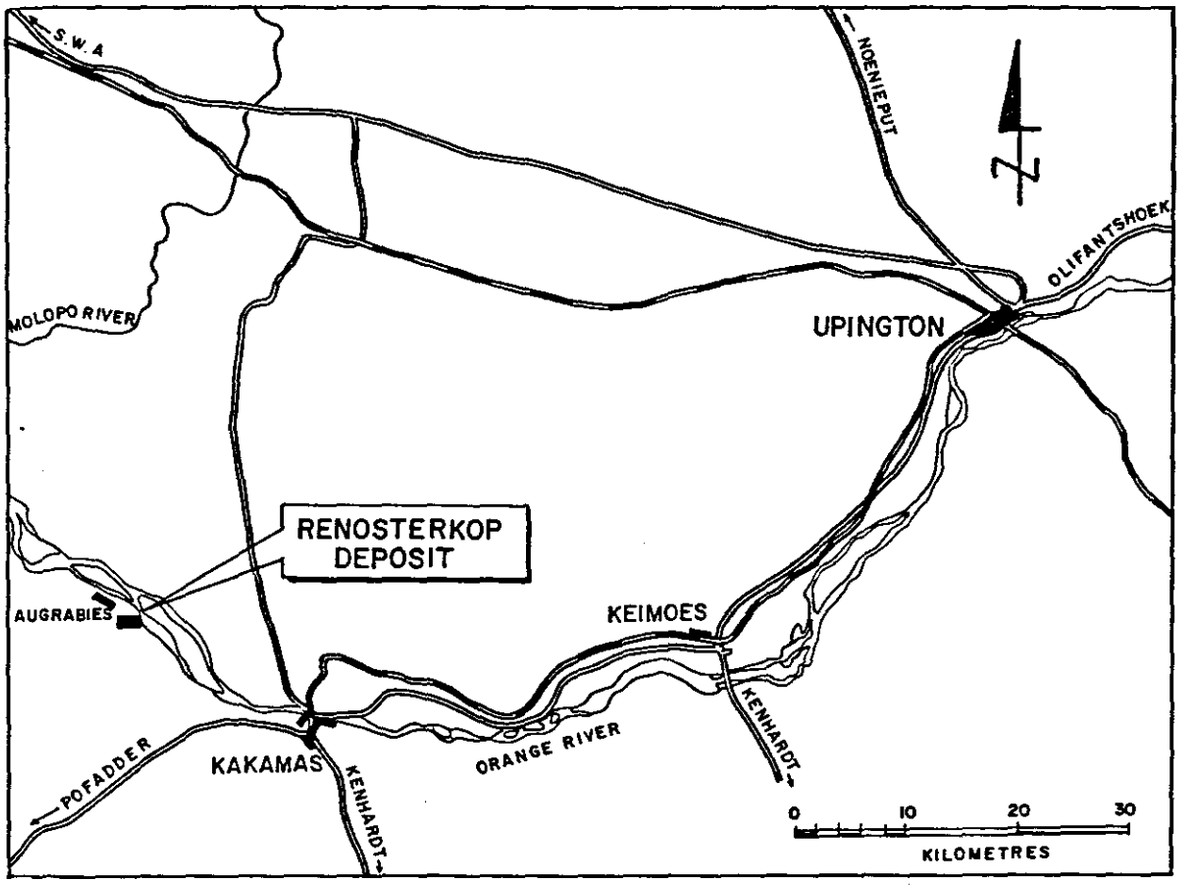

Figure 1: Locality map of the Renosterkop Deposit.

The TBQ occurs as a number of shallow- dipping, sheeted bodies, containing minor intercalations of unmineralized granite gneiss, and forming an erosion resistant ridge (Figure 2) measuring 1500 m by 300 m in plan. The combined mineralized TBQ bodies vary in thickness from a maximum of 60 m to a minimum of 10 cm, with an average thickness of 20 m to 30 m.

The economic potential of the Renosterkop deposit is currently being evaluated by Rio Tinto Exploration (Pty) Limited, which company holds the mineral rights to the area. Rio Tinto has investigated the deposit by detailed geological, geochemical, geophysical and drilling methods.

The purpose of this study was to ascertain the petrographic and petrochemical nature of the mineralized TBQ and its host rocks, and to use this information to outline a probable mode of origin for the TBQ. Such knowledge is deemed useful for further exploration in the area.

Figure 2: Looking north towards Renosterkop, the prominant topographic nature of the ridge as well as the sheeted nature of the TBQ, underlain by granite gneiss country rock, are displayed. The contact between the TBQ and the granite gneiss is indicated by an arrow.

II. REGIONAL GEOLOGY

A. Previous Geological Investigations

The earliest geological work in the area was undertaken by Rogers and Swartz (1900), Rogers (1908), and Rogers and Du Toit (1909 and 1910). They described the geology of the Orange River Valley in the Hopetown and Prieska districts, undertook a geological survey of parts of the districts of Kuruman, Vryburg, Hay, and Gordonia, and reported on the geology of parts of the districts of Kenhardt, Prieska, Hay, Britstown, Carnarvon, and Victoria West respectively.

After the outbreak of the Second World War the Geological Survey embarked on a programme of exploration for strategic minerals, and it was decided to map the rocks in the Orange River Valley between Upington and the sea in order to access the economic potential of the area (Hugo,1969). The task of unravelling the complicated geology and deciphering the complex geological history and structure of an area embracing 5200 square kilometers between Kakamas and Onseepkans fell to J.W. von Backström and D.J.L. Visser.

Work commenced at the beginning of 1941 and was completed during 1946. Von Backström mapped the areas in the vicinity of Kakamas (sheet 2820D) and the Bokvasmaak Native Reserve, i.e. the southern portion of sheet 2820A. Visser surveyed the area south of the Orange River between the Hartbees River and Onseepkans, i.e. the northern parts of Sheets 2820C and 2819D, and thus covered the present study area. Von Backström later completed his PhD thesis on the area 2820D and the major portion of area 2821C, and this map was later published on a scale of 1:125 000 (Von Backström, 1964). The work undertaken by Visser was never published but was used as a base plan by Hugo (1969) who later undertook a detailed study of the pegmatites of the area.

The most recent work covering the study area was undertaken by Praekelt (1984) who remapped Sheet 2820C on a scale of 1:100 000 for his MSc thesis. This mapping included the Renosterkop deposit and surrounding area and has since been partly revised by the Geological Survey and incorporated into a recently compiled geological map of Sheet 2820C (scale 1:250 000) which will soon be published.

B. Regional Geological Setting

The region is underlain by rocks which are described by SACS (Kent, 1980) as forming part of the Korannaland Sequence of the Namaqualand Metamorphic Complex. The lithostratigraphic designation Namaqualand Metamorphic Complex includes metasedimentary, metavolcanic and intrusive rock units which are predominantly gneissic in character. The Complex underlies a Proterozoic tectonic province which has been variously referred to as the Namaqua Mobile Belt, Orange River Belt, Namaqua Province or Sonama Province (Kent, 1980); it is bounded by the Archean Kaapvaal Province, younger cover rocks and the Atlantic coastline.

The lithostratigraphic subdivision of the Namaqualand Metamorphic Complex is presented by SACS (Kent, 1980) as an ad hoc framework for further improvement as more information is obtained, and is given in Table 1.

The Korannaland Sequence loosely groups together a number of rock formations, the stratigraphic relations between which are imperfectly known. These formations are given in Table 2.

The lithology of the constituent formations, and the type areas of the Korannaland Sequence are given in Table 3 and Figure 3 respectively.

Table 1

Lithostratigraphic subdivision of the Namaqualand Metamorphic Complex

Koperberg Suite Spektakel Suite Keimoes Suite Hoogoor Suite Little Namaqualand Suite Gladkop Suite Vioolsdrif Suite	Syntectonic intrusive rock units, radiometrically dated 1100 to 1900 Ma (Kent, 1980)
Orange River Group Okiep Group Bushmanland Group Korannaland Sequence Marydale and Kaaien Groups	Pretectonic metasedimentary and metavolcanic rock units, radiometrically dated 1350 to 2000 Ma (Kent, 1980)

Table 2

Formations of the Korannaland Sequence (Kent,1980)

Toeslaan Formation	Goede Hoop Formation Rautenbach se Kop Formation Kenhardt Formation Biesje Poort Formation Kokerberg Formation	Eierdoppan Formation Jannelsepan Formation

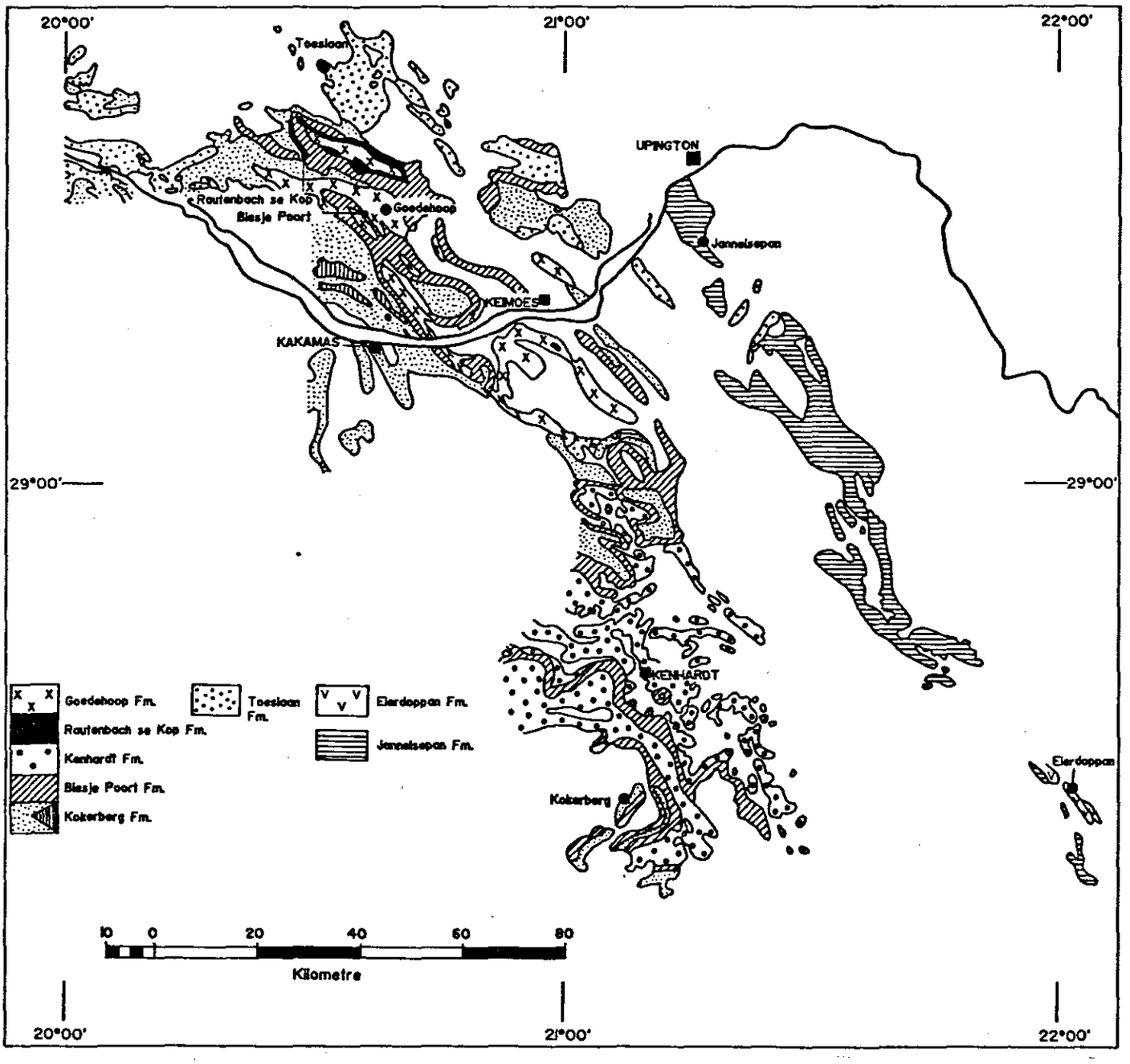

Figure 3: Type areas of the Korannaland Sequence (Kent, 1980)

Table 3

Lithology of the Korannaland Sequence (Kent, 1980)

FORMATION	LITHOLOGY
Goede Hoop	Metaquartzite, muscovite quartzite and conglomerate
Rautenbach se Kop	Quartzo - feldspathic gneiss
Kenhardt	Predominantly a leucocratic biotite gneiss
Biesje Poort	Calc - silicate rocks, streaky leucogneiss, biotite gneiss, marble and amphibolite
Kokerberg	Quartzo - feldspathic gneiss with interlayered metaquartzite
Toeslaan	Garnet - sillimanite - cordierite - biotite gneiss; garnet - bearing quartzo - feldspathic gneiss; biotite gneiss with amphibolite
Eierdoppan	Conglomerate and schist
Jannelsepan	Amphibolitic rocks and associated biotite schists and gneisses; calc silicate rocks; garnet - sillimanite - biotite gneiss

The granite gneiss units found in the immediate vicinity of the study area and underlying the TBQ at Renosterkop are regarded by SACS (Kent, 1980) as belonging to the syntectonic intrusive rocks of the Hoogoor Suite, which are intrusive into the Kokerberg Formations, and are broadly defined as undifferentiated leucocratic quartzo - feldspathic gneiss units that are usually fine- to medium- grained and reddish- brown in outcrop. In places this gneiss - henceforth referred to as granite gneiss - contains nodules with a variable amount of sillimanite (Kent,1980), or it may assume a coarse granitic aspect or become megacrystic. Bands of fine- grained white quartzo- feldspathic rock as well as lenses of calc- silicate rock, quartzite, schist and amphibolite are common (Kent, 1980). The granite gneiss, also referred to as the pink gneiss, underlies a large area and it may not necessarily represent a single rock unit throughout. Accordingly it has been interpreted as intrusive granites by some researchers, and granitized metasediments by others. Suggested parent rocks range from arkose (Poldervaart and von

Backström, 1949; Geringer, 1973; Moore, 1977),to rhyolite (Joubert, 1974; Botha et al., 1976) and granitoid (Coetzee, 1941; Lipson and McCarthy, 1977; Colliston, 1979). Most of these speculations are based either on field relations or on geochemistry. However, owing to the immaturity of clastic sediments such as arkoses and greywackes, the difference in chemical composition between such sedimentary and igneous rocks may not be pronounced (Schultz, 1978).

On the Geological Map of the Republics of South Africa, Transkei, Bophuthatswana, Venda and Ciskei and the Kingdoms of Lesotho and Swaziland (1984, scale 1:1000 000), the pink gneiss units were mapped as the Eendoorn granite, forming part of the Little Namaqualand Suite. The Geological Survey presently classifies the pink gneiss units as forming part of the intrusive Riemvasmaak gneiss (G. Moen, personal communication) and describe it as a pink- weathering granite gneiss with a granular or Augen texture.

Praekelt (1984) mapped the area (Figure 4) in the immediate vicinity of the present study area on a scale of 1:100 000 and considered the Renosterkop deposit as a zenolith of metasediments of Omdraai Formation within the Rooipad granite. He described Renosterkop as a topaz- bearing quartzite and suggested that the topaz formed by reaction of hydrothermally active fluids with the zenolith of Omdraai metasediments as well as with the underlying Rooipad granites.

The Omdraai Formation is described (Praekelt, 1984) as a fine- to medium-grained yellowish leucocratic quartz- feldspar gneiss interbedded with a few thin layers of massive quartzite, biotite schists and amphibolites. The Formation is surrounded by later intrusions of Rooipad and Brabees granites.

The Rooipad granite is a well foliated medium to coarse- grained biotite granite with minor hornblende and it exibits conformable contacts with the Seekoeisteek, Brabees, Eendoorn and Augrabies granites. Xenoliths of the Omdraai formation are common within the Rooipad granite (Praekelt, 1984), but no mineralogical description is given of these xenoliths.

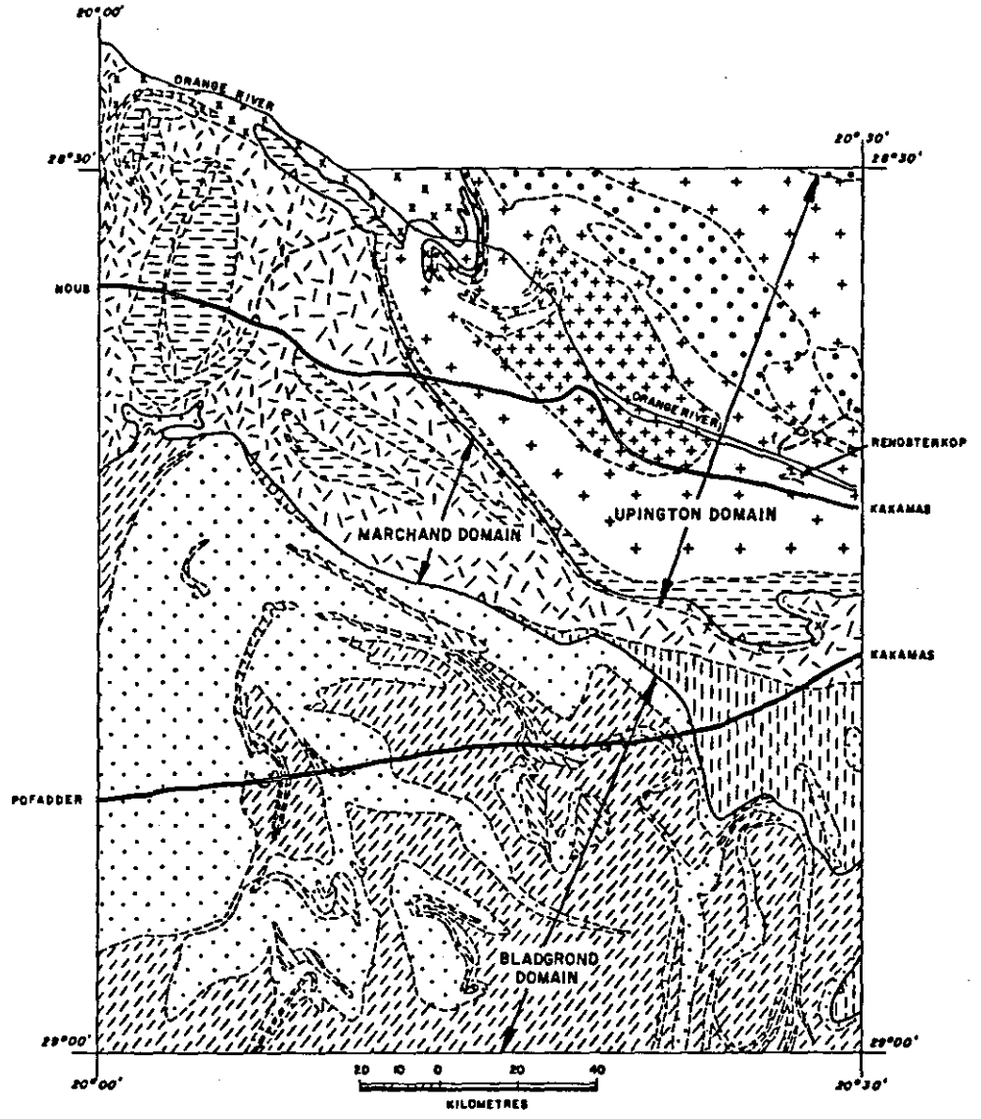

GEOLOGICAL LEGEND

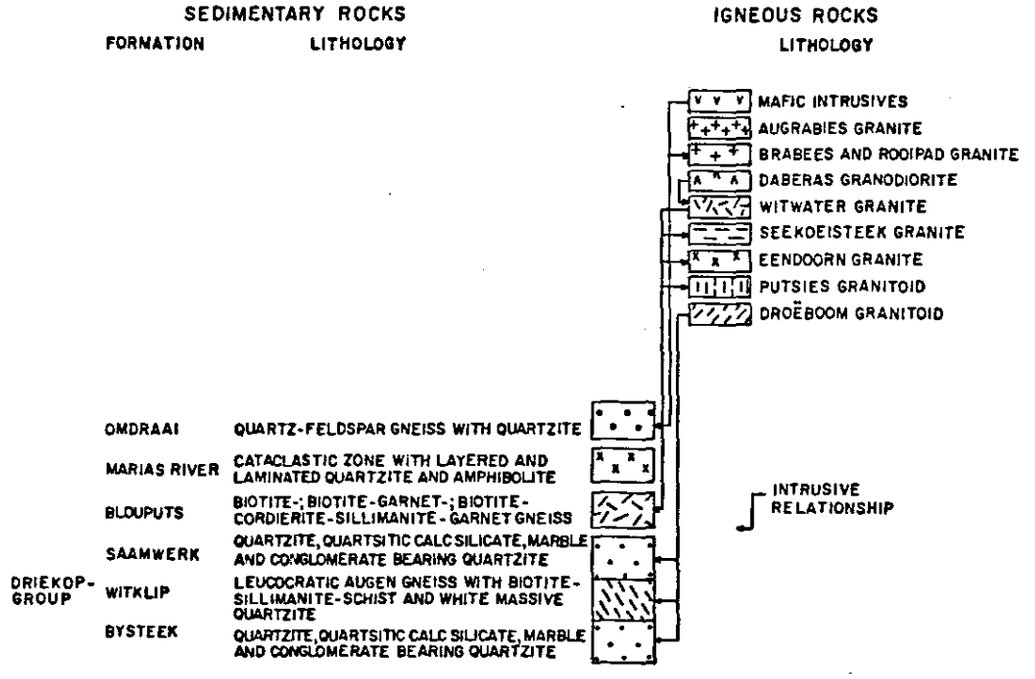

Figure 4: A simplified geological map of the regional geology around Renosterkop (Praekelt, 1984).

The Brabees granite (Praekelt, 1984) is a well foliated and in places porphyroblastic red- brown granite which contains inclusions of quartzitic and mafic inclusions. No relative age relationship between this granite and the Augrabies, Rooipad, or Eendoorn granites could be ascertained by field observations.

The Augrabies granite is described by Praekelt (1984) as medium- to coarse- grained weakly foliated biotite and hornblende- bearing granite which contains zenoliths of a fine- to medium- grained granite of the same composition. Close inspection of the Augrabies granite by the writer however indicated at least two well developed superimposed foliation directions developed in this granite, and although weakly foliated relative to the other gneiss in the area, it is still well- foliated in the absolute sense. Praekelt (1984) furthermore found the Augrabies granite only to be in contact with the Rooipad granite, and all contacts were found to be conformable. No age relationship between these two granites could thus be derived from field observations. The relatively weak foliation that is developed in the Augrabies granite may however point to its younger age.

Praekelt (1984) divided the area 2820C into three structural terranes, ie. the Upington, Marchand and Bladgrond Terranes, which he separated from one another by prominent thrust faults (see Figure 4). Each terrane is considered as containing unique lithological, structural and metamorphic characteristics. The Renosterkop deposit falls within the Upington Terrane in which four phases of deformation were recognized, and which has been thrust- faulted in a south- westerly direction over the Marchand Terrane.

Based on the degree of K- metasomatism as well as the development of rock fabric, Praekelt proposed that the Rooipad granite is older than the Brabees granite, which in turn is older than the Augrabies granite.

For the purpose of the latest 1:250 000 geological map of the area (in press) the Geological Survey has combined the Brabees, Rooipad and Seekoeisteek granites and called them the Riemvasmaak gneiss (G. Moen, personal communication).

It is evident from the above information that the geology of the area in the vicinity of the Renosterkop deposit is not completely understood and that much more detailed work remains to be done. For the purpose of this study, the classification proposed by the Geological Survey is accepted. Accordingly the granite gneiss which hosts the Renosterkop deposit is taken to be part of the Riemvasmaak gneiss.

III. THE RENOSTERKOP TIN - TUNGSTEN DEPOSIT

A. General Geology

The Renosterkop deposit consists of large sheeted bodies of shallow-dipping topaz biotite quartz rock (TBQ) varying in thickness from centimeters up to 60 m in places. The sheets of TBQ overlie a well foliated pink granite gneiss, i.e. Riemvasmaak gneiss, with a consistently flat shallow- dipping bottom contact. Conformable intercalations of granite gneiss are present between the individual TBQ sheets. No contact is identifiable within the TBQ where two sheets merge.

The TBQ hosts low- grade tin, tungsten and zinc mineralization, whereas the granite is not mineralized.

A transition zone, measuring 2 to 3 m in thickness, in which the biotite is partially or totally replaced by chlorite, and in which topaz, quartz and fluorite are formed at the expense of feldspar, is present between the TBQ and the granite gneiss. The contact between this transition zone and the TBQ is generally sharp, but is also seen to be gradational in places. Late stage alteration zones are common within both the TBQ and the granite gneiss.

A plan of the surface geology of the deposit as well as the localities of boreholes used for this study are shown in Figure 5. Figure 6 shows north- south profiles looking east across the three sections used.

B. Structure

An aerial impression of the Renosterkop deposit is that it forms a shallow northerly dipping tight south- vergent synformal fold with a gentle

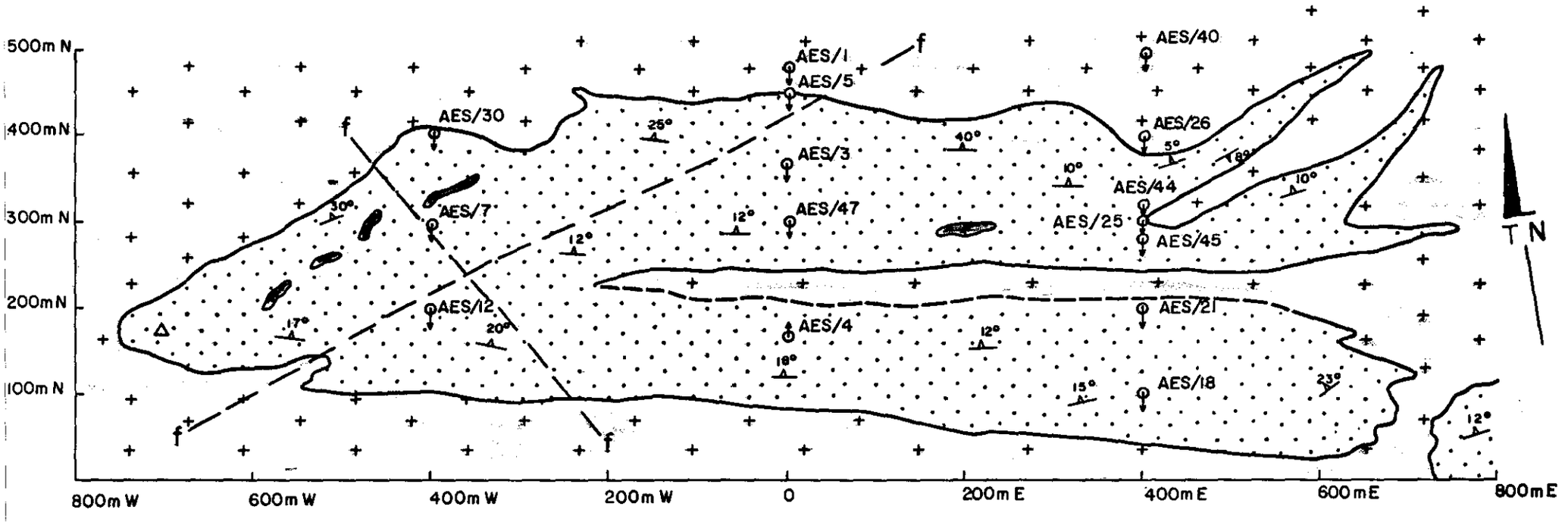

LEGEND

TBQ

GRANITE GNEISS

AES/1 BOREHOLE NUMBER AND INCLINATION

Figure 5: Plan of the surface geology of the Renosterkop deposit.

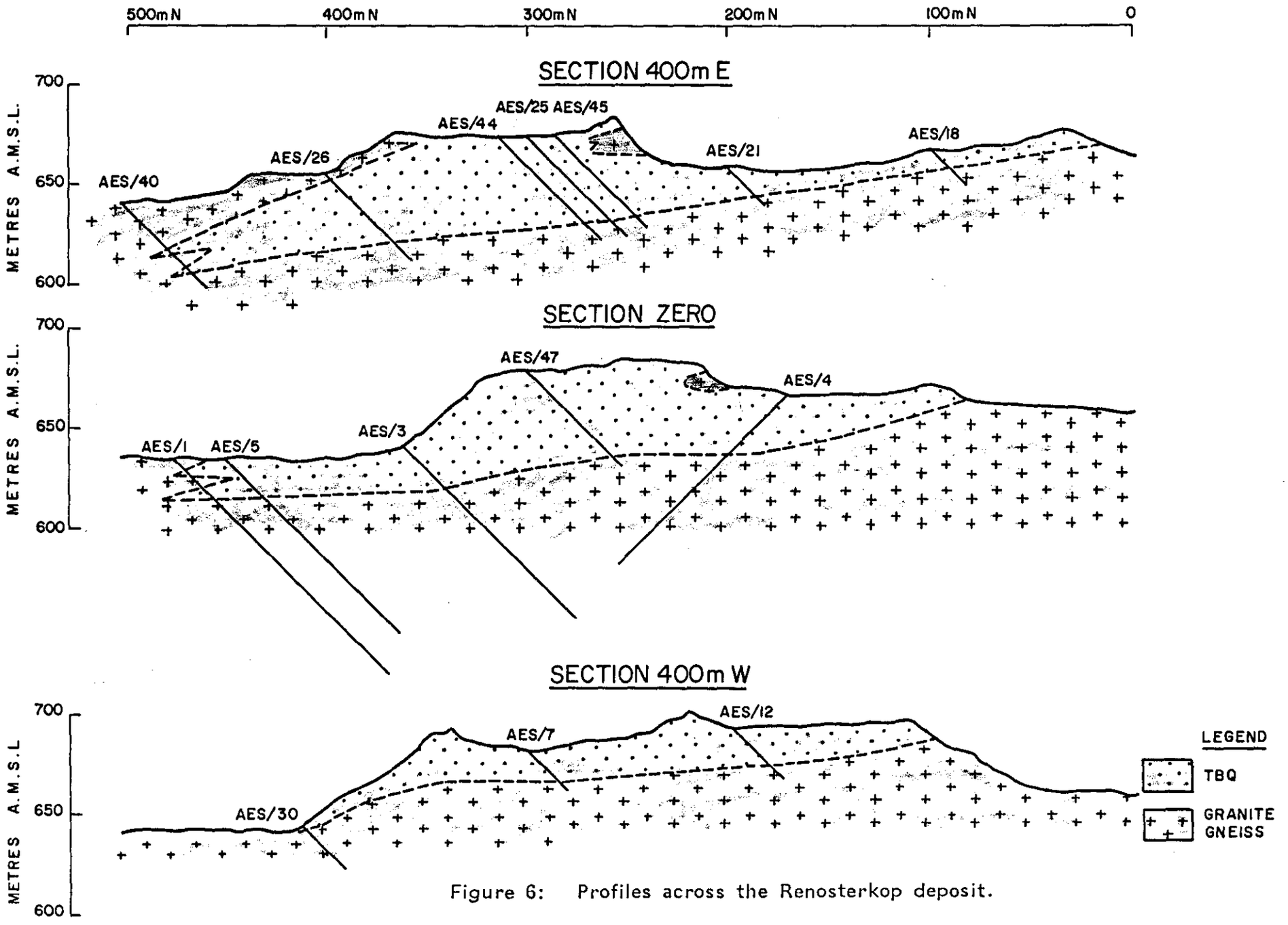

Figure 6: Profiles across the Renosterkop deposit.

eastward plunge and traversed by prominent faults on which no definite direction of movement can be detected (Hartnady, 1985). No field evidence could however be found to substantiate the presence of such a tight south- vergent synformal fold structure. It would rather appear that the deposit comprises a composite of sheetlike bodies of variable thickness as illustrated in Figures 7 and 8. On a local and regional scale, the dominating fabric element observed in the granite gneiss is a tectonic foliation (Hartnady, 1985), and is for practical purposes here referred to as S1. No evidence could be found for S1 being overprinted over an earlier tectonic fabric, and it apparently represents the last major tectonic deformation that was operative in the terrane. As a general rule the sheetlike bodies of TBQ are orientated roughly parallel to this foliation in the granite gneiss. Locally however they cut obliquely across the foliation of the granite gneiss as illustrated in Figure 9.

In the TBQ, S1 is defined by oriented biotite and also by a mm- to cm-scale phase layering defined primarily by variations in biotite abundance. This foliation is parallel to the foliation in the surrounding granite gneiss, which is defined by oriented biotite and elongated Augen- like quartz-feldspar aggregates.

Tight isoclinal folding (Figures 10 and 11) within certain sheets of TBQ, and in the wedges of granitic gneiss between the sheets, are superimposed on S1. These structures do not display axial plane cleavage or foliation, and are non- penetrative with variable plunges of the fold axes.

.The third type of folding seen in the TBQ is represented by open, non-cylindrical, gently or doubly- plunging "whaleback" antiforms and synforms in S1 and may be caused by disharmonic, viscoelastic buckling of the S1 fabric along NW to NNW trends. Later interference patterns trending NE to NNE are superimposed on this event and result in the formation of basin- dome interference patterns (Figure 12).

The major NE and NW trending fault zones (Figure 13) and joints (Figure 8) are superimposed over all the previously discribed structures.

Figure 7: An approximately 1 m wide sheet of dark- coloured TBQ seen along strike within the granite gneiss country rock. This sheet thickens in the distance and eventually merges with other TBQ sheets. In the foreground the sheet thins and eventually pinches out (illustrated in Figure 9).

Figure 8: A section of the northern face of Renosterkop illustrating the composite sheeted bodies of TBQ reaching a thickness of over 40 m in this locality. In the foreground late- stage warping, superimposed on the TBQ, is evident.

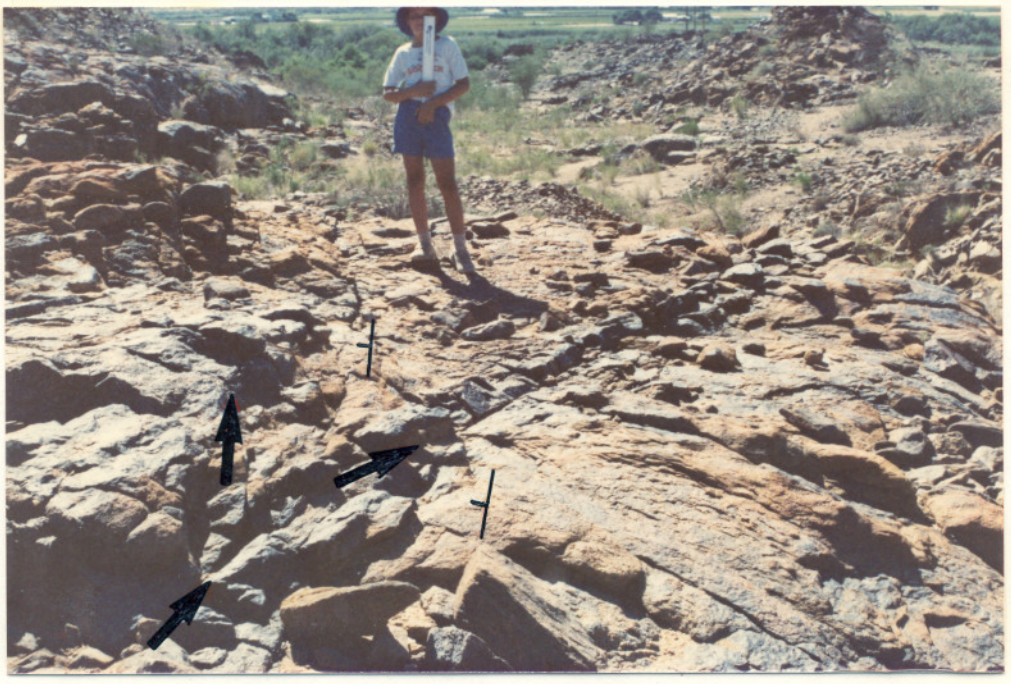

Figure 9: The cross- cutting nature of the TBQ is illustrated by the splitting veins to the left and right of the person standing in the photograph. The right- hand vein cuts across the foliation while the left- hand split runs parallel to the foliation. (⊥ foliation strike and dip)

Figure 10: Looking toward the west, this photograph shows shallow-dipping beds on the northern limb overlying and overturning the beds on the southern limb of this structure. This structure together with other field evidence led to the interpretation that thrust faulting had possibly been responsible for the formation of this structure.

Figure 11: Remnant of a tight isoclinal fold clearly displaying the phase layering within the fold.

.Figure 12: Open non- cyclindrical "whaleback" antiforms and sinforms seen well exposed on the eastern extension of Renosterkop in the vicinity of section 400 E.

Figure 13: Looking SW across a section of Renosterkop a NE trending fault zone may be seen intersecting the TBQ ridge (arrows) and dissapearing into the granite gneiss country rock in the foreground. Hematitic alteration is strongly developed along the northern extensions of this fault zone.

An important observation is that there is no evidence for the existence of non- penetrative isoclinal folding in the granite gneiss country rocks, as is observed in the deformed TBQ.

C. Sampling and Methods of Investigation

The Renosterkop deposit was geologically mapped by a team of six Rio Tinto geologists. A total of 80 ha was covered by grid controlled detailed geological mapping undertaken on a scale of 1:500. A drilling programme totalling 55 diamond drill boreholes and 12 percussion drill boreholes was undertaken between 1981 and 1985.

Three representative geological sections located 400 m apart were selected for diamond drill borehole core sampling across the Renosterkop deposit (Figure 6). Seven boreholes intersected section 400 E, five intersected section ZERO, and three intersected section 400W. Each of the fifteen boreholes was logged in detail and each geological zone was representatively sampled. Except for borehole no. AES/3 which was selectively sampled using assay values as criteria, the number of samples collected depended on the thickness of each apparently uniform geological zone. Field descriptions and depths of samples collected from borehole core are given in Appendix I.

Figures 14, 15 and 16 indicate borehole geology, sample localities, and sample numbers. Special attention was given to the sampling of geological contacts and a total of 198 diamond drill borehole core samples was collected for the purpose of this study. All samples have been numbered AES "X"/"Y", where "X" represents the borehole number, and "Y" represents the sample number. An additional 23 samples numbered RM"Y" were taken from a previous investigation undertaken by De Waal(1985) and included in this study.

Thin, polished and polished thin sections were examined using a conventional petrographic microscope. The microscopic identification of minerals was verified by means of x- ray diffraction techniques and electron microprobe investigations. The chemical analyses of rock samples were carried out by Bergström and Bakker.

Mineral chemistry was ascertained using a Jeol 733 Superprobe at a beam voltage of 15kV and a current of $0,2 \times 10^{-7}$ amp. Table 4 lists the standards which were used for the mineral analyses.

SECTION ZERO

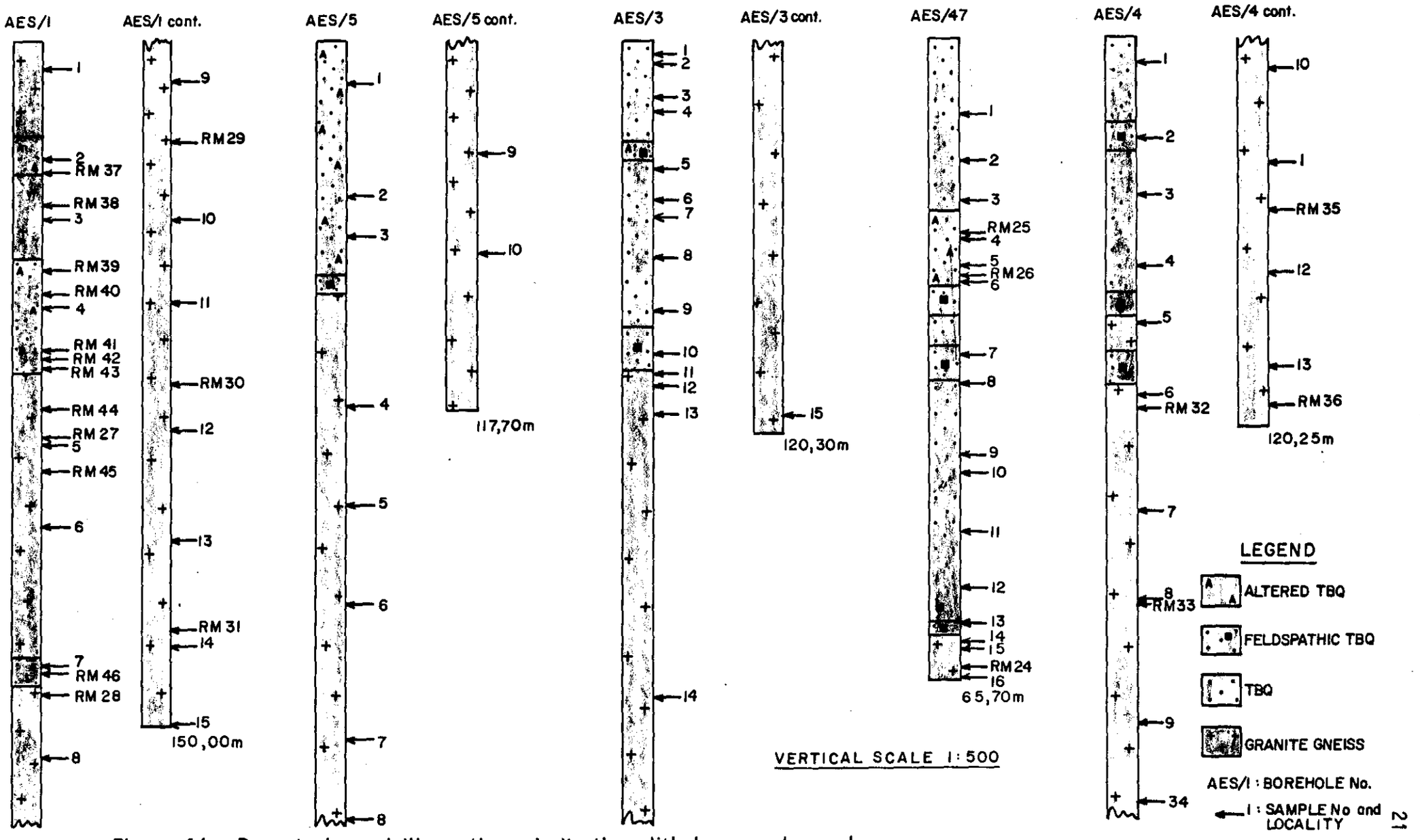

Figure 14: Renosterkop drill sections indicating lithology and sample localities.

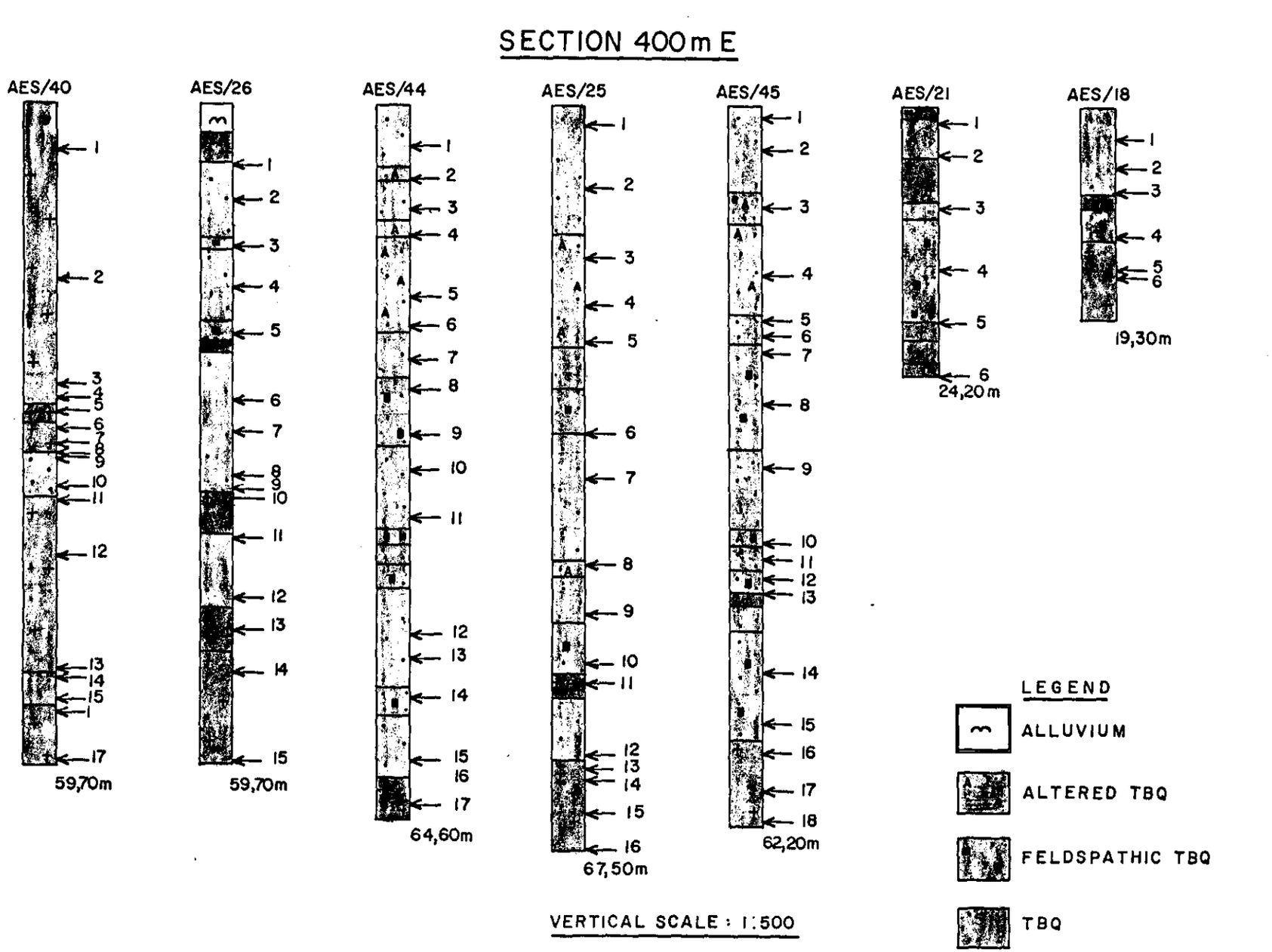

Figure 15: Renosterkop drill sections indicating lithology and sample localities.

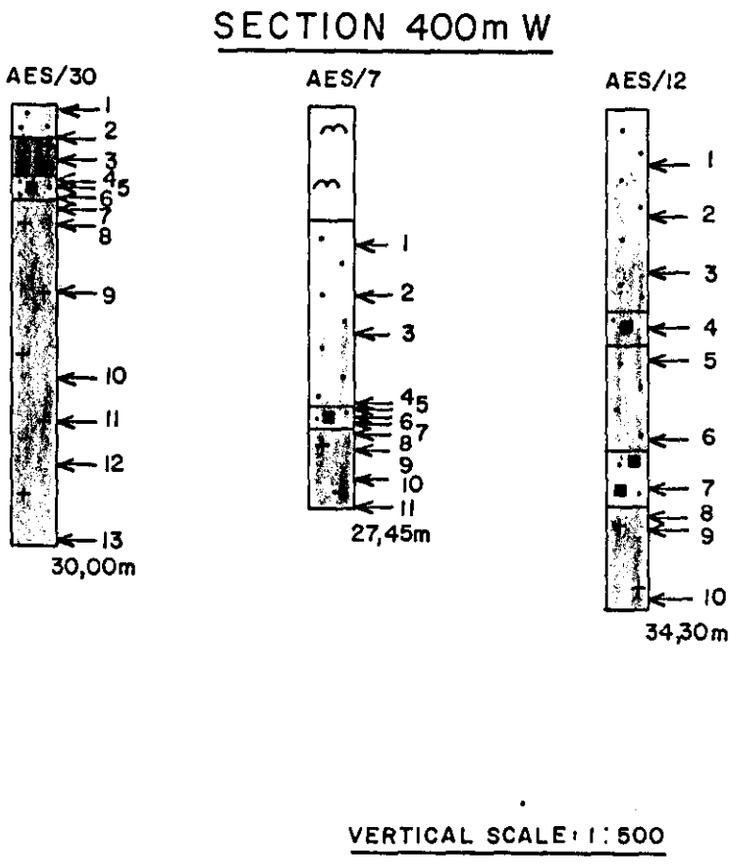

Figure 16: Renosterkop drill sections indicating lithology and sample localities.

Table 4

Table of standards with related elements used for mineral analyses on the Joel microprobe.

STANDARD	MINERAL						
	Amphibole	Biotite	Chlorite	Feldspar	Garnet	Gahnite	Sphalerite
Kakanui Hornblende	Si,Ca,Fe,Na, Al,Ti,Mg	Si,Ca,Fe,Mg, Al,K,Mn,Ti,	Si,Ca,Fe,Mg, Al,K,Mn,Ti,				
Bustamite	Mn				Mn	Mn	
Sanidine	K			Ba			
Biotite (AST.)							
Cassiterite		Sn					Sn
Plagioclase(AST.)				Na,Ca,Al,Si,			
Microcline(Smith)				K			
Augite(Smith)				Mg,Fe.			
Rutile(AST.)				Ti.	Ti	Ti	
Almandite(AST.)					Si,Mg,Ca,Al,		
Pyrope(AST.)					Fe		
Chromite					Cr	Mg,Cr,Fe	
Corundum						Al	
Willemite						Zn	
Sphalerite							Zn,S
Cuprite							Cu
Cobaltite							Co,Fe

D. General Petrographic Description

1. The country rock

The Riemvasmaak gneiss that forms the country rock is a pinkish, medium- to coarse- grained, sporadically porphyroblastic, pronouncedly foliated granite gneiss consisting, per volume, of 40 to 45 % feldspar (roughly 75 % is microcline and 25 % is plagioclase), 30 - 40 % quartz and 10 - 15 % biotite (Figures 17 and 18). Hornblende, up to 15 %, enters the mode of the granite gneiss 50 m below the lower contact and 20 m above the upper contact of the TBQ (Figure 19). The feldspar forms lenticular aggregates set in a matrix of quartz and orientated biotite. The microcline feldspar is commonly replaced by sericite and kaolinite and the biotite by chlorite.

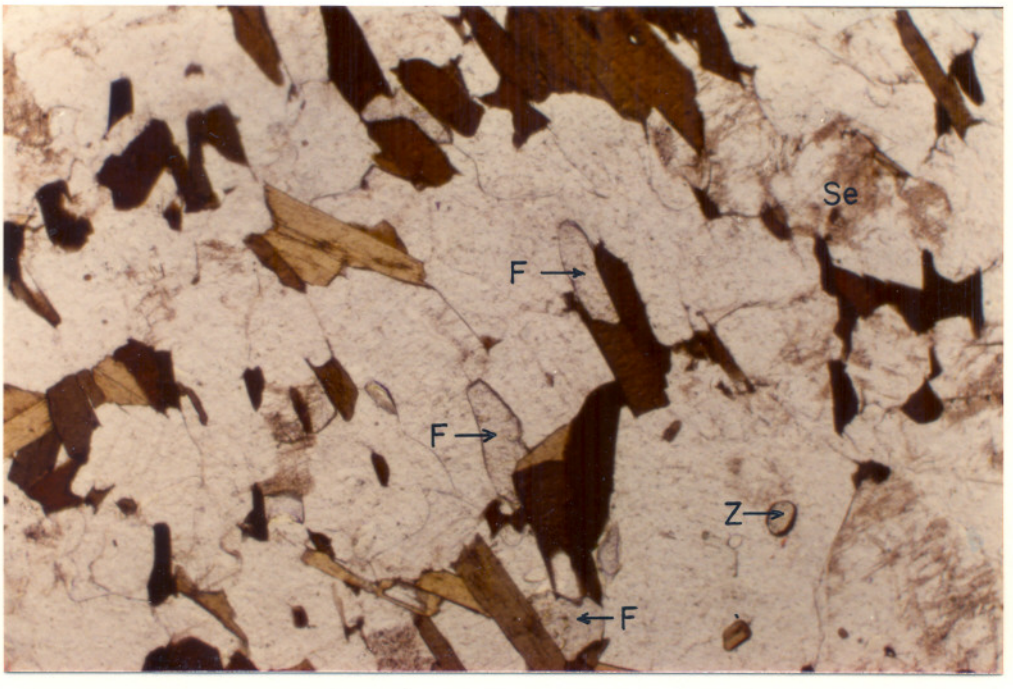

Figure 17: Photomicrograph of a typical granite gneiss displaying greenish- brown biotite in a matrix of quartz and feldspar. Three small fluorite crystals (F) and a single zircon (Z) are present. The feldspar is partly sericitized (Se).
Plane- polarized light
Scale 1 : 0,026

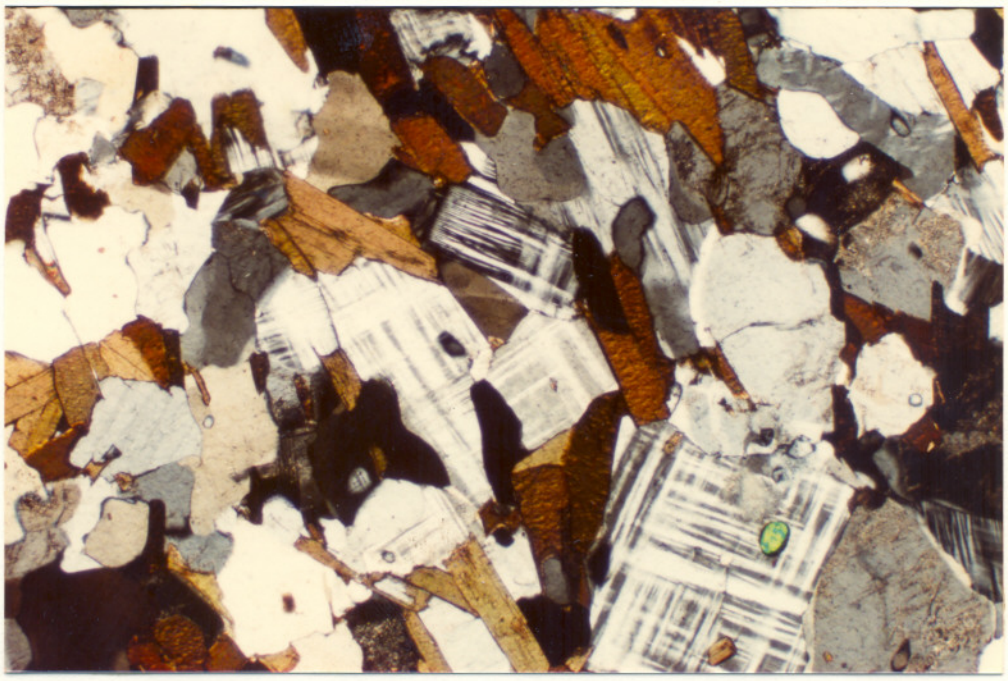

Figure 18: The same field as in Figure 17 is shown here under crossed-nicols. The fluorite displays isotropic characteristics and the zircon shows green interference colours.
Scale 1 : 0,026

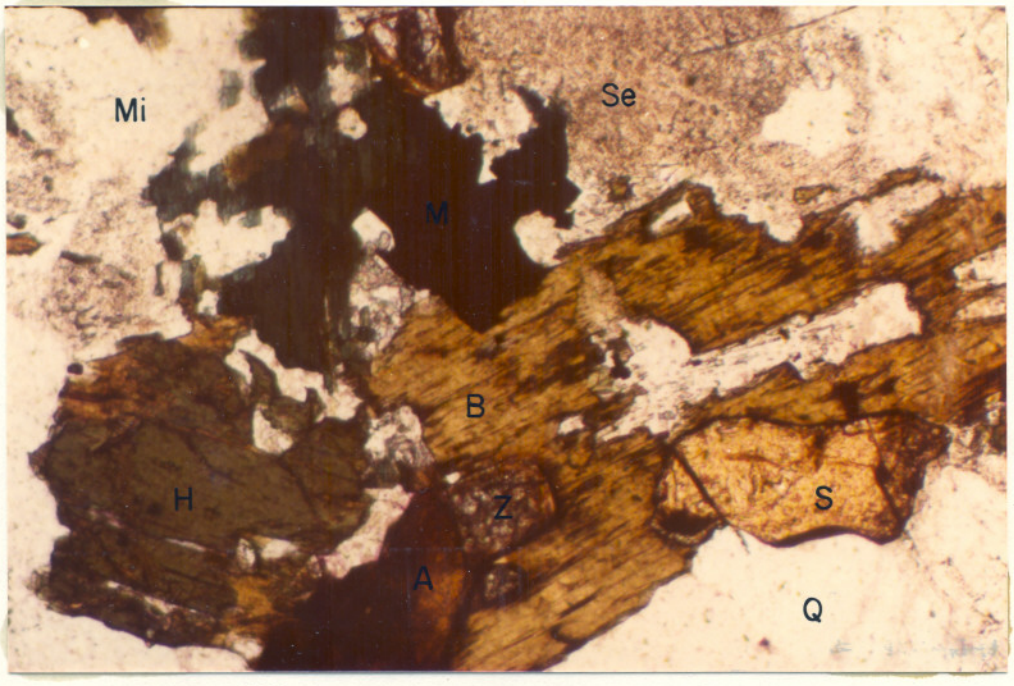

Figure 19: Photomicrograph of the hornblende biotite granite gneiss displaying biotite (B), hornblende (H), allanite (A), sphene (S), zircon (Z), magnetite (M), sericite (Se), microcline (Mi) and quartz (Q).
Plane- polarized light
Scale 1 : 0,0106

Accessory minerals found are small amounts of fluorite (sporadically disseminated), zircon, sphene and garnet. Traces of allanite, apatite, calcite and opaque minerals are also present. Traces of topaz are sparsely disseminated in the granite gneiss.

2. The TBQ host rock

The TBQ is a foliated, grey, homogeneous, fine- to medium- grained topaz biotite quartz rock which typically contains, per volume, 50 to 60 % quartz, 15 - 30 % biotite, 10 - 20 % topaz, less than 5 % fluorite and trace amounts of opaque minerals, zircons and secondary chlorite (Figure 20). Variable amounts of feldspar, usually microcline, are found in the TBQ either as Augen or as small bands developed parallel to the foliation. Depending on the amount of feldspar in the rock, various intermediate stages may be seen between a feldspar- free TBQ and a granite gneiss.

With the exception of topaz, which occurs as larger porphyroblasts, most of the major constituents form a granoblastic aggregate with morphological features typical of grain- surface equilibrium (Figures 20, 21 and 22). The stout biotite flakes (Figure 22) generally show a distinct preferred orientation which defines a foliation that is roughly followed by the elongated grains of quartz and topaz (Figure 21). Fluorite and opaque minerals generally occur as smaller grains disseminated heterogeneously throughout the rock and cassiterite (Figures 23 and 24) is a primary constituent of the TBQ mineral assemblage.

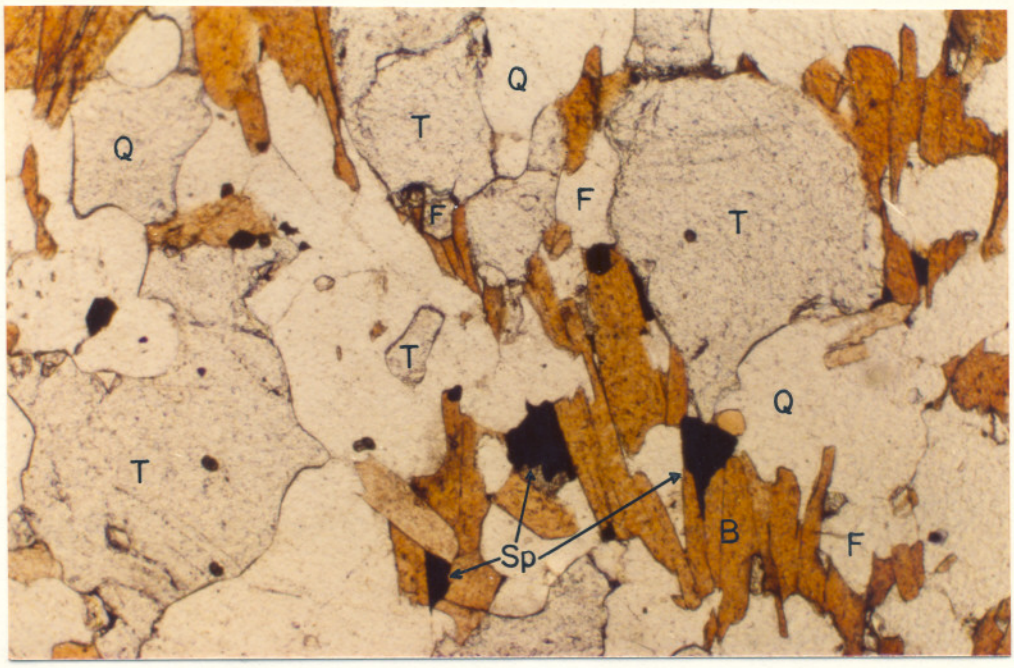

Figure 20: Photomicrograph of the TBQ showing granoblastic aggregates of quartz (Q), topaz (T), red- brown biotite (B), fluorite (F) and sphalerite (Sp.)
Plane- polarized light
Scale 1 : 0,026

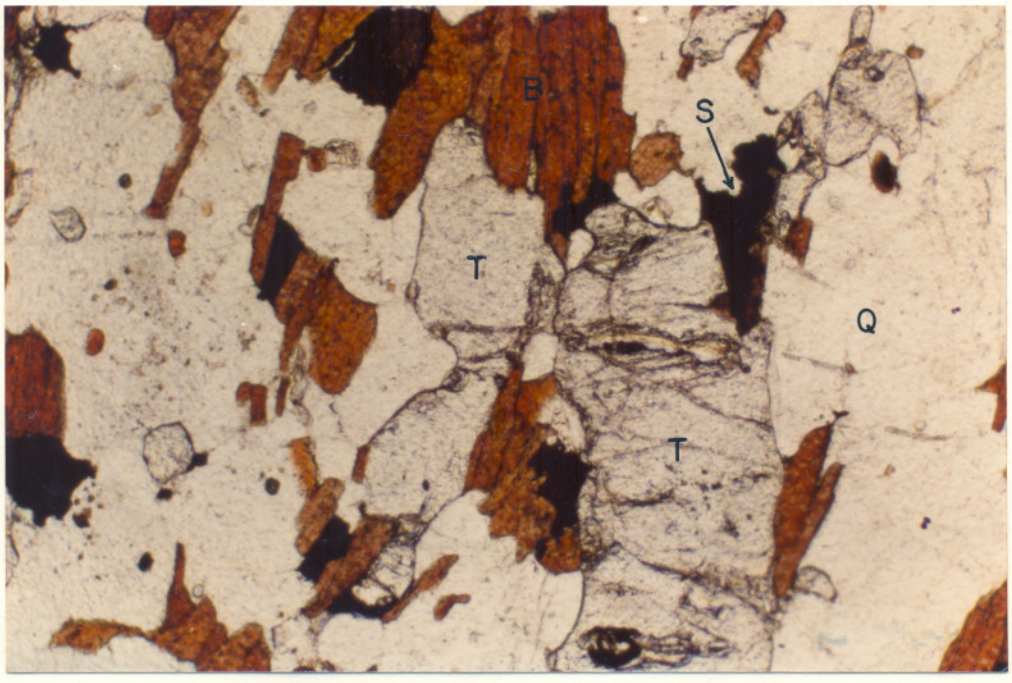

Figure 21: TBQ displaying elongated, porphyroblastic grains of topaz (T), quartz (Q), and orientated red- brown biotite (B). The opaque mineral is sphalerite. The elongation direction in the topaz is parallel to the orientation of the biotite flakes.
Plane- polarized light
Scale 1 : 0,026

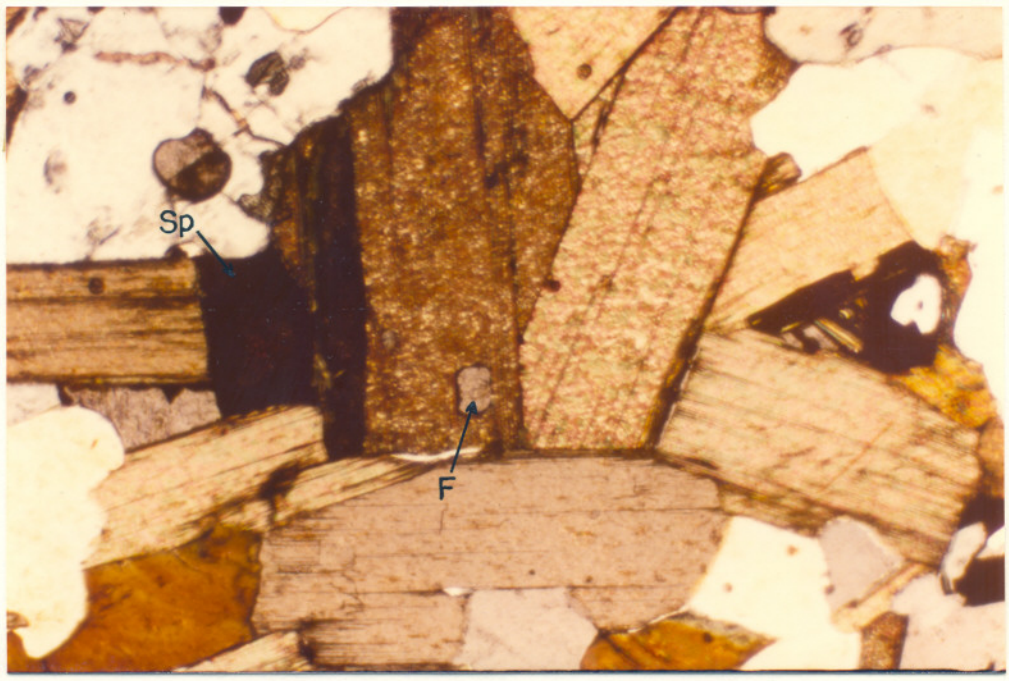

Figure 22: Stout, red- brown biotite flakes in the TBQ that are partly chloritized in places. A small fluorite inclusion (F) is present in the biotite and in the sphalerite (Sp) adjacent to the biotite.
Plane- polarized light
Scale 1 : 0,026

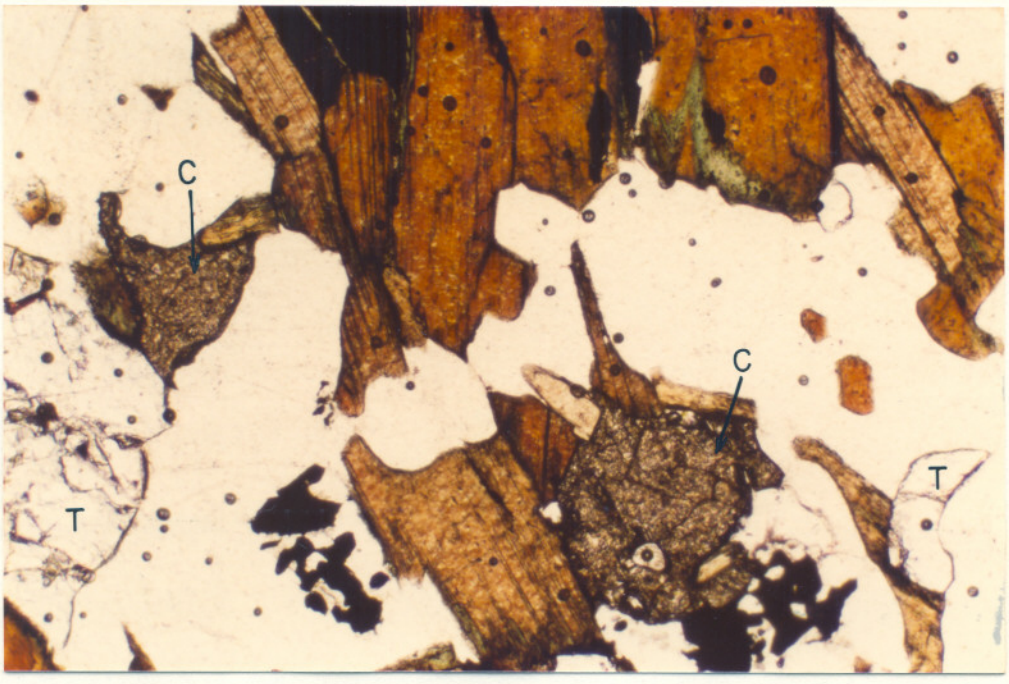

Figure 23: Photomicrograph of the TBQ displaying two cassiterite grains (C), red- brown biotite showing traces of chloritization, quartz, topaz (T) and sphalerite.
Plane- polarized light
Scale 1 : 0,026

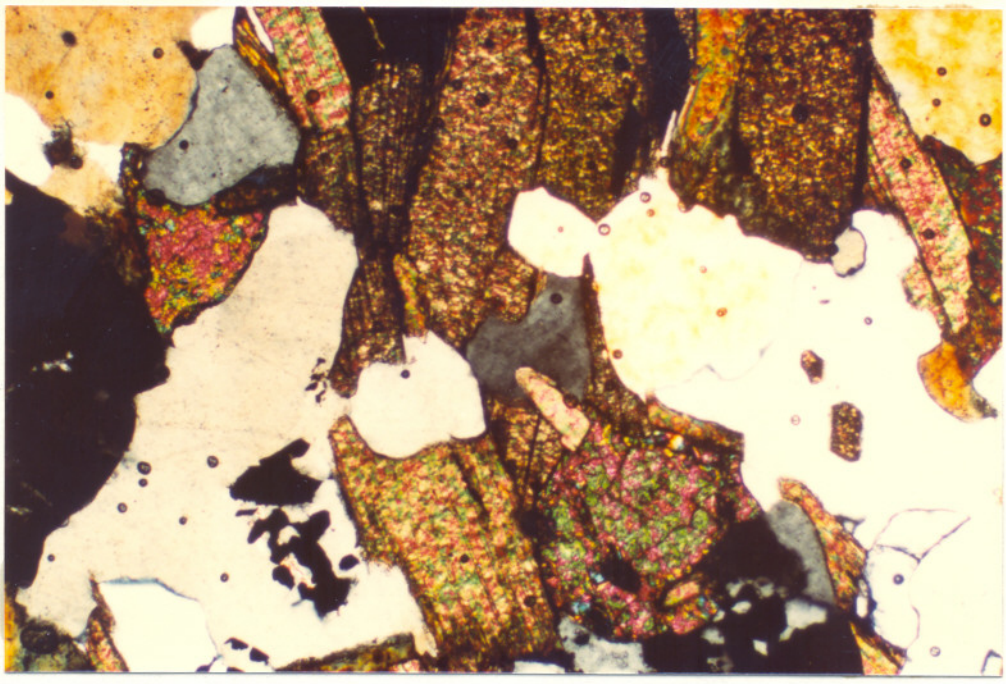

Figure 24: The same field as in Figure 23 shown here under crossed-nicols. The cassiterite displays high- order interference colours.
Scale 1 : 0,026

3. The transition zone

The transition zone is present wherever the TBQ is in contact with the granite gneiss. The transitional rock type basically is a granite gneiss in which the greenish- brown biotite, typical of the granite gneiss, is almost completely broken down to form green chlorite containing many minute rutile crystals (Figure 25), and minor K- feldspar is replacing the biotite aggregates. It is not clear if the latter two reactions are genetically linked or not. Closer to the TBQ, a reddish- brown variety of biotite is formed at the expense of the chlorite (Figures 26 and 27).

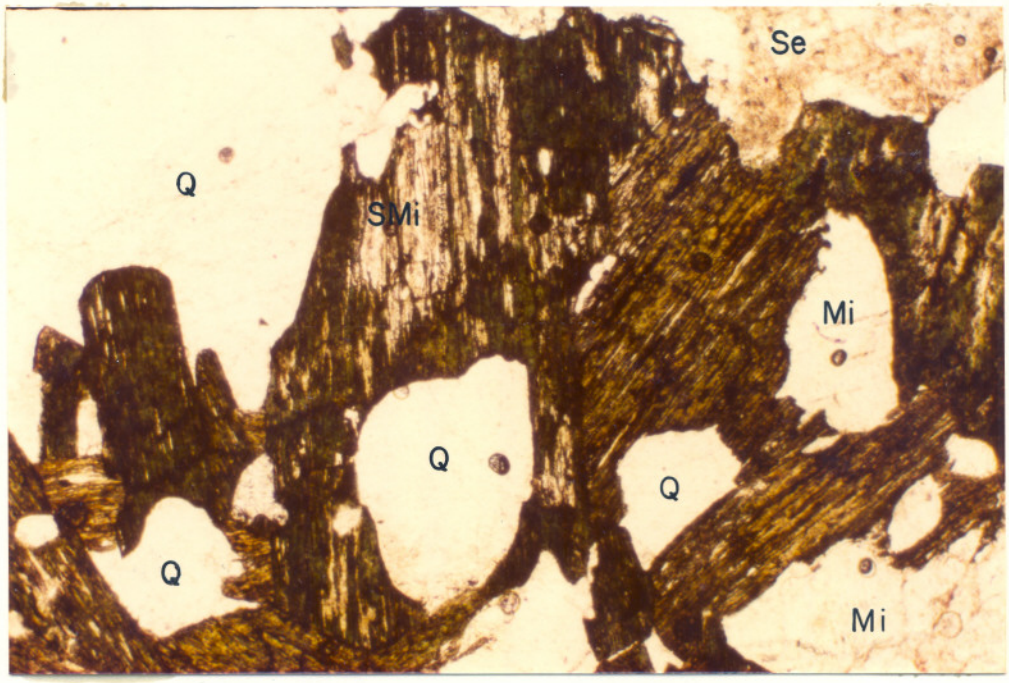

Figure 25: Biotite of the transition zone shown here to be totally replaced by chlorite and surrounded by quartz (Q), microcline (Mi) and sericite (Se). Minute black rutile crystals (not discernable) are present in the biotite. Secondary K - feldspar (SMi) formed at the expense of the biotite.
Plane- polarized light
Scale 1 : 0,026

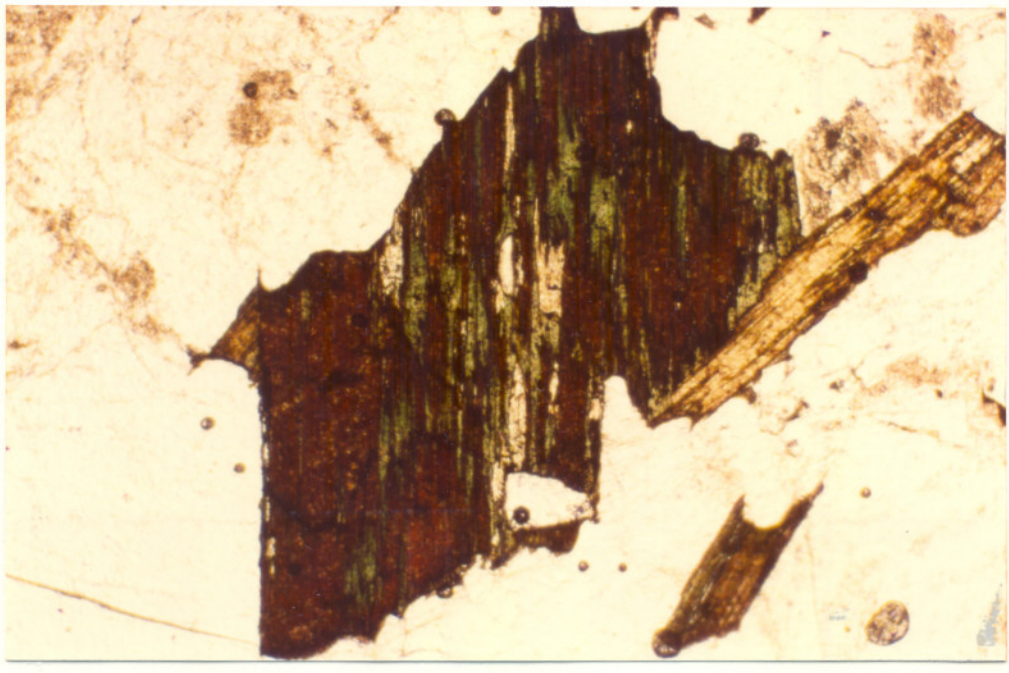

Figure 26: Photomicrograph of red- brown biotite, replacing the green chlorite of the transition zone, surrounded by microcline, quartz and sericite. A small fluorite inclusion is seen in the biotite.
Plane- polarized light
Scale 1 : 0,026

This reddish- brown biotite is characteristically found throughout the TBQ. Minor intercalated lenses of TBQ are also developed in the transition zone.

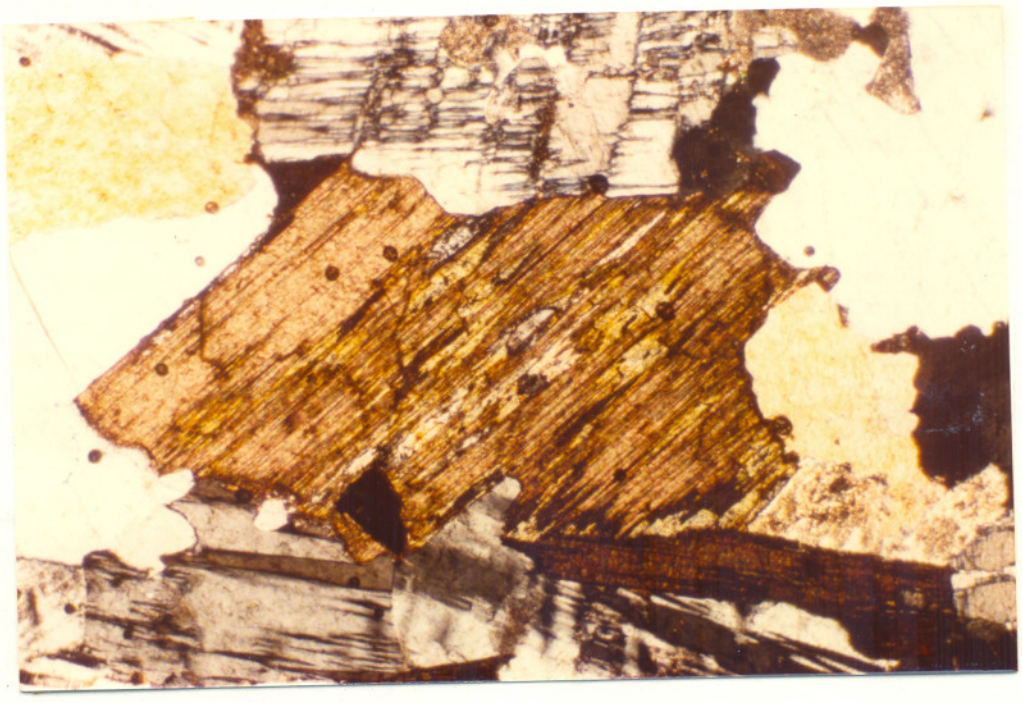

Figure 27: The same field as Figure 26 shown here under crossed- nicols after rotation by 45 °. The twinning in the feldspars is now clearly revealed.
Scale 1 : 0,026

4. The late stage alteration zones

.Late stage alteration of the granite gneiss and TBQ includes silicification, sericitization of feldspars, chloritization of biotite and hematization. The degree of alteration varies from slight to intense and occurs in zones ranging in thickness from centimeters to meters.

Silicification is found in both the granite gneiss and the TBQ. In the vicinity of major fault zones, the silicification is found associated with hematization.

Sericitization of feldspar and topaz is commonly found in the TBQ associated with a corresponding increase in fluorite which is seen to pseudomorphously replace the biotite in the rock. Sericitization and saussuritization of the feldspar in the granite gneiss are common and the microcline may be seen to change colour from clear pink to highly sericitized yellowish- white crystals. Plagioclase is invariably zoned and saussuritized in the core areas.

Chloritization is commonly found in late stage alteration zones in both the TBQ and the granite gneiss, and is seen to form at the expense of biotite.

Hematization is common in the vicinity of fault zones and is associated with an increase in quartz and a decrease in the biotite content of the rock. The hematite is found as mottled reddish- brown patches in the altered rock.

E. Mineral Variation in Borehole Sections

Borehole AES/4 has been selected as a typical example of a cross- section through the TBQ host rocks, the transition zone, and the granite gneiss country rock. The mineral composition of the samples of borehole AES/4 is given in Table 5 and that of all other boreholes together with a brief petrographic description is given in Appendix II.

In borehole AES/4 the red- brown biotite variety is seen developed throughout the TBQ. Wherever feldspar- rich zones are present in the TBQ, as well as in the transition zone, the red- brown biotite takes on a deeper red- brown colour and becomes intermixed with chlorite (Figure 26). Away from the TBQ and beyond the chlorite- bearing transition zone, the biotite found in the granite gneiss has the dark greenish-brown appearance and as one moves further away from the TBQ, hornblende also enters the mode. This general trend, which is illustrated in Figure 28, is observed in all the borehole intersections with the exception of borehole AES/5. Extensive hematitic and chloritic alteration

Table 5

Mineral composition of samples of borehole AES/4

MINERAL	SAMPLE NUMBER																	
	1	2	3	4	5	6	RM 32	7	8	RM 33	9	RM 34	10	11	RM 35	12	13	RM 36
Quartz	xx	xx	xx	xx	xx	xx	xx	xx	xx	xx	xx	xx	xx	xx	xx	xx	xx	xx
Biotite	xx	xx	xx	xx	xx	xx	xx	xx	xx	x	xx	xx	xx	x	x	x	x	x
Topaz	xx	xx	xx	xx	x	x												
Fluorite	x	x	x	x	x	x	x	x	x		xx	xx	x	x		x	x	
Microcline		x			xx	xx	xx	xx	xx	xx	xx	xx	xx	xx	xx	xx	xx	xx
Plagioclase		x			x	x	x	x	x	x	x	x	x	x	x	x	x	xx
Sericite		x			x	xx	x	x	x	x	x	x	x	x	x	x	x	x
Chlorite		x		x	x	x	xx	x	x	x	x	x	x		xx		x	xx
Sphalerite	x	x	x	x														
Zircon	x	x	x	x	x	x	x	x	x	x	x	x	x	x	x	x	x	x
Cassiterite	x	x	x	xx														
Hornblende													x	x	x	x	x	
Sphene							x			x	x	x	x	x	x	x	x	x
Myrmekite					x	x	x	x	x	x	x	x	x	x	x	x	x	x
Allanite																x		
Apatite						x	x	x	x	x	x		x	x	x	x	x	x
Opaque	x	x	x	x	x	x	x	x	x	x	x	x	x	x	x	x	x	x
Monazite					x													
Rock Type	=	=	=	=	*	*	*	+	+	+	+	+	+	+	+	+	+	+

LEGEND

=	TBQ rock
*	Transition zone
+	Granite gneiss

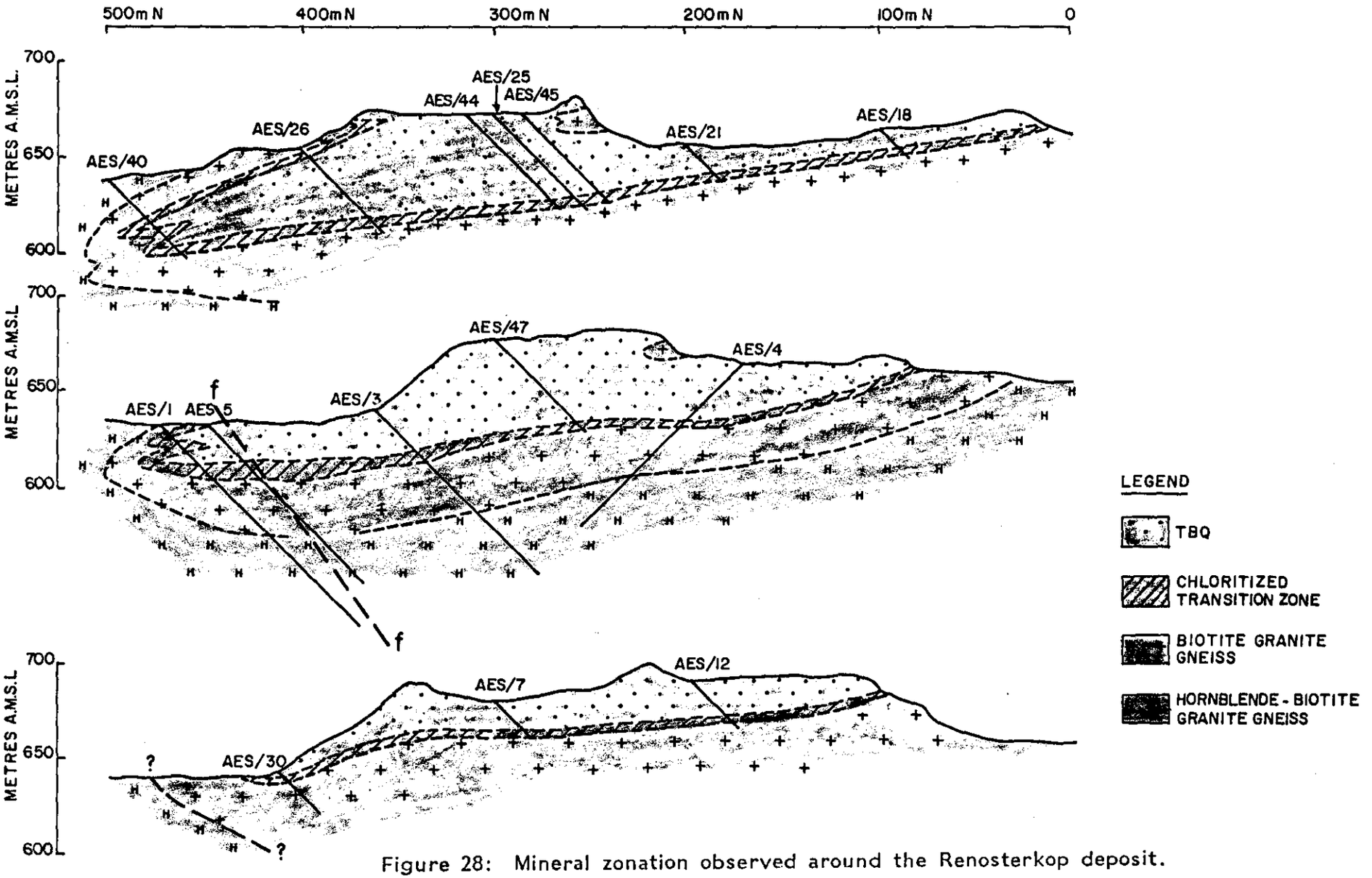

Figure 28: Mineral zonation observed around the Renosterkop deposit.

which is present throughout borehole AES/5, is ascribed to late stage alteration related to the fault seen to pass close to AES/5 in the plan of the surface geology (Figure 5).

In the TBQ and granite gneiss a pronounced antipathetic relationship between feldspar and topaz exists. Topaz is not significantly present in the granite gneiss country rock. This is clearly illustrated in Table 5. Concomitantly with an increase in the topaz content of the rock, a corresponding increase is observed in the sphalerite and cassiterite content. This observation is supported by an increase in the density of the rock.

F. Mineralogy and Mineral Chemistry

In the following sections the constituent minerals will be described roughly in an order of decreasing abundance in the TBQ and granite gneiss.

1. Quartz

In the granite gneiss country rock the quartz is present as medium- to coarse- grained, anhedral crystals which usually show an undulatory extinction. A second generation of smaller quartz grains showing a weak undulatory extinction also is present.

The quartz in the TBQ host rock forms small- to medium- sized grains with irregular outlines, and these too show undulatory extinction. Smaller quartz grains as well as occasional large porphyroblastic quartz grains are also found in the TBQ, and these show no undulatory extinction.

2. Feldspar

The feldspar occurs as medium- to coarse- grained anhedral crystals which commonly exhibit myrmekitic intergrowths. The microcline is invariably Tartan- twinned and the core zones of plagioclase crystals are often saussuritized, indicating a compositional zonation in the original crystals.

Microprobe analyses of a variety of feldspars in granite gneiss located above, below, and intercalated within the TBQ are given in Table 6. The plagioclase has an An content varying between nil and 15 %, ie. albite - oligoclase.

The stoichiometry of the K- feldspars analysed differ from the theoretical in that the number of Si atoms per 32 oxygen atoms is slightly lower, and the numbers of (K + Na) and Al per 32 oxygen atoms are slightly higher than what is to be expected. These deviations, however compare favourably with the analyses of corresponding feldspars quoted by Deer, Howie and Zussman (1963), and is not an artefact as it may appear at first sight.

3. Biotite

Three different biotite varieties are found in the study area. These are the biotite in the granite gneiss country rock, that in the TBQ host rock, and that in the transition zone between the TBQ and the granite gneiss. Microprobe analyses of these three different biotites are given in Table 7.

TABLE 6

Microprobe analyses of feldspars in granite gneiss above, below and intercallated in the TBQ.

	TYPICAL K-FELDSPAR				PLAGIOCLASE VARIATIONS								
	AES 1/1	AES 1/3	AES 1/12	AES 3/12	AES 26/15/1	AES 26/15/2	AES 26/15/3	AES 1/15	AES 26/5	AES 26/10/1	AES 26/10/2	AES 26/10/3	AES 26/10/4
SiO_2	63,80	63,47	63,95	63,52	66,47	66,51	64,83	66,80	67,48	65,8	65,9	62,9	67,86
TiO_2	0,02	0,03	-	0,02	-	0,01	-	0,01	-	-	-	-	-
Al_2O_3	18,95	18,82	18,38	18,34	21,65	21,45	22,19	20,61	19,45	20,30	20,01	22,10	20,44
BaO	0,15	0,14	0,23	0,15	0,02	-	-	-	-	-	-	-	0,01
*FeO	0,04	-	0,01	0,02	0,02	0,06	0,03	0,03	-	0,01	0,01	0,02	0,01
MnO	-	-	-	-	0,01	-	-	-	-	0,02	0,03	0,02	-
MgO	-	-	-	-	-	0,02	-	0,02	-	-	0,03	-	0,02
CaO	0,01	-	0,04	0,02	2,74	0,62	3,16	1,08	0,02	2,06	1,47	3,20	0,77
Na_2O	0,69	0,81	0,99	0,84	9,82	10,31	9,82	10,65	11,50	10,43	11,67	9,82	11,00
K_2O	16,14	16,22	15,61	16,35	0,07	1,10	0,41	0,13	0,17	0,17	0,09	0,25	0,31
TOTAL	99,84	99,50	99,18	99,25	100,80	100,08	100,45	99,33	98,62	98,80	99,21	98,31	100,4

Structural formulae on the basis of 32 (O)

Si	11,88	11,85	11,94	11,90	11,58	11,67	11,39	11,68	11,98	11,80	11,70	11,25	11,80
Ti	-	-	-	-	-	-	-	-	-	-	-	-	-
Al	4,13	4,14	4,03	4,05	4,44	4,44	4,60	4,37	4,04	4,35	4,28	4,79	4,17
Ba	0,01	0,01	0,02	0,01	-	-	-	-	-	-	-	-	-
Fe	0,01	-	-	-	-	0,01	-	-	-	-	-	0,01	-
Mn	-	-	-	-	-	-	-	-	-	-	-	-	-
Mg	-	-	-	-	-	-	-	-	-	-	0,01	-	-
Ca	-	-	-	-	0,51	0,12	0,59	0,20	0,01	0,40	0,27	0,58	0,14
Na	0,18	0,29	0,30	0,31	3,22	3,51	3,35	3,72	3,90	3,68	3,97	3,36	3,86
K	3,87	3,86	3,81	3,91	0,02	0,25	0,09	0,04	0,04	0,04	0,03	0,05	0,07
TOTAL	20,08	20,15	20,10	20,18	20,01	19,77	20,00	20,02	20,01	19,97	20,27	20,03	20,04
Mol% An	0	0	0	0	13,6	3,1	14,6	5,1	0,3	9,7	6,3	14,5	3,4
Mol% Ab	4,4	7,0	7,3	7,3	85,9	90,5	83,1	93,9	98,7	89,3	93,0	84,2	94,8
Mol% Or	95,6	93,0	92,7	92,7	0,5	6,4	2,3	1,0	1,0	1,0	0,7	1,3	1,8

* FeO represents total Fe

Table 7

Microprobe analyses of biotite in the TBQ, the transition zone, and the granite gneiss.

	Red-brown biotite in the TBQ			Red-brown biotite in the chlorite-rich transition zone			Greenish-brown biotite in the granite gneiss		
	AES 4/1	AES 4/4	AES 26/7	AES 1/3	AES 26/10	AES 26/14	AES 4/7	AES 4/8	AES 1/11
SiO_2	41,49	40,45	40,08	37,45	36,91	38,59	35,51	35,37	35,76
TiO_2	1,34	1,24	1,56	3,07	3,38	2,95	3,87	3,73	3,91
Al_2O_3	21,30	20,99	18,78	18,85	18,65	20,34	15,59	15,16	15,10
*FeO	19,37	21,05	25,39	27,57	26,85	26,15	30,62	28,87	31,26
MnO	1,37	1,37	0,92	0,61	0,92	1,33	0,96	0,92	0,56
MgO	1,15	0,81	1,39	1,98	1,91	1,82	2,66	3,41	3,72
CaO	0,01	0,01	0,01	0,00	0,00	0,00	0,12	0,12	0,18
Na_2O	0,31	0,26	0,28	0,20	0,15	0,14	0,17	0,23	0,06
K_2O	9,18	9,13	8,70	7,86	8,42	9,11	8,59	8,92	8,56
SnO_2	0,00	0,00	0,00	0,00	0,00	0,00	0,00	0,00	0,00
TOTAL	95,5	95,3	97,09	97,62	97,27	100,42	98,08	96,72	98,90
Structural formulae on the basis of 16 cations									
Si	6,71	6,59	6,47	6,06	5,99	6,03	5,76	5,77	5,73
Ti	0,16	0,15	0,19	0,37	0,41	0,35	0,47	0,46	0,47
Al	4,06	4,03	3,57	3,59	3,57	3,75	2,98	2,92	2,85
Fe	2,62	2,87	3,43	3,73	3,65	3,42	4,16	3,94	4,19
Mn	0,19	0,19	0,13	0,08	0,13	0,18	0,13	0,13	0,08
Mg	0,28	0,20	0,33	0,48	0,46	0,42	0,64	0,83	0,89
Ca	0,00	0,00	0,00	0,00	0,00	0,00	0,02	0,02	0,03
Na	0,10	0,08	0,09	0,06	0,05	0,04	0,05	0,07	0,02
K	1,89	1,90	1,79	1,62	1,74	1,82	1,78	1,86	1,75
Sn	0,00	0,00	0,00	0,00	0,00	0,00	0,00	0,00	0,00
TOTAL	16,00	16,00	16,00	16,00	16,00	16,00	16,00	16,00	16,00

* FeO represents total Fe

The granite gneiss hosts the dark greenish- brown biotite variety which shows a preferred orientation parallel to the foliation planes in the gneiss and often contains inclusions of sphene and zircons. The zircon in the biotite shows pleochroic haloes due to radioactivity. The microprobe analyses of these biotites show a chemistry that compares favourably with that of biotite from a fine grained granite from Rubideaux, Southern California batholith (Deer, Howie, and Zussman, 1963).

The biotite in the TBQ host rock is a reddish- brown variety which is found as subhedral grains with a distinct orientation defining a foliation. The biotite is sometimes seen mantling opaque mineral grains, and where

hematitic alteration has taken place, the biotite is seen to be pseudomorphously replaced by hematite. Whenever significant amounts of feldspar (over 10 %) are found in the TBQ, chloritization of the biotite is directly related to the amount of feldspar present in the rock. Although no tin was detected in the microprobe analyses of the biotites in the TBQ, a previous investigation carried out by Southwood (1983) revealed that a small proportion of the tin is present in the biotite lattice. The microprobe analyses of the biotites in the TBQ are similar to those of a blue- green siderophyllite in a topaz- bearing greisen vein from Newcastle, Northern Ireland (Deer, Howie, and Zussman, 1963).

In the transition zone a deep reddish- brown biotite variety is found which is partly or totally replaced by chlorite. From the microprobe analyses (Table 7) it may be seen that the chemistry of this biotite is transitional between the biotite in the granite gneiss and that in the TBQ.

A remarkable feature of each of the three biotite varieties is their chemical homogeneity within each of their defined boundaries. The chemistry of the biotite of the granite gneiss which lies above the TBQ is for example the same as that of the biotite in the gneiss at various depths below the TBQ. The chemistry of the biotite in the transition zone between the TBQ host rock and the granite gneiss country rock is similar to that found in a transition zone between the TBQ and a granite gneiss lens within the TBQ (eg.AES 26/10). Unaltered biotite of the TBQ is homogeneous in composition throughout the TBQ body.

Distinct chemical trends may be observed between the three biotite varieties. SiO_2 and Al_2O_3 are seen to increase from the granite gneiss across the transition zone and into the TBQ. At the same time TiO_2 and FeO show a decreasing trend. MgO is also seen to increase slightly while MnO, CaO, Na_2O and K_2O tend to remain constant. Figure 28 illustrates the distribution of the three major rock types which host the different biotite varieties discussed.

4. Chlorite

Chlorite is found replacing the biotite of the granite gneiss wherever the TBQ host rock is in contact with granite gneiss. This occurs at both the upper and lower contacts between the TBQ host rocks and the granite gneiss country rock (Figure 28) as well as in granite gneiss lenses within the TBQ host rock. Chlorite is also common within late stage hydrothermal alteration zones found in both the TBQ and the granite gneiss.

The green pleochroic chlorite either partly or totally replaces the biotite and typically contains minute rutile crystals identified by means of microprobe techniques. The presence of rutile is ascribed to the release of titanium due to the breakdown of biotite and at the same time the inability of chlorite to accommodate large quantities of titanium. Microprobe analyses of the chlorite are given in Table 8.

Table 8

Microprobe analyses of chlorite from the transition zone

	AES 1/3/5	AES 1/5/2	AES 1/11/2	AES 26/15/1	AES 26/15/2	AES 1/3/7	AES 1/3/2	AES 1/3/1
SiO_2	25,96	25,99	26,40	25,52	25,31	23,39	25,86	24,25
TiO_2	0,10	0,80	0,45	0,05	0,10	0,08	0,25	0,14
Al_2O_3	22,05	19,30	18,06	17,79	17,17	21,49	20,03	20,52
*FeO	41,85	41,02	41,84	43,84	43,99	39,26	41,29	43,05
MnO	1,33	1,06	0,50	0,63	0,78	2,80	0,64	0,66
MgO	2,03	3,64	4,96	4,15	4,15	2,78	2,47	2,61
CaO	0,04	0,11	0,20	0,00	0,00	0,09	0,00	0,00
K_2O	0,00	0,04	0,27	0,00	0,00	0,00	0,00	0,00
TOTAL	93,37	91,96	92,68	91,98	91,49	89,89	90,54	91,23

Structural formulae on the basis of 28 (O)

Si	5,58	5,68	5,75	5,67	5,68	5,27	5,73	5,41
Ti	0,02	0,13	0,07	0,01	0,02	0,01	0,04	0,02
Al	5,59	4,97	4,63	4,66	4,54	5,70	5,23	5,40
Fe	7,52	7,50	7,62	8,15	8,26	7,39	7,65	8,04
Mn	0,24	0,20	0,09	0,12	0,15	0,53	0,12	0,12
Mg	0,65	1,19	1,61	1,38	1,39	0,93	0,81	0,87
Ca	0,01	0,03	0,05	0,00	0,00	0,02	0,00	0,00
K	0,00	0,00	0,00	0,00	0,00	0,00	0,00	0,00
TOTAL	19,61	19,71	19,90	19,99	20,04	19,88	19,64	19,87

* FeO represents total Fe

5. Amphibole

The amphibole is a dark green variety which shows a pleochroism ranging from dark to light green and exhibits a characteristic cleavage. The amphibole occurs as small to medium sized anhedral crystals which are commonly broken down to form biotite. Table 9 contains microprobe analyses of various amphibole minerals located both above and below the TBQ, and shows them to be remarkably homogeneous in composition.

Table 9

Microprobe analyses of amphibole from the granite gneiss.

	Amphibole in granite gneiss above the TBQ			Amphibole in granite gneiss below the TBQ						
	AES 1/1	AES 40/1	AES 40/2	AES 1/9	AES 1/12	AES 1/15	AES 3/15	AES 4/10	AES 4/12	AES 4/13
SiO_2	38,41	37,11	37,54	38,43	37,90	38,65	38,25	37,95	37,42	37,80
TiO_2	1,04	0,95	1,04	1,20	1,09	1,29	1,30	1,04	1,09	1,08
Al_2O_3	12,52	11,62	11,85	11,67	11,58	11,74	11,54	12,01	11,64	11,53
*FeO	30,36	31,02	31,51	30,13	29,87	29,09	28,16	30,60	30,90	31,44
MnO	0,77	0,68	0,66	0,58	0,77	0,68	0,74	0,71	0,65	0,60
MgO	1,61	1,71	1,55	2,27	2,30	2,98	3,02	1,78	1,76	1,76
CaO	10,90	11,34	10,77	10,72	11,00	10,81	11,03	10,55	10,63	10,74
Na_2O	1,78	1,84	1,74	1,78	1,67	1,77	1,88	1,70	1,98	1,69
K_2O	1,80	1,76	1,67	0,58	1,85	1,65	1,68	1,61	1,66	1,60
TOTAL	99,20	98,02	98,34	98,43	98,02	98,65	97,59	97,95	97,72	98,23

Structural formulae on the basis of 23(O)

Si	6,16	6,08	6,12	6,23	6,16	6,19	6,18	6,17	6,13	6,16
Ti	0,13	0,12	0,13	0,15	0,13	0,16	0,16	0,13	0,13	0,13
Al	2,37	2,25	2,28	2,23	2,22	2,21	2,20	2,30	2,25	2,21
Fe	4,07	4,25	4,30	4,08	4,06	3,89	3,81	4,16	4,23	4,28
Mn	0,10	0,09	0,09	0,08	0,11	0,09	0,10	0,10	0,09	0,08
Mg	0,38	0,42	0,38	0,55	0,56	0,71	0,73	0,43	0,43	0,43
Ca	1,87	1,99	1,88	1,86	1,92	1,85	1,91	1,84	1,87	1,87
Na	0,55	0,59	0,55	0,56	0,53	0,55	0,59	0,54	0,63	0,53
K	0,37	0,37	0,35	0,12	0,38	0,34	0,35	0,33	0,35	0,33
TOTAL	16,00	16,16	16,08	15,86	16,07	15,99	16,03	16,00	16,11	16,02

• FeO represents total Fe

Based on a standard amphibole formula written as:

$$A_{0-1}B_2C_5T_8O_{22}(OH,F,Cl)_2, \text{ where}$$

A = Na, K

B = Na, Li, Ca, Mn, Fe^{2+}, Mg

C = Mg, Fe^{2+}, Mn, Al, Fe^{3+}, Ti, and

T = Si, Al,

Hawthorne (1981) divided the amphiboles into four principal groups on the basis of the B group cation occupancy:

$(Ca + Na)_B < 1,34$ Iron- magnesium- manganese group

$(Ca + Na)_B \geq 1,34$ and $Na_B < 0,67$ — Calcic amphibole group

$(Ca + Na)_B \geq 1,34$ and $0,67 \leq Na_B < 1,34$ — Sodic- calcic amphibole group

$Na_B \geq 1,34$ — Alkali amphibole group

Using the abovementioned classification it can be shown (Table 9) that all the amphiboles from Renosterkop fall within the calcic amphibole group and may be termed hornblende. This may be illustrated using sample AES1/1 as an example.

$(Ca + Na)_B = 2,42$, and

$Na_B = 0,55$

A further subdivision of the calcic amphibole group (Hawthorne, 1981) shows (sample AES1/1):

$Mg/(Mg + Fe) = 0,09$

$Na + K = 0,92$

$Ti = 0,13$

$Al^{vi} = 1,84$, and

$Si = 6,16$

Based on the classification used by Hawthorne (1981) it is necessary to furthermore distinguish whether $Fe^{3+} > Al^{vi}$ or $< Al^{vi}$ in order to differentiate ferro-pargasite from hastingite. Unfortunately the microprobe does not allow the determination of ferrous and ferric iron and accordingly no further subdivision is possible. It could be either a ferro-pargasite or a hastingite.

The microprobe analyses of the amphibole in Table 9 compare favourably to analyses of a hornblende from a quartz monzonitic syenite from Sokuchankoge, Kogen-do, Korea, quoted by Deer, Howie and Zussman (1963).

6. Topaz

The occurence of topaz is restricted to the TBQ, in which it is scattered throughout the quartz- biotite matrix, mainly as colourless, porphyroblastic, irregular to lenticular grains. The grains are generally larger than those of quartz, and commonly contain small rounded inclusions of quartz or fluorite. Late stage alteration has resulted in the sericitization of topaz in places.

7. Fluorite

Fluorite is found mainly within the TBQ and generally only minor amounts are present in the granite gneiss. Fluorite is common in the transition zone but is present in much smaller amounts than in the TBQ. Chloritic and sericitic alteration zones in the granite gneiss generally contain a higher concentration of fluorite than the unaltered granite gneiss.

The TBQ host rock contains approximately 5 % fluorite by volume. The mineral takes the form of small anhedral crystals which are commonly found enclosed in topaz or on grain boundaries of quartz crystals. Fluorite often occupies the angular interstices between biotite flakes and can thus be said to have formed later than both the quartz and the biotite. Small concentrations of fluorite are found in the TBQ in alteration zones where sericitization and chloritization are pronounced. Purple fluorite is common on fracture surfaces.

8. Zircon

Zircon is commonly found within the granite gneiss and the TBQ host rock and generally occurs as small rounded crystals, showing distinct

pleochroic haloes in biotite. Minute euhedral crystals of short prismatic habit are restricted to the granite gneiss country rock. The rounded zircon crystals in the granite gneiss are generally larger than those in the TBQ. Growth zones of the zircon in the TBQ are seen ending discordantly against grain surfaces indicating that the zircons have been exposed to either chemical dissolution or physical abration.

9. Gahnite

Gahnite is restricted to the TBQ in which it is found in small amounts in some samples. It appears to be in complete grain surface and chemical equilibrium with biotite and shows slight signs of incipient alteration to sphalerite and chlorite. The gahnite takes on a bright green colour and microprobe analyses of typical gahnite samples are given in Table 10.

The gahnite has been compared to gahnite from Aggeneys as well as blue and green gahnite from Oranjefontein (Hicks,et.al., 1985). The gahnite compositions, normalized to molar proportions of end- member gahnite, hercynite and spinel, are plotted on a triangular diagram (Figure 29) and show the Renosterkop gahnite to be enriched in the $FeAl_2O_4$ molecule relative to the other three gahnite varieties described by Hicks et. al., 1985.

Table 10

Microprobe analyses of representative gahnite samples

	AES 47/5/1	AES 47/5/2	AES 47/5/3	AES 47/5/4	AES 47/5/5
Al_2O_3	57,38	56,51	57,27	56,67	57,01
ZnO	27,57	26,51	28,91	27,59	27,74
MgO	0,08	0,12	0,07	0,10	0,09
Cr_2O_3	0,01	0,00	0,01	0,00	0,03
*FeO	14,75	15,02	12,83	14,98	14,65
MnO	0,50	0,54	0,48	0,55	0,52
TiO_2	0,00	0,00	0,00	0,00	0,00
TOTAL	100,27	98,70	99,56	99,89	100,05

Structural formulae on the basis of 32(O)

Al	16,07	16,07	16,14	15,99	16,03
Zn	4,84	4,72	5,10	4,88	4,89
Mg	0,03	0,04	0,02	0,04	0,03
Cr	0,00	0,00	0,00	0,00	0,01
Fe	2,93	3,03	2,57	3,00	2,92
Mn	0,10	0,11	0,10	0,11	0,10
Ti	0,00	0,00	0,00	0,00	0,00
TOTAL	23,97	23,97	23,93	24,02	23,98

* FeO represents total Fe

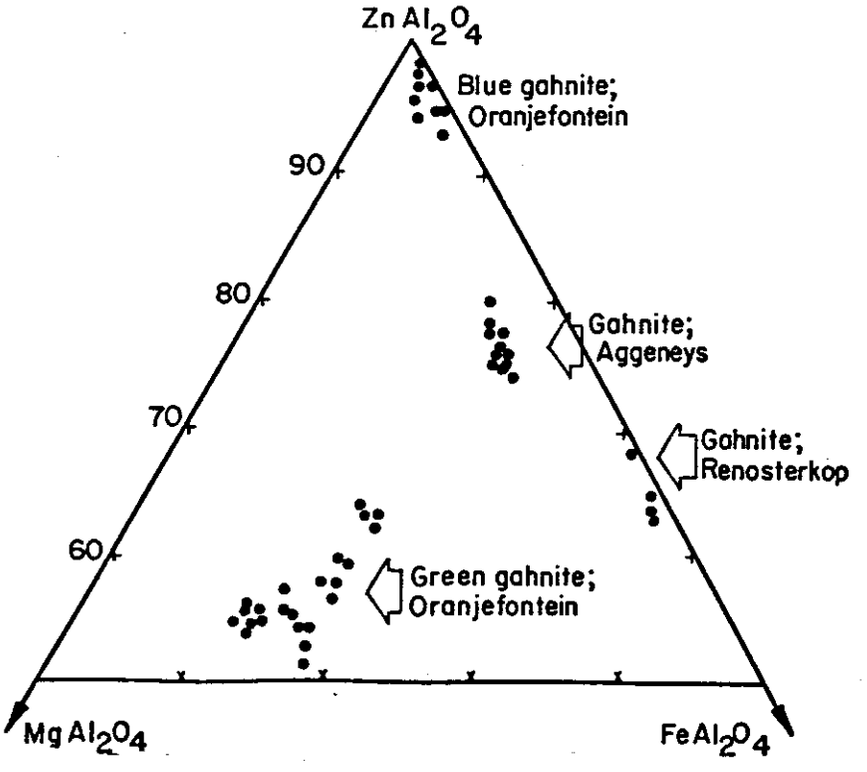

Figure 29: Triangular plot showing the composition of green gahnite from Renosterkop, blue and green gahnite from Oranjefontein, and gahnite from the Broken Hill orebody, Aggeneys. Compositions have been normalized to end- member gahnite, spinel and hercynite (after removal of calculated galaxite, chromite and magnetite). (Adapted from Hicks, et al 1985).

10. Accessory non-opaque minerals

In the granite gneiss, small amounts of apatite, allanite, sphene and calcite are found as accessory minerals. Apatite is found in small amounts taking on the form of minute six- sided, prismatic crystals. Allanite occurs sparsely distributed throughout the granites away from the TBQ and trace amounts of calcite are found in small cracks and veins. Sphene is found sporadically disseminated throughout the granite gneiss country rock.

Traces of brown radioactive monazite are also sporadically disseminated in the TBQ. Sillimanite, as well developed prisms and associated with muscovite, is sparsely developed as a breakdown product of the topaz in the TBQ (De Waal, 1985).

11. Accessory opaque minerals

(a). General statement

In this section the opaque minerals are discussed. Sphalerite and cassiterite, although strictly- speaking transparent, are included in order to group together all the minerals of potential economic value. The opaque minerals microscopically identified are listed in Table 11.

(b). The granite gneiss

The opaque minerals in the granite gneiss consist of minor amounts of pyrite, pyrrhotite, hematite and magnetite as well as trace amounts of

Table 11

Distribution of opaque minerals in 30 selected samples of TBQ and granite gneiss

	TBQ												ALTERATION ZONES						
	AES 3/1	AES 3/2	AES 3/3	AES 3/4	AES 3/5	AES 3/6	AES 3/7	AES 3/8	AES 3/9	AES 3/10	AES 44/2	AES 44/11	AES 1/2	AES 1/4	AES 5/3	AES 47/4	AES 5/8	AES 25/4	AES 44/5
Pyrite	x	x	x	x	x	x	xx	x	x	x	x	x				x		x	x
Arsenopyrite	x			x	x						x								
Pyrrhotite	x		x		x		x				x	x							
Marcasite	x			x	x	x													
Chalcopyrite	x	x	x	x	x	x	x	x	x	x	x	x						x	x
Covellite	x			x	x	x	x	x	x										
Digenite	x			x	x	x	x		x										
Sphalerite	xx	xx	xx	x	xx	x	xx	x	xx	x	x	xx						xx	xx
Cassiterite	x	x	x	x	x		x	x	x			x				xx		x	
Ilmenite					x														
Hematite	x	x			x								x	x	x		x		
Magnetite													x		x				
Wolframite																			

xx	Minor
x	Trace

Table 11

Distribution of opaque minerals in 30 selected samples of TBQ and granite gneiss (cont.)

	BIOTITE - BEARING GRANITE GNEISS					HORNBLENDE - BEARING GRANITE GNEISS					
	AES 4/9	AES 3/13	AES 3/14	AES 26/14	AES 26/15	AES 1/1	AES 1/15	AES 3/15	AES 40/1	AES 4/13	AES 1/9
Pyrite	×	×		×	×		×				×
Arsenopyrite				×							
Pyrrhotite	×	×	×	×			×	×			
Marcasite											
Chalcopyrite			×				×				
Covellite				×							
Digenite											
Sphalerite											
Cassiterite											
Ilmenite							×		×		
Hematite		×	×	×	×	×	×		×		
Magnetite		×			×	×	×	×	×	×	×
Wolframite											

copper sulphides. There is a stronger tendency for magnetite to be associated with the hornblende- bearing granite gneiss than with the biotite- bearing granite gneiss.

(c). The TBQ

Cassiterite, wolframite, sphalerite, arsenopyrite, marcasite and blue sulphides are found disseminated within the TBQ rocks.

(i).Cassiterite is the main source of tin and occurs as brownish monocrystalline grains disseminated in the TBQ. The grains are often twinned and are irregularly shaped. Cassiterite is often associated with sphalerite in microscopic bands developed parallel to the foliation. This is a common feature wherever sphalerite becomes a significant component of the rock. Cassiterite is also seen to be in grain surface equilibrium with quartz, biotite, topaz, fluorite and sulphides. A definite antipathetic relationship however exists between cassiterite and feldspar. The length and breadth of each of 270 cassiterite grains were measured and the statistical analysis of the results are presented in Table 12.

Table 12

Results of statistical analyses of cassiterite grain sizes

	Variable dimension of cassiterite grains		
	Length	Breadth	Square root of length x breadth
Moments			
Mean	362	208	269
Sum	97819	56074	72689
Standard deviation	213	125	152
Variance	45569	15646	23252
Skewness	1,76	1,99	2,02
Kurtosis	5,07	5,84	6,41
Uncorrected sum of squares	47597161	15854474	25822343
Corrected sum of squares	12258062	4208943	6254727
Coefficient of variation	58,9	60,2	56,6
Standard mean	13,0	7,6	9,3
Quantiles			
100% Max	1500	900	1102
99%	1244	750	910
95%	750	450	520
90%	600	378	447
75%Q3	450	250	336
50% MED	300	180	232
25% QI	210	120	164
10%	150	90	134
5%	120	81	107
1%	90	48	64
0% Min	60	35	55
Range	1440	865	1048
Q3 - QI	240	130	172
Mode	300	150	134
Lowest extreme	60	35	55
Highest extreme	1500	900	1102

Frequency bar charts for the dimensions of the cassiterite grains are given in Figure 30 a, b and c. It may be seen from Figure 30 that the majority of cassiterite grains vary between 100 and 500 µm in size.

(ii). **Sphalerite** is the most common mineral in the opaque group and occurs disseminated throughout most of the TBQ host rocks. Concentrations of sphalerite are sometimes found along microscopic bands developed parallel to the foliation and in these instances are usually associated with small amounts of cassiterite.

The sphalerite typically contains numerous chalcopyrite inclusions in the form of fine exsolved droplets, and is pseudomorphously replaced by fluorite, quartz and biotite. In places only the original chalcopyrite inclusions remain in the pseudomorphs. A second generation of sphalerite has also been identified and is characterized by a lighter colour and the absence of chalcopyrite inclusions. The sphalerite is most commonly found in contact with biotite, and to a lesser extent with fluorite. It typically occupies the interstices between biotite flakes.

(iii). **Wolframite**, sparsely disseminated and distributed in patches, was identified in field outcrops of TBQ but was not observed in any of the polished sections studied. The wolframite observed in outcrops forms tabular subhedral crystals ranging in size from 2 to 15 mm.

(iv). **Chalcopyrite** is mainly found as inclusions in sphalerite but also occurs in the form of anhedral grains disseminated within the TBQ host rock. Qualitative analyses of the chalcopyrite carried out on the electron microprobe indicated a significant amount of osmium associated with the chalcopyrite inclusions in the sphalerite as well as the individual chalcopyrite grains. Lesser amounts of zinc, palladium and silver were also identified in some of the chalcopyrite grains. These findings are however subject to quantitative confirmation. Deer, Howie and Zussman (1962) have reported minor and trace amounts of many elements present in chalcopyrite, eg. Ag,Au,Pt,Pb,Co,Ni,Mn, Sn, and Zn replacing Cu or Fe, and As of Se replacing S. No mention was made of Os.

(v). **Pyrite** is the most widely distributed sulphide mineral and occurs as

Fluorine values in the granite gneiss decrease consistently with depth below the TBQ. This implies a definite transitional trend rather than a sharp contact relationship between the granite gneiss and the TBQ. With the exception of Ce and Ba, the trace element chemistry in the granite gneiss is generally lower than in the TBQ. This transitional chemical trend over the granite gneiss - TBQ contact is also illustrated by SiO_2, TiO_2, Fe_2O_3, Al_2O_3, CaO, MnO, K_2O, P_2O_5 and S (Appendix III).

Table 13

Major and trace element chemistry for rock samples

SAMPLE NO.	AES/26/1	AES/26/2	AES/26/3	AES26/4	AES/4/1	AES/26/5	AES/26/6
DESCRIPTION	TBQ 5% feldspar	TBQ 5% feldspar	Granite gneiss lens	TBQ with sericitized topaz	TBQ	Granite gneiss lens -biotite rich	TBQ
Depth above(+) or below(-) lower granite gneiss/ TBQ contact	+28,1m	+26,4m	+23,3m	+20,7m	+18,4m	+17,7m	+13,4m
SiO_2	70,30	70,10	62,40	63,90	67,30	71,50	66,40
TiO_2	0,17	0,10	0,69	0,51	0,50	0,34	0,43
Al_2O_3	16,10	14,50	15,10	13,00	14,50	13,20	18,30
Fe_2O_3	0,49	0,20	0,30	0,12	0,27	0,26	0,41
FeO	3,05	4,85	4,60	5,55	6,10	3,33	5,30
MnO	0,03	0,12	0,14	0,16	0,47	0,16	0,30
MgO	<0,10	<0,10	0,70	0,40	0,30	0,20	0,20
CaO	2,99	2,25	2,62	6,80	1,56	0,73	1,30
Na_2O	0,40	0,30	2,70	0,20	0,30	1,70	0,40
K_2O	1,49	2,29	6,91	2,72	3,25	6,58	2,06
P_2O_5	0,05	0,01	0,23	0,16	0,06	0,05	0,01
H_2O-	0,08	0,07	0,13	0,06	0,11	0,09	0,05
H_2O+	1,02	0,61	0,92	0,80	0,74	0,75	0,57
M.CH	-1,23	-0,67	-1,00	-0,77	-0,02	-0,38	0,10
F	2,05	1,90	2,17	4,54	1,52	1,13	1,90
S	0,50	0,81	0,23	0,43	0,74	<0,01	1,22
	98,72	98,11	99,84	99,35	97,72	100,02	98,85
O≡F	0,86	0,80	0,91	1,91	0,64	0,48	0,80
TOTAL	97,86	97,31	98,93	97,44	97,08	99,54	98,05
ppm							
*Sn	10	75	16	173	60	69	138
*W	3	15	3	7	15	1	16
Ta	< 20	< 20	< 20	< 20	< 20	< 20	< 20
Ce	63	51	114	90	55	144	3
La	26	17	76	39	19	76	2
Nb	59	123	40	43	31	38	33
Zr	176	133	526	335	320	370	259
Y	97	194	137	122	71	25	43
Sr	20	45	115	164	51	178	53
As	24	11	257	0	12	13	476
Rb	360	825	866	642	1240	1057	717
Ba	55	91	843	151	308	396	84
*Zn	290	602	139	245	646	47	799
Cu	198	122	182	500	170	29	658

* Relative value represented as a factor of true confidential value.

Table 13

Major and trace element chemistry for rock samples (cont.)

SAMPLE NO.	AES/4/2	AES/26/7	AES/4/3	AES/26/8	AES/26/9	AES/26/10	AES/26/11	AES/4/4	AES/26/12
DESCRIPTION	TBQ 5% feldspar	TBQ	TBQ	TBQ 5% feldspar	TBQ 5% feldspar	Granite gneiss lens	TBQ	TBQ	TBQ
Depth above(+) or below(-) lower granite gneiss/ TBQ contact	+13,0m	+11,5m	+8,8m	+8,6m	+7,8m	+7,1m	+4,6m	+3,9m	+0,7m
SiO_2	70,80	65,90	68,40	67,40	69,30	72,70	61,50	64,00	70,20
TiO_2	0,50	0,46	0,35	0,51	0,53	0,44	0,58	0,44	0,40
Al_2O_3	12,40	15,90	14,60	14,50	11,40	11,70	6,00	17,80	14,50
Fe_2O_3	0,21	0,29	0,36	0,50	0,00	0,00	1,32	0,73	0,11
FeO	5,30	6,10	5,40	6,70	6,70	3,30	7,40	5,90	5,60
MnO	0,18	0,29	0,54	0,30	0,23	0,09	0,21	0,41	0,23
MgO	0,20	0,30	0,20	0,30	0,60	0,30	0,40	0,20	0,10
CaO	1,27	2,21	1,14	2,17	1,84	1,13	10,06	1,50	1,26
Na_2O	0,80	0,40	0,30	0,20	0,40	2,50	0,30	0,40	0,20
K_2O	3,47	2,31	2,80	2,45	6,37	5,23	2,73	2,84	2,05
P_2O_5	0,02	0,21	0,04	0,01	0,04	0,04	0,02	0,44	0,00
H_2O-	0,25	0,09	0,16	0,15	0,26	0,23	0,19	0,18	0,20
H_2O+	0,65	0,56	0,77	0,80	1,14	0,97	0,84	0,93	0,61
M.CH	-0,51	0,46	-0,23	-0,13	-1,67	-0,85	-3,50	-0,40	-1,67
F	1,50	1,81	1,44	2,33	1,90	0,72	6,63	1,69	1,56
S	0,54	1,37	0,69	0,58	0,19	0,01	1,43	0,95	0,47
	98,09	98,21	97,19	98,90	100,86	99,36	100,15	98,41	97,49
O≡F	0,63	0,76	0,61	0,98	0,80	0,30	2,79	0,71	0,66
TOTAL	97,46	97,45	96,58	97,92	100,06	99,06	97,36	97,70	96,83
ppm									
*Sn	58	144	50	15	17	7	29	97	27
*W	6	46	7	9	5	1	3	25	4
Ta	< 20	< 20	< 20	< 20	< 20	< 20	< 20	< 20	< 20
Ce	134	9	83	40	133	108	88	130	87
La	64	24	32	40	63	45	25	63	43
Nb	34	29	25	36	41	29	55	33	23
Zr	424	298	284	358	440	372	728	324	298
Y	75	67	70	104	72	74	631	96	82
Sr	46	71	48	49	160	74	83	69	46
As	280	977	47	223	24	28	44	96	7
Rb	790	750	1048	746	985	445	646	1029	738
Ba	378	162	138	179	642	536	328	219	176
*Zn	487	838	591	412	231	55	147	688	408
Cu	187	886	115	295	59	34	1337	198	185

* Relative value represented as a factor of true confidential value.

Table 13

Major and trace element chemistry for rock samples (cont.)

SAMPLE NO.	AES/4/5	AES/26/13	AES/26/14	AES/4/6	AES/26/15	AES/4/7
DESCRIPTION	Granite gneiss, biotite rich	Granite gneiss, Augen	Granite gneiss, biotite rich	Granite gneiss, biotite rich	Granite gneiss	Granite gneiss
Depth above(+) or below(-) lower granite gneiss/ TBQ contact	-0,35m	-1,4m	-4,2m	-5,7m	-9,9m	-14,1m
SiO_2	71,70	73,20	72,10	71,70	74,10	73,50
TiO_2	0,46	0,51	0,49	0,45	0,49	0,41
Al_2O_3	12,30	11,90	12,30	12,10	11,70	12,00
Fe_2O_3	0,06	0,31	0,38	0,03	0,85	0,20
FeO	3,40	3,20	3,35	3,30	2,70	3,00
MnO	0,09	0,03	0,09	0,05	0,05	0,03
MgO	0,30	0,30	0,20	0,30	0,20	0,30
CaO	1,32	1,04	1,32	1,26	1,24	1,52
Na_2O	1,70	2,40	2,00	2,40	2,20	2,70
K_2O	6,83	5,27	5,76	5,15	5,29	4,70
P_2O_5	0,07	0,05	0,07	0,05	0,07	0,05
H_2O-	0,18	0,19	0,20	0,16	0,19	0,18
H_2O+	0,65	0,69	0,90	0,90	0,70	0,63
M.CH	-0,77	-0,61	-1,09	-0,72	-0,51	-0,54
F	1,32	0,94	1,06	1,01	0,29	0,67
S	0,02	< 0,01	0,03	0,01	< 0,01	< 0,01
	100,40	100,03	100,25	98,87	100,07	99,89
O≡F	0,56	0,40	0,45	0,43	0,12	0,28
TOTAL	99,84	99,63	99,80	98,44	99,95	99,61
ppm						
*Sn	11	3	18	10	1	6
*W	2	1	1	1	0	0
Ta	< 20	< 20	< 20	< 20	< 20	< 20
Ce	92	106	116	129	129	44
La	41	44	54	54	73	32
Nb	33	33	30	28	33	38
Zr	405	406	409	410	411	389
Y	85	72	81	75	88	96
Sr	122	63	84	73	77	70
As	16	13	26	11	10	23
Rb	799	266	579	400	274	317
Ba	534	564	527	572	595	481
*Zn	69	30	60	76	7	24
Cu	66	34	79	74	32	19

* Relative value represented as a factor of true confidential value.

Table 13

Major and trace element chemistry for rock samples (cont.)

SAMPLE NO.	AES/4/8	AES/4/9	AES/4/10	AES/4/11	AES/4/12	AES/4/13
DESCRIPTION	Granite gneiss	Granite gneiss	Granite gneiss	Granite gneiss	Granite gneiss	Granite gneiss
Depth above(+) or below(-) lower granite gneiss/ TBQ contact	-20,2	-29,3	-33,6	-40,3	-48,0	-55,2
SiO_2	74,40	71,30	73,60	75,40	74,40	77,00
TiO_2	0,48	0,54	0,50	0,42	0,33	0,35
Al_2O_3	11,60	11,10	12,00	11,70	12,10	11,00
Fe_2O_3	0,49	0,54	0,29	0,09	0,12	0,00
FeO	3,35	4,05	2,90	2,70	2,20	2,40
MnO	0,07	0,07	0,07	0,03	0,03	0,05
MgO	0,20	0,30	0,30	0,20	0,20	0,20
CaO	1,13	1,41	1,28	1,14	0,87	0,90
Na_2O	2,50	2,00	2,50	2,80	2,70	2,40
K_2O	4,73	5,61	5,00	4,89	5,62	5,17
P_2O_5	0,08	0,07	0,04	0,05	0,03	0,02
H_2O-	0,18	0,15	0,12	0,13	0,07	0,08
H_2O+	0,53	0,65	0,61	0,61	0,29	0,59
M.CH	-0,32	-0,55	-0,42	-0,24	-0,21	-0,34
F	0,37	0,86	0,27	0,25	0,25	0,19
S	<0,01	0,08	<0,01	<0,01	<0,01	<0,01
	100,11	98,73	99,48	100,41	99,21	100,33
O≡F	0,16	0,36	0,11	0,11	0,11	0,08
TOTAL	99,95	98,37	99,37	100,30	99,10	100,25
ppm						
*Sn	5	3	1	1	1	0
*W	0	1	0	0	0	0
Ta	<20	<20	<20	<20	<20	<20
Ce	133	179	174	176	120	123
La	56	83	82	72	53	62
Nb	35	29	29	26	27	21
Zr	432	504	427	380	291	336
Y	82	74	74	81	76	76
Sr	78	71	70	69	64	57
As	24	6	7	7	5	5
Rb	320	466	234	220	260	244
Ba	520	563	552	460	461	418
*Zn	13	66	6	7	5	5
Cu	1	51	18	30	11	19

* Relative value represented as a factor of true confidential value.

IV. DISCUSSION AND INTERPRETATION

A. The Nature of the Granite Gneiss

1. Trace element correlations

Based on a technique used by Schultz (1977) an attempt has been made to ascertain whether the granite gneiss is derived from sedimentary rocks or from igneous rocks. The technique makes use of the postulation that the interelement correlations for sedimentary rocks differ from those of igneous rocks. Table 14 shows various element pairs and the signs of their correlation coefficients for the igneous and sedimentary systems investigated by Schultz (1977). The results of the correlation studies of element pairs for the Renosterkop granite gneiss and the TBQ are also included in this table. Scores based on the similarity of the signs of correlation coefficients are given for each of the rocks. The Zr - Ti and Zr - Rb correlations are ignored because they are the same for both igneous and sedimentary systems. The graphical plots of the Renosterkop data are given in Appendix IV.

Table 14

Signs of interelement correlation coefficients for sedimentary and igneous systems after Schultz (1977) compared to the granite gneiss and TBQ from the Renosterkop deposit

	SYSTEMS		RENOSTERKOP	
Element pair	Igneous	Sedimentary	Granite gneiss	TBQ
Ti-K	-	+	0	+
Al-K	-	+	+	-
Mg-K	-	+	0	+
Ti-Rb	-	+	+	-
Zr-Ti	+	+	+	+
Zr-K	-	+	0	+
Zr-Rb	+	+	0	0
Rb-Sr	-	0	+	0
Ca-K	-	0	0	-
K-Si	+	0	-	0
Rb-Si	+	0	-	0
Score	I S 9 0	I S 0 9	I S 0 3	I S 3 6

LEGEND
- = negative correlation
+ = positive correlation
0 = undefined correlation
I = igneous
S = sedimentary
Score = sum of signs the signs that correspond to the igneous or sedimentary system excluding Zr - Ti and Zr - Rb.

From these results it may be seen that the granite gneiss at Renosterkop shows a weak tendency towards the sedimentary system. This method is however felt to be unreliable and inconclusive largely because of the inherent variability of rock systems from one locality to the other. Less variation in trace element chemistry could be expected in the sedimentary enviroment because the global factors controlling sedimentation tend to be similar in most sedimentary systems. This same argument cannot be put forward for the igneous system. Furthermore, the validity of using the chemistry of these metamorphosed and altered rocks in correlations of this nature must be questioned.

2. De la Roche classification

Figure 31 shows a chemical classification diagram of rocks by De la Roche (1980) on which the Renosterkop granite gneiss is seen to plot in the granite field. The values used in this diagram are listed with the Niggli values and norm in Appendix V.

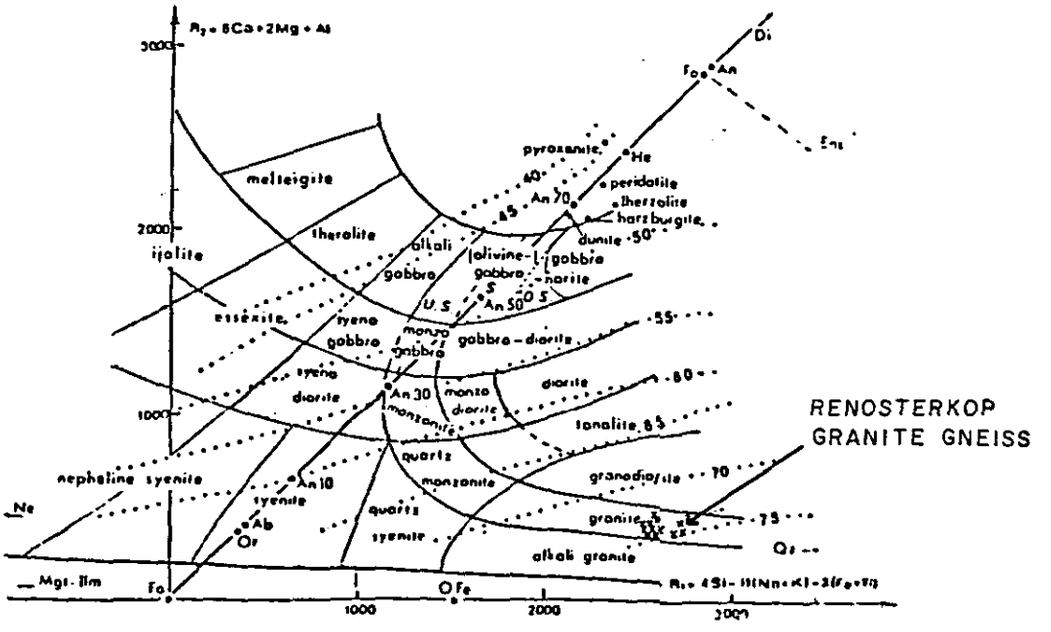

Figure 31: De la Roche diagram showing the Renosterkop granite gneiss plotting as a "granite". (After De la Roche et.al.,1980).

3. Qz - Ab - Or variation diagrams

Graphical plots of the normative residua values of the granite gneiss, derived from the Niggli norms in Appendix V, are shown on the Qz - Ab - Or diagram in Figure 32.

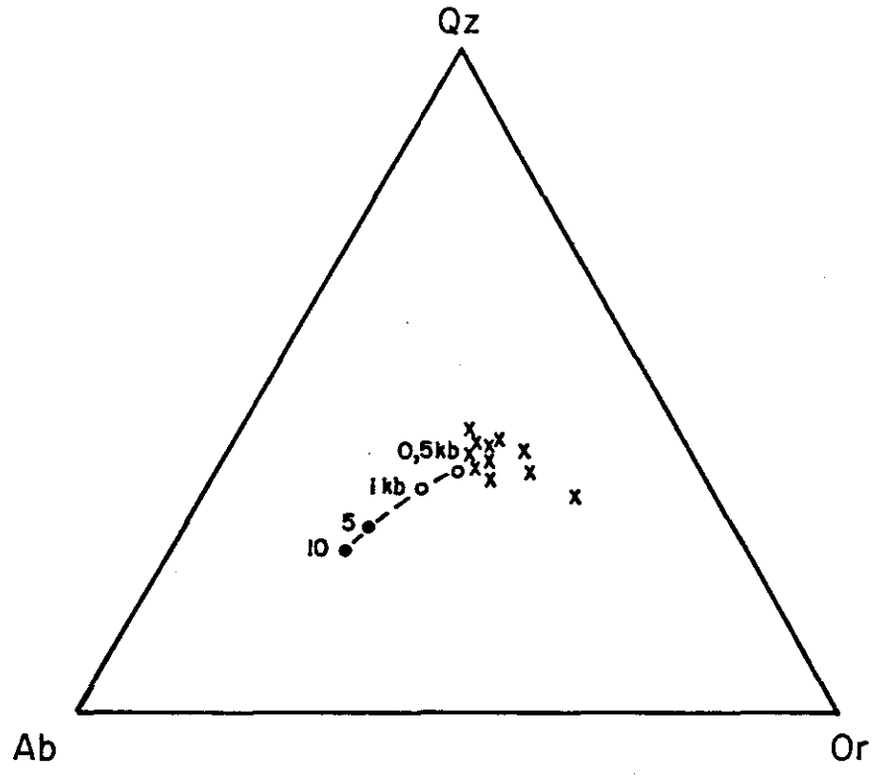

Figure 32: Residua plot of the granite gneiss at Renosterkop.

The granite gneiss clusters close to the 0,5Kb position of the minimum melt composition. Recent experimental studies carried out by Manning and Pichavant (1983) have shown that F, in addition to water, may have a pronounced effect on phase relationships in the hydrous, silica- saturated residua system, Qz - Ab - Or. The presence of both water and F causes a marked reduction in solidus temperature at 1Kb, i.e. from 715°C (water alone) to less than 550°C with 4 % F in the charge. This is clearly illustrated in Figure 33 and the results suggest that (a) F- bearing rocks may begin to melt at lower temperatures than similar F- free rocks, and (b) that enrichment in F by fluid - rock interaction may allow melting to take place at lower temperatures than would otherwise be possible.

The fact that the granite gneiss at Renosterkop clusters around the 0,5Kb position would imply that neither F nor pH_2O played a particularly important role in decreasing the minimum melt composition of the granite gneiss precursor at the time of formation. The system most likely crystallized under dry conditions.

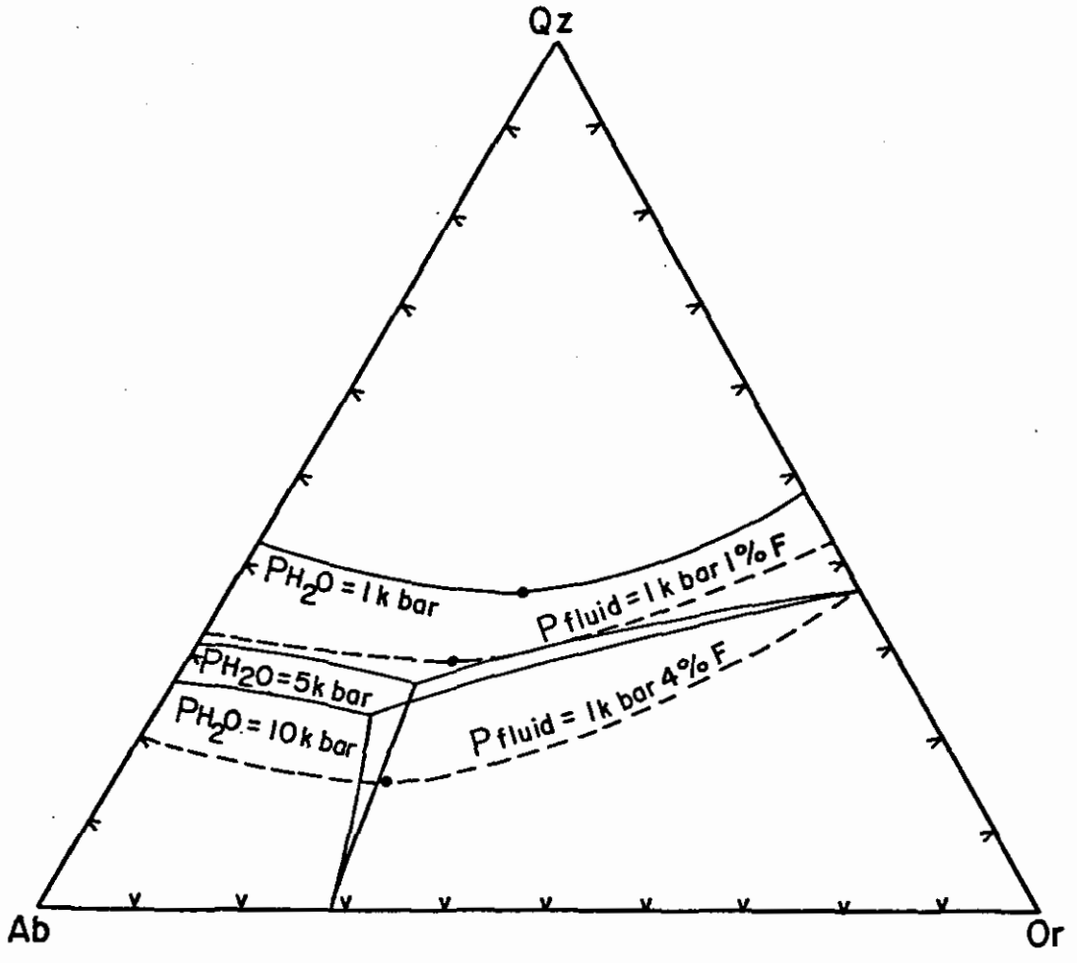

Figure 33: The dependence of the position of the quartz- alkali- feldspar field boundary on PH_2O and F concentration (After Manning and Pichavant, 1983).

4. Trace element ratio's

Plots of the incompatible trace elements of the granite gneiss illustrated (Figure 34) on diagrams Rb Vs (Y + Nb) and Nb Vs Y (Pearce, 1984) show the granite gneiss to fall into the category of a "within plate" granite.

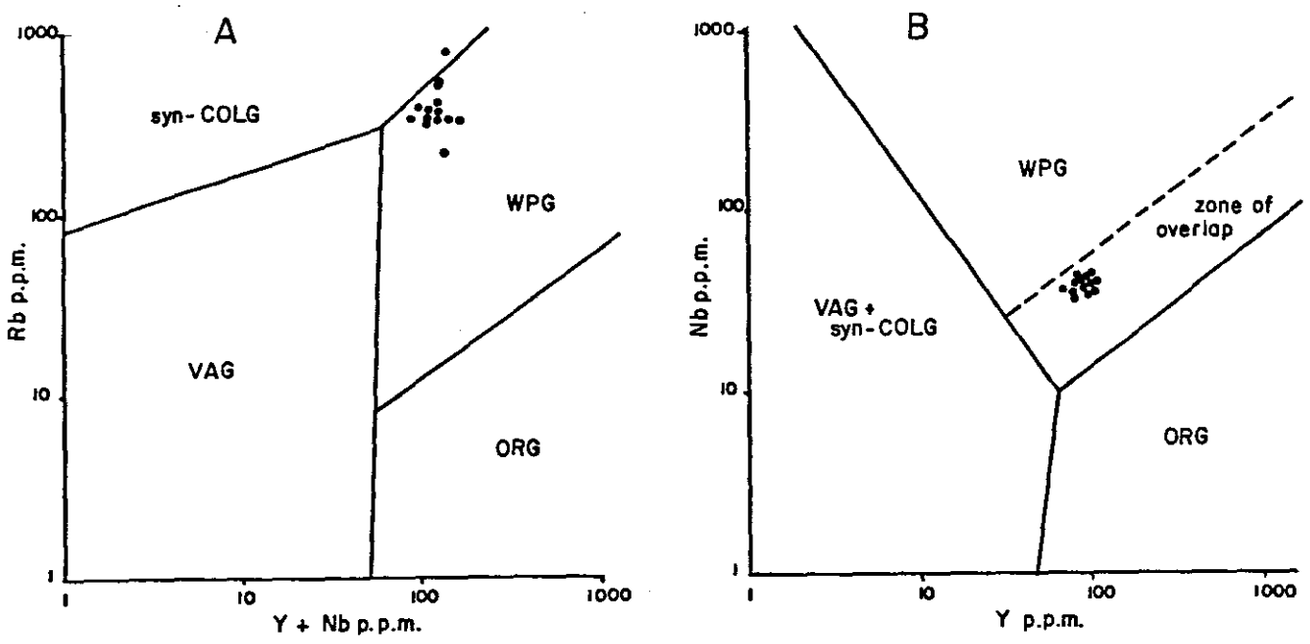

Figure 34: Plots of incompatible trace elements of the granite gneiss.
WPG : Within plate granite
ORG : Ocean ridge granite
VAG : Volcanic arc granite
syn- COLG : Syn- collision granite
(After Pearce,J.A.,et. al, 1984).

Furthermore, comparison of normalised element ratio's as in Figure 35 show the Renosterkop granite gneiss to be comparable to "within plate" granite over an attenuated continental lithosphere. However, it must again be noted that the metamorphosed and altered nature of these rocks renders most plots of this nature questionable.

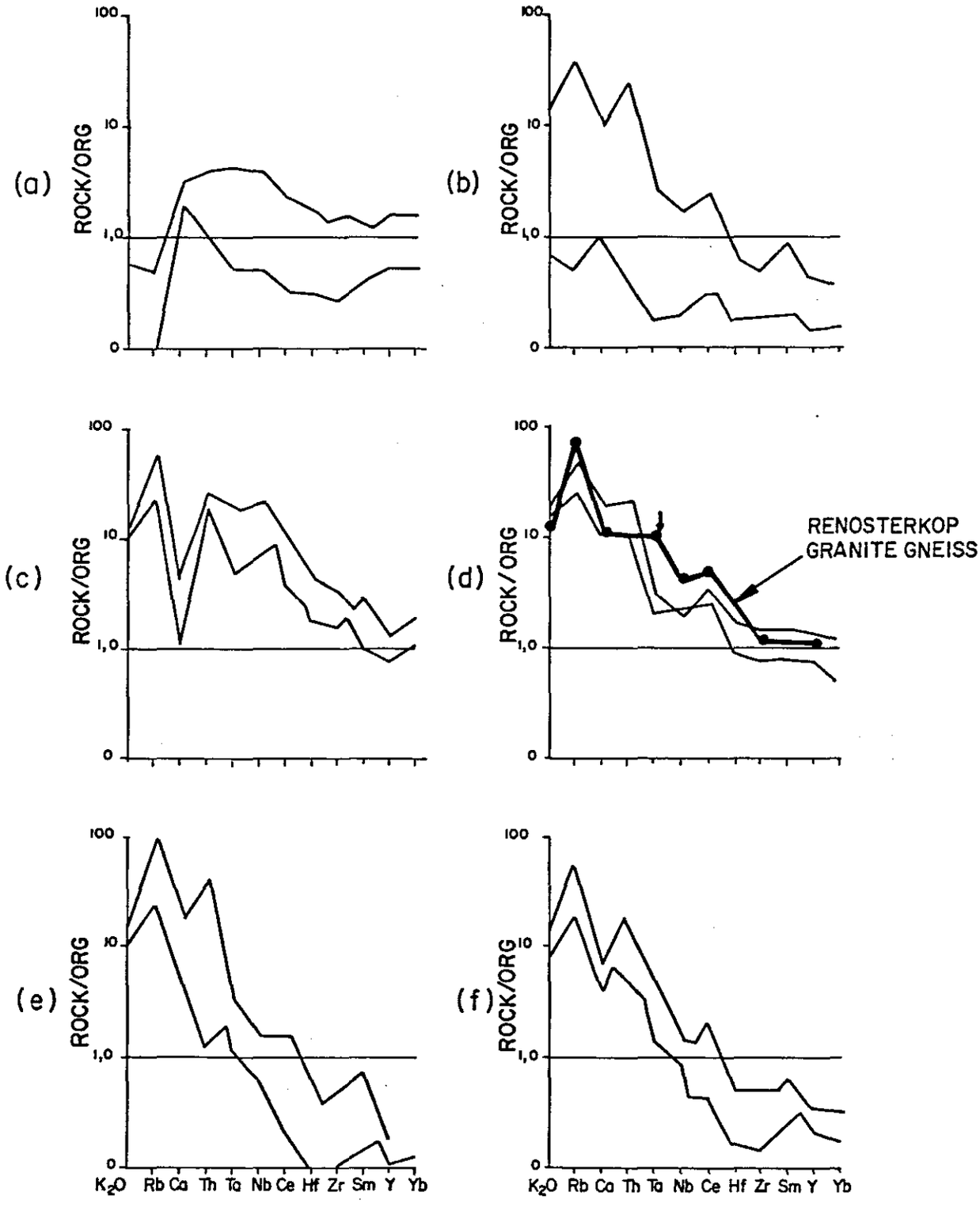

Figure 35: Normalized geochemical patterns for representative analyses of ocean ridge granites (ORG) from various tectonic settings and sub - settings (Pearce,J.A.,et.al.,1984). (a) Ocean ridge granites, (b) volcanic arc granites, (c) within plate granites, (d) within plate granites (attenuated continental lithosphere) (e) syn- collision granites, (f) post- collision granites.

5. Aluminium saturation

From the Niggli values (Appendix V) the granite gneiss can be shown to be metaluminous rather than peraluminous (Shand, 1927), and the average al/(c + alk) value for the granite gneiss is calculated to be 0,998. This value is acceptable for A- type granites but not so for S- type granites which as a rule have al/(c + alk)>1.0.

6. Comparison with A- type granites in southeastern Australia

Collins et. al (1982) identified two A- type granite suites (Gabo and Mumbulla) in the Lachlan Fold Belt in southeastern Australia and compared them to I- type granites of the Bega Batholith. This comparison is based on average compositions of samples with similar SiO_2 contents, and is illustrated in Table 15 together with an average composition of the granite gneiss from Renosterkop.

Table 15

Average compositions of the granite gneiss from Renosterkop, the Gabo and Mumbulla A- type granites and of I- type granites of the Bega Batholith (adapted from Collins,et.al.,1982).

%	Granite gneiss from Renosterkop	Mumbulla A-type	Bega I-type	Gabo A-type	Bega I-type
SiO_2	74,63	77,21	76,03	73,04	72,50
TiO_2	0,43	0,13	0,11	0,37	0,31
Al_2O_3	11,73	11,79	12,64	12,62	13,63
Fe_2O_3	0,29	0,36	0,46	1,63	0,70
FeO	2,75	0,85	0,70	1,51	1,65
MnO	0,05	0,03	0,03	0,08	0,06
MgO	0,23	0,04	0,24	0,33	0,72
CaO	1,15	0,39	0,80	0,96	2,32
Na_2O	2,54	3,08	3,43	3,70	3,09
K_2O	5,06	5,00	4,46	4,11	3,67
P_2O_5	0,05	0,02	0,02	0,08	0,08
ppm					
Ba	498	575	331	767	577
Rb	267	242	212	167	160
Sr	71	43	67	148	165
Pb	-	37	24	28	19
Th	-	26	25	21	20
U	-	6	6	5	4
Zr	381	170	95	490	147
Nb	30	19	11	25	9
Y	82	90	46	83	29
La	61	64	30	62	33
Ce	128	150	68	153	71
Sc	-	16	6	17	9
V	-	2	6	6	30
Cu	19	9	2	4	3
Zn	>100	122	20	133	37
Ga	-	20	14	21	15

A- type granites which are alkaline, anorogenic, anhydrous and metaluminous granites (Collins,et.al.,1982) are chemically distinguished from I- type granites with similar SiO_2 contents by higher abundances of large highly charged cations such as Nb, Ga, Zr, Y and the REE, and lower Al, Mg and Ca. Total FeO and $Na_2O + K_2O$ are also generally higher.

As may be seen from Table 15 the granite gneiss at Renosterkop complies with many of the proposed requirements for that of an A- type granite and is more similar in composition to the Gabo A- type granite than to the other granite types reported here.

7. Comparison with the Bobbejaankop granite at Zaaiplaats Tin Mine

Coetzee (1984) carried out a geochemical and petrographical investigation of the Bobbejaankop granite at the Zaaiplaats Tin Mine and by basing his classification on the work of Collins (1982) concluded that the Bobbejaankop granite can be classified as an A- type granite. Table 16 lists the average composition of the granite gneiss at Renosterkop as well as that of the mineralised (Sn) and unmineralized Bobbejaankop Granite. Except for small differences, these two granites are very similar to each other. Kent (1980) gives the radiometric ages of the pretectonic rock units of the Namaqualand Metamorphic Complex to vary between 1350 and 2000 Ma, and those of the syntectonic rock units to vary between 1100 and 1900 Ma. The Bobbejaankop granite is dated at 1920 ± 40 Ma.

Table 16

Average composition of the granite gneiss from Renosterkop, and the unmineralized and mineralized Bobbejaankop granite (adapted from Coetzee, 1984).

%	Granite gneiss from Renosterkop	Unmineralized Bobbejaankop granite	Mineralized Bobbejaankop granite
SiO_2	74,63	74,92	74,89
TiO_2	0,43	0,08	0,08
Al_2O_3	11,73	11,27	11,29
Fe_2O_3	0,29	1,58	1,58
FeO	2,75	-	-
MnO	0,05	0,03	0,04
MgO	0,23	0,13	0,14
CaO	1,15	0,88	0,99
Na_2O	2,54	2,91	3,17
K_2O	5,06	5,21	5,04
P_2O_5	0,05	0,01	0,02
S	<0,01	0,02	0,03
ppm			
Ba	498	180	178
Rb	267	443	419
Sr	71	14	14
Th	-	44	43
U	-	12	11
Zr	381	285	278
Nb	30	35	32
Y	82	158	162
Cu	19	39	58
Zn	>100	65	88
Sn	30	14	267
W	2	7	24
F	327	3674	4600

8. Comparison with an S- type granite

The granite gneiss at Renosterkop differs from S- type granites (Chappell, et.al., 1974) in that the latter are characteristically peraluminous, have a lower SiO_2 content (65 - 76 %), contain ilmenite in place of magnetite, and are furthermore characterized by the presence of muscovite, monazite, cordierite and garnet as opposed to hornblende and sphene in I- and A- type granites. A further distinguishing feature is that S- type granites commonly contain white feldspar, whereas in I-type granites pink feldspar is common and A- type granites are characteristically perthitic.

9. Conclusion

It is concluded from the abovementioned information that although the rocks are not in their pristine state, the chemistry of the granite gneiss is generally more typical that of the A- type rather than the I- or S-type granite. This finding is contradictory to a possible formation of the granite gneiss by granitization of pre-existing sedimentary rocks.

B. Nature of the TBQ and its Relationship to the Granite Gneiss

1. General hypothesis

In the descriptive section (Chapter III) of this treatise a large amount of information has been compiled which tends to support the general hypothesis that the TBQ bodies are in fact the result of the metasomatism of the granite gneiss country rock through a medium of mineralized HF-rich fluids. These metasomatizing fluids followed a pre-existing zone of fracturing, permeated the walls of the conduits, and gave rise to Al-, Ca- and F- fixation and alkali- solution, as implicitly supported by the diagrams contained in Appendix III, and more explicitly by the following three sets of evidence.

2. The topaz - feldspar antipathy

From the petrography it is evident that there is a very quantitative antipathetic relationship between topaz and feldspar be shown in thin section under the microscope that the K broken down by reaction to topaz, quartz and minor fl

9. Conclusion

It is concluded from the abovementioned information that although the rocks are not in their pristine state, the chemistry of the granite gneiss is generally more typical that of the A- type rather than the I- or S-type granite. This finding is contradictory to a possible formation of the granite gneiss by granitization of pre-existing sedimentary rocks.

B. Nature of the TBQ and its Relationship to the Granite Gneiss

1. General hypothesis

In the descriptive section (Chapter III) of this treatise a large amount of information has been compiled which tends to support the general hypothesis that the TBQ bodies are in fact the result of the metasomatism of the granite gneiss country rock through a medium of mineralized HF-rich fluids. These metasomatizing fluids followed a pre-existing zone of fracturing, permeated the walls of the conduits, and gave rise to Al-, Ca- and F- fixation and alkali- solution, as implicitly supported by the diagrams contained in Appendix III, and more explicitly by the following three sets of evidence.

2. The topaz - feldspar antipathy

From the petrography it is evident that there is a very definite quantitative antipathetic relationship between topaz and feldspar. It can be shown in thin section under the microscope that the K- feldspar is broken down by reaction to topaz, quartz and minor fluorite. This is

especially visible on the contact zones between typical TBQ and granite gneiss, and clearly suggests the following HF- consuming reactions:

$2KAlSi_3O_8 + 2HF = Al_2SiO_4F_2 + 5SiO_2 + 2KOH^*$ ----------(1)
microcline topaz + quartz

$2NaAlSi_3O_8 + 2HF = Al_2SiO_4F_2 + 5SiO_2 + 2NaOH^*$ ----------(2)
albite

$CaAl_2Si_2O_8 + 4HF = CaF_2 + Al_2SiO_4F_2 + SiO_2 + 2H_2O^*$ ----------(3)
anorthite fluorite

*(removed in solution)

All of these reactions are in essence acid- base reactions. It is logical that a high activity of HF will drive such reactions to the right, and that as long as a flux of HF is maintained, the feldspar will continuously be destroyed up to the point where it disappears from the mode. Concurrently topaz, fluorite and quartz will precipitate and the alkali will be removed in solution. The antipathetic relationship between topaz and feldspar, in general, and microline, being the major feldspar, in particular, is a manifestation of the degree to which a high HF- flux could be maintained along a concentration gradient outward from the conduits for the HF- rich fluids.

3. The chlorite- bearing granite gneiss

The intermediate zone of chlorite- bearing rock between the biotite-bearing granite gneiss and the TBQ rock has two main characteristics, ie. (i) the original biotite in the granite gneiss has broken down by reaction to chlorite and rutile, and (ii) neoformed K- feldspar has in part replaced the chlorite, implying that when these reactions took place, K-feldspar was a stable mineral signifying high temperatures or low pH_2O or both.

The reason for the breakdown and restabilization of the biotite in the advancing transition zone may be explained by comparing the following formulae obtained from the analyses in Table 7 and 8.

(i) biotite in granite gneiss:

$K_{1,8}Fe_{4,1}Mg_{0,8}Ti_{0,47}Al_{0,65}(Al_{2,25}Si_{5,75})O_{20}(OH)_4$

(ii) chlorite in granite gneiss:

$Fe_{7,8}Mg_{1,1}Al_{2,7}(Al_{2,4}Si_{5,5})O_{20}(OH)_{16}$

(iii) biotite in TBQ

$K_{1,9}Fe_3Mg_{0,27}Ti_{0,17}Al_{2,5}(Al_{1,4}Si_{6,6})O_{20}(OH)_4$

It is obvious that the biotite in the granite gneiss has higher Ti, Fe, Mg and lower Al^{vi} values than the biotite in the TBQ. The chlorite may be seen to have high Al^{vi} values as well as high Fe and no K. It could therefore be argued that if the fluid in the conduits was basically water-poor, the activity gradient of water may have lagged behind that of HF away from the conduits. In this way a relatively dry zone is created, away from the main fluid conduits, so that K- feldspar was stabilised in these regions. Because the Al / Si ratio in K- feldspar is lower than that in the biotite of the granite gneiss, an Al- rich chlorite was initially produced as a complimentary by-product to the K- feldspar. As the reaction front was propagated and pHF and pH_2O increased, the high Al- chlorite was again replaced by biotite when K- feldspar became unstable and yielded to topaz, as described in the previous section.

4. The chemical connection

Probably the strongest indicator of the inherent connection between the granite gneiss and the TBQ comes from the major and trace element chemistry of the rocks. The technique which will be used to study this connection was advanced by Pearce (1968), who since then has applied it amongst others to the Dundonald Sill (1969) and the Palisade Sill (1970). Pearce (1968) has shown that by dividing two variables by a third parameter does not change the slope of the relationship between them if the third parameter is an inert component.

This is better illustrated by means of an example:

Assume we have a four component geological system A,B,C and D with concentrations 10,40,20 and 30 percent respectively. If we now remove one of the components, say D, then in absolute terms A,B and C increase from 10, 40 and 20 percent to 14,3, 57,1 and 28,6 percent respectively. This is illustrated below.

Component	Concentration		New Concentration
A	10	Geological process ——————> removes D	14,3
B	40		57,1
C	20		28,6
D	30		0

A comparison of the original with the new concentration does not give a true picture of the process, because in actual fact the only thing that happened was that D was removed from the system, and no addition was made to any of the other three components as it may appear from a direct comparison. To assess the process itself we need to find an inert component that did not participate in the process reaction. Say by inductive reasoning we can prove A to be such a component. Using the concentration of A as a divisor we can change all the concentrations to ratios.

Component ratios	Concentration		New Concentration ratios
A	1	Geological process ——————> removes D	1
B	4		4
C	2		2
D	3		0

Looking at the new ratios after the removal of D we now clearly see that A,B and C remained constant, ie. they did not participate in the process reaction, but only D decreased from 3 to 0, as indeed happened in the process.

For the purpose of this study Al_2O_3 was chosen as an inert component. This is based on the strong antipathetic relationship that exists between

potassium feldspar and topaz, and on the premise that in the high HF-environment, any Al contained in the original granite system and resulting from the breakdown of potassium feldspar, will be directly precipitated as topaz. This means that Al_2O_3 is not really participating in the reaction between the fluids and the granite gneiss. Much the same reasoning can be advanced for Ca which would precipitate as CaF_2 with an increase in HF. The reason for choosing Al_2O_3 above CaO may be illustrated by comparing Figures 36 (a) and (b). Less scatter may be seen where Al_2O_3 is used as a divisor than when CaO is used as a divisor. The basic reason is not only the closure effect due to the preponderance of Al_2O_3 over CaO, but also one can expect that the Al_2O_3 determinations, owing to the larger concentrations are more accurate than those for CaO. Two obvious outliers are present and such outliers merit special treatment in the discussion of these Pearce diagrams.

In Appendix VI, Pearce diagrams for all the major and trace element analyses using Al_2O_3 as a divisor are given. All values are plotted against relative depth, with the datum line representing the approximate granite gneiss - TBQ contact. Prominent outliers have been numbered for comparison and discussion. The following observations may be made from these diagrams:

(i) SiO_2 has a slight negative slope in the granite gneiss and transitional zone, but decreases more pronouncedly from the granite gneiss into the TBQ.

(ii) The outlier 26.11 is characterised by enrichment in SiO_2, TiO_2, total FeO, MnO, MgO, CaO, S, F as well as most of the trace elements, but is not enriched in either Sn, W or Zn. This phenomenon could be ascribed to either an analytical error or a late- stage metasomatic event. The outlier 26.4 is enriched in F, Sn and Sr, most probably due to a late-stage metasomatic event. Other outliers are seen enriched in certain REE, but never consistently throughout. This feature could probably be explained by a multiphase intrusion of metasomatic fluids.

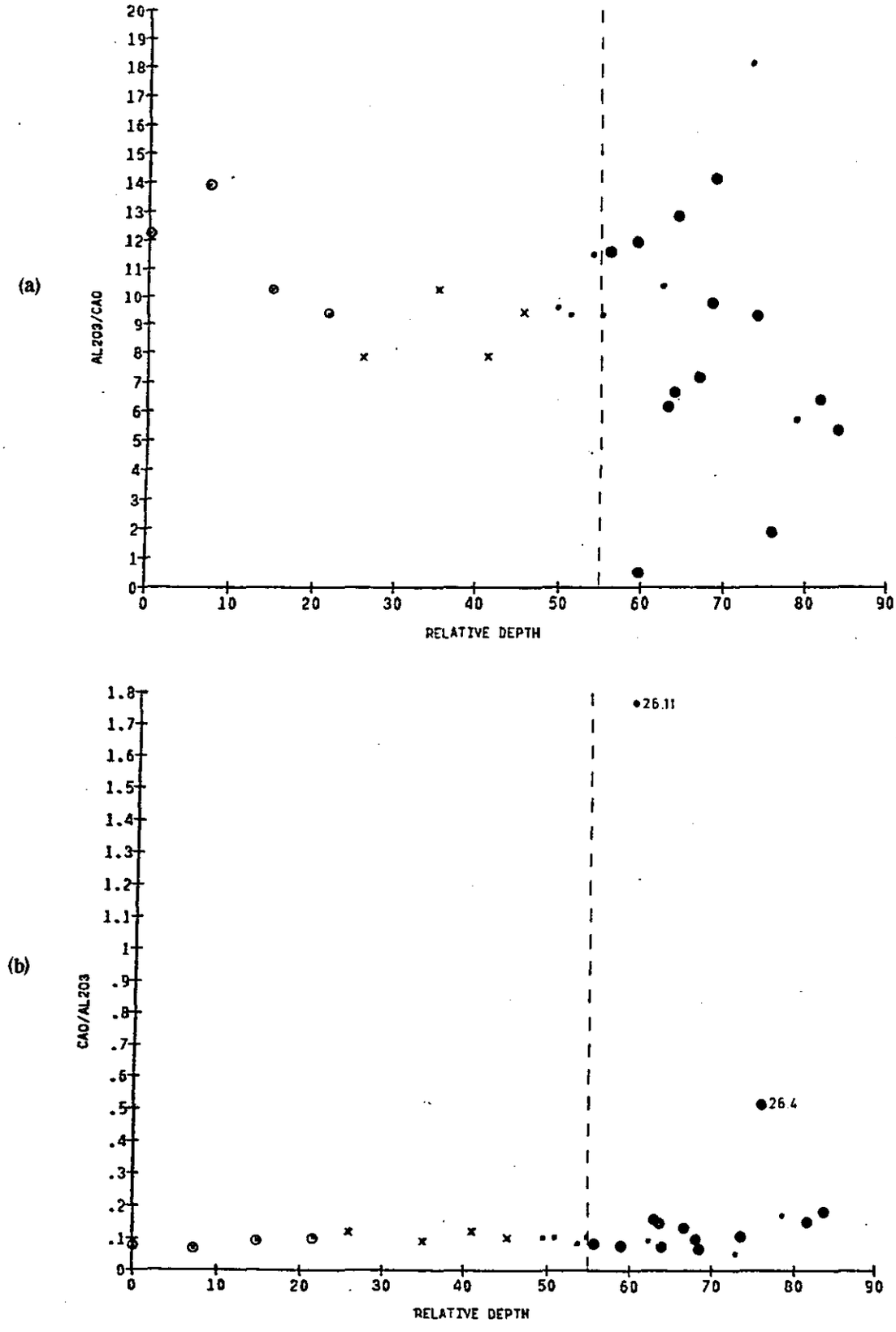

Figure 36: (a) CaO/Al_2O_3 Vs relative depth (m)
(b) Al_2O_3/CaO Vs relative depth (m)
⊗ Hornblende- bearing granite gneiss
× Biotite- bearing granite gneiss
• Transition zone and granitic gneiss lenses
● TBQ

(iii) TiO_2 increases in the hornblende- bearing granite gneiss towards the biotite- bearing granite gneiss. It then decreases towards the transition zone from where it follows a random to weakly decreasing trend in the TBQ.

(iv) FeO follows a similar trend to that displayed by TiO_2.

(v) Fe_2O_3 has a tendency to increase moderately towards the TBQ, and in broad terms is also similar to TiO_2.

(vi) MnO shows a remarkably linear enrichment in the TBQ, decreasing sharply in intensity further away from the lower granite gneiss - TBQ contact. The two additional outliers 4.1 and 4.3 may be ascribed to a possible late stage metasomatic event, but are not consistently enriched in other elements as would be expected in late stage metasomatic enrichment. Whatever factor is responsible for the decreasing linear trend in MnO away from the lower granite gneiss - TBQ contact is probably also responsible for the two outliers 4.1 and 4.3.

(vii) MgO shows a roughly linear trend with no significant slope in the granite gneiss, but is randomly distributed throughout the TBQ.

(viii) CaO shows a smooth linear trend throughout both the granite gneiss and the TBQ (Figure 36a, not repeated in Appendix VI). The outlier 26.4 shows chemical and mineralogical properties similar to, but less pronounced than that of 26.11

(ix) Na_2O and K_2O decrease sharply in the TBQ which is a typical phenomenon observed in the formation of greisens and tallies with the proposed reactions. The outlier 26.9 observed on the K_2O graph is related to the presence of feldspar in the TBQ.

(x) P_2O_5 is seen to increase gradually from the hornblende- bearing granite gneiss into the biotite- bearing granite gneiss from which it decreases steadily towards the TBQ. It is of interest to note that the outliers 4.4 and 26.7 are associated with anomalous tungsten values. This

would suggest that some of the tungsten mineralization was introduced in one of the later stage metasomatic events.

(xi) H_2O^+ remains relatively consistent throughout while H_2O^- increases across the transition zone.

(xii) F shows a weak gradational increase from the deepest hornblende-bearing granite gneiss through into the furthest TBQ sample. The two outliers are both ascribed to a late- stage metasomatic event which was responsible for the precipitation of CaF_2. Only one of the two outliers is associated with an anomalous tin value, thus indicating that not all of the multiphase metasomatic events were enriched in Sn, W or Zn mineralization, but probably remobilized existing mineralization, and concentrated it in F- rich alteration zones in the TBQ.

(xiii) S is present in noteworthy amounts only in the TBQ.

(xiv) Sn, W and Zn mineralization are all enriched only in the TBQ. No other relationship is seen between these three elements, although a weak pattern may be observed between Sn and Zn mineralization.

(xv) Ce, La and Zr show a parabolic pattern similar to that displayed by TiO_2 and Fe_2O_3. The elements increase from the deepest hornblende-bearing granite gneiss towards the biotite- bearing granite gneiss from where it decreases steadily towards the furthest point of the TBQ. Zr is the only element enriched in a later metasomatic event. The leaching of Zr in the TBQ would explain the rounded and reduced form of the zircon crystals in the TBQ relative to those found in the granite gneiss. The shape of the zircons is apparently the result of partial dissolution under the chemical conditions induced by the HF- rich fluids.

(xvi) Nb shows a weak increasing trend throughout most of the hornblende- and biotite- bearing granite gneiss, but drops across the transition zone and increases once again toward the furthest point of the TBQ body.

(xvii) Y displays a smooth trend throughout the granite gneiss and TBQ.

(xviii) Sr increases weakly throughout the granite gneiss and then decreases fairly sharply from the transition zone to the furthest point of the TBQ body. Four outliers are associated with late- stage metasomatic enrichment also seen in the feldspar- rich TBQ.

(xix) Rb, As and Cu show a marked increase in the TBQ, the latter two related to the introduction of sulphides during the process responsible for the formation of the TBQ.

(xx) Ba remains relatively constant in the granite gneiss, but decreases sharply in the TBQ where it shows a random distribution. Ba is also enriched in a late- stage metasomatic event.

From the above observations it may thus be seen that a definite relationship exists between the granite gneiss and the TBQ. This is clearly indicated by the transitional trend observed from the hornblende-bearing granite gneiss, through the biotite- bearing granite gneiss, across the chlorite zone and into the TBQ. This mineralogical halo surrounding the TBQ, supported by transitional chemistry, is evidence that the TBQ is indeed an alteration product of the granite gneiss.This process of alteration chemically had a very wide sphere of influence in that elemental haloes formed more than 50m away from the central zone of reaction. The inconsistency of the outliers (except for 26.11) would seem to represent overprinting due to numerous localized late stage events in which the reactive fluids differed slightly in composition from one another, and were not necessarily all enriched in Sn, W or Zn. A precise chemical definition of each of these events is not possible with the present data set, and beyond the scope of this study.

C. Reference and Comparison to Similar Rocks in other Parts of the World

Very little literature is available on mineral associations similar to those at Renosterkop. The limited literature encountered will be discussed in

this section, and comparisons will be made to the rocks found at Renosterkop.

1. Mineralization associated with the Mole Granite and the Torrington wolframite- bearing quartz - topaz rock (silexite), Australia

The Mole granite, located in northern New South Wales, Australia, intruded sediments and volcanics of Permian and Carboniferous age. An area of 650 square kilometres of sediments and volcanics has been unroofed leaving a similar area of exposed granite (Figure 37). A prominent roof pendant is present towards the central part of the exposed granite outcrop. The major rocks involved are a porphyritic pressure-quenched roof zone granite which grades inwards into a coarse phaneritic facies with seriate texture. Both varieties are cut by dykes, sills and irregular masses of microgranite. The granite has undergone post-magmatic alteration resulting in the development of K- feldspar megacrysts rimmed by albite (commonly kaolinized), biotite and quartz clots. The three major textural varieties show no systematic chemical difference. They are characterized by high SiO_2, alkalis, Rb, LIL, HREE and Sn and low CaO, Sr and Eu. Table 17 shows representative analyses of varieties of the Mole Granite. A considerable quantity of tin, and lesser tungsten, is found associated with the roof, in veins and in the granite, but much more so in the roof cover (Kleeman,1982). Five episodes of mineralization have been recognized:

(i) sheeted quartz and greisen- bordered veins containing tin and base metals

(ii) complex pegmatite bodies containing cassiterite

(iii) stockwork with quartz veins containing molybdenite, wolframite and bismuth minerals

(iv) quartz - white muscovite - Li biotite - topaz greisen with W, Bi, Mo and Sn minerals, and

(v) quartz - green muscovite - chlorite greisen with Sn- W- Bi- base metal minerals.

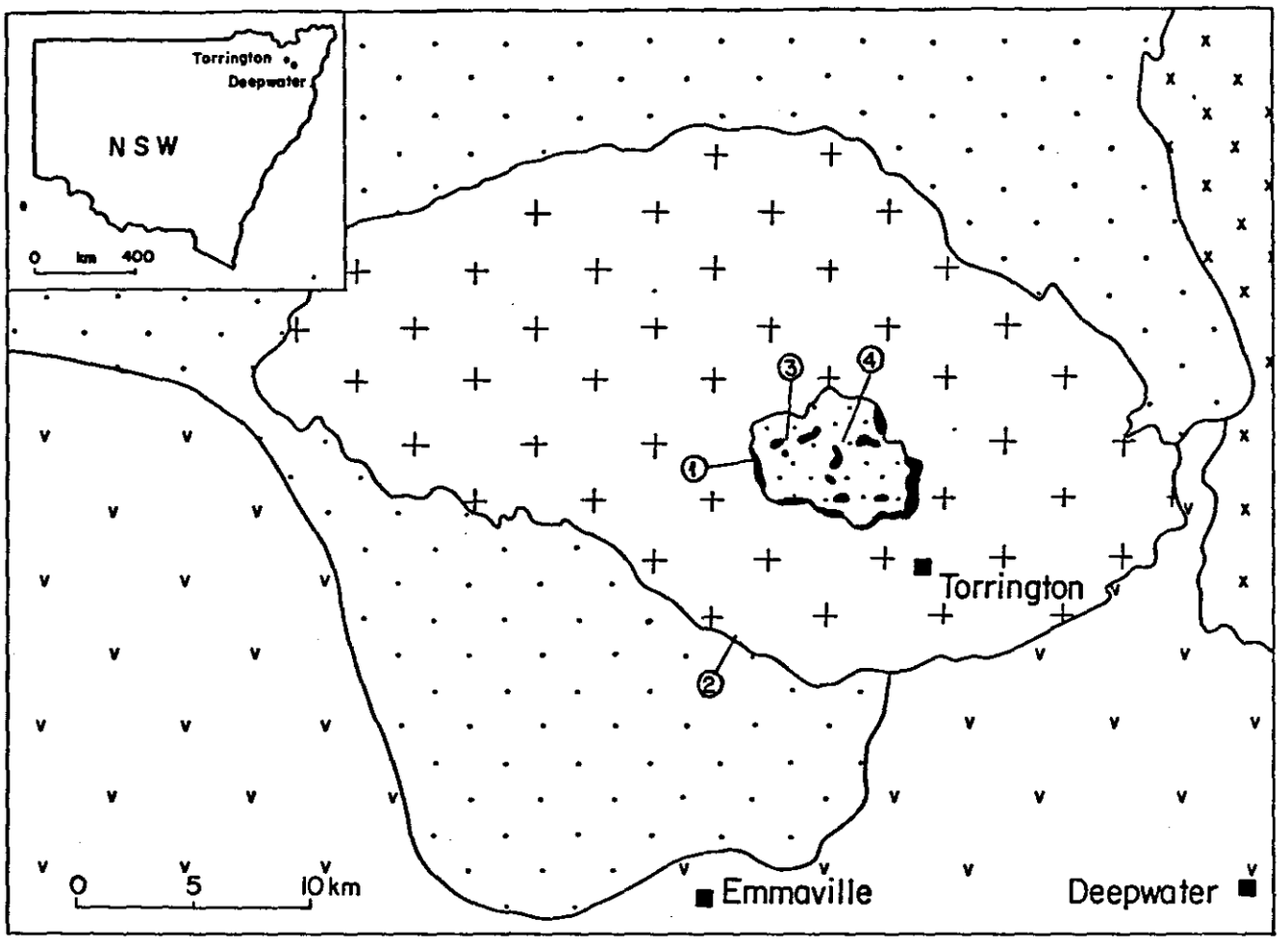

Coarse and porphyritic Mole granite
microgranite
other granites
Permian volcanics
Silexite
Permian and Carboniferous sediments
Coarse silexite
Fine silexite
Biotite-quartz-topaz rock
Biotite-rich selvage
Silicified country rock
Flow layering in microgranite
Layering in silexite
Localities of sections

Sketch sections of silexite:

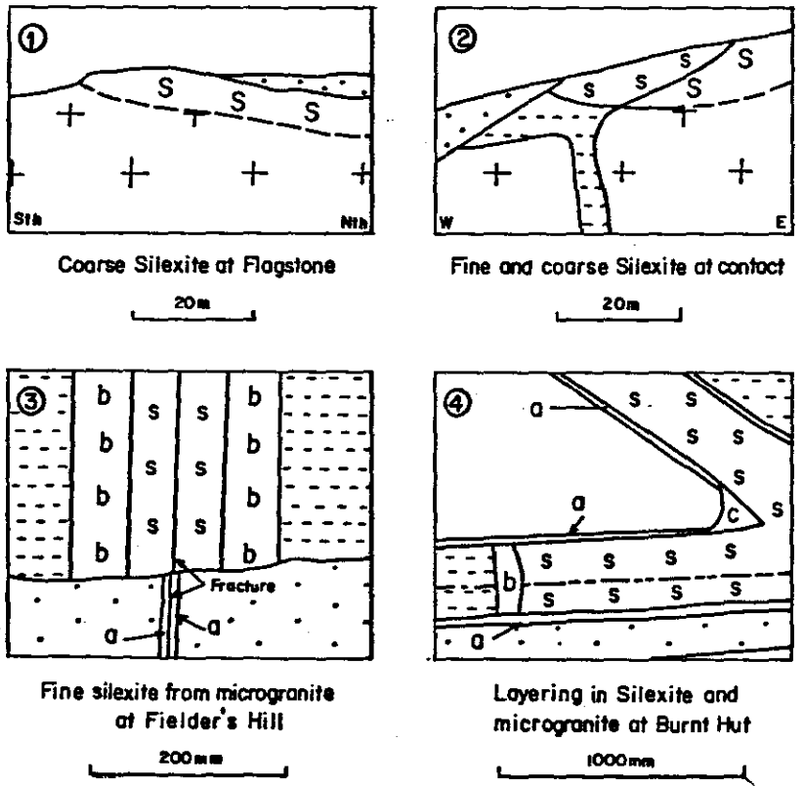

Coarse Silexite at Flagstone

Fine and coarse Silexite at contact

Fine silexite from microgranite at Fielder's Hill

Layering in Silexite and microgranite at Burnt Hut

Figure 37: Geological setting and sketch sections of silexite (After Kleeman, 1982).

Table 17

Representative analyses of varieties of the Mole Granite (Plimer, et. al., 1982)

	PRESSURE-QUENCE VARIETY	SERIATE VARIETY	MICROGRANITE
SiO_2	77,08	77,23	76,55
TiO_2	0,13	0,15	0,11
Al_2O_3	12,39	11,87	12,49
*Fe_2O_3	1,19	1,29	1,04
MnO	0,04	0,04	0,04
MgO	0,15	0,20	0,09
CaO	0,34	0,42	0,32
Na_2O	3,20	3,44	3,49
K_2O	4,67	4,51	5,02
P_2O_5	bld	bld	bld
LOI	0,73	0,66	0,86
TOTAL	99,90	99,75	100,08
Sr	19	22	11
Rb	507	517	638
Y	87	99	77
Pb	34	35	32
Th	34	36	44
Cu	14	297	11
Zn	29	30	23
Ce	74	87	83
Nd	32	38	37
Nb	17	19	20
Li	79	118	90
Ga	20	20	24
Sn	5	9	8
Zr	108	121	89
Ba	90	88	39
La	25	28	27
NORMS			
Q	38,28	37,54	35,11
Or	27,99	27,02	29,95
Ab	28,69	30,95	27,93
An	1,74	2,15	1,62
Cor	1,60	0,58	0,80
En	0,03	0,11	0,14
Fs	1,65	1,01	0,79
Mt	0,06	0,27	0,33
Il	0,26	0,47	0,20
DI	96,26	96,86	96,23

bld = below limit of detection; Fe_2O_3* = total iron as Fe_2O_3

Silexite is the local name for the quartz - topaz rock which is hosted dominantly, but not exclusively, in the sedimentary rocks of the roof pendant (Kleeman, 1982). The other occurrences are near the exposed margin of the granite or close to its roof. In the roof pendant the silexite is dominantly a fine grained rock, resembling quartzite in the field. It is a xenomorphic mixture of quartz and topaz (average 20 to 25 %), with

minor wolframite, zinnwaldite, kaolinite and various other accessory minerals.

The origin of the silexite is regarded as being the result of hydrothermal alteration of granite. Following emplacement of granite, net- vein systems were introduced in the fractured roof. This episode is important in producing significant volumes of tin- mineralized vein systems. A complex pegmatite of orthoclase, biotite, beryl, topaz, fluorite, quartz and muscovite was emplaced next. The microgranite invaded fractures in the solid upper porphyritic carapace of the granite, and in the overlying roof, especially in the roof pendant. Silexite formation postdates microgranite intrusion. Where the hydrothermal alteration is complete, the silexite occupies the intrusive forms of the microgranite, retaining the sharp contacts with only a thin biotite selvage in the country rock. The latter rock is silicified and contains topaz. Sketch sections of silexite are illustrated in Figure 37. Evidence for silexite occurring as an obvious replacement may be seen at Fielders Hill, for example, where low angle dykes in a sedimentary host are traversed by fractures. A fluid passing through the fracture has caused very little alteration in the country rock, just a biotite selvage a few millimetres wide, but there is a vigorous reaction in the microgranite. Symmetrically about the central fracture three zones are present: silexite, a biotite- quartz- topaz rock, then unaltered microgranite. These zones are at least one or two centimetres wide, but occur at all scales. Where large patches of silexite are formed, the shapes become irregular, and the biotite- quartz- topaz rock decreases in volume relative to the silexite.

The nature of the alteration may be described as follows: At an incipient stage, microgranite is first altered by partial replacement of alkali feldspar by quartz and the growth of scattered clots of additional biotite up to two millimetres in diameter. Table 18 shows the chemical composition of this rock. Topaz is present, but its texture is ambiguous, and not definitely magmatic or replacement in origin. This stage passes abruptly into the biotite- quartz- topaz rock, which retains the general texture of the microgranite, but all of the feldspar is replaced by quartz, biotite and topaz. Biotite and topaz each constitute between 10 - 20 % of this rock, which is also represented in Table 18. This rock grades rapidly,

as the process becomes more profound, into a low- biotite transitional silexite (see also Table 18), with only an average of 5 % biotite and up to 20 % or more topaz. Finally complete transformation of silexite results in an almost biotite- free quartz - topaz rock, with typically 20 to 25 % topaz (Table 18).

Table 18

Analyses of microgranite, silexite, and transition rocks (Kleeman, 1982)

	1	2	3	4	5
SiO_2	77,22	75,65	74,85	78,46	80,50
TiO_2	0,05	0,08	0,08	0,04	0,07
Al_2O_3	12,20	13,78	12,42	15,45	14,68
*Fe_2O_3	1,10	1,13	5,76	1,52	0,21
MnO	0,02	0,05	0,11	0,06	0,05
MgO	0,04	0,03	0,15	0,23	0,03
CaO	0,45	0,24	0,81	0,06	0,10
Na_2O	3,44	2,91	0,05	0,03	0,02
K_2O	4,68	4,88	1,94	0,74	0,15
P_2O_5	0,01	0,00	0,00	0,00	0,00
H_2O	0,69	0,57	1,69	1,31	1,51
F	0,12	0,46	2,96	3,47	3,48
Less O-F	0,05	0,19	1,24	1,46	1,46
TOTAL	99,97	99,59	99,84	99,91	99,34
Ga	23	27	39	10	1
Rb	566	910	898	288	30
Sr	4	14	0	0	0
Y	101	116	145	187	111
Zr	99	59	43	62	32
Nb	19	18	32	13	31
Ba	65	67	48	33	8
La	33	30	51	34	25
Ce	88	73	126	100	93
Nd	47	38	62	55	42
Th	43	27	88	92	112

1.Unaltered microgranite. 2.Incipiently altered microgranite. 3.Biotite-quartz-topaz rock. 4.Low biotite transitional silexite. 5.Silexite.

* Total Fe.

Total transformation to silexite results in almost complete removal of Ca, Na, K, Ga, Rb and Sr, and notable depletion of Fe and Ba. These are balanced by minor increases in Si and Al, and substantial increases in F and OH as well as Th. All of these chemical changes are consistent with the mineralogical changes.

(a). Discussion and comparison to Renosterkop

Renosterkop is the only tin occurrence known in the granite gneiss country rock in the area. Owing to the obvious intense structural deformation of the granite gneiss no roof zone has been identified and the only textural variation is the presence of an Augen gneiss in places. Pegmatites are common, but are not found in the TBQ.

Chemically the granite gneiss at Renosterkop differs from the Mole Granite (see Tables 13 and 17) in that it has a higher total FeO, CaO, Sr, Zn, Ce, Zr and Ba content, and a lower Rb content.

At Torrington, transformation to silexite results in almost complete removal of Ca, Na, K, Ga, Rb and Sr, and notable depletion of Fe and Ba. These are balanced by minor increases in Si and Al, and substantial increases in F and OH as well as Th. On the other hand, the transformation at Renosterkop from granite gneiss to TBQ is characterized by no noteworthy change in Ca, Al or total FeO, an increase in Rb, and a decrease in Na, K, Si, Sr, and Ba. An increase in F is however consistent.

Mineralization at Renosterkop is found associated with only one rock type exposed to various degrees of alteration and differs from the five episodes of mineralization identified in the Mole Granite.

The difference in mode of occurrence and chemistry between the two deposits leads to the conclusion that the only common feature between the deposits is the mineral assemblage biotite - quartz - topaz and the presence of Sn and WO_3 in both.

2. Quartz- topaz- loellingite rocks near Eldorado, Victoria

Two dykes consisting of a quartz- topaz loellingite rock type have recently been discovered within the aplitic phase of the Pilot Range granite pluton near Eldorado, in NE Victoria (Birch,1984). Minor biotite, muscovite, chlorite, kaolinite, anatase and pharmacosiderite are associated. Apart from the loellingite, the dykes are similar mineralogically to the "topazites" from New England, NSW. The northern-most dyke is approximately 200m long and 2,5 - 3,0 m wide. The southern dyke is approximately 170 m long and 6 m wide. The dykes have been termed "topazites" and at both localities the immediate country rock is a pink porphyritic granite with an aplitic or microgranitic groundmass. The contact between the topazite and the porphyritic microgranite is sharp rather than gradational. No mention is made of mineralization in the topazites by the author of the paper, but he does record that small occurrences of tin, tungsten and molybdenum mineralization may be found in the granite rocks of the region.

(a). Mineralogy of the topazites

The modal abundances of the minerals present in the topazite is given as follows (Birch, 1984):

Quartz	80 - 90 %
Topaz	10 - 15 %
Loellingite	5 %
Micas	> 5 %

For the purpose of this study only the mineralogy of the micas will be discussed.

Micas

Micas are not generally conspicuous in the Eldorado topazites, but mineralogical banding resulting from concentrations of biotite may be seen in some specimens. Microprobe analyses of the biotite from these rocks, listed in Table 19, are comparable to the biotite found at Renosterkop (Table 7).

Table 19

Microprobe analyses of biotite in the Eldorado topazite dykes (Birch,1984)

	1	2	3
SiO_2	45,76	35,53	35,22
TiO_2	0,46	3,01	2,74
Al_2O_3	20,93	20,56	20,83
FeO	8,04	23,72	25,55
MnO	0,15	0,49	0,55
MgO	6,73	3,20	1,49
Na_2O	0,23	0,24	0,25
K_2O	10,83	9,94	9,37
F	4,41	1,75	1,53
H_2Ocalc	2,08	3,08	3,10
O≡F	2,06	0,74	0,64
TOTAL	97,56	100,78	99,23

Structural formulae based on 25(O) and 4(OH,F)

Si	6,570	5,446	5,514
Al	1,430	2,554	2,486
Al	2,112	1,159	1,358
Ti	0,049	0,347	0,323
Fe	0,965	3,042	3,346
Mn	0,018	0,063	0,073
Mg	1,441	0,731	0,347
Na	0,065	0,074	0,076
K	1,985	1,990	1,872
F	2,004	0,850	0,756
OH	1,994	3,150	3,243

SAMPLES

1. Biotite,Silver Mine topazite
2. Biotite, Weinerts topazite
3. Biotite, Byawatha aplite, Weinerts

(b). Paragenesis of the topazites

According to Birch (1984), the formation of the topazites probably involved both magmatic and hydrothermal components. The topazite melt itself appears likely to have been derived by extreme fractionation of the granitic magma forming the Pilot Range pluton. This fractionation may pass through an intermediate stage with the formation of melts rich in Si, Al , Na, K and F. Continued crystallization and increasing F concentration may have led to the removal of feldspars, resulting in a topazite magma.

Hydrothermal solutions may have arisen due to immiscibility in the upper levels of the magma body when separation of a vapour saturated aqueous fluid phase occurred, or on the other hand, a topazite magma could have persisted as an extremely water-, and halide- rich melt into the final stages of intrusion, when a boiling process gave rise to a water- rich fluid phase. The crystallization of topaz would be the major phase reducing the HF content of these solutions during cooling and thereby compounding the effect of removal of HF in any vapour phase and increasing the alkali chloride content of the solution.

(c). Discussion and comparison to Renosterkop

Once again very little comparison can be drawn between these rocks described and the topaz- bearing biotite quartz rocks found at Renosterkop. The biotite and topaz contents of the rocks found at Eldorado are lower and the quartz content is higher than the rocks found at Renosterkop.

No mention is made of any accessory minerals similar to those found at Renosterkop. A generally weak comparison may be seen to exist between the microprobe analyses of the biotite found at Renosterkop and those found at Eldorado. On the limited information available on the Eldorado

occurrence, it would seem appropriate to conclude that no relationship exists between the nature and origin of the two deposits.

D. Genesis of the Renosterkop Tin Deposit

1.Previous models proposed

Genetic models which have been proposed for the origin of the TBQ which hosts the Renosterkop tin deposit are as follows:

(a). Origin by greisenization of a granitoid host rock

i. Proposal: Armstrong(1985) suggested that the granite gneiss units at Renosterkop and vicinity represent the granitoids from which the tin mineralization was derived. The process of tin deposition took place at sites of intense and complex metasomatic activity in the apical zone of a tin bearing granitoid. The quartz - biotite rocks which carry the tin originated by pervasive metasomatic alteration and replacement of granitic host rocks to form sheeted greisen bodies. The mineralized environment is therefore plutonic and no sedimentary rock types are represented. The tin- bearing solutions could further have metasomatized the granite either before, during, or after the major structural events and have thus inherited most of the structural features present.

ii. Discussion: This proposal is the most acceptable of all other explanations for the origin of the TBQ at Renosterkop, but differs slightly from the model based on the outcome of this study.

(b). Sedimentary origin

i. Proposal: Southwood (1983) regards both the TBQ and the granite gneiss to be of sedimentary origin and refers to them as metaquartzite and pink gneiss respectively. He further suggests their origin to be derived from the denudation of an ancient stanniferous granite. He regards the mineralization as hydrothermal with tin leached from the biotite in the pink gneiss, probably as alkali- oxyflurostannate complexes. The ore- bearing solutions migrated upwards into the metaquartzite, with which they re-equilibrated. The resulting physiochemical changes led to the formation and precipitation of the cassiterite.

ii. Discussion: The nature of the granite gneiss has since been shown in this study to be of probable igneous origin, more typical that of an A- type than an S- type granite. In the latest classification by the Geological Survey the granite is also regarded to be of igneous origin, a finding based on the results of various regional researchers (G. Moen, pers. comm.). Furthermore, the chemical zonation found around the TBQ, as well as the presence of rock types that are transitional in mineralogy and chemistry between the granite gneiss and the TBQ, are not typical of what would be expected of two genetically different rock types.

(c). Sedimentary xenolith within intrusive granite gneiss

i. Proposal: Praekelt (1984) proposes that the TBQ is a xenolith of sedimentary origin within the intrusive granite gneiss and mineralized by means of hydrothermally active fluids.

ii. Discussion: The granite gneiss has undergone numerous and intense deformational phases since emplacement, and a xenolith of that size would thus be expected to have undergone the same deformational events. No primary sedimentary features are recognisable at Renosterkop. What might appear to be bedding in the TBQ is in actual fact the inherited foliation

from the original granite gneiss which was metasomized by the hydrothermally active fluids. Further evidence against a sedimentary xenolith is the presence of isolated granite gneiss lenses found in the host rock, and which are better explained as being areas unaltered by the hydrothermal fluids. Final evidence against this postulate is derived from the petrochemistry of the host and country rocks. The transitional chemical variation observed from the country rock through into the host rock is characteristic of an alteration process taking place in a once homogeneous rock type.

(d). Volcanic exhalative origin

i. **Proposal:** A proposal was made that the tin mineralization could be controlled by volcanic exhalative processes, and that the TBQ and gneiss would thereby be volcanic in origin.

ii. **Discussion:** The proposed model would not be able to explain the chemical zonation seen in the country and host rocks at Renosterkop. The formation of the body would have to had taken place prior to the deformational events responsible for the development of the foliation, and had this taken place, the form of the body would no longer be recognizable and zonation would be absent.

2. Preferred model

An interpretation of the results of this work supports an origin for the TBQ by greisenization of a once homogeneous granitoid host rock, but the genetic model proposed here is more elaborate and differs slightly from that proposed by Armstrong (1985).

The granite gneiss units at Renosterkop and vicinity represent ancient "within plate", probably A- type hornblende- bearing granites which have undergone numerous phases of intense structural deformation and recrystallization, giving rise to the pronounced gneissosity.

After the development of the final deformational event, responsible for the present foliation developed in the gneiss, a later stage structural event took place in the form of a thrust fault or a wide fault or fracture zone in which the ductility of the rocks, caused by chemical softening, allowed tight isoclinal folding to develop. It is along this structurally weak and possibly fractured zone that metasomatic HF- rich fluids found conduits along which they migrated. These conduits could possibly be identified with quartz veins existing in places within the TBQ as illustrated in Figure 38.

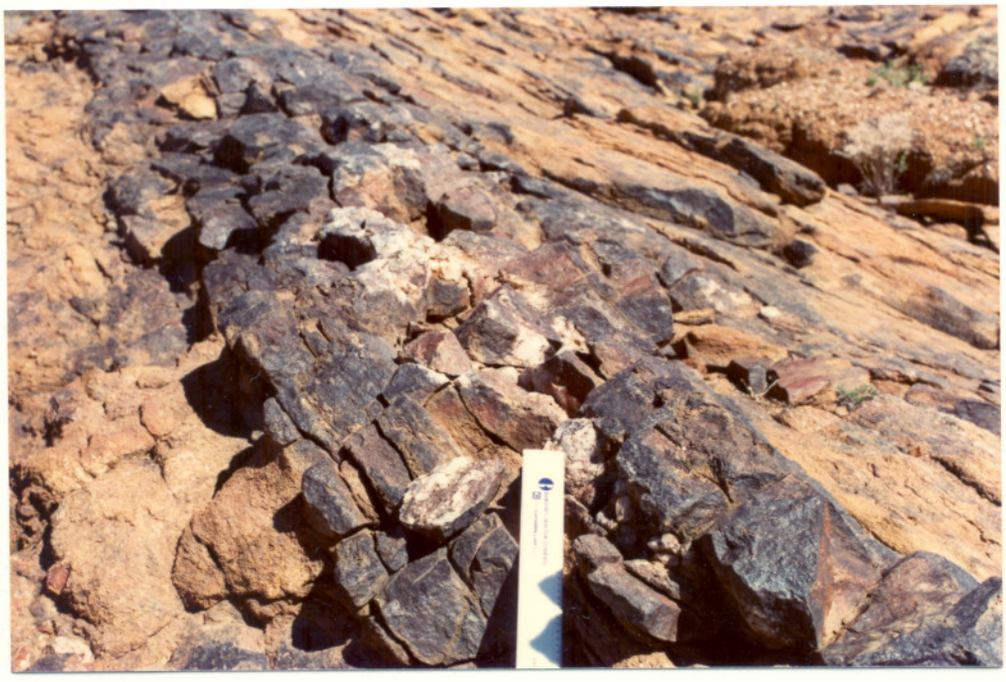

Figure 38: A quartz vein seen developed in this ±1 m wide sheet of TBQ possibly represents a one- time conduit along which greisenizing fluids migrated.

The granite gneiss thus became greisenized in situ, thereby inheriting the existing foliation and tight isoclinal folding found only in this zone and not in the surrounding granite gneiss. Further away from the zone of intense and complete greisenization, the migrating fluids effected the replacement of hornblende by biotite, thus giving rise to the envelope of biotite gneiss that surrounds the greisen bodies in the country rock of hornblende- bearing gneiss. In one locality the greisenizing fluids are seen to cross- cut the foliation developed in the gneiss, (Figure 9), and thus substantiating the theory that the fluids were emplaced after the development of the foliation. The possibility exists that the fault zone could pinch and swell along strike and that similar mineralized extensions may be found elsewhere.

A multiphase invasion by metasomatic fluids in a composite conduit system is proposed, each fluid phase differing slightly in chemistry from the other and probably remobilizing and concentrating mineralization emplaced by the previous event. This would explain the lack of obvious metal zonation in the biotite greisen as well as the poor relationship between Sn, W and Zn mineralization.

The preferred orientation of the biotite is also thought to be inherited from the foliation in the granite gneiss. The granoblastic nature of the TBQ is an indication that it has crystallized under low stress conditions and has not undergone intense tectonic deformation after formation. The mineral and chemical zonation around the TBQ host rock as a whole, together with the remarkably flat bottom contact, is further substantive evidence for the emplacement of the hydrothermal fluids after the last major stress event. The halo pattern is only disturbed by later fault zones.

Attempts to bracket the temperature - pressure field of formation of the TBQ have not been all successful. It stands to reason that the well developed grain surface equilibrium observed in the TBQ is a manifestation of a high temperature, low stress environment of formation. Unfortunately, the co-existing biotite and garnet proved to be unsuitable because of the high Mn- content of the latter mineral. Probably the most valuable geothermometer in the TBQ is the presence of sparsely developed

sillimanite crystals which point to a lower temperature limit of formation at approximately 600°C. From the coexistence in the same rock of K-feldspar, muscovite, quartz and sillimanite (be they not grain contact), as well as the apparent solid or near- solid state of the granite gneiss during the metasomatic reactions, one may tentatively derive a pressure of about 3 Kbar and a temperature of formation of about 650° C. These figures are subject to confirmation.

The emplacement of the metasomatic fluids is thought to have taken place in the waning stages of a major tectono- metamorphic event after consolidation of the granitoid country rock and subsequent to the last intense foliation event. The fluids were obviously not derived from the fractional crystallization of the Augrabies granite on which at least two foliation directions are imprinted. The source of the fluids remains an enigma and no speculation is made as to their origin.

Subject to various definitions and descriptions of greisens, and with the exception of biotite, the metasomatic alteration process and mineral assemblage is typically that of a greisen deposit. The presence of biotite in place of muscovite is ascribed to the replacement of Al by Fe in this relatively Fe- rich environment. Because the Al was preferentially tied up in topaz under the high pHF conditions that prevailed, causing Fe to act as substitute for Al, biotite was stabilised instead of muscovite. Accordingly it is felt that the TBQ may confidently be termed a "biotite greisen". The biotite greisen is genetically related to the Riemvasmaak granite gneiss country rock only in the sense that the latter is the mother rock from which the greisen was derived by F- metasomatism.

E. Conclusions

The mineralized topaz biotite quartz rock (TBQ) at Renosterkop contains a mineral assemblage that, apart from the abundance of biotite and absence of muscovite, is typical of a greisen. This rock is therefore referred to as a biotite greisen.

The granite gneiss country rock, in which the greisenized bodies are developed, has been identified as a "within plate" A- type granite belonging to the Riemvasmaak gneiss of the Namaqualand Metamorphic Complex. Mineralogical and chemical evidence support an origin for the TBQ by progressive alteration and replacement of a once homogeneous granite by F- bearing metasomatic fluids along structurally controlled conduits within a pre-existing fault or fracture zone. This is based on the observation that the biotite greisen units display evidence of folding and possibly thrust or low- angle faulting. Greisenization is furthermore concluded to have taken place after the final event responsible for the development of foliation in the gneiss. In the process the greisen inherited all structures in the granite gneiss with the biotite defining the original foliation.

The petrographic study identified a wide mineralogical halo surrounding the biotite greisen which is characterized by (i) an inner ±2 m wide chlorite- rich transition zone situated between the biotite greisen and the granite gneiss, (ii) an intermediate biotite gneiss zone, and (iii) an outer biotite - hornblende gneiss. The presence of this mineralogical halo was chemically substantiated by means of rock analyses and the subsequent identification of a chemical transition between the biotite greisen and the granite gneiss using Pearce diagrams.

The halo effect, together with the remarkably flat bottom contact between the biotite greisen and the granite gneiss, is important evidence for the emplacement of the greisenizing fluids after the last major stress event in the area.

No literature could be traced referring to mineral deposits similar to that at Renosterkop in other parts of the world. Although comparable mineral associations have been recorded, these in their geological context, bear only little relationship to the Renosterkop deposit.

V. ACKNOWLEDGEMENTS

I would like to express my sincere thanks and gratitude to the following persons and institutions for making this investigation possible:

1. Prof. S.A. De Waal for his continuous support, motivation, guidance and encouragement throughout the duration of this investigation.

2. Rio Tinto Exploration (Pty)Ltd. for kindly providing borehole core and other exploration data and for generous financial support during the investigation. Special thanks are extended to Dr. Vaughan Armstrong for firstly discovering Renosterkop, and furthermore for commenting on the manuscript and for advancing constructive ideas and criticism. Bob Cooke, Jos Haumann, Vaughan Armstrong, Tony Bloomer and Bernie Green were all responsible for contributions towards the compilation of a surface plan as well as for advancing ideas towards the structure and geology of the Renosterkop deposit. Appreciation is extended towards Laurie Lavis for organizing the draughting of the figures, and to Brenda Brunner for draughting the figures.

3. The department of Geology, Potchefstroom University for C.H.E. and the C.S.I.R. for offering financial assistance during the period of my study. Also to the staff of the same department for patient assistance in all fields of research. Leon Smuts for the preparation of thin and polished sections, Johan Engelbrecht and Miekie van Rensburg for assistance on the microprobe and Martie Coetzee and Koos Elsenbroek for assistance on the computer and other general matters.

4.Elise van Dijken and other staff members of the Computer Sciences department for their patient assistance with the word processor.

5. Maj. Edwards of the S.A. Defence Force for allowing me time to continue my investigation during the duration of a two - month military camp.

6. To my parents for their moral and financial support throughout my student years. Their interest, love and encouragement have served as an example that I would be proud to display towards my own children.

7. Last but not least I express my thanks towards my wife Gigi, my daughter Charlie, and my son Allan, who have sacrificed a way of life to bear with me during the course of this investigation. Over and above her call of duties as a mother, my wife found the time to type this thesis. I am extremely grateful.

VI. REFERENCES

Armstrong,N.V.(1985). A metasomatic origin for the Renosterkop tin mineralization by greisenization of granitoid host rocks. Rio Tinto Exploration (Pty)Ltd., Internal report, 7 June 1985, 8pp.

Atherton,M.P. and Gribble,C.D.(1983). Magmatites, melting and metamorphism. Shiva Publishing Ltd.,Cheshire, 326pp.

Atherton,M.P. and Tarney,J.(1979). Origin of granite batholiths: geochemical evidence. Shiva Publishing Ltd., Cheshire, 148pp.

Birch,W.D.(1984). Quartz - topaz - loellingite rocks near Eldorado,Victoria. Australian Journal of Earth Sciences, 31,269-278.

Botha,B.J.V., Grobler,M.J., Linstrom,W. and Smith,L.A.(1976). Stratigraphic correlation between the Kheis and Matsap formations and their relation to the Namaqualand Metamorphic Complex. Trans. geol. Soc. S. Afr., 79,304-311.

Chappell,B.W. and White,A.J.R.(1974).Two contrasting granite types. Pacific Geology,8,173-174.

Coetzee,C.B.(1941). The petrology of the Goodhouse - Pella area, Namaqualand, South Africa. Trans. geol. Soc. S. Afr.,44,167-206.

Collins,W.J., Beams,S.D., White,A.J.R. and Chappell,B.W.(1982). Nature and origin of A- type granites with particular reference to Southeastern Australia. Contrib. Mineral. Petrol.,80,189 - 200.

Colliston,W.P. (1979). The stratigraphy of the Namaqualand Metamorphic Complex in Bushmanland. Geol. Soc. S. Afr. 18th Congr. Abstracts 1,85-105.

Deer,W.A., Howie,R.A. and Zussman,J.(1962). Rock forming minerals: Sheet silicates. Longmans, Green and Co. Ltd., London, 3,270pp.

_____(1962). Rock forming minerals: Non - silicates. Longmans, Green and Co.Ltd.,London, 5,371pp.

_____(1963). Rock forming minerals: Chain silicates. Longmans, Green and Co.Ltd., London, 2,379pp.

_____(1964). Rock forming minerals: Framework silicates. Longmans, Green and Co. Ltd., London, 4,435pp.

De la Roche,H., Leterrier,J., Grandclaude,P. and Marchal,M. (1980). A classification of volcanic and plutonic rocks using R^1R^2 - diagram and major element analyses - its relationship with current nomenclature. Chem. Geol.,29,183-210.

De Waal,S.A.(1985). Petrological investigation of the rocks of the Renosterkop prospect. Rio Tinto Exploration (Pty)Ltd., Internal report, October,1985, 39pp.

Eadington,P.J. and Nashar,B.(1978). Evidence for the magmatic origin of quartz - topaz rocks from the New England batholith, Australia. Contrib. Mineral. Petrol., 67,433-438.

Evans,A.M.(1982). Metallization associated with acid magmatism. John Wiley and Sons, Inc., New York, 385pp.

Fourie,P.H.(1969). Die geochemie van granitiese gesteentes van die Bosveldstollingskompleks. Unpubl. DSc thesis, Pretoria University, 289pp.

Geringer,G.J.(1973). Die geologie van die argeise gesteentes en jongere formasies in die gebied wes van Upington met spesiale verwysing na die verskillende granietvoorkomste. Unpubl. DSc thesis, Univ. O.F.S., Bloemfontein, 203pp.

Hartnady,C.J.H.(1985). Report on reconnaissance in connection with proposed structural analysis. Rio Tinto Exploration (Pty)Ltd., Internal report, 4th January, 1985, 18pp.

Hawthorne, F.C.(1981). Crystal chemistry of the amphiboles. Reviews in mineralogy: Amphiboles and other hydrous pyriboles - mineralogy. Mineralogical Society of America, Washington, 9A,1-102.

Hicks,J.A., Moore,J.M. and Reid,A.M.(1985). The co-occurrence of green and blue gahnite in the Namaqualand Metamorphic Complex, South Africa. Canadian Mineralogist, 25,535-542.

Hugo,P.J.(1965). The pegmatites of the Kenhardt and Gordonia Districts. Unpubl. DSc thesis, Univ. Orange Free State, Bloemfontein, 207pp.

Hugo,P.J.(1969). The pegmatites of the Kenhardt and Gordonia Districts, Cape Province. Geol. Surv. S. Afr. Mem. 58,94pp.

Joubert,P.(1974). The gneisses of Namaqualand and their deformation. Trans. geol. Soc. S. Afr., 77,339-345.

Kent,L.E.(1980). Compiler. South African Committee for Stratigraphy (SACS). Stratigraphy of South Africa, Part 1: Lithostratigraphy of the Republic of South Africa, South West Africa / Namibia, and the Republics of Bophuthatswana, Transkei and Venda: Handb. geol Surv. S.Afr.,8,690pp.

Kleeman,J.D.(1985). Origin of disseminated wolframite- bearing quartz - topaz rock at Torrington, New South Wales, Australia. In: High heat production (HHP) granites, hydrothermal circulation and ore genesis. Institution of Mining and Metallurgy, London, 197-201.

Lipson,R.D. and McCarthy,T.S.(1977). Geochemical correlation between some rock - types of the Namaqualand granite - gneiss complex. Trans. geol. Soc. S. Afr.,80,177-181.

Lister,L.A.(1973). Symposium on granites, gneisses and related rocks. Geol. Soc. S. Afr. Spec. Publ.3,411-418.

Manning, D.A.C. and Pichavant, M.(1983). The role of fluorine and boron in the generation of granitic melts.In: Atherton,M.P. and Gribble,

C.D.(Editors) - **Migmatites, melting and metamorphism,** Shiva Publications Ltd., Cheshire, 94-109.

Mehnert,K.R.(1968). Migmatites and the origin of granitic rocks. Elsevier Publishing Co. Ltd., Amsterdam, 393pp.

Moore,J.M.(1977). The geology of Namiesberg, northern Cape. Precambrian Res.Unit,Univ. Cape Town, Bull No.20,69pp.

Mueller,R.F. and Saxena,S.K.(1977). Chemical petrology. Springer - Verlag, New York, 394pp.

Pearce,J.A., Haris,N.B.W. and Tindle,A.G.(1984). Trace element discrimination diagrams for the tectonic interpretation of granitic rocks. Journal of Petrology, 25,956-983.

Pearce,T.H.(1968). A contribution to the theory of variation diagrams: Contrib. Mineral and Petrol.,19,142-257.

_____(1970). Chemical variations in the Palisade Sill. Journal of Petrology, 11(1),15-32.

Plimer,I.R. and Kleeman,J.D.(1985). Mineralization associated with the Mole Granite, Australia. In: High heat production (HHP) granites, hydrothermal circulation and ore genesis. Institution of Mining and Metallurgy, London, 563-569.

Poldervaart,A. and Von Backström, J.W.(1949). A study of an area at Kakamas (Cape Province). Geol. Soc. S. Afr. Trans. 52,433-495.

Praekelt,H.E.(1984).Die geologie van die gebied rondom Augrabies(2820C).Unpubl. MSc thesis, Univ. Orange Free State, Bloemfontein, 80pp.

Ramdor,P.(1969). The ore minerals and their intergrowths. Permagon Press, Oxford, 1174pp.

Rogers,A.W. and Schwartz, E.H.L.(1900). Geology of the Orange River Valley in the Hope Town and Prieska Districts. 4th a. Rep. geol. Commn Cape Good Hope, (1899), 65-97.

Rogers,A.W.(1908). Geological survey of parts of Vryburg, Kuruman, Hay, and Gordonia. 12th a Rep. geol. Commn Cape Good Hope, (1907), 10-122.

Rogers,A.W. and Du Toit, A.L.(1909). Report on the geology of parts of Prieska, Hay, Britstown, Carnarvon and Victoria West. 13 th a. Rep. geol. Commn Cape Good Hope,(1908), 8-109.

Rosenberg,P.E.(1972). Compositional variations in synthetic topaz. American Mineralogist,57,169-187.

Schultz,R.(1977). Origin of the so- called charnockitic adamellite porphyry from the Upington Geotraverse, South Africa. Annual report, P.R.U., Univ. Cape Town, 14,48-83.

Shand,S.J.(1927). The Eruptive Rocks. Van Nostrand, New York, 360pp.

Sederholm,J.J.(1967). Selected works: granites and migmatites. Oliver and Boyd, London, 608pp.

Southwood,M.J.(1983). A mineralogical investigation of samples from the Renosterkop tin prospect near Upington. MINTEK Confidential Report No.M91, Randburg 11pp.

Streckeisen,A.(1976). To each plutonic rock it's proper name. Earth Sci. Rev.,12,1-33.

Uytenbogaardt,W. and Burke,E.A.J.(1971). Tables for microscopic identification of ore minerals. Elsevier Publishing Co.Ltd., Amsterdam, 430pp.

Van Bever Donker,J.M.(1980). Structural and metamorphic evolution of an area around Kakamas and Keimoes, Cape Province, South Africa. P.R.U., Univ. Cape Town, Bull 31,243pp.

Von Backström,J.W.(1964). The geology of an area around Keimoes, Cape Province, with special reference to phacoliths of charnockitic adamellite - porphyry. Mem. geol. Surv. S. Afr.,53,218pp.

APPENDIX I

Field descriptions and depths of samples collected from borehole core

Abbreviations used:

Alt	=	altered
Biot	=	biotite
Chl	=	chlorite
Feldsp	=	feldspathic
Gran	=	granite
Hem	=	hematite
Kaol	=	kaolin
QV	=	quartz vein
Si	=	silicification
Sn	=	tin
TBQ	=	topaz - bearing biotite quartz rock

BOREHOLE AES/1		
SAMPLE NO.	DEPTH(m)	DESCRIPTION
AES/1/1	2,60	Granite gneiss
AES/1/2	12,0	Altered TBQ with mottled hematite staining
RM 37	13,2	Greenish fine grained altered granite gneiss
RM 38	16,6	Granite gneiss
AES/1/3	18,0	Granite gneiss (weakly kaolinized)
RM 39	23,1	Altered kaolinized + chloritized TBQ
RM 40	25,6	Altered TBQ with mottled hematite
AES/1/4	26,8	Altered TBQ with Si,Hem,Chl, and Kaol.
RM 41	31,4	Silicified TBQ
RM 42	32,2	Hematized + kaolinized TBQ
RM 43	33,1	Altered pegmatitic zone
RM 44	37,3	Granite gneiss
RM 27	40,05	Granite gneiss
AES/1/5	40,75	Granite gneiss
RM 45	43,6	Granite gneiss
AES/1/6	49,5	Granite gneiss
AES/1/7	63,6	Sphene-rich biotite-quartz-diorite
RM 46	64,3	Sphene-rich biotite-quartz-diorite
RM 28	66,5	Granite gneiss
AES/1/8	72,90	Granite gneiss
AES/1/9	84,15	Granite gneiss
AES/1/10	98,25	Granite gneiss
AES/1/11	106,60	Granite gneiss
RM 30	115,0	Granite gneiss
AES/1/12	119,6	Granite gneiss
AES/1/13	131,0	Granite gneiss
RM 31	140,05	Granite gneiss
AES/1/14	141,70	Granite gneiss
AES/1/15	149,5	Granite gneiss

BOREHOLE AES/3		
*SAMPLE NO.	DEPTH(m)	DESCRIPTION
AES/3/1	1,25	TBQ, low % Sn
AES/3/2	2,35	TBQ, high % Sn
AES/3/3	5,85	TBQ, med % Sn
AES/3/4	7,15	TBQ, high % Sn
AES/3/5	13,10	TBQ, high % Sn
AES/3/6	16,35	TBQ, med % Sn
AES/3/7	18,05	TBQ, high % Sn
AES/3/8	22,25	TBQ, low % Sn
AES/3/9	27,70	TBQ, med % Sn
AES/3/10	31,95	TBQ, low % Sn
AES/3/11	34,00	Granite gneiss
AES/3/12	35,25	Granite gneiss
AES/3/13	38,25	Granite gneiss
AES/3/14	66,95	Granite gneiss
AES/3/15	118,25	Granite gneiss

* TBQ sampled using high + low assay values as criteria

BOREHOLE AES/4		
SAMPLE NO.	DEPTH(m)	DESCRIPTION
AES/4/1	2,60	TBQ
AES/4/2	10,30	TBQ (5% feldspathic)
AES/4/3	16,10	TBQ
AES/4/4	23,50	TBQ
AES/4/5	29,20	Granite gneiss (biot- rich)
AES/4/6	36,50	Granite gneiss (biot- rich)
RM 32	38,00	Granite gneiss
AES/4/7	48,50	Granite gneiss
AES/4/8	57,50	Granite gneiss
RM 33	58,00	Granite gneiss
AES/4/9	69,90	Granite gneiss (biot- rich)
RM 34	78,00	Granite gneiss
AES/4/10	83,50	Granite gneiss
AES/4/11	93,10	Granite gneiss
RM 35	98,00	Granite gneiss
AES/4/12	104,35	Granite gneiss
AES/4/13	114,00	Granite gneiss
RM 36	118,00	Granite gneiss (biot- rich)

BOREHOLE AES/5		
SAMPLE NO.	DEPTH(m)	DESCRIPTION
AES/5/1	4,4	Silicified TBQ with mottled hematite
AES/5/2	15,9	Silicified TBQ
AES/5/3	20,0	Silicified TBQ
AES/5/4	37,3	Granite gneiss
AES/5/5	47,5	Granite gneiss (kaolinized)
AES/5/6	57,5	Granite gneiss with feldspar porphyroblasts
AES/5/7	71,3	Granite gneiss
AES/5/8	79,4	Granite gneiss, altered + kaolinized
AES/5/9	91,6	Granite gneiss, altered + kaolinized
AES/5/10	102,7	Granite gneiss, altered + kaolinized

BOREHOLE AES/7		
SAMPLE NO.	DEPTH(m)	DESCRIPTION
AES/7/1	9,0	TBQ
AES/7/2	12,4	TBQ
AES/7/3	15,3	TBQ
AES/7/4	20,0	TBQ (10% feldspathic, banded)
AES/7/5	20,3	Feldspar- rich TBQ (banded + porphyroblastic, 30 %) representing gradational contact with gneiss
AES/7/6	21,0	TBQ (lens forming part of gradational contact zone
AES/7/7	21,3	Feldpar- rich TBQ (30%) banded- forming part of gradational contact
AES/7/8	22,15	Granite gneiss (pink)- just below bottom contact
AES/7/9	23,30	Granite gneiss (pink)
AES/7/10	25,4	Granite gneiss (pink)
AES/7/11	27,45	Granite gneiss (pink)

BOREHOLE AES/12		
SAMPLE NO.	DEPTH(m)	DESCRIPTION
AES/12/1	3,5	TBQ
AES/12/2	7,1	TBQ (5% feldsp.)
AES/12/3	10,8	TBQ
AES/12/4	14,5	Very feldspathic TBQ
AES/12/5	16,8	TBQ
AES/12/6	22,4	TBQ (10% feldsp.)
AES/12/7	25,8	Gran. gneiss with porphyroblasts
AES/12/8	27,7	Gran. gneiss (kaolinized) just below TBQ contact
AES/12/9	28,35	Gran. gneiss
AES/12/10	33,3	Gran. gneiss

BOREHOLE AES/18		
SAMPLE NO.	DEPTH(m)	DESCRIPTION
AES/18/1	3,00	TBQ
AES/18/2	5,45	TBQ
AES/18/3	7,70	TBQ (5% feldspathic)
AES/18/4	11,70	TBQ (10% feldspar porphyroblasts)
AES/18/5	14,80	Granite gneiss(grey)
AES/18/6	15,05	Granite gneiss(pink)

BOREHOLE AES/21		
SAMPLE NO.	DEPTH(m)	DESCRIPTION
AES/21/1	1,60	TBQ (20% feldspathic)
AES/21/2	4,45	TBQ / granite gneiss contact
AES/21/3	9,10	TBQ
AES/21/4	14,60	TBQ (5% feldspathic)
AES/21/5	19,50	Gran. gneiss (biot- rich) porphyroblastic
AES/21/6	24,15	Gran. gneiss (pink)

BOREHOLE AES/25		
SAMPLE NO.	DEPTH(m)	DESCRIPTION
AES/25/1	1,80	TBQ
AES/25/2	7,50	TBQ
AES/25/3	13,7	TBQ
AES/25/4	17,95	TBQ
AES/25/5	21,2	Silicified TBQ
AES/25/6	29,4	TBQ (10% feldspathic, partly porphyroblastic
AES/25/7	33,75	TBQ
AES/25/8	41,4	Granitic gneiss
AES/25/9	45,8	TBQ
AES/25/10	50,4	Granitic gneiss or very feldspathic TBQ
AES/25/11	52,2	Feldspathic TBQ with large feldspar porphyroblastis
AES/25/12	58,8	TBQ
AES/25/13	60,0	Biotite- rich granite gneiss
AES/25/14	61,0	Biotite- rich granite gneiss
AES/25/15	63,9	Biotite- rich granite gneiss
AES/25/16	67,2	Granite gneiss (pink)

BOREHOLE AES/26		
SAMPLE NO.	DEPTH(m)	DESCRIPTION
AES/26/1	5,7	Silicified TBQ 20 cm from QV
AES/26/2	8,5	TBQ (5% kaolinized feldsp.)
AES/26/3	12,75	Gran. gneiss in feldspar- rich TBQ zone
AES/26/4	16,3	TBQ with minor altered feldspar porhyroblast and sericitized topaz
AES/26/5	20,55	Feldspar- rich TBQ
AES/26/6	26,6	TBQ (coarse- grained)
AES/26/7	29,3	TBQ (coarse- grained)
AES/26/8	33,4	TBQ (fine- grained)
AES/26/9	34,7	TBQ on upper gradational contact with granitic gneiss
AES/16/10	35,3	Granite gneiss
AES/26/11	39,0	TBQ 20 cm below sharp lower contact with granitic gneiss
AES/26/12	44,4	TBQ
AES/26/13	47,20	Augen granite gneiss
AES/26/14	51,15	Granite gneiss (biotite- rich)
AES/26/15	59,45	Granite gneiss (pink)

BOREHOLE AES/30		
SAMPLE NO.	DEPTH(M)	DESCRIPTION
AES/30/1	0,30	TBQ
AES/30/2	2,30	TBQ / gran. gneiss contact
AES/30/3	3,60	Granite gneiss
AES/30/4	5,30	TBQ
AES/30/5	5,50	Granite gneiss (biotite- rich)
AES/30/6	6,30	TBQ / gran. gneiss contact
AES/30/7	7,0	Granite gneiss (pink)
AES/30/8	8,25	Granite gneiss (pink)
AES/30/9	12,70	Granite gneiss (pink)
AES/30/10	18,5	Granite gneiss (pink
AES/30/11	21,6	Granite gneiss (grey, altered)
AES/30/12	24,55	Granite gneiss (pink)
AES/30/13	29,80	Granite gneiss (pink)

BOREHOLE AES/40		
SAMPLE NO.	DEPTH(m)	DESCRIPTION
AES/40/1	4,0	Granite gneiss (pink)
AES/40/2	15,4	Granite gneiss (pink)
AES/40/3	24,9	Granite gneiss (pink)
AES/40/4	26,2	Granite gneiss (grey);± 1m from upper TBQ contact
AES/40/5	27,3	TBQ
AES/40/6	29,0	Granite gneiss (grey) with much biotite and porphyroblasts
AES/40/7	30,3	Granite gneiss (pink)
AES/40/8	31,25	Silicified altered TBQ forming part of gradational upper TBQ gran.gneiss contact
AES/40/9	31,50	TBQ (just below contact)
AES/40/10	34,20	TBQ
AES/40/11	35,60	Silicified altered TBQ representig gradational lower TBQ/ gran. gneiss contact
AES/40/12	40,40	Granite gneiss (pink)
AES/40/13	51,55	Granite gneiss, grey and silicified, representing upper TBQ / gran.gneiss contact
AES/40/14	51,80	Silicified TBQ just below upper contact
AES/40/15	53,70	TBQ
AES/40/16	54,70	Granite gneiss (grey) just below TBQ contact
AES/40/17	59,30	Granite gneiss(pink)

BOREHOLE AES/44		
SAMPLE NO.	DEPTH(m)	DESCRIPTION
AES/44/1	3,60	TBQ
AES/44/2	6,50	Chloritized + silicified TBQ
AES/44/3	9,35	TBQ
AES/44/4	11,60	Chloritized, silicified + kaolinized TBQ
AES/44/5	17,10	TBQ
AES/44/6	19,65	TBQ
AES/44/7	22,65	TBQ
AES/44/8	25,3	Granitic gneiss (coarse-grained)
AES/44/9	29,6	TBQ (porphyroblastic feldspar 5 %)
AES/44/10	32,7	TBQ
AES/44/11	37,0	TBQ
AES/44/12	47,7	TBQ (15% feldspathic)
AES/44/13	49,75	TBQ (10% feldsp., partly porphyroblastic
AES/44/14	53,5	Granitic gneiss (biotite- rich) or feldspathic TBQ
AES/44/15	58,9	TBQ
AES/44/16	60,6	Granite gneiss (pinkish)
AES/44/17	63,1	Granite gneiss (pink)

BOREHOLE AES/45		
SAMPLE NO.	DEPTH	DESCRIPTION
AES/45/1	1,10	TBQ
AES/45/2	4,0	TBQ
AES/45/3	9,2	Silicified TBQ
AES/45/4	15,1	Kaolinized + silicified TBQ
AES/45/5	19,4	TBQ
AES/45/6	20,7	TBQ
AES/45/7	22,4	TBQ (high Sn)
AES/45/8	26,85	TBQ (feldspatic)
AES/45/9	32,6	TBQ
AES/45/10	39,6	TBQ (feldsp. alt. + structural deformation
AES/45/11	41,0	TBQ
AES/45/12	42,75	Granitic gneiss
AES/45/13	44,0	Granitic gneiss
AES/45/14	51,35	TBQ (5-10% porphyroblastic feldspar)
AES/45/15	56,0	TBQ (10% porphyroblastic feldspar)
AES/45/16	58,6	Granitic gneiss (biot- rich)
AES/45/17	62,0	Granite gneiss (pink)
AES/45/18	64,9	Granite gneiss (pink)

BOREHOLE AES/47		
SAMPLE NO.	DEPTH(M)	DESCRIPTION
AES/47/1	7,75	TBQ
AES/47/2	12,50	TBQ
AES/46/3	16,55	TBQ
AES/47/4	20,65	TBQ Silicified (biot- poor)
AES/47/5	23,30	TBQ Weakly silicified
AES/47/6	24,75	TBQ Silicified
AES/47/7	32,40	TBQ Weakly silicified
AES/47/8	35,40	TBQ
AES/47/9	42,70	TBQ
AES/47/10	44,50	TBQ
AES/47/11	50,45	TBQ
AES/47/12	56,20	TBQ Weakly feldspathic
AES/47/13	59,65	TBQ Weakly feldspathic
AES/47/14	61,60	TBQ Feldspathic
AES/47/15	62,30	Gran. gneiss (biotite- rich)
AES/47/16	65,45	Gran. gneiss (pink)

APPENDIX II

Mineral composition of samples of all boreholes together with brief petrographic descriptions

LEGEND

+ Granite gneiss
A+ Altered granite gneiss
* Transition zone
+. Feldspar - rich TBQ
. TBQ
A. Altered TBQ

BOREHOLE AES/1															
	1	2	RM 37	RM 38	3	RM 39	RM 40	4	RM 41	RM 42	RM 43	RM 44	RM 27	5	RM 45
Quartz	xx	xx	xx	xx	xx	xx	xx	xx	xx	xx	xx	xx	xx	xx	xx
Biotite	x	x	x	x	x	x	x	x	x	x	x	xx	x	x	x
Topaz		x	x		x	x	x	x	x			x			
Fluorite	x	x	x	x	x		xx	x	xx		x	x	x	x	
Microcline	xx			xx	xx							xx	xx	xx	xx
Plagioclase				x	x							x	x	x	x
Sericite	x	x	xx	xx	x	xx	xx		xx	xx	xx	x	x	xx	x
Chlorite	x		xx	xx	xx		xx	xx		xx	x	xx	xx	xx	xx
Sphalerite															
Zircon	x	x	x	x	x	x	x	x	x	x	x	x	x	x	x
Cassiterite															
Garnet															
Gahnite															
Sillimanite															
Hornblende	x														
Sphene	x		x	x											
Myrmekite				x	x							x	x	x	x
Allanite															
Apatite	x			x	x							x	x	x	
Calcite					x										
Opaque		xx	x	x		x	xx	xx	xx	xx		x	x	x	x
Monazite															
Rutile					x										
Muscovite															
Rock Type	+	A.	*	+	+	A.	A.	A.	A.	A.	A.	*	*	*	A+

AES/1: The rocks in this borehole have undergone intense alteration and no definite clear pattern may be seen. Hornblende is found in the upper portion of the borehole together with a greenish brown biotite variety. As one moves down the borehole towards a zone of altered TBQ, the hornblende dissapears and the biotite in the granite gneiss becomes chloritized. In the altered TBQ the biotite remains strongly chloritized and in places hematized, and traces of red- brown biotite are present.

Below the zone of altered TBQ, both chlorite and a dark- brown biotite variety are found in varying quantities up to sample no. 7, where only brown biotite is present.

BOREHOLE AES/1 (cont)															
	6	7	RM 46	RM 28	8	9	RM 29	10	11	RM 30	12	13	RM 31	14	15
Quartz	xx	xx	xx	xx	xx	xx	xx	xx	xx	xx	xx	xx	xx	xx	xx
Biotite	x	xx	xx	xx	xx	x	xx	x	x	x	x			x	x
Topaz															
Fluorite	x	x	x	x	x		x				x	x			x
Microcline	xx	x	x	xx	xx	xx	xx	xx	xx	xx	xx	xx	xx	xx	xx
Plagioclase	x	xx	xx	x	x	x	xx	x	x	x	x	x	x	x	x
Sericite	xx	x	x	x	x	x	x	x	x	x	xx	x	x	xx	x
Chlorite	x	x	x	x	x	x	xx	x	x	x	x	xx	x	x	x
Sphalerite															
Zircon	x	x	x	x	x	x	x	x	x	x	x	x	x	x	x
Cassiterite															
Garnet															
Gahnite															
Sillimanite															
Hornblende				x		x		x	x	xx	x	x			x
Sphene		xx	xx	x	x	x	x	x		x	x	x	x		x
Myrmekite	x	x	x	x	x	x		x	x	x	x	x	x	x	x
Allanite				x						x	x	x			
Apatite	x			x			x		x	x		x			x
Calcite				x			x								
Opaque	x	x	x	x	x	x	x	x		x	x	x	xx	x	x
Monazite					x						x			x	
Rutile															
Muscovite															
Rock Type	A+			+	+	+	A+	+	+	+	+	A+	A+	A+	+

Below sample no. 7, the biotite becomes weakly chloritized and in sample no. 9 hornblende is seen for the first time. Below sample RM28 varying amounts of hornblende, brown biotite and chlorite are present. In RM29 biotite and chlorite are present in equal amounts. In samples RM31 and 14 alteration has taken place and all biotite has been chloritized and replaced by opaques. A fault zone is expected to have passed through the vicinity of this position. The hornblende generally appears to increase in quantity between samples 9 and 15.

BOREHOLE AES/3															
	1	2	3	4	5	6	7	8	9	10	11	12	13	14	15
Quartz	xx	xx	xx	xx	xx	xx	xx	xx	xx	xx	xx	xx	xx	xx	xx
Biotite	xx	xx	xx	xx	x	xx	xx	xx	xx	xx	x	x	x	xx	x
Topaz	xx	xx	xx	xx	xx	x	xx	x	xx	x					
Fluorite	x	x	x	x	x	x	x	x	x	x	x	x		x	
Microcline											xx	xx	xx	xx	xx
Plagioclase											x	x	x	x	x
Sericite					x						x	x	xx	x	x
Chlorite	x	x	x	x	x	x	x	x	x	x	x	xx	x	x	
Sphalerite	x	xx	x	x	x	x	x			x					
Zircon	x	x	x	x	x	x	x	x	x	x	x	x	x	x	x
Cassiterite	x	xx	x	xx	xx		x	x	x						
Garnet															
Gahnite															
Sillimanite															
Hornblende															x
Sphene														x	x
Myrmekite											x			x	x
Allanite															
Apatite													x	x	
Calcite															
Opaque	x	xx	xx	xx	xx	x	xx	x	x	x	x	x	x	x	x
Muscovite					x					x					
ROCK TYPE	=	=	=	=	=	=	=	=	=	=	*	*	+	+	+

AES/3: Red- brown biotite is present throughout the TBQ with traces of chlorite occurring sporadically. Below the TBQ the biotite becomes completely chloritized and with depth alters to a brown biotite. This brown biotite is joined by hornblende as one moves further down the borehole.

In sample 5 biotite alters to muscovite, and this sample is particularly rich in tin.

Borehole AES/3 was selectively sampled according to high and low tin values. Special attention was given to determine microscopically whether a relationship exists between the number of cassiterite grains and the grain size of the host rock matrix. No relationship could however be determined.

BOREHOLE AES/5										
	1	2	3	4	5	6	7	8	9	10
Quartz	xx	xx	xx	xx	xx	xx	xx	xx	xx	xx
Biotite	x	x	x	xx		x	x	x	x	x
Topaz	xx	xx	xx	x		x	x			
Fluorite	xx	x	xx	x		x	x		x	x
Microcline				xx	xx	xx	xx		xx	xx
Plagioclase				x	x	x	x	x	xx	xx
Sericite	x			xx		xx	xx	xx	xx	x
Chlorite	x	xx	xx	x	xx	xx	xx	x	x	x
Sphalerite										
Zircon	x	x	x	x		x	x	x	x	x
Cassiterite			x							
Garnet										
Gahnite										
Sillimanite										
Hornblende										
Sphene					x		x			
Myrmekite							x			
Allanite							x		x	
Apatite					x		x			x
Calcite										
Opaque	x	x	xx	x		x	x	x	x	x
Muscovite			x							
ROCK TYPE	A.	A.	A.	A+	A+	A+	A+	A+	A+	A+

AES/5: The TBQ at the top of the borehole is altered and carries only traces of red- brown biotite. The remainder of the biotite has been chloritized or replaced by opaque minerals.

Below the TBQ, the biotite is replaced by chlorite in samples 4 and 5, and in samples 6 and 7 traces of brown biotite are found. In samples 8 and 9 the biotite is once again chloritized and replaced by opaques. Quartz with a bowtie- type extinction is found in these samples. In sample 10, brown biotite may be seen with traces of chlorite, indicating that the chlorite altered to the biotite. A major fault zone is expected to have passed through the vicinity of samples 8 and 9, explaining the absence of hornblende and the intense alteration throughout the borehole.

BOREHOLE AES/7											
	1	2	3	4	5	6	7	8	9	10	11
Quartz	xx	xx	xx	xx	xx	xx	xx	xx	xx	xx	xx
Biotite	xx	xx	xx	xx	xx	xx	x	xx	x	x	xx
Topaz	xx	xx	xx	x		x					
Fluorite	x	x	x	x	x	x	x	x	x	x	x
Microcline				x	xx		xx	xx	xx	xx	xx
Plagioclase				x	x		x	x	x	x	x
Sericite				x	x		x	xx	xx	xx	x
Chlorite	x						x	x	x	x	x
Sphalerite	x	x	xx			xx					
Zircon	x	x	x	x	x	x	x	x	x	x	x
Cassiterite			x			xx					
Garnet											
Gahnite											
Sillimanite											
Hornblende											
Sphene					x				x		x
Myrmekite					x		x	x	x	x	x
Allanite											
Apatite											x
Calcite											
Opaque	x	x	x	x	x	x	x	x	x	x	x
ROCK TYPE	.	.	.	+	+	.	*	*	*	+	+

AES/7: The biotite throughout the TBQ is red- brown in colour. Just below the TBQ this biotite changes to a deep red- brown variety and becomes chloritized. Further down the hole chloritization decreases and the biotite takes on a dark greenish- brown colour.

This is a typical unaltered borehole passing through the transition zone and into the granite gneiss.

BOREHOLE AES/12										
	1	2	3	4	5	6	7	8	9	10
Quartz	xx	xx	xx	xx	xx	xx	xx	xx	xx	xx
Biotite	xx	xx	xx	xx	xx	xx	x	x	x	x
Topaz	x	x	x	x	xx	x				
Fluorite	x	x	x	x	x	x	x	x	x	x
Microcline		x		x		x	xx	xx	xx	xx
Plagioclase				x		x	x	x	x	x
Sericite		xx		x		x	x	xx	xx	x
Chlorite	x	x				x	x	xx	x	x
Sphalerite	xx	x	x	x	xx	x				
Zircon	x	x	x	x	x	x	x	x	x	x
Cassiterite	xx	x			xx	x				
Garnet										
Gahnite										
Sillimanite										
Hornblende										
Sphene							x			
Myrmekite							x	x		x
Allanite										
Apatite							x			
Calcite										
Opaque	x	x	x	x	x	x	x	x	x	x
Muscovite		x								
Monazite			x		x					
ROCK TYPE	.	+.	.	+.	.	+.	*	*	*	+

AES/12: Red- brown biotite is found throughout the borehole from samples 1 to 6. Samples 7,8 and 9 are seen to pass through the transition zone and in sample 9 only the dark greenish- brown biotite is seen remaining with traces of chlorite. In sample 10, deep red- brown partly chloritized biotite is once again seen. This is typical of a reaction zone in the vicinity of TBQ and it would appear that if this borehole were drilled deeper, another lens of TBQ would have been intersected.

BOREHOLE AES/18						
	1	2	3	4	5	6
Quartz	xx	xx	xx	xx	xx	xx
Biotite	xx	xx	xx	xx	xx	xx
Topaz	xx	·xx	xx	x	x	
Fluorite	xx	xx	x	x	x	x
Microcline			x	x	xx	xx
Plagioclase					x	xx
Sericite			x	x	x	x
Chlorite	x			x		x
Sphalerite	xx	x		x		
Zircon	x	x	x	x	x	x
Cassiterite	x					
Garnet						
Gahnite						
Sillimanite						
Hornblende						
Sphene						
Myrmekite						
Allanite						
Apatite					x	x
Calcite						
Opaque	x	x	x	x	x	x
Muscovite					x	x
Monazite					x	
ROCK TYPE	.	.	+.	+.	+	+

AES/18: In samples 1 and 2 most fluorite is associated with biotite. Zircon and fluorite inclusions may be seen in biotite in sample 4, and zircon inclusions in biotite in sample 5.

Biotite takes on a bright red- brown colour in samples 1 to 5 with traces of green chloritized biotite in 5. Sample 6 contains a dull brown biotite.

BOREHOLE AES/21						
	1	2	3	4	5	6
Quartz	xx	xx	xx	xx	xx	xx
Biotite	xx	xx	xx	xx	xx	xx
Topaz	xx	x	x	x		x
Fluorite	x	x	x	x	x	x
Microcline	x	xx		x	xx	xx
Plagioclase		x			x	x
Sericite	xx	xx		x	x	x
Chlorite						x
Sphalerite	x	x	x	x		
Zircon	x	x	x	x	x	x
Cassiterite						
Garnet						
Gahnite					x	
Sillimanite						
Hornblende						
Sphene						
Myrmekite						
Allanite						
Apatite					x	
Calcite						
Opaque	x	x	x	x	x	x
ROCK TYPE	+.	+.	.	+.	+	*

AES/21: The biotite appears to be in complete physical equilibrium with all other minerals and takes on a red- brown colour in samples 1 to 5. Chloritic alteration of the biotite is present in sample 6. No cassiterite grains were found in any of the samples.

BOREHOLE AES/25																
	1	2	3	4	5	6	7	8	9	10	11	12	13	14	15	16
Quartz	xx	xx	xx	xx	xx	xx	xx	xx	xx	xx	xx	xx	xx	xx	xx	xx
Biotite	xx	xx	x	xx	x	xx	xx	x	xx	xx	xx	xx	xx	xx	xx	x
Topaz	xx	x	xx	xx	x	x	xx		x			xx				
Fluorite	x	x	xx	x	x	x	x	x	x	x	x	x	x	x	x	x
Microcline			xx		xx	xx		xx		xx	xx		xx	xx	xx	xx
Plagioclase			x			x		x		x	x		x	x	x	x
Sericite			x		x	x		x		xx	x		x	x	x	x
Chlorite	x		x		x		x			x	x	x	x	x	x	xx
Sphalerite	x	x		xx	x	x	x		x			x				
Zircon	x	x		x		x	x	x	x	x	x	x	x	x	x	x
Cassiterite	x			xx			x		x			x				
Garnet																
Gahnite					x											
Sillimanite																
Hornblende																
Sphene													x			
Myrmekite								x		x	x				x	x
Allanite																
Apatite										x						
Calcite							x									
Opaque	x	x	x	x	x	x	x		x	x		x	x	x	x	x
Muscovite					x											
ROCK TYPE	.	.	+.	.	+.	+.	.	+.	.	+.	+.	.	*	*	*	*

AES/25: Red- brown biotite is seen throughout the TBQ and is chloritized along the edges wherever feldspar is seen to enter the mode. In sample no. 15, biotite is foliated around large feldspar phenocrysts. Many cassiterite and sphalerite grains were identified in sample no. 4. The majority of cassiterite grains are seen in contact with sphalerite and biotite. Gahnite was identified in sample no. 5.

BOREHOLE AES/26															
	1	2	3	4	5	6	7	8	9	10	11	12	13	14	15
Quartz	xx	xx	xx	xx	xx	xx	xx	xx	xx	xx	xx	xx	xx	xx	xx
Biotite	xx	xx	x	xx	xx	xx	xx	xx	xx	xx	xx	xx	x	x	x
Topaz	xx	xx		x	x	xx	x	x			x	xx			
Fluorite	x	x	x	x	x	x	x	x	x	x	xx	x	x	x	x
Microcline	x		xx		xx				x	xx			xx	xx	xx
Plagioclase			x		x				x				x	x	x
Sericite	x	x	x	x	x				x	x			x	xx	xx
Chlorite	x	x	x	x				x	x	x	x		x	xx	x
Sphalerite	x	xx		x		x	xx	x	x		x	x			
Zircon	x		x	x	x		x	x	x	x	x	x	x	x	x
Cassiterite		xx		xx		xx	x					xx			
Garnet															
Gahnite	x														
Sillimanite															
Hornblende															
Sphene					x								x		
Myrmekite			x									x			
Allanite															
Apatite													x		x
Calcite															
Opaque	x	x			x	x	x	x	x	x	x	x	x	x	x
Muscovite								x							
ROCK TYPE	.	.	+.	.	+.	.	.	.	+.	+	.	.	*	*	+

AES/26: In this borehole a reaction zone may be seen in which the red-brown biotite of the TBQ is chloritized as one moves from the TBQ into the granite gneiss. This zone may be seen both above and below the TBQ.

Gahnite was found in sample no. 1 and cassiterite was identified in samples 2,4,6,7 and 12.

BOREHOLE AES/30													
	1	2	3	4	5	6	7	8	9	10	11	12	13
Quartz	xx	xx	xx	xx	xx	xx	xx	xx	xx	xx	xx	xx	xx
Biotite	xx	xx	xx	xx	xx	xx	x	xx	xx	xx	xx	xx	xx
Topaz	x	xx		x	x	x							
Fluorite	x	x	x	x	xx	x	x	x	x	x	x	x	x
Microcline			xx		x	x	xx	xx	xx	xx	xx	xx	xx
Plagioclase			x				x	x	x	x	x	x	x
Sericite			x	x	x	xx	xx	xx	xx	xx	xx	xx	xx
Chlorite			x	x			x	xx	x	x	x	x	x
Sphalerite	x	xx		x									
Zircon	x	x	x	x	x	x	x	x	x	x	x	x	
Cassiterite	x	x											
Garnet													
Gahnite													
Sillimanite													
Hornblende													
Sphene								x	x		x		
Myrmekite							x	x	x	x	x		x
Allanite													
Apatite			x			x			x		x	x	
Calcite													
Opaque	x	xx	x	x		x				x	x	x	
Muscovite							x						
ROCK TYPE	.	.	+	.	+.	+.	*	*	+	+	A+	+	+

AES/30: Few cassiterite grains associated with a relative abundance of sphalerite were found in samples 1 and 2.

Alteration within the granite gneiss is seen in sample no. 11 in which partly chloritized reddish- brown biotite typical of the TBQ may be found.

BOREHOLE AES/40																	
	1	2	3	4	5	6	7	8	9	10	11	12	13	14	15	16	17
Quartz	xx	xx	xx	xx	xx	xx	xx	xx	xx	xx	xx	xx	xx	xx	xx	xx	xx
Biotite	xx	x	xx	xx	xx	xx	xx	x	xx	xx	x	x	x	xx	xx	xx	x
Topaz			x		x	x		xx	xx	xx	x				xx		
Fluorite	x	x	x	x	x	x		xx	x	x	x	x	x	x	xx	x	
Microcline	xx	xx	xx	xx		xx	xx	xx			x	xx	xx		x	xx	xx
Plagioclase			x	x			x					x	x			x	x
Sericite	x	x	x	x		x	x	x			x	xx	x	x	x	x	xx
Chlorite	x		x	x		x	x					xx	x	x	x	xx	xx
Sphalerite					x				xx	xx					x		
Zircon	x	x	x	x	x	x	x	x	x	x	x	x	x	x	x	x	x
Cassiterite								xx									
Garnet																	
Gahnite																	
Sillimanite																	
Hornblende	x	x															
Sphene	x	x											x				
Myrmekite	x	x					x					x	x			x	x
Allanite																	
Apatite	x	x	x	x			x					x	x	x			x
Calcite																	
Opaque	x	x	x	x	x	x	x	x	x	x	x	x	x	x	x	x	x
Monazite						x			x						x	x	
Muscovite						x		x			x						
ROCK TYPE	+	+	+	+	.	+	+	.	.	.	.	*	*	.	+.	*	*

AES/40: Hornblende is found in samples 1 and 2 in the granite gneiss overlying the TBQ. This hornblende occurs together with a light brown biotite. As one approaches the upper TBQ, the hornblende dissapears and the biotite becomes chloritized. The remaining biotite gradually becomes darker red- brown as seen in samples 3 and 4. In the TBQ itself the biotite takes on a red- brown colour. Below the TBQ the biotite is once again chloritized as seen in sample 12. Approaching the lower TBQ, the chlorite once again transforms to a red- brown biotite as seen in samples 13 to 15. In sample 16 the red- brown biotite is once again broken down to chlorite below the TBQ. In sample 17 the chlorite alters to a dark brown biotite variety.

Cassiterite grains were only found in sample no. 8 associated with anomolous topaz.

BOREHOLE AES/44																	
	1	2	3	4	5	6	7	8	9	10	11	12	13	14	15	16	17
Quartz	xx	xx	xx	xx	xx	xx	xx	xx	xx	xx	xx	xx	xx	xx	xx	xx	xx
Biotite	xx	x	xx	x	xx	x	xx	x	xx	xx	xx	xx	xx	xx	xx	xx	x
Topaz	xx	x	xx	xx	xx	xx	xx		x	xx	xx	x		x	x		
Fluorite	x	x	x	x	x	xx	x	x	x	x		x	x	x	x	x	x
Microcline		xx		xx		x		xx	xx			x	x	xx		xx	xx
Plagioclase				x		x		x				x	x	x		x	x
Sericite		x		xx		x		xx	xx			x	x	xx		xx	x
Chlorite	x					x							x			x	x
Sphalerite	xx		x		x	x	x		x	x	xx	x			xx		
Zircon	x		x		x		x	x	x	x	x	x	x	x	x	x	x
Cassiterite	xx				x		x			xx	xx	x					
Garnet																	
Gahnite													x	x			
Sillimanite																	
Hornblende																	
Sphene														x			
Myrmekite		x		x		x		x						x		x	x
Allanite																	
Apatite								x									
Calcite																	
Opaque	x		x	x	x	x	x	x	x	x	xx	x	x	x	x	x	
Monazite									x								
ROCK TYPE	.	+.	.	+.	.	+.	.	+	+.	.	.	+.	+.	+.	.	*	*

AES/44: Biotite is generally red- brown throughout the TBQ except for sample 7 in which it is brown. Minor chlorite alteration is found associated with the development of feldspar within the TBQ. The feldspar is assumed to be secondary due to the foliation of the biotite around the feldspar phenocrysts. An increase in chloritization is found below the TBQ into the granite gneiss.

Gahnite is found in samples 13 and 14.

BOREHOLE AES/45																		
	1	2	3	4	5	6	7	8	9	10	11	12	13	14	15	16	17	18
Quartz	xx	xx	xx	xx	xx	xx	xx	xx	xx	xx	xx	xx	xx	xx	xx	xx	xx	xx
Biotite	xx	xx	x	x	xx	x	xx	xx	xx	xx	xx	xx	x	xx	xx	xx	xx	
Topaz	x	x	x	x	xx	xx	x	x	xx	x	x			x				
Fluorite	x	x	x	xx	x	x	x	x	x	xx	x	x	x	x	x	x	x	x
Microcline			x	x				x		x		xx	xx	x	xx	x	xx	xx
Plagioclase				x				x		x		x	x		x	x	x	x
Sericite			x	x				xx		x		x	x	x	xx	x	x	x
Chlorite										x	x		x			x	xx	xx
Sphalerite	xx	x		x	xx	xx	xx	x	xx		xx		x	x	x			
Zircon		x		x	x		x	x	x	x	x	x	x	x	x	x	x	x
Cassiterite	x	x		xx	x	x	x		x		xx			x				
Garnet																		
Gahnite			x		x											x		
Sillimanite																		
Hornblende																		
Sphene			x															
Myrmekite													x		x	x	x	
Allanite																		
Apatite													x	x				x
Calcite																		
Opaque	x	x	x	x	x		x		x	x	x	x	x	x	x			x
Monazite										x								
Muscovite										x								
ROCK TYPE	.	.	A.	A.	.	.	.	+.	.	+.	.	+	+	+.	+.	*	*	*

AES/45: The biotite is generally red- brown throughout the TBQ except for sample 6 in which it is very pale brown. Chloritization may be seen in zones enriched in feldspar. Below the TBQ the biotite is chloritized. Cassiterite grains observed appeared to be locked primarily to fluorite and to a lesser degree to sphalerite and biotite.

Gahnite is identified in samples 3 and 5.

BOREHOLE AES/47																
	1	2	3	4	5	6	7	8	9	10	11	12	13	14	15	16
Quartz	xx	xx	xx	xx	xx	xx	xx	xx	xx	xx	xx	xx	xx	xx	xx	xx
Biotite	xx	xx	xx	x	xx	x	xx	xx	xx	xx	xx	xx	xx	x	x	x
Topaz	xx	xx	x	x	xx	x	xx	xx	x	x	x	x	x	x		
Fluorite	x	x	x	x	x	x	x	x	x	x	x	x	x	x	x	
Microcline						x						x		xx	xx	xx
Plagioclase						x						x		x	x	x
Sericite						xx	x					x	x	x	xx	xx
Chlorite											x		x		x	x
Sphalerite	xx	x	x	x			x	xx	x	x	x	x	x			
Zircon	x	x	x		x	x			x	x	x	x	x	x	x	x
Cassiterite	xx		x	x	x						xx					
Garnet																
Gahnite				xx	xx	x								x		
Sillimanite																
Hornblende																
Sphene				x								x			x	
Myrmekite														x		
Allanite																
Apatite																
Calcite							x							x	x	
Opaque	x	x	x	x	x	x	x	x	x	x	x		x	x	x	
Monazite	x										x		x			
Muscovite																
ROCK TYPE	.	.	.	.	.	+.	.	.	.	.	.	+.	.	+.	*	+

AES/47: The biotite is seen to take on a red- brown colour throughout the TBQ. Smaller amounts of biotite are present in the alteration zone between samples 4 and 6 which are characterized by the presence of gahnite throughout the zone. Directly below the TBQ the biotite changes to a brown colour. Topaz is present mainly as large porphyroblasts and gahnite is found in abundance in samples 4 and 5 and to a lesser degree in 6.

APPENDIX III

Graphical presentation of major and trace element chemistry .

LEGEND

- – – – : TBQ / Granite gneiss contact
- × : Hornblende - biotite granite gneiss
- ✦ : Biotite granite gneiss
- ◇ : Transition zone and granitic gneiss lenses
- □ : TBQ

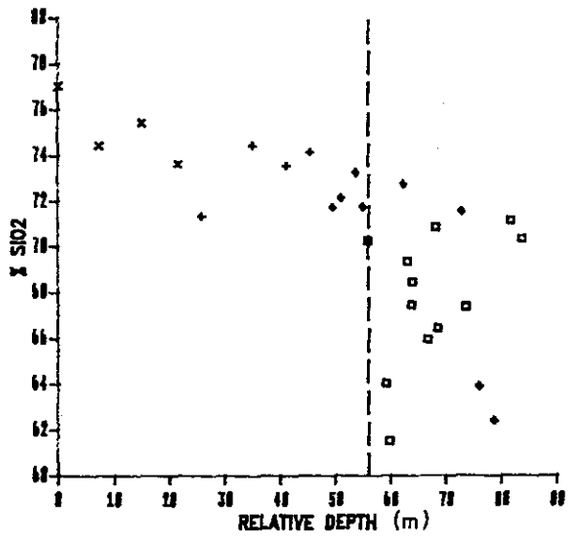
% SiO2
RELATIVE DEPTH (m)

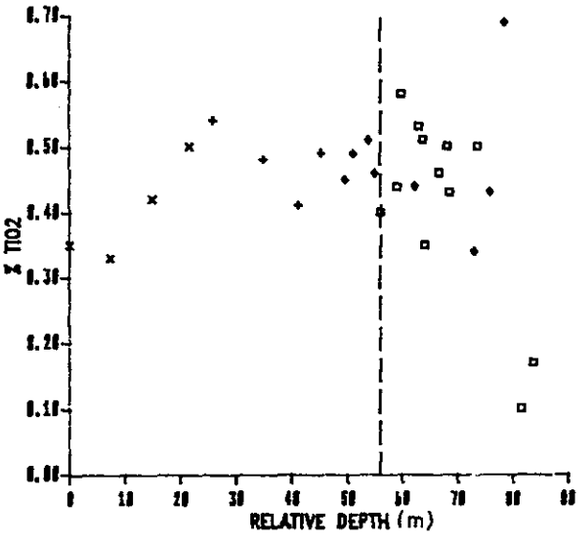
% TiO2
RELATIVE DEPTH (m)

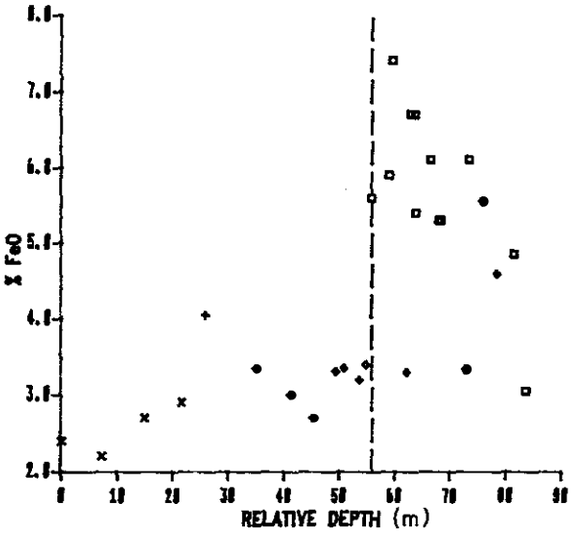
% FeO
RELATIVE DEPTH (m)

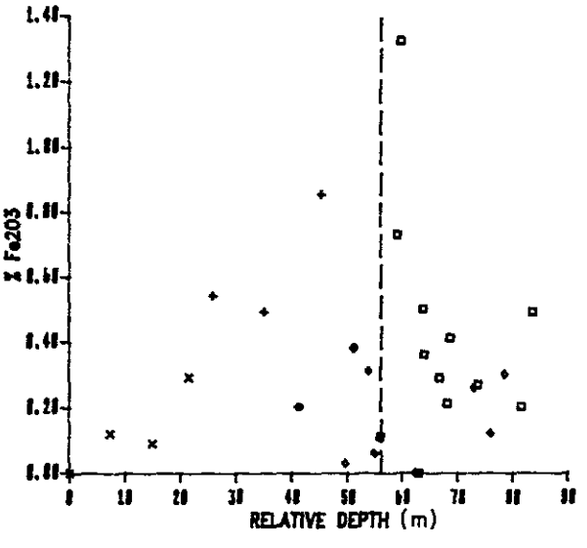
% Fe2O3
RELATIVE DEPTH (m)

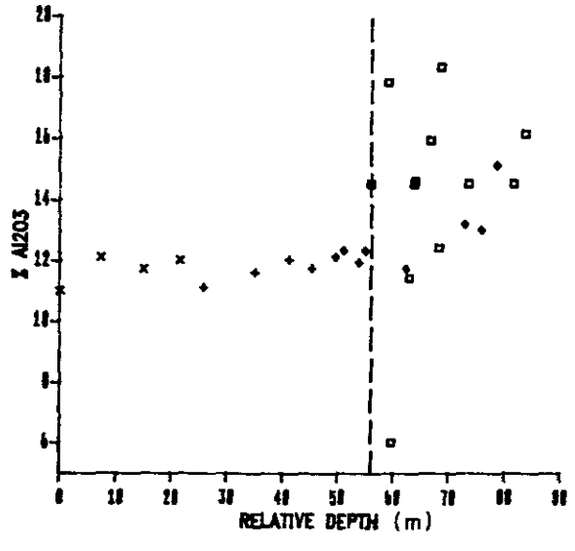
% Al2O3
RELATIVE DEPTH (m)

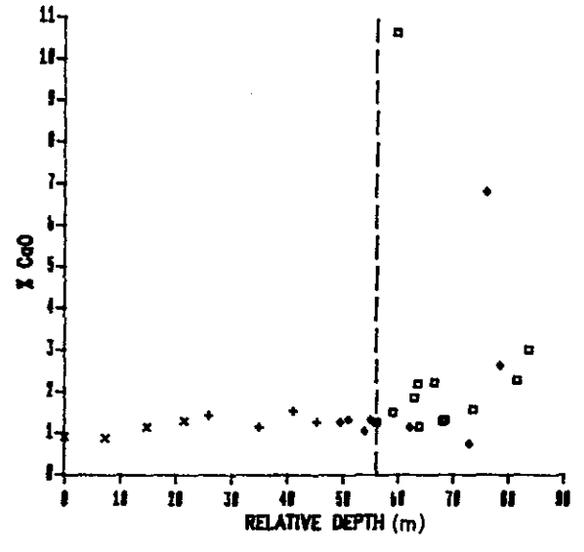
% CaO
RELATIVE DEPTH (m)

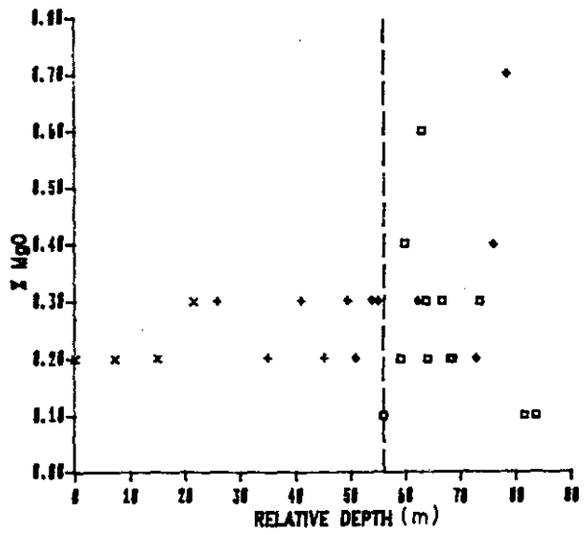
% MgO
RELATIVE DEPTH (m)

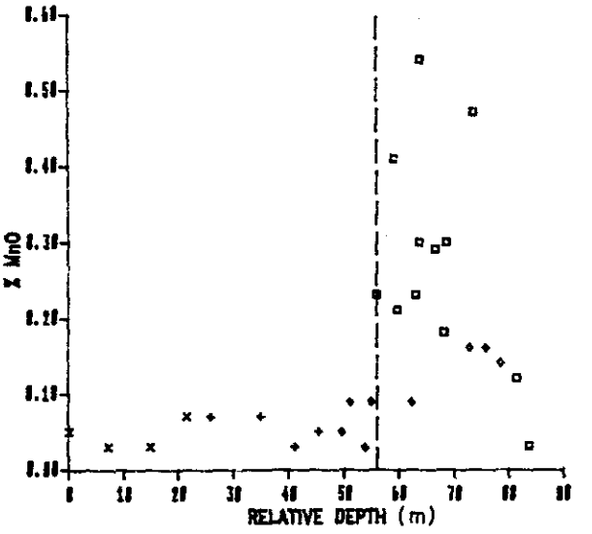
% MnO
RELATIVE DEPTH (m)

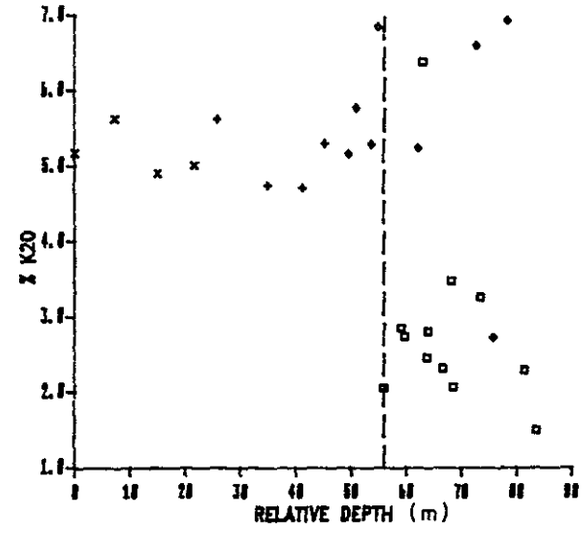
% K20
RELATIVE DEPTH (m)

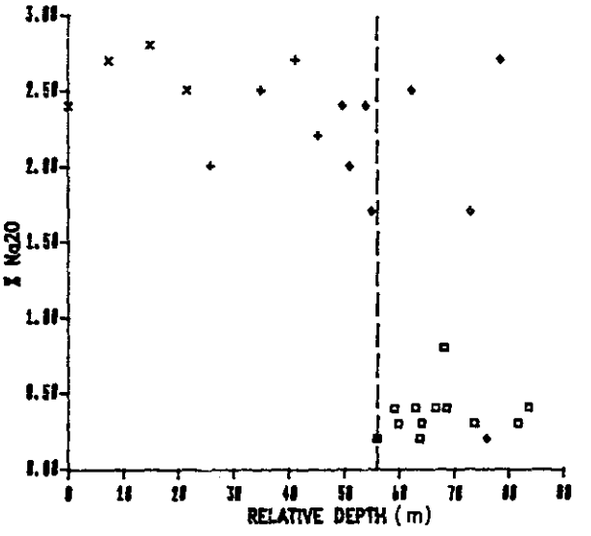
% Na20
RELATIVE DEPTH (m)

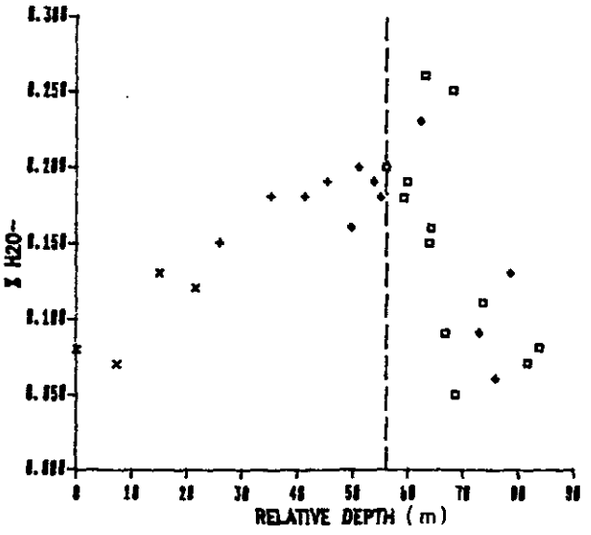
% H20-
RELATIVE DEPTH (m)

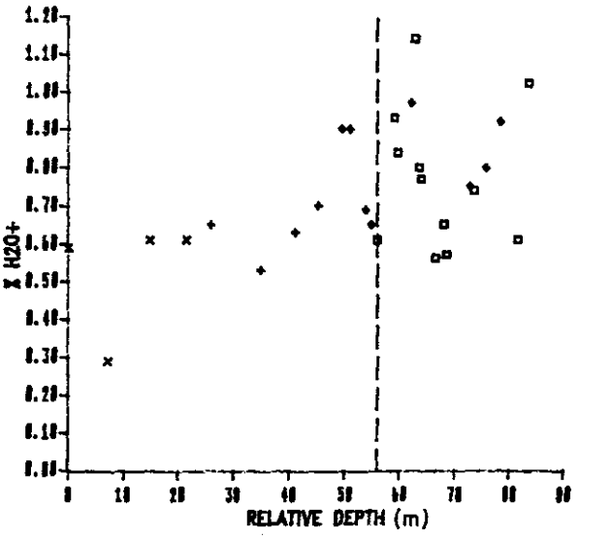
% H20+
RELATIVE DEPTH (m)

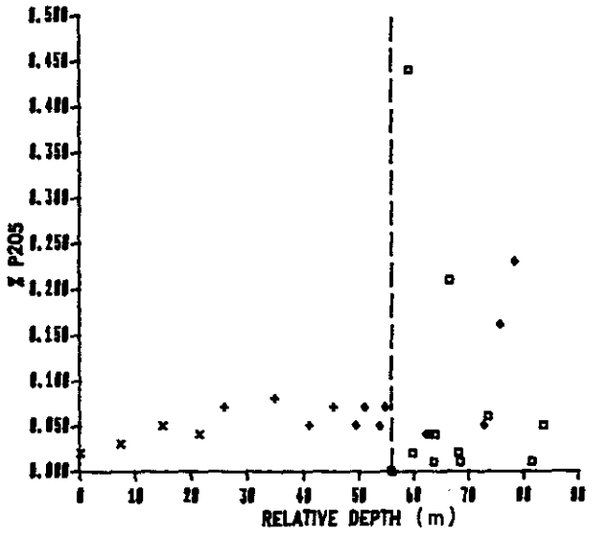
% P2O5
RELATIVE DEPTH (m)

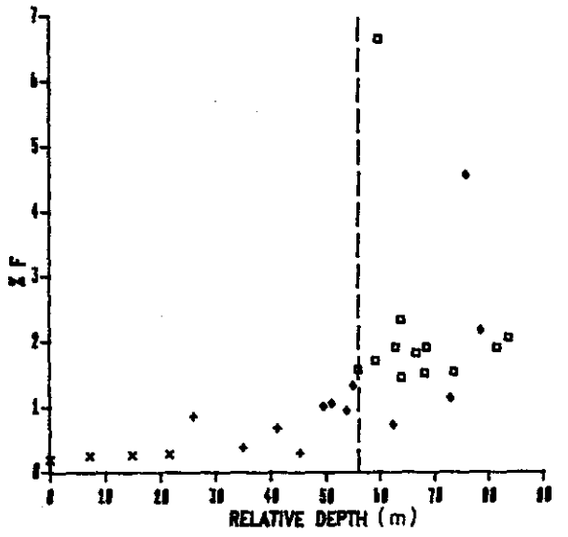
% F
RELATIVE DEPTH (m)

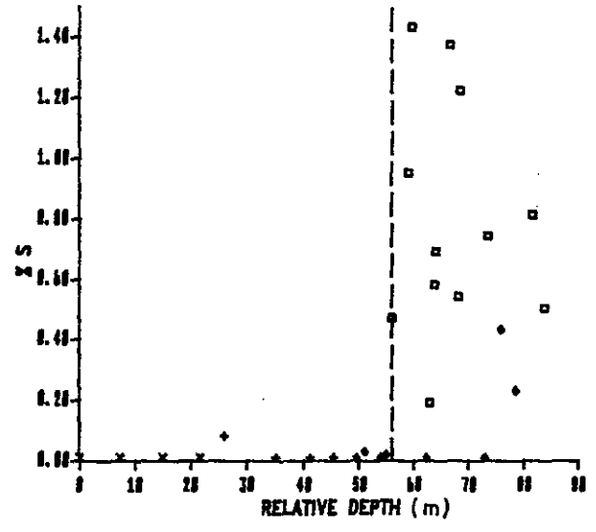
% S
RELATIVE DEPTH (m)

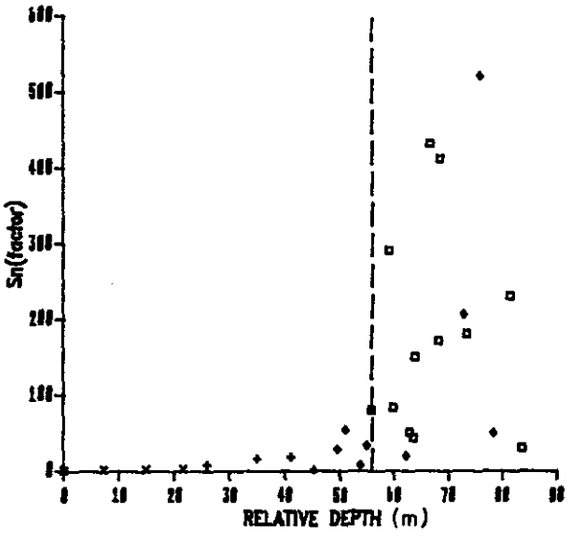
Sn(factor)
RELATIVE DEPTH (m)

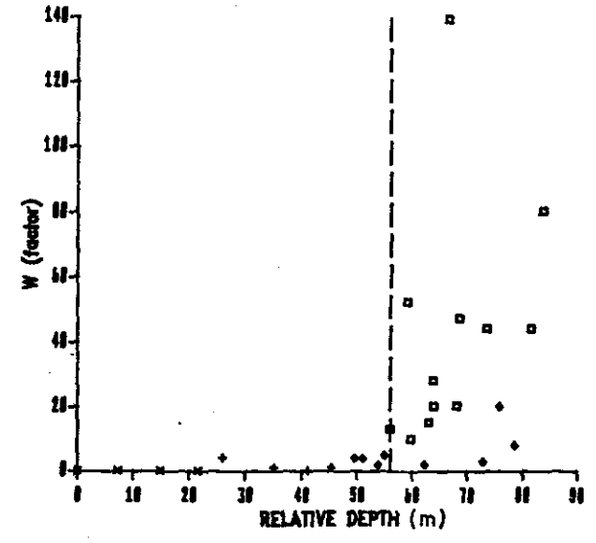
W (factor)
RELATIVE DEPTH (m)

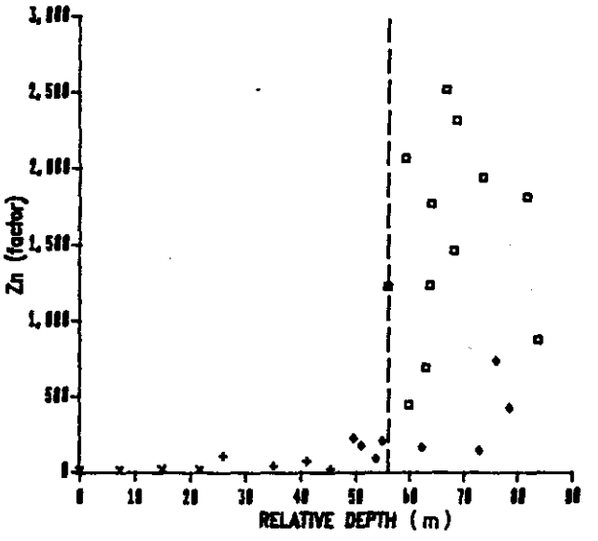
Zn (factor)
RELATIVE DEPTH (m)

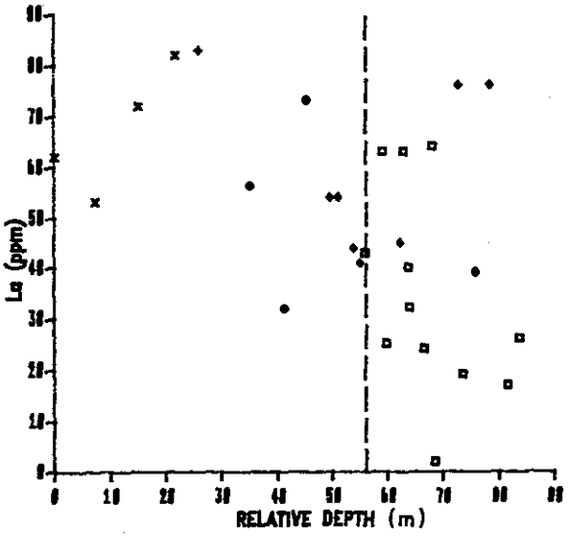
La (ppm)
RELATIVE DEPTH (m)

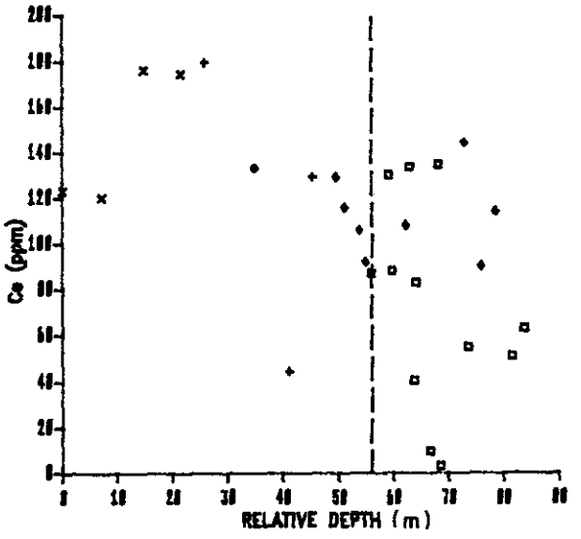
Ce (ppm)
RELATIVE DEPTH (m)

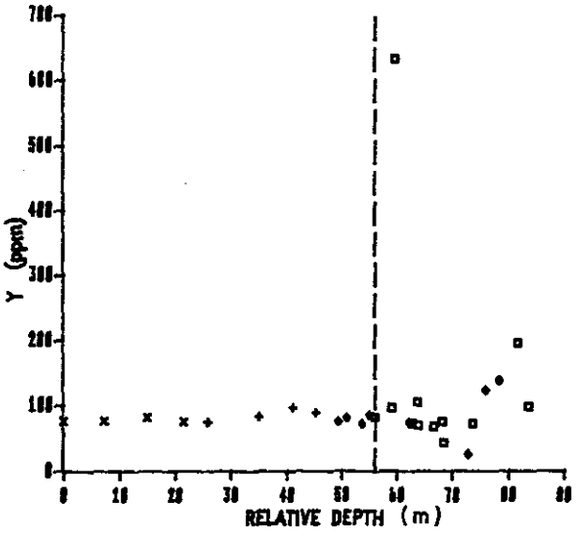
Y (ppm)
RELATIVE DEPTH (m)

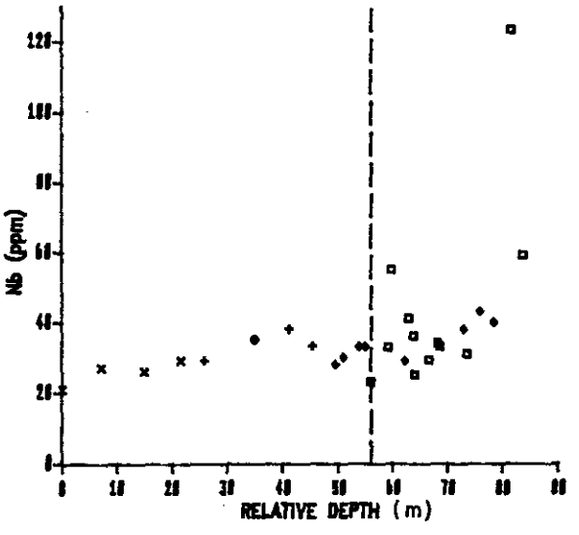
Nb (ppm)
RELATIVE DEPTH (m)

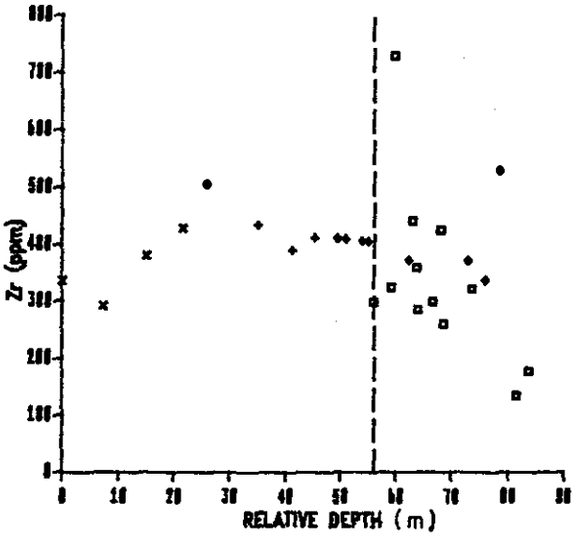
Zr (ppm)
RELATIVE DEPTH (m)

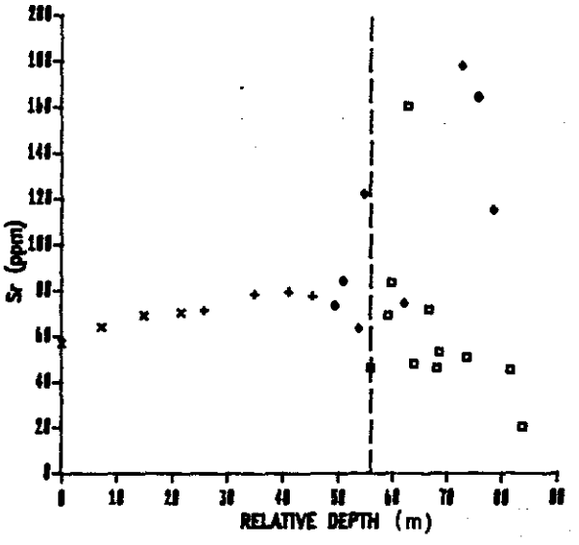
Sr (ppm)
RELATIVE DEPTH (m)

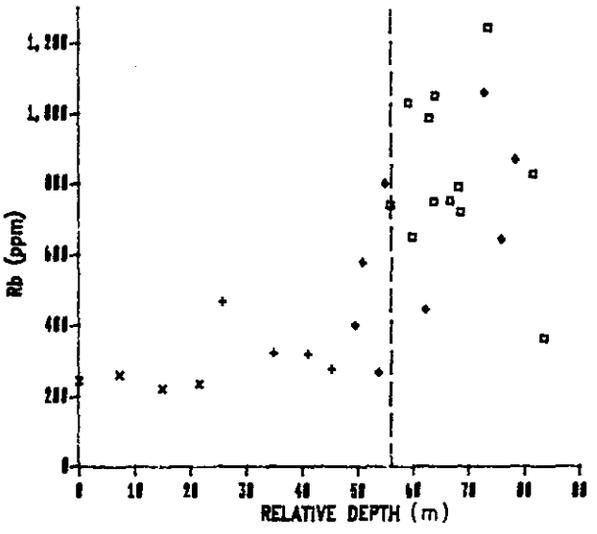
Rb (ppm)
RELATIVE DEPTH (m)

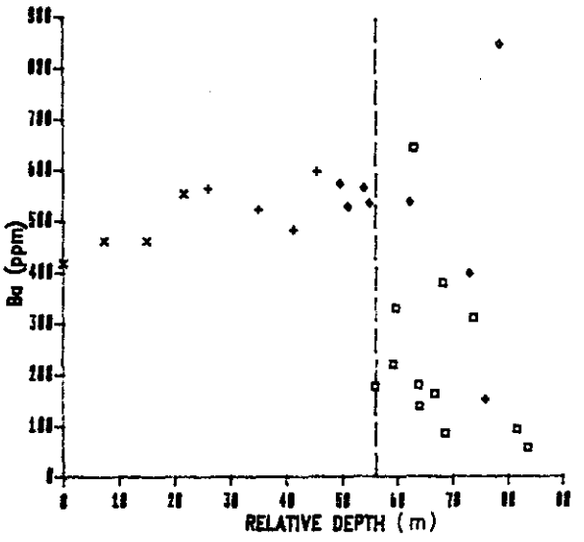
Ba (ppm)
RELATIVE DEPTH (m)

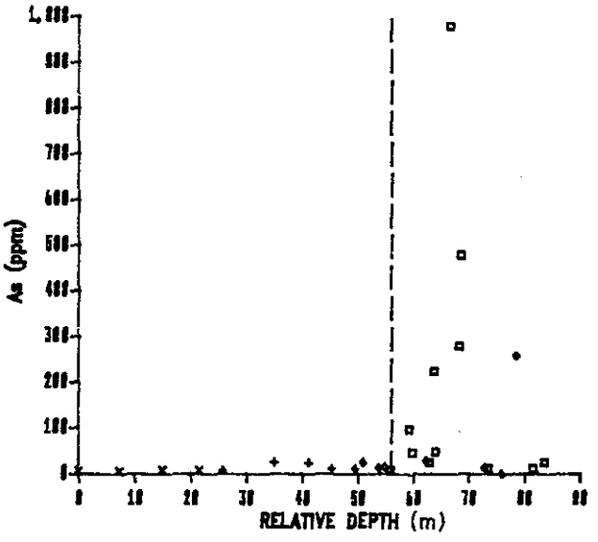
As (ppm)
RELATIVE DEPTH (m)

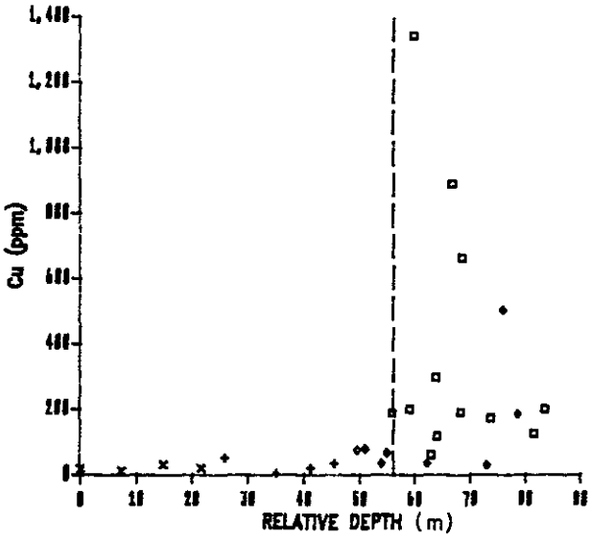
Cu (ppm)
RELATIVE DEPTH (m)

APPENDIX IV

Trace element correlations

LEGEND

- ● : TBQ
- • : Transition zone and granite gneiss lenses
- × : Granite gneiss

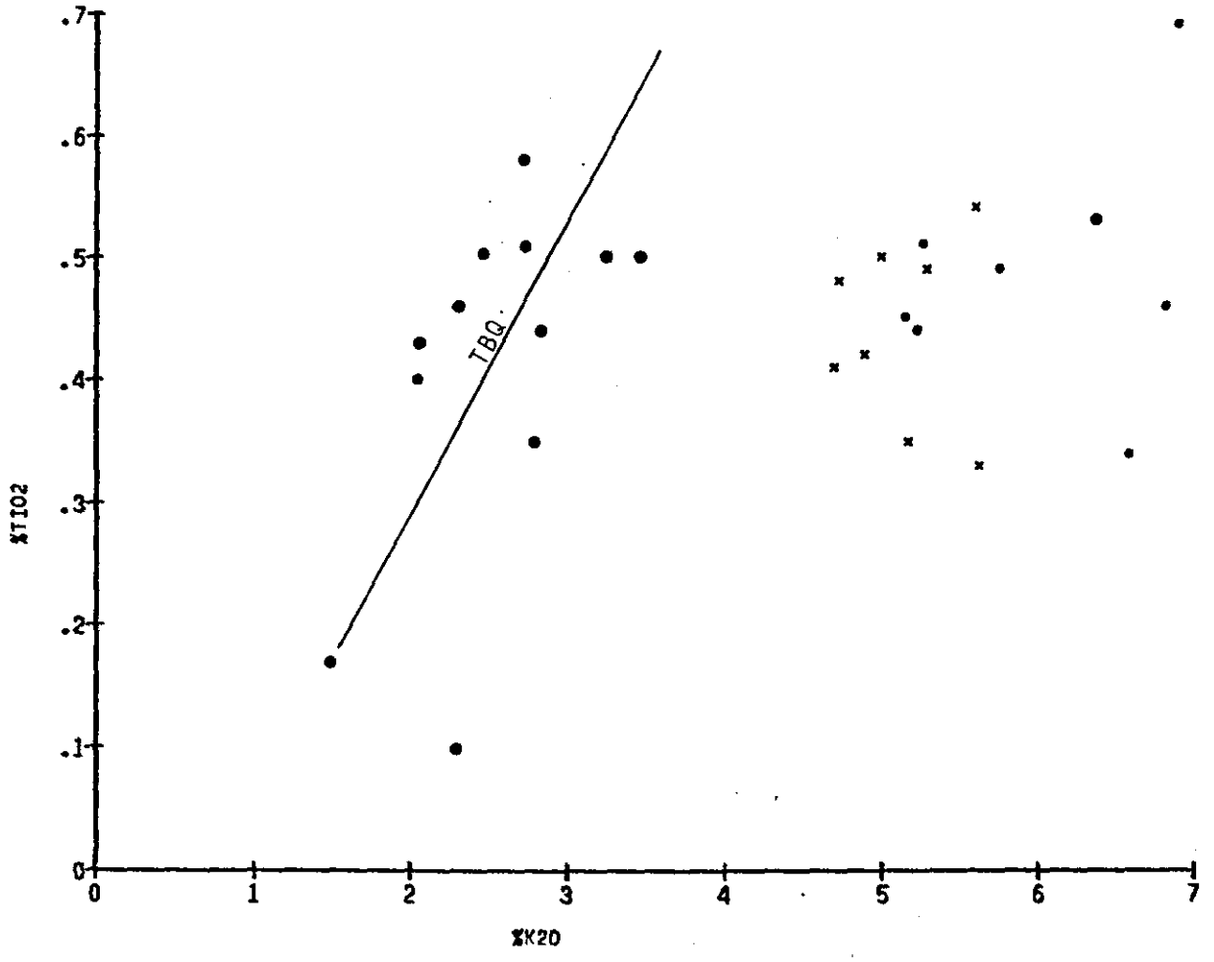
.7
.6
.5
.4
.3
.2
.1
0
0
1
2
3
4
5
6
7
%TIO2
%K2O
TBQ

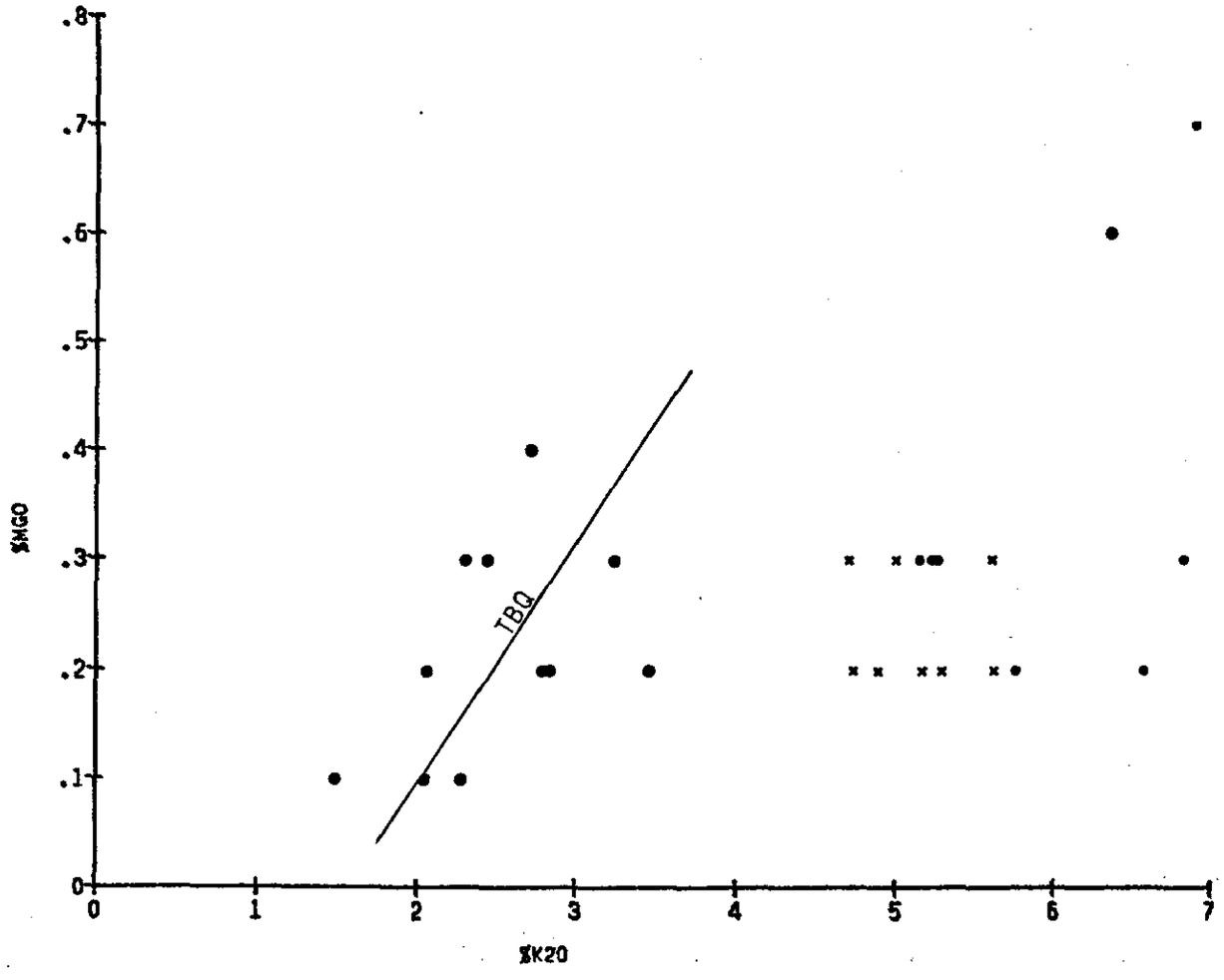
%MGO
%K2O
TBQ
0
.1
.2
.3
.4
.5
.6
.7
.8
1
2
3
4
5
6
7

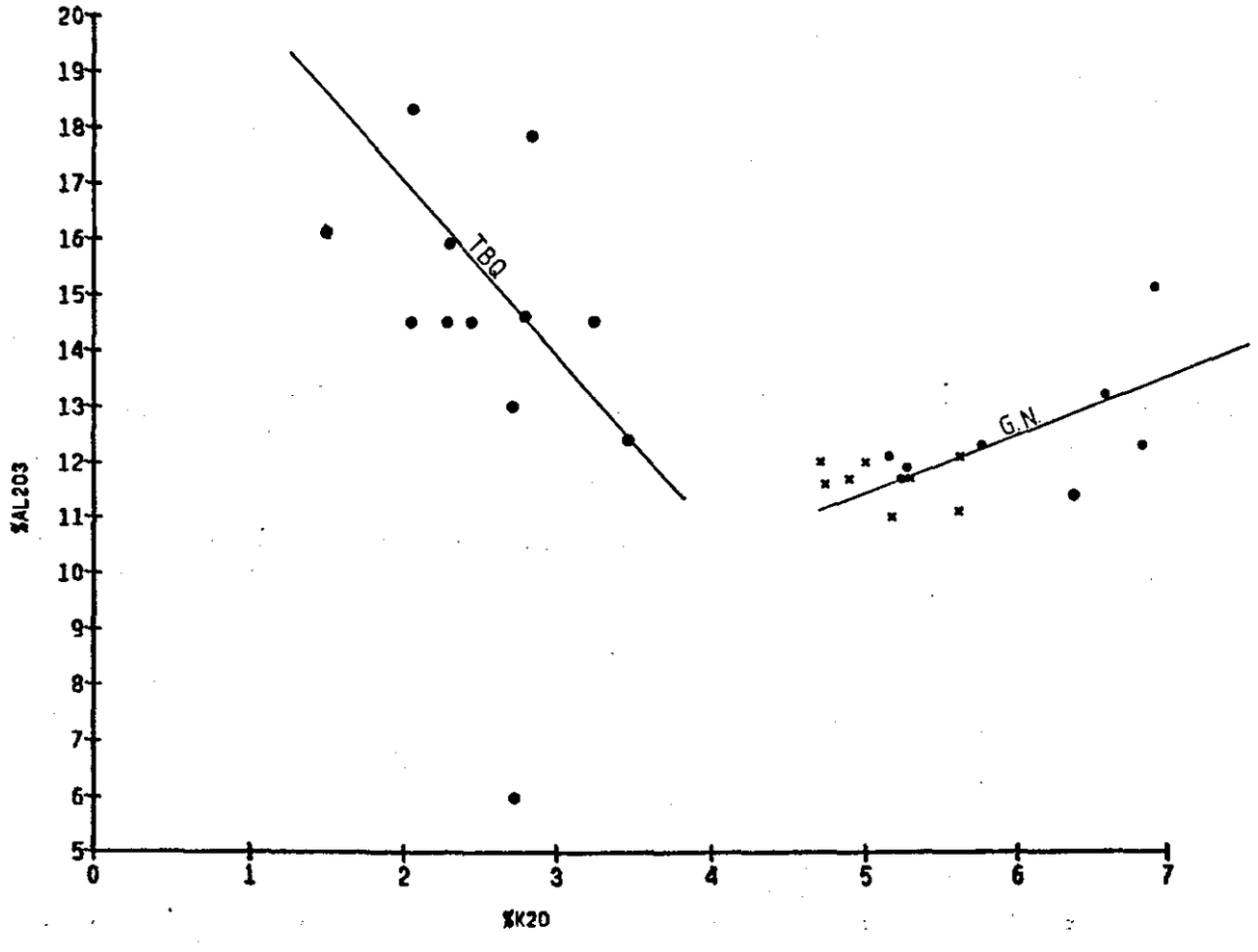
%AL2O3
%K2O
TBQ
G.N.
5
6
7
8
9
10
11
12
13
14
15
16
17
18
19
20
0
1
2
3
4
5
6
7

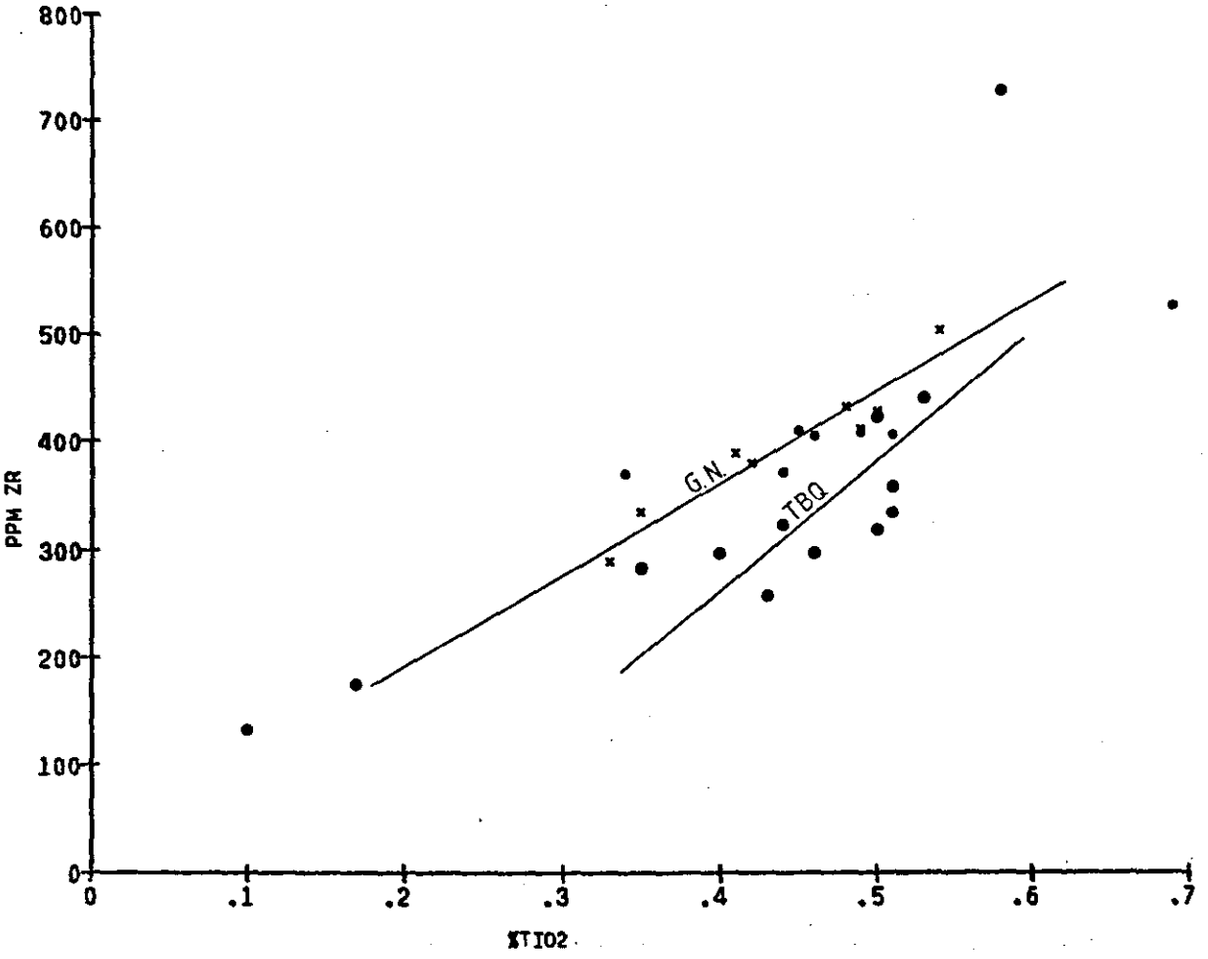
PPM ZR
%TIO2
G.N.
TBQ
0
100
200
300
400
500
600
700
800
.1
.2
.3
.4
.5
.6
.7

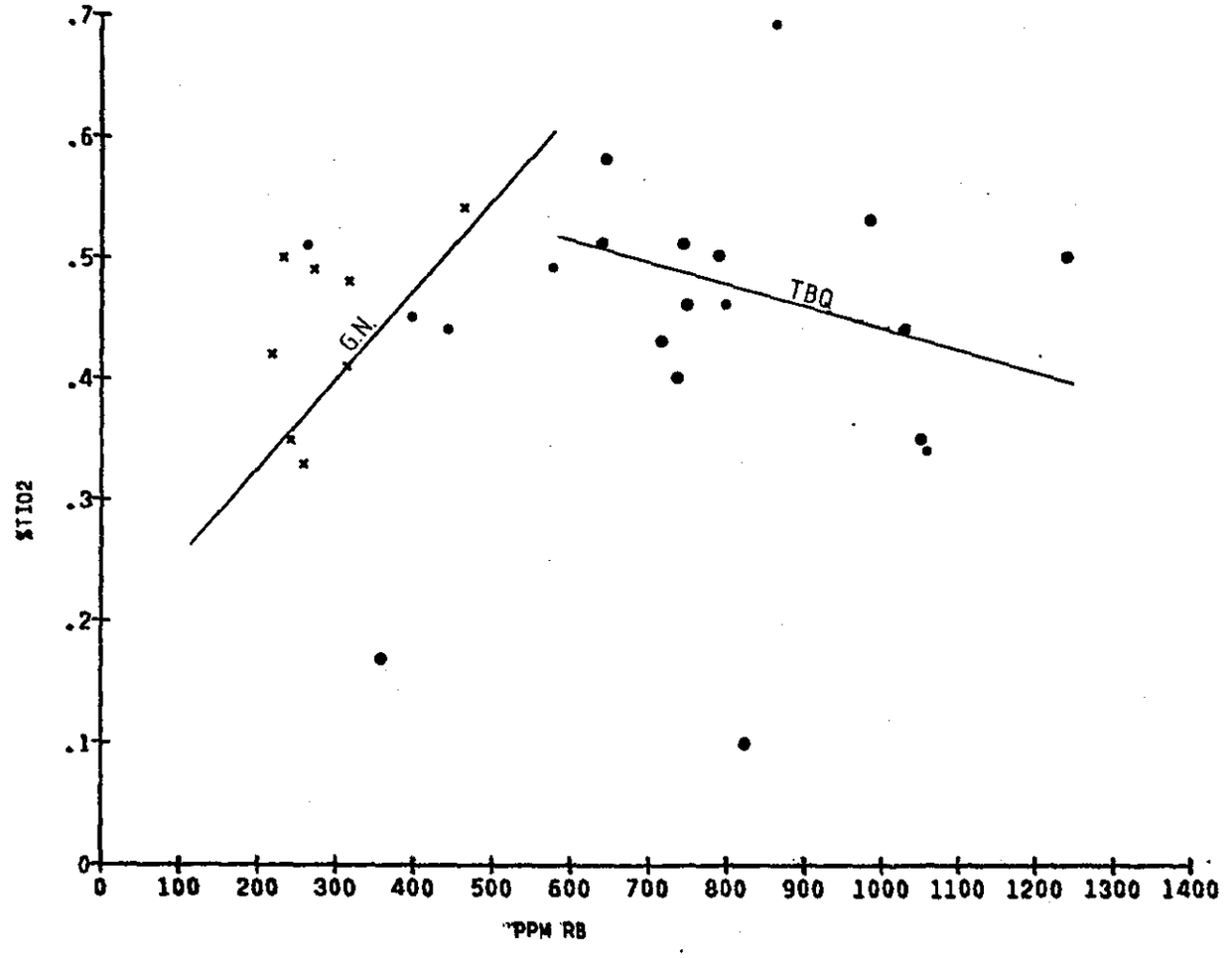
%TIO2
PPM RB
G.N.
TBQ
0
.1
.2
.3
.4
.5
.6
.7
100
200
300
400
500
600
700
800
900
1000
1100
1200
1300
1400

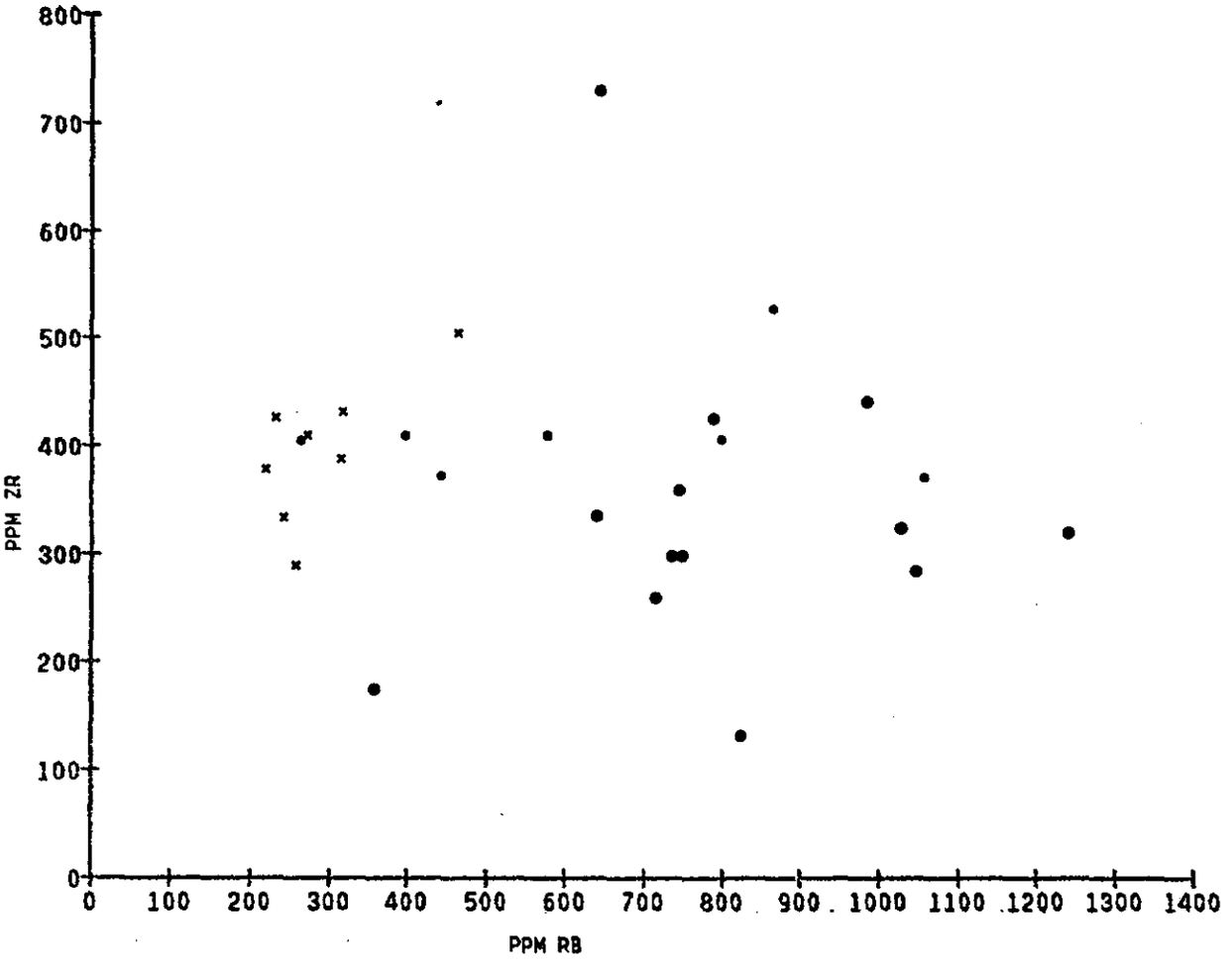
PPM ZR
PPM RB
0
100
200
300
400
500
600
700
800
900
1000
1100
1200
1300
1400

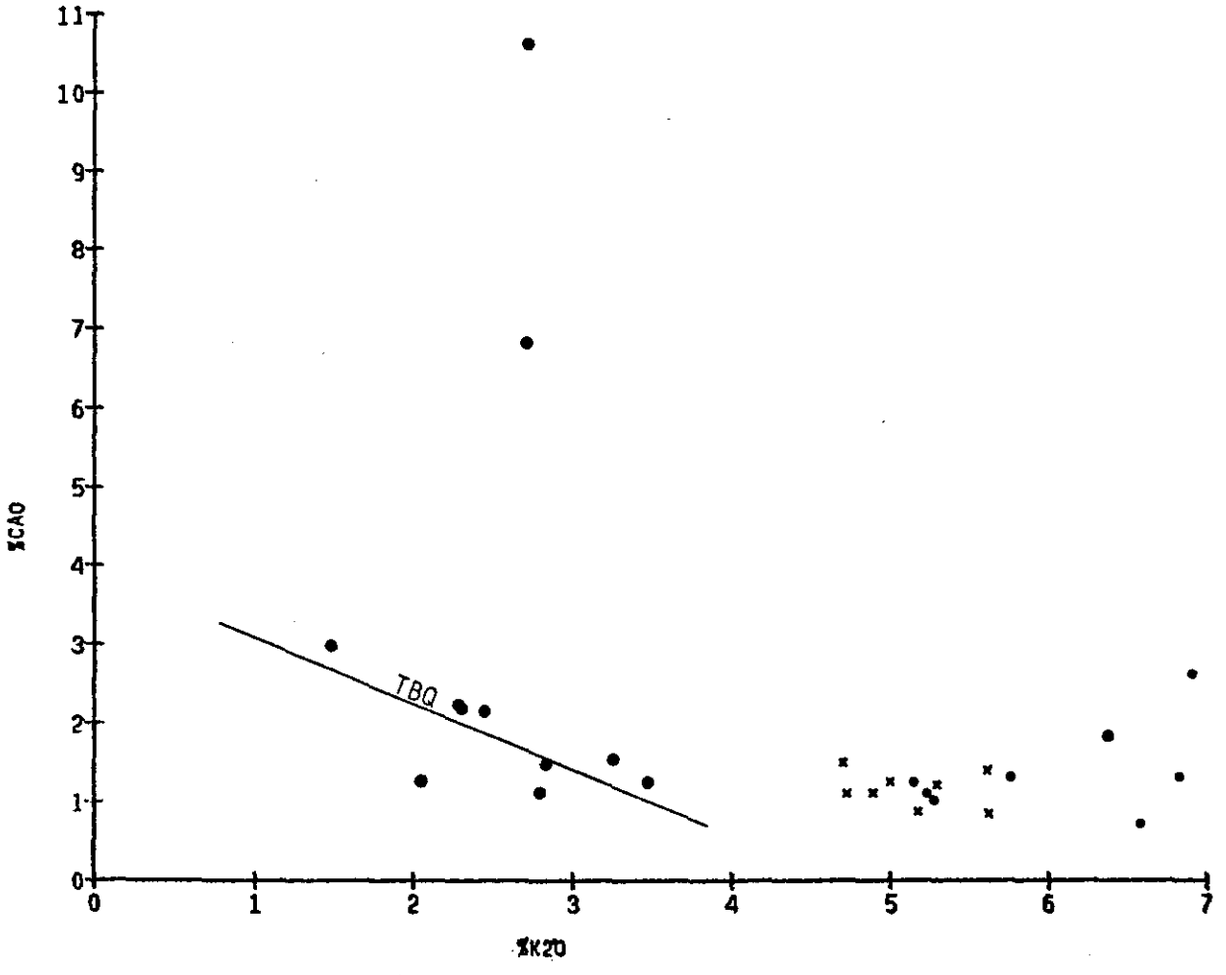
%CAO
%K2O
TBQ
0
1
2
3
4
5
6
7
8
9
10
11

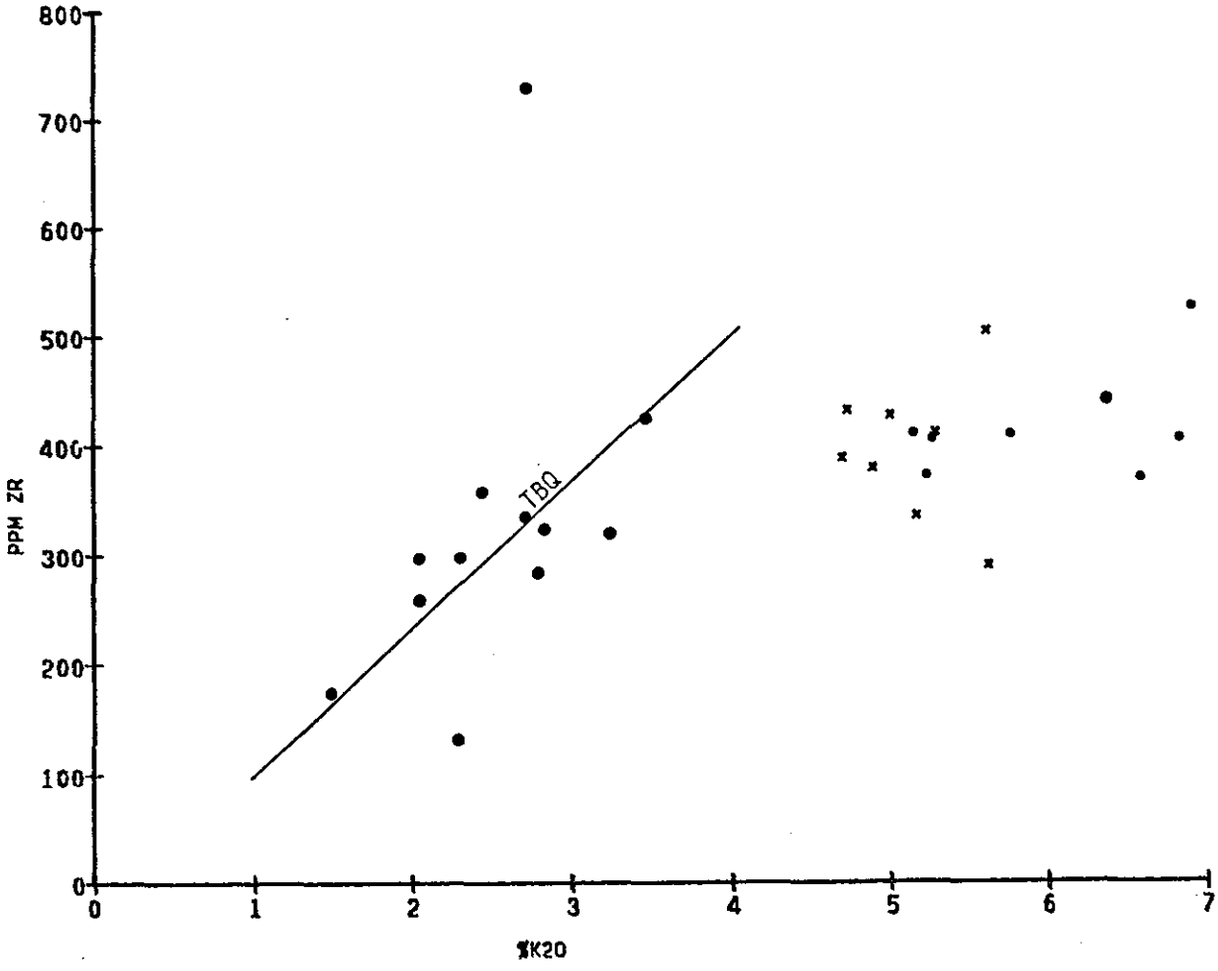
PPM ZR
%K2O
TBQ
0
100
200
300
400
500
600
700
800
0
1
2
3
4
5
6
7

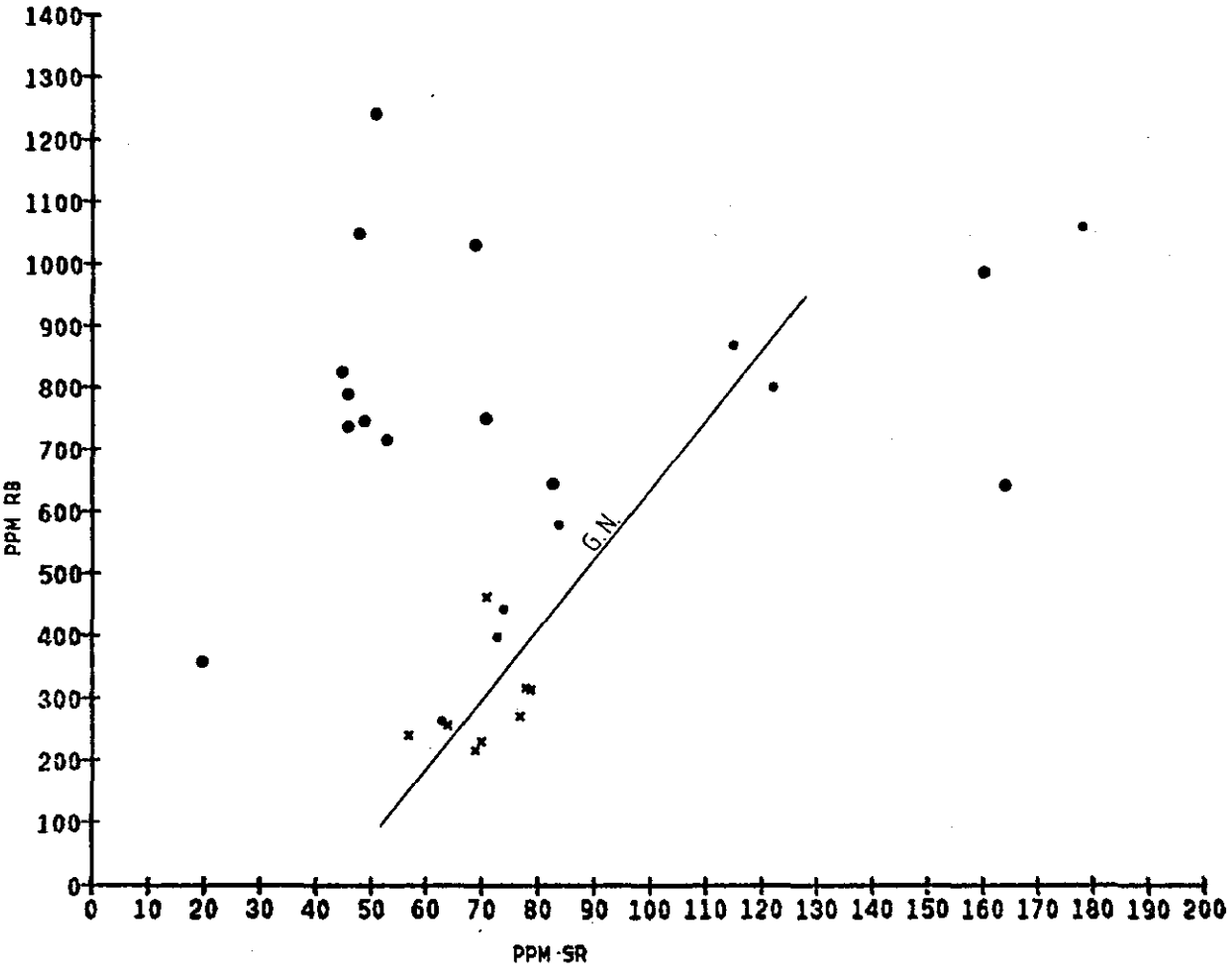
PPM RB
PPM SR
G.N.
0
100
200
300
400
500
600
700
800
900
1000
1100
1200
1300
1400
0
10
20
30
40
50
60
70
80
90
100
110
120
130
140
150
160
170
180
190
200

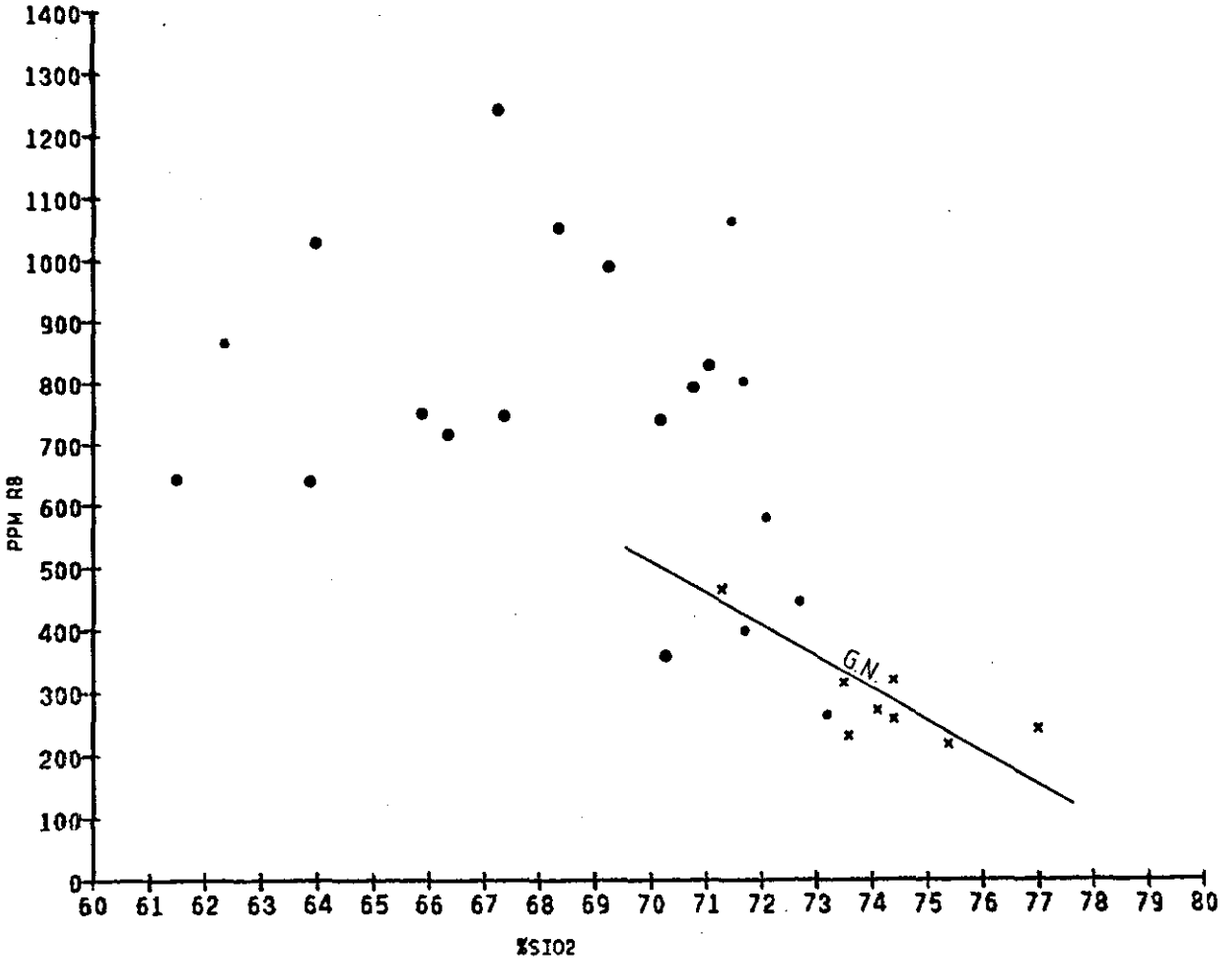
PPM RB
%SIO2
G.N.

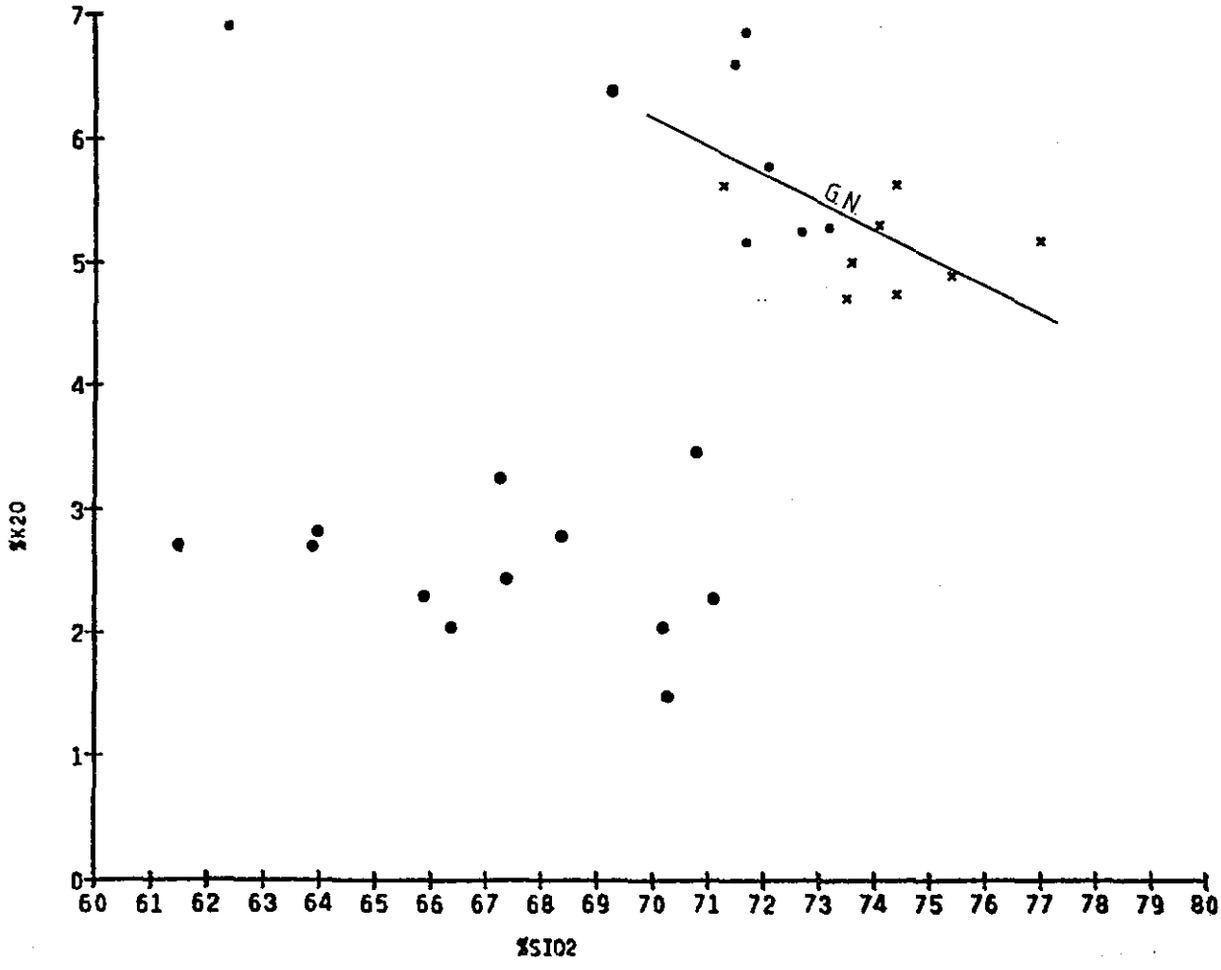
%K2O
%SIO2
G.N.

APPENDIX V

Niggli values and Niggli norms

NIGGLI-VALUES AND NIGGLI-NORM

SAMPLE NUMBER: AES/4/1

1.MASS PERCENTAGES OF OXIDES

SIO2	TIO2	AL2O3	CR2O3	FE2O3	FEO	MNO	MGO
CAO	NA2O	K2O	P2O5	CO2	H2O	H2O	S
67.300	0.500	14.500	0.000	0.270	6.100	0.470	0.300
1.560	0.300	3.250	0.060	0.000	0.740	0.110	0.740

2.NIGGLI-VALUES
AL= 45.62 FM= 32.83
C= 8.92 ALK= 12.62 SUM=100.00
SI= 359.4 K=0.88 MG=0.07 QZ= 208.9
AL/(C+ALK)= 2.12

3.CATION PERCENTAGES

68.124	0.429	17.295	0.000	0.206	5.162	0.403	0.452
1.691	0.588	4.195	0.051	0.000	0.000		

TOTAL = 100.000

4.NIGGLI-NORM
PHOS. NOT ALLOCATED TO CAO= 0.000
CO2 NOT ALLOC. TO CAO = 0.000
CALCITE= 0.000 APATITE= 0.137 PYRITE= 2.105 ILMENITE= 0.857
ORTHOCLASE 0.000 ALBITE= 2.942 ANORTHITE 8.027
BIOTITE= 15.309 MUSCOVITE= 15.972

DIOPSIDE= 0.000 EN= 0.000 FS= 0.000 WO= 0.000 HYPERSTHENE 0.000 FS= 0.000 EN= 0.000

OLIVINE= 0.000 FO= 0.000 FA= 0.000

LEUCITE= 0.000 NEPHELINE 0.000 AKMITE= 0.000
CORUND. 2.823 OR SILLIMANITE= 4.235

CHROMITE= 0.000 MAGNETITE= 0.308 HEMATITE= 0.000
RUTILE= 0.000 TITANITE= 0.000

SODIUM METASILICATE = 0.000 KALIOPHILITE= 0.000
WOLASTONITE= 0.000

QUARTZ(IF CORUNDUM IS USED)= 51.519
QUARTZ(IF SILLIMANITE IS USED)= 50.107
DIFF. SIO2= 0.000 TOTAL =100.000

%AN IN PLAGIOCLASE=73.2
FELDSPAR RATIO :%OR= 0.0 %AB= 26.8 %AN= 73.2
RESIDUA:OR= 0.0 AB= 5.5 QZ= 94.5
MUSCOVITE FACT. 17.9
DE LA ROCHE-VALUES : R1= 3593.0 R2= 489.0

NIGGLI-VALUES AND NIGGLI-NORM

SAMPLE NUMBER: AES/4/2

1.MASS PERCENTAGES OF OXIDES

SIO2	TIO2	AL2O3	CR2O3	FE2O3	FEO	MNO	MGO
CAO	NA2O	K2O	P2O5	CO2	H2O	H2O	S
70.800	0.500	12.400	0.000	0.210	5.300	0.180	0.200
1.270	0.800	3.470	0.020	0.000	0.650	0.250	0.540

2.NIGGLI-VALUES
AL= 43.77 FM= 30.19
C= 8.15 ALK= 17.90 SUM=100.00
SI= 424.1 K=0.74 MG=0.06 QZ= 252.5
AL/(C+ALK)= 1.68

3.CATION PERCENTAGES

71.344	0.427	14.724	0.000	0.159	4.465	0.154	0.300
1.371	1.562	4.459	0.017	0.000	0.000		

TOTAL = 100.000

4.NIGGLI-NORM
PHOS. NOT ALLOCATED TO CAO= 0.000
CO2 NOT ALLOC. TO CAO = 0.000
CALCITE= 0.000 APATITE= 0.045 PYRITE= 1.529 ILMENITE= 0.854
ORTHOCLASE 3.347 ALBITE= 7.810 ANORTHITE 6.711
BIOTITE= 12.488 MUSCOVITE= 15.600

DIOPSIDE= 0.000 EN= 0.000 FS= 0.000 WO= 0.000 HYPERSTHENE 0.000 FS= 0.000 EN= 0.000

OLIVINE= 0.000 FO= 0.000 FA= 0.000

LEUCITE= 0.000 NEPHELINE 0.000 AKMITE= 0.000
CORUND. 0.000 OR SILLIMANITE= 0.000

CHROMITE= 0.000 MAGNETITE= 0.239 HEMATITE= 0.000
RUTILE= 0.000 TITANITE= 0.000

SODIUM METASILICATE = 0.000 KALIOPHILITE= 0.000
WOLASTONITE= 0.000

QUARTZ(IF CORUNDUM IS USED)= 51.376
QUARTZ(IF SILLIMANITE IS USED)= 51.376
DIFF. SIO2= 0.000 TOTAL =100.000

%AN IN PLAGIOCLASE=46.2
FELDSPAR RATIO :%OR= 18.7 %AB= 43.7 %AN= 37.6
RESIDUA:OR= 5.4 AB= 12.5 QZ= 82.2
MUSCOVITE FACT. 25.2
DE LA ROCHE-VALUES : R1= 3609.6 R2= 406.6

SAMPLE NUMBER: AES/4/3

1.MASS PERCENTAGES OF OXIDES

SIO2	TIO2	AL2O3	CR2O3	FE2O3	FEO	MNO	MGO
CAO	NA2O	K2O	P2O5	CO2	H2O	H2O	S
68.400	0.350	14.600	0.000	0.360	5.400	0.540	0.200
1.140	0.300	2.800	0.040	0.000	0.770	0.160	0.690

2.NIGGLI-VALUES
AL= 49.32 FM= 31.77
C= 7.00 ALK= 11.90 SUM=100.00
SI= 392.2 K=0.86 MG=0.05 QZ= 244.6
AL/(C+ALK)= 2.61

3.CATION PERCENTAGES

69.696	0.302	17.530	0.000	0.276	4.600	0.466	0.304
1.244	0.592	3.638	0.034	0.000	0.000		

TOTAL = 100.000

4.NIGGLI-NORM
PHOS. NOT ALLOCATED TO CAO= 0.000
CO2 NOT ALLOC. TO CAO = 0.000
CALCITE= 0.000 APATITE= 0.092 PYRITE= 1.976 ILMENITE= 0.604
ORTHOCLASE 0.000 ALBITE= 2.961 ANORTHITE 5.933
BIOTITE= 13.667 MUSCOVITE= 13.510

DIOPSIDE= 0.000 EN= 0.000 FS= 0.000 WO= 0.000 HYPERSTHENE 0.000 FS= 0.000 EN= 0.000

OLIVINE= 0.000 FO= 0.000 FA= 0.000

LEUCITE= 0.000 NEPHELINE 0.000 AKMITE= 0.000
CORUND. 5.358 OR SILLIMANITE= 8.036

CHROMITE= 0.000 MAGNETITE= 0.414 HEMATITE= 0.000
RUTILE= 0.000 TITANITE= 0.000

SODIUM METASILICATE = 0.000 KALIOPHILITE= 0.000
WOLASTONITE= 0.000

QUARTZ(IF CORUNDUM IS USED)= 55.485
QUARTZ(IF SILLIMANITE IS USED)= 52.806
DIFF. SIO2= 0.000 TOTAL =100.000

%AN IN PLAGIOCLASE=66.7
FELDSPAR RATIO :%OR= 0.0 %AB= 33.3 %AN= 66.7
RESIDUA:OR= 0.0 AB= 5.3 QZ= 94.7
MUSCOVITE FACT. 16.8
DE LA ROCHE-VALUES : R1= 3823.8 R2= 441.2

SAMPLE NUMBER: AES/4/4

1.MASS PERCENTAGES OF OXIDES

SIO2	TIO2	AL2O3	CR2O3	FE2O3	FEO	MNO	MGO
CAO	NA2O	K2O	P2O5	CO2	H2O	H2O	S
64.000	0.440	17.800	0.000	0.730	5.900	0.410	0.200
1.500	0.400	2.840	0.440	0.000	0.930	0.180	0.950

2.NIGGLI-VALUES
AL= 51.36 FM= 30.01
C= 7.87 ALK= 10.77 SUM=100.00
SI= 313.4 K=0.82 MG=0.05 QZ= 170.4
AL/(C+ALK)= 2.76

3.CATION PERCENTAGES

64.238	0.374	21.053	0.000	0.551	4.951	0.348	0.299
1.612	0.778	3.635	0.374	0.000	0.000		

TOTAL = 100.000

4.NIGGLI-NORM
PHOS. NOT ALLOCATED TO CAO= 0.000
CO2 NOT ALLOC. TO CAO = 0.000
CALCITE= 0.000 APATITE= 0.997 PYRITE= 2.679 ILMENITE= 0.748
ORTHOCLASE 0.000 ALBITE= 3.890 ANORTHITE 4.947
BIOTITE= 12.978 MUSCOVITE= 14.091

DIOPSIDE= 0.000 EN= 0.000 FS= 0.000 WO= 0.000 HYPERSTHENE 0.000 FS= 0.000 EN= 0.000

OLIVINE= 0.000 FO= 0.000 FA= 0.000

LEUCITE= 0.000 NEPHELINE 0.000 AKMITE= 0.000
CORUND. 9.012 OR SILLIMANITE= 13.518

CHROMITE= 0.000 MAGNETITE= 0.827 HEMATITE= 0.000
RUTILE= 0.000 TITANITE= 0.000

SODIUM METASILICATE = 0.000 KALIOPHILITE= 0.000
WOLASTONITE= 0.000

QUARTZ(IF CORUNDUM IS USED)= 49.831
QUARTZ(IF SILLIMANITE IS USED)= 45.325
DIFF. SIO2= 0.000 TOTAL =100.000

%AN IN PLAGIOCLASE=56.0
FELDSPAR RATIO :%OR= 0.0 %AB= 44.0 %AN= 56.0
RESIDUA:OR= 0.0 AB= 7.9 QZ= 92.1
MUSCOVITE FACT. 20.1
DE LA ROCHE-VALUES : R1= 3412.0 R2= 543.5

NIGGLI-VALUES AND NIGGLI-NORM

SAMPLE NUMBER: AES/4/5

1.MASS PERCENTAGES OF OXIDES

SIO2	TIO2	AL2O3	CR2O3	FE2O3	FEO	MNO	MGO
CAO	NA2O	K2O	P2O5	CO2	H2O	H2O	S
71.700	0.460	12.300	0.000	0.060	3.400	0.090	0.300
1.320	1.700	6.830	0.070	0.000	0.650	0.180	0.020

2.NIGGLI-VALUES
AL= 40.10 FM= 18.87
C= 7.82 ALK= 33.21 SUM=100.00
SI= 396.7 K=0.73 MG=0.13 QZ= 163.9
AL/(C+ALK)= 0.98

3.CATION PERCENTAGES

69.270	0.376	14.002	0.000	0.044	2.746	0.074	0.432
1.366	3.182	8.415	0.057	0.000	0.000		

TOTAL = 100.000

4.NIGGLI-NORM
PHOS. NOT ALLOCATED TO CAO= 0.000
CO2 NOT ALLOC. TO CAO = 0.000
CALCITE= 0.000 APATITE= 0.153 PYRITE= 0.054 ILMENITE= 0.753
ORTHOCLASE 42.074 ALBITE= 15.911 ANORTHITE 6.013
BIOTITE= 0.000 MUSCOVITE= 0.000

DIOPSIDE= 0.271 EN= 0.021 FS= 0.115 WO= 0.136 HYPERSTHENE 5.535 FS= 4.692 EN= 0.843

OLIVINE= 0.000 FO= 0.000 FA= 0.000

LEUCITE= 0.000 NEPHELINE 0.000 AKMITE= 0.000
CORUND. 0.000 OR SILLIMANITE= 0.000

CHROMITE= 0.000 MAGNETITE= 0.065 HEMATITE= 0.000
RUTILE= 0.000 TITANITE= 0.000

SODIUM METASILICATE = 0.000 KALIOPHILITE= 0.000
WOLASTONITE= 0.000

QUARTZ(IF CORUNDUM IS USED)= 29.170
QUARTZ(IF SILLIMANITE IS USED)= 29.170
DIFF. SIO2= 0.000 TOTAL =100.000

%AN IN PLAGIOCLASE=27.4
FELDSPAR RATIO :%OR= 65.7 %AB= 24.9 %AN= 9.4
RESIDUA:OR= 48.3 AB= 18.3 QZ= 33.5
MUSCOVITE FACT. 0.0
DE LA ROCHE-VALUES : R1= 2511.5 R2= 404.5

NIGGLI-VALUES AND NIGGLI-NORM

SAMPLE NUMBER: AES/4/6

1.MASS PERCENTAGES OF OXIDES

SIO2	TIO2	AL2O3	CR2O3	FE2O3	FEO	MNO	MGO
CAO	NA2O	K2O	P2O5	CO2	H2O	H2O	S
71.700	0.450	12.100	0.000	0.030	3.300	0.050	0.300
1.260	2.400	5.150	0.050	0.000	0.900	0.160	0.010

2.NIGGLI-VALUES
AL= 41.07 FM= 18.84
C= 7.77 ALK= 32.31 SUM=100.00
SI= 413.1 K=0.59 MG=0.14 QZ= 183.8
AL/(C+ALK)= 1.02

3.CATION PERCENTAGES

70.131	0.373	13.946	0.000	0.022	2.698	0.041	0.437
1.320	4.548	6.424	0.041	0.000	0.000		

TOTAL = 100.000

4.NIGGLI-NORM
PHOS. NOT ALLOCATED TO CAO= 0.000
CO2 NOT ALLOC. TO CAO = 0.000
CALCITE= 0.000 APATITE= 0.110 PYRITE= 0.027 ILMENITE= 0.746
ORTHOCLASE 29.761 ALBITE= 22.742 ANORTHITE 6.255
BIOTITE= 3.773 MUSCOVITE= 0.000

DIOPSIDE= 0.000 EN= 0.000 FS= 0.000 WO= 0.000 HYPERSTHENE 3.209 FS= 2.706 EN= 0.504

OLIVINE= 0.000 FO= 0.000 FA= 0.000

LEUCITE= 0.000 NEPHELINE 0.000 AKMITE= 0.000
CORUND. 0.000 OR SILLIMANITE= 0.000

CHROMITE= 0.000 MAGNETITE= 0.033 HEMATITE= 0.000
RUTILE= 0.000 TITANITE= 0.000

SODIUM METASILICATE = 0.000 KALIOPHILITE= 0.000
WOLASTONITE= 0.000

QUARTZ(IF CORUNDUM IS USED)= 33.343
QUARTZ(IF SILLIMANITE IS USED)= 33.343
DIFF. SIO2= 0.000 TOTAL =100.000

%AN IN PLAGIOCLASE=21.6
FELDSPAR RATIO :%OR= 50.7 %AB= 38.7 %AN= 10.6
RESIDUA:OR= 34.7 AB= 26.5 QZ= 38.8
MUSCOVITE FACT. 0.0
DE LA ROCHE-VALUES : R1= 2701.8 R2= 399.9

SAMPLE NUMBER: AES/4/7

1.MASS PERCENTAGES OF OXIDES

SIO2	TIO2	AL2O3	CR2O3	FE2O3	FEO	MNO	MGO
CAO	NA2O	K2O	P2O5	CO2	H2O	H2O	S
73.500	0.410	12.000	0.000	0.200	3.000	0.030	0.300
1.520	2.700	4.700	0.050	0.000	0.630	0.180	0.000

2.NIGGLI-VALUES
AL= 40.54 FM= 17.95
C= 9.33 ALK= 32.18 SUM=100.00
SI= 421.4 K=0.53 MG=0.14 QZ= 192.7
AL/(C+ALK)= 0.98

3.CATION PERCENTAGES

70.664	0.334	13.594	0.000	0.145	2.411	0.024	0.430
1.565	5.030	5.762	0.041	0.000	0.000		

TOTAL = 100.000

4.NIGGLI-NORM
PHOS. NOT ALLOCATED TO CAO= 0.000
CO2 NOT ALLOC. TO CAO = 0.000
CALCITE= 0.000 APATITE= 0.108 PYRITE= 0.000 ILMENITE= 0.668
ORTHOCLASE 28.812 ALBITE= 25.148 ANORTHITE 7.006
BIOTITE= 0.000 MUSCOVITE= 0.000

DIOPSIDE= 0.384 EN= 0.034 FS= 0.159 WO= 0.192 HYPERSTHENE 4.726 FS= 3.900 EN= 0.826

OLIVINE= 0.000 FO= 0.000 FA= 0.000

LEUCITE= 0.000 NEPHELINE 0.000 AKMITE= 0.000
CORUND. 0.000 OR SILLIMANITE= 0.000

CHROMITE= 0.000 MAGNETITE= 0.217 HEMATITE= 0.000
RUTILE= 0.000 TITANITE= 0.000

SODIUM METASILICATE = 0.000 KALIOPHILITE= 0.000
WOLASTONITE= 0.000

QUARTZ(IF CORUNDUM IS USED)= 32.930
QUARTZ(IF SILLIMANITE IS USED)= 32.930
DIFF. SIO2= 0.000 TOTAL =100.000

%AN IN PLAGIOCLASE=21.8
FELDSPAR RATIO :%OR= 47.3 %AB= 41.2 %AN= 11.5
RESIDUA:OR= 33.2 AB= 28.9 QZ= 37.9
MUSCOVITE FACT. 0.0
DE LA ROCHE-VALUES : R1= 2783.3 R2= 419.6

SAMPLE NUMBER: AES/4/8

1.MASS PERCENTAGES OF OXIDES

SIO2	TIO2	AL2O3	CR2O3	FE2O3	FEO	MNO	MGO
CAO	NA2O	K2O	P2O5	CO2	H2O	H2O	S
74.400	0.480	11.600	0.000	0.490	3.350	0.070	0.200
1.130	2.500	4.730	0.080	0.000	0.530	0.180	0.000

2.NIGGLI-VALUES
AL= 40.18 FM= 20.73
C= 7.12 ALK= 31.97 SUM=100.00
SI= 437.4 K=0.55 MG=0.08 QZ= 209.5
AL/(C+ALK)= 1.03

3.CATION PERCENTAGES

71.432	0.390	13.123	0.000	0.354	2.689	0.057	0.286
1.162	4.651	5.791	0.065	0.000	0.000		

TOTAL = 100.000

4.NIGGLI-NORM
PHOS. NOT ALLOCATED TO CAO= 0.000
CO2 NOT ALLOC. TO CAO = 0.000
CALCITE= 0.000 APATITE= 0.173 PYRITE= 0.000 ILMENITE= 0.781
ORTHOCLASE 26.086 ALBITE= 23.254 ANORTHITE 5.268
BIOTITE= 4.593 MUSCOVITE= 0.000

DIOPSIDE= 0.000 EN= 0.000 FS= 0.000 WO= 0.000 HYPERSTHENE 2.058 FS= 1.819 EN= 0.239

OLIVINE= 0.000 FO= 0.000 FA= 0.000

LEUCITE= 0.000 NEPHELINE 0.000 AKMITE= 0.000
CORUND. 0.000 OR SILLIMANITE= 0.000

CHROMITE= 0.000 MAGNETITE= 0.531 HEMATITE= 0.000
RUTILE= 0.000 TITANITE= 0.000

SODIUM METASILICATE = 0.000 KALIOPHILITE= 0.000
WOLASTONITE= 0.000

QUARTZ(IF CORUNDUM IS USED)= 37.256
QUARTZ(IF SILLIMANITE IS USED)= 37.256
DIFF. SIO2= 0.000 TOTAL =100.000

%AN IN PLAGIOCLASE=18.5
FELDSPAR RATIO :%OR= 47.8 %AB= 42.6 %AN= 9.6
RESIDUA:OR= 30.1 AB= 26.9 QZ= 43.0
MUSCOVITE FACT. 0.0
DE LA ROCHE-VALUES : R1= 2871.9 R2= 361.9

NIGGLI-VALUES AND NIGGLI-NORM

SAMPLE NUMBER: AES/4/9

1.MASS PERCENTAGES OF OXIDES

SIO2	TIO2	AL203	CR203	FE203	FEO	MNO	MGO
CAO	NA20	K20	P205	CO2	H20	H20	S
71.300	0.540	11.100	0.000	0.540	4.050	0.070	0.300
1.410	2.000	5.610	0.070	0.000	0.650	0.150	0.080

2.NIGGLI-VALUES
AL= 36.61 FM= 24.06
C= 8.45 ALK= 30.87 SUM=100.00
SI= 399.2 K=0.65 MG=0.10 QZ= 175.7
AL/(C+ALK)= 0.93

3.CATION PERCENTAGES

69.982	0.449	12.838	0.000	0.399	3.323	0.058	0.439
1.482	3.804	7.022	0.058	0.000	0.000		

TOTAL = 100.000

4.NIGGLI-NORM
PHOS. NOT ALLOCATED TO CAO= 0.000
CO2 NOT ALLOC. TO CAO = 0.000
CALCITE= 0.000 APATITE= 0.155 PYRITE= 0.221 ILMENITE= 0.898
ORTHOCLASE 35.110 ALBITE= 19.018 ANORTHITE 5.031
BIOTITE= 0.000 MUSCOVITE= 0.000

DIOPSIDE= 1.517 EN= 0.107 FS= 0.651 WO= 0.758 HYPERSTHENE 5.438 FS= 4.668 EN= 0.770

OLIVINE= 0.000 FO= 0.000 FA= 0.000

LEUCITE= 0.000 NEPHELINE 0.000 AKMITE= 0.000
CORUND. 0.000 OR SILLIMANITE= 0.000

CHROMITE= 0.000 MAGNETITE= 0.598 HEMATITE= 0.000
RUTILE= 0.000 TITANITE= 0.000

SODIUM METASILICATE = 0.000 KALIOPHILITE= 0.000
WOLASTONITE= 0.000

QUARTZ(IF CORUNDUM IS USED)= 32.016
QUARTZ(IF SILLIMANITE IS USED)= 32.016
DIFF. SIO2= 0.000 TOTAL =100.000

%AN IN PLAGIOCLASE=20.9
FELDSPAR RATIO :%OR= 59.3 %AB= 32.1 %AN= 8.5
RESIDUA:OR= 40.8 AB= 22.1 QZ= 37.2
MUSCOVITE FACT. 0.0
DE LA ROCHE-VALUES : R1= 2665.1 R2= 395.1

NIGGLI-VALUES AND NIGGLI-NORM

SAMPLE NUMBER: AES4/10

1.MASS PERCENTAGES OF OXIDES

SIO2	TIO2	AL203	CR203	FE203	FEO	MNO	MGO
CAO	NA20	K20	P205	CO2	H20	H20	S
73.600	0.500	12.000	0.000	0.290	2.900	0.070	0.300
1.280	2.500	5.000	0.040	0.000	0.610	0.120	0.000

2.NIGGLI-VALUES
AL= 41.11 FM= 18.31
C= 7.97 ALK= 32.62 SUM=100.00
SI= 427.9 K=0.57 MG=0.14 QZ= 197.4
AL/(C+ALK)= 1.01

3.CATION PERCENTAGES

70.812	0.408	13.604	0.000	0.210	2.333	0.057	0.430
1.319	4.661	6.135	0.033	0.000	0.000		

TOTAL = 100.000

4.NIGGLI-NORM
PHOS. NOT ALLOCATED TO CAO= 0.000
CO2 NOT ALLOC. TO CAO = 0.000
CALCITE= 0.000 APATITE= 0.087 PYRITE= 0.000 ILMENITE= 0.815
ORTHOCLASE 29.275 ALBITE= 23.303 ANORTHITE 6.323
BIOTITE= 2.239 MUSCOVITE= 0.000

DIOPSIDE= 0.000 EN= 0.000 FS= 0.000 WO= 0.000 HYPERSTHENE 3.215 FS= 2.616 EN= 0.599

OLIVINE= 0.000 FO= 0.000 FA= 0.000

LEUCITE= 0.000 NEPHELINE 0.000 AKMITE= 0.000
CORUND. 0.000 OR SILLIMANITE= 0.000

CHROMITE= 0.000 MAGNETITE= 0.315 HEMATITE= 0.000
RUTILE= 0.000 TITANITE= 0.000

SODIUM METASILICATE = 0.000 KALIOPHILITE= 0.000
WOLASTONITE= 0.000

QUARTZ(IF CORUNDUM IS USED)= 34.429
QUARTZ(IF SILLIMANITE IS USED)= 34.429
DIFF. SIO2= 0.000 TOTAL =100.000

%AN IN PLAGIOCLASE=21.3
FELDSPAR RATIO :%OR= 49.7 %AB= 39.6 %AN= 10.7
RESIDUA:OR= 33.6 AB= 26.8 QZ= 39.6
MUSCOVITE FACT. 0.0
DE LA ROCHE-VALUES : R1= 2787.0 R2= 393.2

SAMPLE NUMBER: AES4/11

1.MASS PERCENTAGES OF OXIDES

SIO2	TIO2	AL203	CR203	FE203	FEO	MNO	MGO
CAO	NA20	K20	P205	CO2	H20	H20	S
75.400	0.420	11.700	0.000	0.090	2.700	0.030	0.200
1.140	2.800	4.890	0.050	0.000	0.610	0.130	0.000

2.NIGGLI-VALUES
AL= 41.54 FM= 15.96
C= 7.36 ALK= 35.14 SUM=100.00
SI= 454.4 K=0.53 MG=0.11 QZ= 213.8
AL/(C+ALK)= 0.98

3.CATION PERCENTAGES

71.731	0.338	13.116	0.000	0.064	2.147	0.024	0.283
1.161	5.161	5.933	0.040	0.000	0.000		

TOTAL = 100.000

4.NIGGLI-NORM
PHOS. NOT ALLOCATED TO CAO= 0.000
CO2 NOT ALLOC. TO CAO = 0.000
CALCITE= 0.000 APATITE= 0.107 PYRITE= 0.000 ILMENITE= 0.677
ORTHOCLASE 29.663 ALBITE= 25.807 ANORTHITE 5.055
BIOTITE= 0.000 MUSCOVITE= 0.000

DIOPSIDE= 0.334 EN= 0.023 FS= 0.144 WO= 0.167 HYPERSTHENE 4.002 FS= 3.458 EN= 0.544

OLIVINE= 0.000 FO= 0.000 FA= 0.000

LEUCITE= 0.000 NEPHELINE 0.000 AKMITE= 0.000
CORUND. 0.000 OR SILLIMANITE= 0.000

CHROMITE= 0.000 MAGNETITE= 0.097 HEMATITE= 0.000
RUTILE= 0.000 TITANITE= 0.000

SODIUM METASILICATE = 0.000 KALIOPHILITE= 0.000
WOLASTONITE= 0.000

QUARTZ(IF CORUNDUM IS USED)= 34.260
QUARTZ(IF SILLIMANITE IS USED)= 34.260
DIFF. SIO2= 0.000 TOTAL =100.000

%AN IN PLAGIOCLASE=16.4
FELDSPAR RATIO :%OR= 49.0 %AB= 42.6 %AN= 8.4
RESIDUA:OR= 33.1 AB= 28.8 QZ= 38.2
MUSCOVITE FACT. 0.0
DE LA ROCHE-VALUES : R1= 2812.9 R2= 363.5

SAMPLE NUMBER: AES4/12

1.MASS PERCENTAGES OF OXIDES

SIO2	TIO2	AL203	CR203	FE203	FEO	MNO	MGO
CAO	NA20	K20	P205	CO2	H20	H20	S
74.400	0.330	12.100	0.000	0.120	2.200	0.030	0.200
0.870	2.700	5.620	0.030	0.000	0.290	0.070	0.000

2.NIGGLI-VALUES
AL= 43.17 FM= 13.64
C= 5.64 ALK= 37.54 SUM=100.00
SI= 450.6 K=0.58 MG=0.13 QZ= 200.4
AL/(C+ALK)= 1.00

3.CATION PERCENTAGES

71.165	0.267	13.638	0.000	0.086	1.759	0.024	0.285
0.891	5.004	6.855	0.024	0.000	0.000		

TOTAL = 100.000

4.NIGGLI-NORM
PHOS. NOT ALLOCATED TO CAO= 0.000
CO2 NOT ALLOC. TO CAO = 0.000
CALCITE= 0.000 APATITE= 0.065 PYRITE= 0.000 ILMENITE= 0.535
ORTHOCLASE 33.892 ALBITE= 25.020 ANORTHITE 4.254
BIOTITE= 0.616 MUSCOVITE= 0.000

DIOPSIDE= 0.000 EN= 0.000 FS= 0.000 WO= 0.000 HYPERSTHENE 3.131 FS= 2.623 EN= 0.508

OLIVINE= 0.000 FO= 0.000 FA= 0.000

LEUCITE= 0.000 NEPHELINE 0.000 AKMITE= 0.000
CORUND. 0.000 OR SILLIMANITE= 0.000

CHROMITE= 0.000 MAGNETITE= 0.130 HEMATITE= 0.000
RUTILE= 0.000 TITANITE= 0.000

SODIUM METASILICATE = 0.000 KALIOPHILITE= 0.000
WOLASTONITE= 0.000

QUARTZ(IF CORUNDUM IS USED)= 32.358
QUARTZ(IF SILLIMANITE IS USED)= 32.358
DIFF. SIO2= 0.000 TOTAL =100.000

%AN IN PLAGIOCLASE=14.5
FELDSPAR RATIO :%OR= 53.7 %AB= 39.6 %AN= 6.7
RESIDUA:OR= 37.1 AB= 27.4 QZ= 35.5
MUSCOVITE FACT. 0.0
DE LA ROCHE-VALUES : R1= 2647.7 R2= 345.2

NIGGLI-VALUES AND NIGGLI-NORM

SAMPLE NUMBER: AES4/13

1.MASS PERCENTAGES OF OXIDES

SIO2	TIO2	AL203	CR203	FE203	FEO	MNO	MGO
CAO	NA2O	K2O	P2O5	CO2	H2O	H2O	S
77.000	0.350	11.000	0.000	0.000	2.400	0.050	0.200
0.900	2.400	5.170	0.020	0.000	0.590	0.080	0.000

2.NIGGLI-VALUES
AL= 42.05 FM= 15.23
C= 6.25 ALK= 36.47 SUM=100.00
SI= 499.6 K=0.59 MG=0.13 QZ= 253.7
AL/(C+ALK)= 0.98

3.CATION PERCENTAGES

73.453	0.283	12.365	0.000	0.000	1.914	0.040	0.284
0.919	4.436	6.289	0.016	0.000	0.000		

TOTAL = 100.000

4.NIGGLI-NORM
PHOS. NOT ALLOCATED TO CAO= 0.000
CO2 NOT ALLOC. TO CAO = 0.000
CALCITE= 0.000 APATITE= 0.043 PYRITE= 0.000 ILMENITE= 0.566
ORTHOCLASE 31.447 ALBITE= 22.180 ANORTHITE 4.098
BIOTITE= 0.000 MUSCOVITE= 0.000

DIOPSIDE= 0.292 EN= 0.021 FS= 0.125 WO= 0.146 HYPERSTHENE 3.766 FS= 3.218 EN= 0.547

OLIVINE= 0.000 FO= 0.000 FA= 0.000

LEUCITE= 0.000 NEPHELINE 0.000 AKMITE= 0.000
CORUND. 0.000 OR SILLIMANITE= 0.000

CHROMITE= 0.000 MAGNETITE= 0.000 HEMATITE= 0.000
RUTILE= 0.000 TITANITE= 0.000

SODIUM METASILICATE = 0.000 KALIOPHILITE= 0.000
WOLASTONITE= 0.000

QUARTZ(IF CORUNDUM IS USED)= 37.609
QUARTZ(IF SILLIMANITE IS USED)= 37.609
DIFF. SIO2= 0.000 TOTAL =100.000

%AN IN PLAGIOCLASE=15.6
FELDSPAR RATIO :%OR= 54.5 %AB= 38.4 %AN= 7.1
RESIDUA:OR= 34.5 AB= 24.3 QZ= 41.2
MUSCOVITE FACT. 0.0
DE LA ROCHE-VALUES : R1= 3007.6 R2= 323.7

NIGGLI-VALUES AND NIGGLI-NORM

SAMPLE NUMBER: AES26/1

1.MASS PERCENTAGES OF OXIDES

SIO2	TIO2	AL203	CR203	FE203	FEO	MNO	MGO
CAO	NA2O	K2O	P2O5	CO2	H2O	H2O	S
70.300	0.170	16.100	0.000	0.490	3.050	0.030	0.000
2.990	0.400	1.490	0.050	0.000	1.020	0.080	0.500

2.NIGGLI-VALUES
AL= 55.90 FM= 17.35
C= 18.87 ALK= 7.88 SUM=100.00
SI= 414.3 K=0.71 MG=0.00 QZ= 282.7
AL/(C+ALK)= 2.09

3.CATION PERCENTAGES

70.856	0.145	19.121	0.000	0.372	2.570	0.026	0.000
3.228	0.781	1.915	0.043	0.000	0.000		

TOTAL = 100.000

4.NIGGLI-NORM
PHOS. NOT ALLOCATED TO CAO= 0.000
CO2 NOT ALLOC. TO CAO = 0.000
CALCITE= 0.000 APATITE= 0.114 PYRITE= 1.416 ILMENITE= 0.290
ORTHOCLASE 0.000 ALBITE= 3.906 ANORTHITE 15.782
BIOTITE= 5.737 MUSCOVITE= 8.387

DIOPSIDE= 0.000 EN= 0.000 FS= 0.000 WO= 0.000 HYPERSTHENE 0.000 FS= 0.000 EN= 0.000

OLIVINE= 0.000 FO= 0.000 FA= 0.000

LEUCITE= 0.000 NEPHELINE 0.000 AKMITE= 0.000
CORUND. 6.999 OR SILLIMANITE= 10.498

CHROMITE= 0.000 MAGNETITE= 0.557 HEMATITE= 0.000
RUTILE= 0.000 TITANITE= 0.000

SODIUM METASILICATE = 0.000 KALIOPHILITE= 0.000
WOLASTONITE= 0.000

QUARTZ(IF CORUNDUM IS USED)= 56.813
QUARTZ(IF SILLIMANITE IS USED)= 53.313
DIFF. SIO2= 0.000 TOTAL =100.000

%AN IN PLAGIOCLASE=80.2
FELDSPAR RATIO :%OR= 0.0 %AB= 19.8 %AN= 80.2
RESIDUA:OR= 0.0 AB= 6.8 QZ= 93.2
MUSCOVITE FACT. 9.5
DE LA ROCHE-VALUES : R1= 4279.6 R2= 665.2

SAMPLE NUMBER: AES26/2

1.MASS PERCENTAGES OF OXIDES

SIO2	TIO2	AL203	CR203	FE203	FEO	MNO	MGO
CAO	NA2O	K2O	P2O5	CO2	H2O	H2O	S
70.100	0.100	14.500	0.000	0.200	4.850	0.120	0.000
2.250	0.300	2.290	0.010	0.000	0.610	0.070	0.810

2.NIGGLI-VALUES
AL= 50.22 FM= 25.32
C= 14.17 ALK= 10.29 SUM=100.00
SI= 412.1 K=0.83 MG=0.00 QZ= 270.9
AL/(C+ALK)= 2.05

3.CATION PERCENTAGES

70.798	0.086	17.256	0.000	0.152	4.095	0.103	0.000
2.434	0.587	2.949	0.009	0.000	0.000		

TOTAL = 100.000

4.NIGGLI-NORM
PHOS. NOT ALLOCATED TO CAO= 0.000
CO2 NOT ALLOC. TO CAO = 0.000
CALCITE= 0.000 APATITE= 0.023 PYRITE= 2.299 ILMENITE= 0.171
ORTHOCLASE 0.000 ALBITE= 2.935 ANORTHITE 12.097
BIOTITE= 10.464 MUSCOVITE= 11.490

DIOPSIDE= 0.000 EN= 0.000 FS= 0.000 WO= 0.000 HYPERSTHENE 0.000 FS= 0.000 EN= 0.000

OLIVINE= 0.000 FO= 0.000 FA= 0.000

LEUCITE= 0.000 NEPHELINE 0.000 AKMITE= 0.000
CORUND. 4.290 OR SILLIMANITE= 6.435

CHROMITE= 0.000 MAGNETITE= 0.228 HEMATITE= 0.000
RUTILE= 0.000 TITANITE= 0.000

SODIUM METASILICATE = 0.000 KALIOPHILITE= 0.000
WOLASTONITE= 0.000

QUARTZ(IF CORUNDUM IS USED)= 56.003
QUARTZ(IF SILLIMANITE IS USED)= 53.859
DIFF. SIO2= 0.000 TOTAL =100.000

%AN IN PLAGIOCLASE=80.5
FELDSPAR RATIO :%OR= 0.0 %AB= 19.5 %AN= 80.5
RESIDUA:OR= 0.0 AB= 5.2 QZ= 94.8
MUSCOVITE FACT. 12.5
DE LA ROCHE-VALUES : R1= 4066.2 R2= 549.8

SAMPLE NUMBER: AES26/3

1.MASS PERCENTAGES OF OXIDES

SIO2	TIO2	AL203	CR203	FE203	FEO	MNO	MGO
CAO	NA2O	K2O	P2O5	CO2	H2O	H2O	S
62.400	0.690	15.100	0.000	0.300	4.600	0.140	0.700
2.620	2.700	6.910	0.230	0.000	0.920	0.130	0.230

2.NIGGLI-VALUES
AL= 37.14 FM= 21.84
C= 11.71 ALK= 29.31 SUM=100.00
SI= 260.5 K=0.63 MG=0.20 QZ= 43.2
AL/(C+ALK)= 0.91

3.CATION PERCENTAGES

60.299	0.565	17.194	0.000	0.218	3.716	0.115	1.008
2.711	5.055	8.515	0.188	0.000	0.000		

TOTAL = 100.000

4.NIGGLI-NORM
PHOS. NOT ALLOCATED TO CAO= 0.000
CO2 NOT ALLOC. TO CAO = 0.000
CALCITE= 0.000 APATITE= 0.502 PYRITE= 0.625 ILMENITE= 1.130
ORTHOCLASE 42.577 ALBITE= 25.277 ANORTHITE 9.058
BIOTITE= 0.000 MUSCOVITE= 0.000

DIOPSIDE= 2.346 EN= 0.299 FS= 0.874 WO= 1.173 HYPERSTHENE 6.740 FS= 5.023 EN= 1.716

OLIVINE= 0.000 FO= 0.000 FA= 0.000

LEUCITE= 0.000 NEPHELINE 0.000 AKMITE= 0.000
CORUND. 0.000 OR SILLIMANITE= 0.000

CHROMITE= 0.000 MAGNETITE= 0.327 HEMATITE= 0.000
RUTILE= 0.000 TITANITE= 0.000

SODIUM METASILICATE = 0.000 KALIOPHILITE= 0.000
WOLASTONITE= 0.000

QUARTZ(IF CORUNDUM IS USED)= 11.421
QUARTZ(IF SILLIMANITE IS USED)= 11.421
DIFF. SIO2= 0.000 TOTAL =100.000

%AN IN PLAGIOCLASE=26.4
FELDSPAR RATIO :%OR= 55.4 %AB= 32.9 %AN= 11.8
RESIDUA:OR= 53.7 AB= 31.9 QZ= 14.4
MUSCOVITE FACT. 0.0
DE LA ROCHE-VALUES : R1= 1478.7 R2= 632.7

NIGGLI-VALUES AND NIGGLI-NORM

SAMPLE NUMBER: AES26/4

1.MASS PERCENTAGES OF OXIDES

SIO2	TIO2	AL203	CR203	FE203	FEO	MNO	MGO
CAO	NA2O	K2O	P2O5	CO2	H2O	H2O	S
63.900	0.510	13.000	0.000	0.120	5.550	0.160	0.400
6.800	0.200	2.720	0.160	0.000	0.800	0.060	0.430

2.NIGGLI-VALUES
AL= 34.30 FM= 24.46
C= 32.61 ALK= 8.63 SUM=100.00
SI= 286.1 K=0.90 MG=0.11 QZ= 151.6
AL/(C+ALK)= 0.83

3.CATION PERCENTAGES

65.747	0.445	15.761	0.000	0.093	4.774	0.139	0.613
7.493	0.399	3.569	0.139	0.000	0.000		

TOTAL = 100.000

4.NIGGLI-NORM
PHOS. NOT ALLOCATED TO CAO= 0.000
CO2 NOT ALLOC. TO CAO = 0.000
CALCITE= 0.000 APATITE= 0.372 PYRITE= 1.243 ILMENITE= 0.889
ORTHOCLASE 17.845 ALBITE= 1.994 ANORTHITE 29.483
BIOTITE= 0.000 MUSCOVITE= 0.000

DIOPSIDE= 5.457 EN= 0.362 FS= 2.366 WO= 2.728
HYPERSTHENE 6.514 FS= 5.650 EN= 0.864

OLIVINE= 0.000 FO= 0.000 FA= 0.000

LEUCITE= 0.000 NEPHELINE 0.000 AKMITE= 0.000
CORUND. 0.000 OR SILLIMANITE= 0.000

CHROMITE= 0.000 MAGNETITE= 0.139 HEMATITE= 0.000
RUTILE= 0.000 TITANITE= 0.000

SODIUM METASILICATE = 0.000 KALIOPHILITE= 0.000
WOLASTONITE= 0.000

QUARTZ(IF CORUNDUM IS USED)= 36.065
QUARTZ(IF SILLIMANITE IS USED)= 36.065
DIFF. SIO2= 0.000 TOTAL =100.000

%AN IN PLAGIOCLASE=93.7
FELDSPAR RATIO :%OR= 36.2 %AB= 4.0 %AN= 59.8
RESIDUA:OR= 31.9 AB= 3.6 QZ= 64.5
MUSCOVITE FACT. 0.0
DE LA ROCHE-VALUES : R1= 3595.1 R2= 1067.0

NIGGLI-VALUES AND NIGGLI-NORM

SAMPLE NUMBER: AES26/5

1.MASS PERCENTAGES OF OXIDES

SIO2	TIO2	AL203	CR203	FE203	FEO	MNO	MGO
CAO	NA2O	K2O	P2O5	CO2	H2O	H2O	S
71.500	0.340	13.200	0.000	0.260	3.330	0.160	0.200
0.730	1.700	6.580	0.050	0.000	0.750	0.090	0.000

2.NIGGLI-VALUES
AL= 43.66 FM= 19.16
C= 4.39 ALK= 32.80 SUM=100.00
SI= 401.4 K=0.72 MG=0.09 QZ= 170.2
AL/(C+ALK)= 1.17

3.CATION PERCENTAGES

69.240	0.279	15.062	0.000	0.189	2.696	0.131	0.288
0.757	3.190	8.126	0.041	0.000	0.000		

TOTAL = 100.000

4.NIGGLI-NORM
PHOS. NOT ALLOCATED TO CAO= 0.000
CO2 NOT ALLOC. TO CAO = 0.000
CALCITE= 0.000 APATITE= 0.109 PYRITE= 0.000 ILMENITE= 0.558
ORTHOCLASE 31.965 ALBITE= 15.949 ANORTHITE 3.444
BIOTITE= 8.775 MUSCOVITE= 4.453

DIOPSIDE= 0.000 EN= 0.000 FS= 0.000 WO= 0.000
HYPERSTHENE 0.000 FS= 0.000 EN= 0.000

OLIVINE= 0.000 FO= 0.000 FA= 0.000

LEUCITE= 0.000 NEPHELINE 0.000 AKMITE= 0.000
CORUND. 0.000 OR SILLIMANITE= 0.000

CHROMITE= 0.000 MAGNETITE= 0.284 HEMATITE= 0.000
RUTILE= 0.000 TITANITE= 0.000

SODIUM METASILICATE = 0.000 KALIOPHILITE= 0.000
WOLASTONITE= 0.000

QUARTZ(IF CORUNDUM IS USED)= 34.463
QUARTZ(IF SILLIMANITE IS USED)= 34.463
DIFF. SIO2= 0.000 TOTAL =100.000

%AN IN PLAGIOCLASE=17.8
FELDSPAR RATIO :%OR= 62.2 %AB= 31.1 %AN= 6.7
RESIDUA:OR= 38.8 AB= 19.4 QZ= 41.8
MUSCOVITE FACT. 20.0
DE LA ROCHE-VALUES : R1= 2562.9 R2= 353.9

NIGGLI-VALUES AND NIGGLI-NORM

SAMPLE NUMBER: AES26/6

1.MASS PERCENTAGES OF OXIDES

SIO2	TIO2	AL203	CR203	FE203	FEO	MNO	MGO
CAO	NA2O	K2O	P2O5	CO2	H2O	H2O	S
66.400	0.430	18.300	0.000	0.410	5.300	0.300	0.200
1.300	0.400	2.060	0.010	0.000	0.570	0.050	1.220

2.NIGGLI-VALUES
AL= 56.25 FM= 27.61
C= 7.26 ALK= 8.88 SUM=100.00
SI= 346.4 K=0.77 MG=0.06 QZ= 210.9
AL/(C+ALK)= 3.49

3.CATION PERCENTAGES

65.934	0.362	21.412	0.000	0.306	4.400	0.252	0.296
1.382	0.770	2.609	0.008	0.000	0.000		

TOTAL = 100.000

4.NIGGLI-NORM
PHOS. NOT ALLOCATED TO CAO= 0.000
CO2 NOT ALLOC. TO CAO = 0.000
CALCITE= 0.000 APATITE= 0.022 PYRITE= 3.404 ILMENITE= 0.723
ORTHOCLASE 0.000 ALBITE= 3.848 ANORTHITE 6.842
BIOTITE= 10.555 MUSCOVITE= 9.025

DIOPSIDE= 0.000 EN= 0.000 FS= 0.000 WO= 0.000
HYPERSTHENE 0.000 FS= 0.000 EN= 0.000

OLIVINE= 0.000 FO= 0.000 FA= 0.000

LEUCITE= 0.000 NEPHELINE 0.000 AKMITE= 0.000
CORUND. 11.399 OR SILLIMANITE= 17.099

CHROMITE= 0.000 MAGNETITE= 0.459 HEMATITE= 0.000
RUTILE= 0.000 TITANITE= 0.000

SODIUM METASILICATE = 0.000 KALIOPHILITE= 0.000
WOLASTONITE= 0.000

QUARTZ(IF CORUNDUM IS USED)= 53.722
QUARTZ(IF SILLIMANITE IS USED)= 48.022
DIFF. SIO2= 0.000 TOTAL =100.000

%AN IN PLAGIOCLASE=64.0
FELDSPAR RATIO :%OR= 0.0 %AB= 36.0 %AN= 64.0
RESIDUA:OR= 0.0 AB= 7.4 QZ= 92.6
MUSCOVITE FACT. 12.4
DE LA ROCHE-VALUES : R1= 3767.5 R2= 527.4

NIGGLI-VALUES AND NIGGLI-NORM

SAMPLE NUMBER: AES26/7

1.MASS PERCENTAGES OF OXIDES

SIO2	TIO2	AL203	CR203	FE203	FEO	MNO	MGO
CAO	NA2O	K2O	P2O5	CO2	H2O	H2O	S
65.900	0.460	15.900	0.000	0.290	6.100	0.290	0.300
2.210	0.400	2.310	0.210	0.000	0.560	0.090	1.370

2.NIGGLI-VALUES
AL= 47.78 FM= 30.66
C= 12.07 ALK= 9.49 SUM=100.00
SI= 336.1 K=0.79 MG=0.07 QZ= 198.2
AL/(C+ALK)= 2.22

3.CATION PERCENTAGES

65.988	0.390	18.760	0.000	0.218	5.107	0.246	0.447
2.370	0.776	2.950	0.178	0.000	0.000		

TOTAL = 100.000

4.NIGGLI-NORM
PHOS. NOT ALLOCATED TO CAO= 0.000
CO2 NOT ALLOC. TO CAO = 0.000
CALCITE= 0.000 APATITE= 0.475 PYRITE= 3.855 ILMENITE= 0.780
ORTHOCLASE 0.000 ALBITE= 3.880 ANORTHITE 10.367
BIOTITE= 12.850 MUSCOVITE= 9.405

DIOPSIDE= 0.000 EN= 0.000 FS= 0.000 WO= 0.000
HYPERSTHENE 0.000 FS= 0.000 EN= 0.000

OLIVINE= 0.000 FO= 0.000 FA= 0.000

LEUCITE= 0.000 NEPHELINE 0.000 AKMITE= 0.000
CORUND. 6.595 OR SILLIMANITE= 9.892

CHROMITE= 0.000 MAGNETITE= 0.328 HEMATITE= 0.000
RUTILE= 0.000 TITANITE= 0.000

SODIUM METASILICATE = 0.000 KALIOPHILITE= 0.000
WOLASTONITE= 0.000

QUARTZ(IF CORUNDUM IS USED)= 51.466
QUARTZ(IF SILLIMANITE IS USED)= 48.169
DIFF. SIO2= 0.000 TOTAL =100.000

%AN IN PLAGIOCLASE=72.8
FELDSPAR RATIO :%OR= 0.0 %AB= 27.2 %AN= 72.8
RESIDUA:OR= 0.0 AB= 7.5 QZ= 92.5
MUSCOVITE FACT. 11.4
DE LA ROCHE-VALUES : R1= 3673.9 R2= 588.3

NIGGLI-VALUES AND NIGGLI-NORM

SAMPLE NUMBER: AES26/8

1.MASS PERCENTAGES OF OXIDES

SIO2	TIO2	AL203	CR203	FE203	FEO	MNO	MGO
CAO	NA20	K20	P205	CO2	H20	H2O	S
67.400	0.510	14.500	0.000	0.500	6.700	0.300	0.300
2.170	0.200	2.450	0.010	0.000	0.800	0.150	0.580

2.NIGGLI-VALUES
AL= 44.26 FM= 34.60
C= 12.04 ALK= 9.10 SUM=100.00
SI= 349.2 K=0.89 MG=0.07 QZ= 212.8
AL/(C+ALK)= 2.09

3.CATION PERCENTAGES

68.408	0.438	17.341	0.000	0.382	5.685	0.258	0.454
2.359	0.393	3.171	0.009	0.000	0.000		

TOTAL = 100.000

4.NIGGLI-NORM
PHOS. NOT ALLOCATED TO CAO= 0.000
CO2 NOT ALLOC. TO CAO = 0.000
CALCITE= 0.000 APATITE= 0.023 PYRITE= 1.654 ILMENITE= 0.877
ORTHOCLASE 0.000 ALBITE= 1.967 ANORTHITE 11.722
BIOTITE= 16.690 MUSCOVITE= 7.594

DIOPSIDE= 0.000 EN= 0.000 FS= 0.000 WO= 0.000 HYPERSTHENE 0.000 FS= 0.000 EN= 0.000

OLIVINE= 0.000 FO= 0.000 FA= 0.000

LEUCITE= 0.000 NEPHELINE 0.000 AKMITE= 0.000
CORUND. 4.832 OR SILLIMANITE= 7.248

CHROMITE= 0.000 MAGNETITE= 0.573 HEMATITE= 0.000
RUTILE= 0.000 TITANITE= 0.000

SODIUM METASILICATE = 0.000 KALIOPHILITE= 0.000
WOLASTONITE= 0.000

QUARTZ(IF CORUNDUM IS USED)= 54.069
QUARTZ(IF SILLIMANITE IS USED)= 51.653
DIFF. SIO2= 0.000 TOTAL =100.000

%AN IN PLAGIOCLASE=85.6
FELDSPAR RATIO :%OR= 0.0 %AB= 14.4 %AN= 85.6
RESIDUA:OR= 0.0 AB= 3.7 QZ= 96.3
MUSCOVITE FACT. 8.1
DE LA ROCHE-VALUES : R1= 3798.6 R2= 555.9

NIGGLI-VALUES AND NIGGLI-NORM

SAMPLE NUMBER: AES26/9

1.MASS PERCENTAGES OF OXIDES

SIO2	TIO2	AL203	CR203	FE203	FEO	MNO	MGO
CAO	NA20	K20	P205	CO2	H20	H2O	S
69.300	0.530	11.400	0.000	0.040	6.700	0.230	0.600
1.840	0.400	6.370	0.040	0.000	1.140	0.260	0.190

2.NIGGLI-VALUES
AL= 33.83 FM= 33.84
C= 9.92 ALK= 22.41 SUM=100.00
SI= 349.0 K=0.91 MG=0.13 QZ= 159.4
AL/(C+ALK)= 1.05

3.CATION PERCENTAGES

68.505	0.444	13.279	0.000	0.030	5.537	0.193	0.883
1.948	0.766	8.030	0.033	0.000	0.000		

TOTAL = 100.000

4.NIGGLI-NORM
PHOS. NOT ALLOCATED TO CAO= 0.000
CO2 NOT ALLOC. TO CAO = 0.000
CALCITE= 0.000 APATITE= 0.089 PYRITE= 0.528 ILMENITE= 0.88
ORTHOCLASE 36.661 ALBITE= 3.831 ANORTHITE 9.461
BIOTITE= 5.585 MUSCOVITE= 0.000

DIOPSIDE= 0.000 EN= 0.000 FS= 0.000 WO= 0.000 HYPERSTHENE 8.466 FS= 7.21 EN= 1.25

OLIVINE= 0.000 FO= 0.000 FA= 0.000

LEUCITE= 0.000 NEPHELINE 0.000 AKMITE= 0.000
CORUND. 0.000 OR SILLIMANITE= 0.000

CHROMITE= 0.000 MAGNETITE= 0.045 HEMATITE= 0.000
RUTILE= 0.000 TITANITE= 0.000

SODIUM METASILICATE = 0.000 KALIOPHILITE= 0.000
WOLASTONITE= 0.000

QUARTZ(IF CORUNDUM IS USED)= 34.447
QUARTZ(IF SILLIMANITE IS USED)= 34.447
DIFF. SIO2= 0.000 TOTAL =100.000

%AN IN PLAGIOCLASE=71.2
FELDSPAR RATIO :%OR= 73.4 %AB= 7.7 %AN= 18.9
RESIDUA:OR= 48.9 AB= 5.1 QZ= 46.0
MUSCOVITE FACT. 0.0
DE LA ROCHE-VALUES : R1= 2850.4 R2= 461.2

SAMPLE NUMBER: AE26/10

1.MASS PERCENTAGES OF OXIDES

SIO2	TIO2	AL203	CR203	FE203	FEO	MNO	MGO
CAO	NA20	K20	P205	CO2	H20	H2O	S
72.700	0.440	11.700	0.000	0.000	3.300	0.090	0.300
1.130	2.500	5.230	0.040	0.000	0.970	0.230	0.010

2.NIGGLI-VALUES
AL= 40.21 FM= 19.15
C= 7.06 ALK= 33.58 SUM=100.00
SI= 424.1 K=0.58 MG=0.14 QZ= 189.8
AL/(C+ALK)= 0.99

3.CATION PERCENTAGES

70.639	0.362	13.396	0.000	0.000	2.681	0.074	0.434
1.176	4.707	6.481	0.033	0.000	0.000		

TOTAL = 100.000

4.NIGGLI-NORM
PHOS. NOT ALLOCATED TO CAO= 0.000
CO2 NOT ALLOC. TO CAO = 0.000
CALCITE= 0.000 APATITE= 0.088 PYRITE= 0.027 ILMENITE= 0.724
ORTHOCLASE 32.403 ALBITE= 23.533 ANORTHITE 5.521
BIOTITE= 0.000 MUSCOVITE= 0.000

DIOPSIDE= 0.067 EN= 0.005 FS= 0.028 WO= 0.034 HYPERSTHENE 5.602 FS= 4.738 EN= 0.863

OLIVINE= 0.000 FO= 0.000 FA= 0.000

LEUCITE= 0.000 NEPHELINE 0.000 AKMITE= 0.000
CORUND. 0.000 OR SILLIMANITE= 0.000

CHROMITE= 0.000 MAGNETITE= 0.000 HEMATITE= 0.000
RUTILE= 0.000 TITANITE= 0.000

SODIUM METASILICATE = 0.000 KALIOPHILITE= 0.000
WOLASTONITE= 0.000

QUARTZ(IF CORUNDUM IS USED)= 32.034
QUARTZ(IF SILLIMANITE IS USED)= 32.034
DIFF. SIO2= 0.000 TOTAL =100.000

%AN IN PLAGIOCLASE=19.0
FELDSPAR RATIO :%OR= 52.7 %AB= 38.3 %AN= 9.0
RESIDUA:OR= 36.8 AB= 26.8 QZ= 36.4
MUSCOVITE FACT. 0.0
DE LA ROCHE-VALUES : R1= 2697.9 R2= 374.9

SAMPLE NUMBER: AE26/11

1.MASS PERCENTAGES OF OXIDES

SIO2	TIO2	AL203	CR203	FE203	FEO	MNO	MGO
CAO	NA20	K20	P205	CO2	H20	H2O	S
61.500	0.580	6.000	0.000	1.320	7.400	0.210	0.400
10.600	0.300	2.730	0.020	0.000	0.840	0.190	1.430

2.NIGGLI-VALUES
AL= 14.21 FM= 31.98
C= 45.64 ALK= 8.17 SUM=100.00
SI= 247.3 K=0.86 MG=0.07 QZ= 114.6
AL/(C+ALK)= 0.26

3.CATION PERCENTAGES

64.652	0.517	7.432	0.000	1.044	6.504	0.187	0.626
11.934	0.611	3.660	0.018	0.000	0.000		

TOTAL = 100.000

4.NIGGLI-NORM
PHOS. NOT ALLOCATED TO CAO= 0.000
CO2 NOT ALLOC. TO CAO = 0.000
CALCITE= 0.000 APATITE= 0.047 PYRITE= 4.224 ILMENITE= 1.033
ORTHOCLASE 18.299 ALBITE= 3.055 ANORTHITE 7.903
BIOTITE= 0.000 MUSCOVITE= 0.000

DIOPSIDE= 19.482 EN= 1.253 FS= 8.488 WO= 9.741 HYPERSTHENE 0.000 FS= 0.000 EN= 0.000

OLIVINE= 0.000 FO= 0.000 FA= 0.000

LEUCITE= 0.000 NEPHELINE 0.000 AKMITE= 0.000
CORUND. 0.000 OR SILLIMANITE= 0.000

CHROMITE= 0.000 MAGNETITE= 1.566 HEMATITE= 0.000
RUTILE= 0.000 TITANITE= 0.000

SODIUM METASILICATE = 0.000 KALIOPHILITE= 0.000
WOLASTONITE= 10.907

QUARTZ(IF CORUNDUM IS USED)= 33.483
QUARTZ(IF SILLIMANITE IS USED)= 33.483
DIFF. SIO2= 0.000 TOTAL =100.000

%AN IN PLAGIOCLASE=72.1
FELDSPAR RATIO :%OR= 62.5 %AB= 10.4 %AN= 27.0
RESIDUA:OR= 33.4 AB= 5.6 QZ= 61.1
MUSCOVITE FACT. 0.0
DE LA ROCHE-VALUES : R1= 3347.8 R2= 1374.9

NIGGLI-VALUES AND NIGGLI-NORM

SAMPLE NUMBER: AE26/12

1.MASS PERCENTAGES OF OXIDES

SIO2	TIO2	AL2O3	CR2O3	FE2O3	FEO	MNO	MGO
CAO	NA2O	K2O	P2O5	CO2	H2O	H2O	S
70.200	0.400	14.500	0.000	0.110	5.600	0.230	0.100
1.260	0.200	2.050	0.000	0.000	0.610	0.200	0.470

2.NIGGLI-VALUES
AL= 51.77 FM= 30.96
C= 8.18 ALK= 9.10 SUM=100.00
SI= 425.4 K=0.87 MG=0.03 QZ= 289.0
AL/(C+ALK)= 3.00

3.CATION PERCENTAGES

71.659	0.346	17.441	0.000	0.084	4.779	0.199	0.152
1.377	0.396	2.669	0.000	0.000	0.000		

TOTAL = 100.000

4.NIGGLI-NORM
PHOS. NOT ALLOCATED TO CAO= 0.000
CO2 NOT ALLOC. TO CAO = 0.000
CALCITE= 0.000 APATITE= 0.000 PYRITE= 1.348 ILMENITE= 0.692
ORTHOCLASE 0.000 ALBITE= 1.978 ANORTHITE 6.887
BIOTITE= 13.736 MUSCOVITE= 6.662

DIOPSIDE= 0.000 EN= 0.000 FS= 0.000 WO= 0.000 HYPERSTHENE 0.000 FS= 0.000 EN= 0.000

OLIVINE= 0.000 FO= 0.000 FA= 0.000

LEUCITE= 0.000 NEPHELINE 0.000 AKMITE= 0.000
CORUND. 8.002 OR SILLIMANITE= 12.002

CHROMITE= 0.000 MAGNETITE= 0.127 HEMATITE= 0.000
RUTILE= 0.000 TITANITE= 0.000

SODIUM METASILICATE = 0.000 KALIOPHILITE= 0.000
WOLASTONITE= 0.000

QUARTZ(IF CORUNDUM IS USED)= 60.570
QUARTZ(IF SILLIMANITE IS USED)= 56.569
DIFF. SIO2= 0.000 TOTAL =100.000

%AN IN PLAGIOCLASE=77.7
FELDSPAR RATIO :%OR= 0.0 %AB= 22.3 %AN= 77.7
RESIDUA:OR= 0.0 AB= 3.4 QZ= 96.6
MUSCOVITE FACT. 7.9
DE LA ROCHE-VALUES : R1= 4158.5 R2= 446.0

NIGGLI-VALUES AND NIGGLI-NORM

SAMPLE NUMBER: AE26/13

1.MASS PERCENTAGES OF OXIDES

SIO2	TIO2	AL2O3	CR2O3	FE2O3	FEO	MNO	MGO
CAO	NA2O	K2O	P2O5	CO2	H2O	H2O	S
73.200	0.510	11.900	0.000	0.310	3.200	0.030	0.300
1.040	2.400	5.270	0.050	0.000	0.690	0.190	0.000

2.NIGGLI-VALUES
AL= 40.78 FM= 19.67
C= 6.48 ALK= 33.07 SUM=100.00
SI= 425.8 K=0.59 MG=0.13 QZ= 193.5
AL/(C+ALK)= 1.03

3.CATION PERCENTAGES

70.682	0.417	13.540	0.000	0.225	2.583	0.025	0.432
1.076	4.490	6.490	0.041	0.000	0.000		

TOTAL = 100.000

4.NIGGLI-NORM
PHOS. NOT ALLOCATED TO CAO= 0.000
CO2 NOT ALLOC. TO CAO = 0.000
CALCITE= 0.000 APATITE= 0.109 PYRITE= 0.000 ILMENITE= 0.834
ORTHOCLASE 29.721 ALBITE= 22.452 ANORTHITE 5.037
BIOTITE= 4.363 MUSCOVITE= 0.000

DIOPSIDE= 0.000 EN= 0.000 FS= 0.000 WO= 0.000 HYPERSTHENE 2.292 FS= 1.898 EN= 0.394

OLIVINE= 0.000 FO= 0.000 FA= 0.000

LEUCITE= 0.000 NEPHELINE 0.000 AKMITE= 0.000
CORUND. 0.000 OR SILLIMANITE= 0.000

CHROMITE= 0.000 MAGNETITE= 0.338 HEMATITE= 0.000
RUTILE= 0.000 TITANITE= 0.000

SODIUM METASILICATE = 0.000 KALIOPHILITE= 0.000
WOLASTONITE= 0.000

QUARTZ(IF CORUNDUM IS USED)= 34.855
QUARTZ(IF SILLIMANITE IS USED)= 34.855
DIFF. SIO2= 0.000 TOTAL =100.000

%AN IN PLAGIOCLASE=18.3
FELDSPAR RATIO :%OR= 52.0 %AB= 39.2 %AN= 8.8
RESIDUA:OR= 34.2 AB= 25.8 QZ= 40.1
MUSCOVITE FACT. 0.0
DE LA ROCHE-VALUES : R1= 2730.2 R2= 366.2

SAMPLE NUMBER: AE26/14

1.MASS PERCENTAGES OF OXIDES

SIO2	TIO2	AL2O3	CR2O3	FE2O3	FEO	MNO	MGO
CAO	NA2O	K2O	P2O5	CO2	H2O	H2O	S
72.100	0.490	12.300	0.000	0.380	3.350	0.090	0.200
1.320	2.000	5.760	0.070	0.000	0.900	0.200	0.030

2.NIGGLI-VALUES
AL= 40.87 FM= 19.52
C= 7.97 ALK= 31.64 SUM=100.00
SI= 406.6 K=0.65 MG=0.09 QZ= 180.1
AL/(C+ALK)= 1.03

3.CATION PERCENTAGES

69.852	0.402	14.042	0.000	0.277	2.713	0.074	0.289
1.370	3.754	7.116	0.057	0.000	0.000		

TOTAL = 100.000

4.NIGGLI-NORM
PHOS. NOT ALLOCATED TO CAO= 0.000
CO2 NOT ALLOC. TO CAO = 0.000
CALCITE= 0.000 APATITE= 0.153 PYRITE= 0.082 ILMENITE= 0.804
ORTHOCLASE 32.468 ALBITE= 18.772 ANORTHITE 6.370
BIOTITE= 4.983 MUSCOVITE= 0.000

DIOPSIDE= 0.000 EN= 0.000 FS= 0.000 WO= 0.000 HYPERSTHENE 1.901 FS= 1.683 EN= 0.219

OLIVINE= 0.000 FO= 0.000 FA= 0.000

LEUCITE= 0.000 NEPHELINE 0.000 AKMITE= 0.000
CORUND. 0.000 OR SILLIMANITE= 0.000

CHROMITE= 0.000 MAGNETITE= 0.415 HEMATITE= 0.000
RUTILE= 0.000 TITANITE= 0.000

SODIUM METASILICATE = 0.000 KALIOPHILITE= 0.000
WOLASTONITE= 0.000

QUARTZ(IF CORUNDUM IS USED)= 34.052
QUARTZ(IF SILLIMANITE IS USED)= 34.052
DIFF. SIO2= 0.000 TOTAL =100.000

%AN IN PLAGIOCLASE=25.3
FELDSPAR RATIO :%OR= 56.4 %AB= 32.6 %AN= 11.1
RESIDUA:OR= 38.1 AB= 22.0 QZ= 39.9
MUSCOVITE FACT. 0.0
DE LA ROCHE-VALUES : R1= 2681.4 R2= 400.1

SAMPLE NUMBER: AE26/15

1.MASS PERCENTAGES OF OXIDES

SIO2	TIO2	AL2O3	CR2O3	FE2O3	FEO	MNO	MGO
CAO	NA2O	K2O	P2O5	CO2	H2O	H2O	S
74.100	0.490	11.700	0.000	0.850	2.700	0.050	0.200
1.240	2.200	5.290	0.070	0.000	0.700	0.190	0.000

2.NIGGLI-VALUES
AL= 40.64 FM= 19.08
C= 7.83 ALK= 32.45 SUM=100.00
SI= 436.8 K=0.61 MG=0.09 QZ= 207.0
AL/(C+ALK)= 1.01

3.CATION PERCENTAGES

71.295	0.399	13.265	0.000	0.615	2.172	0.041	0.287
1.278	4.101	6.491	0.057	0.000	0.000		

TOTAL = 100.000

4.NIGGLI-NORM
PHOS. NOT ALLOCATED TO CAO= 0.000
CO2 NOT ALLOC. TO CAO = 0.000
CALCITE= 0.000 APATITE= 0.152 PYRITE= 0.000 ILMENITE= 0.799
ORTHOCLASE 30.919 ALBITE= 20.507 ANORTHITE 5.914
BIOTITE= 2.457 MUSCOVITE= 0.000

DIOPSIDE= 0.000 EN= 0.000 FS= 0.000 WO= 0.000 HYPERSTHENE 2.049 FS= 1.721 EN= 0.328

OLIVINE= 0.000 FO= 0.000 FA= 0.000

LEUCITE= 0.000 NEPHELINE 0.000 AKMITE= 0.000
CORUND. 0.000 OR SILLIMANITE= 0.000

CHROMITE= 0.000 MAGNETITE= 0.923 HEMATITE= 0.000
RUTILE= 0.000 TITANITE= 0.000

SODIUM METASILICATE = 0.000 KALIOPHILITE= 0.000
WOLASTONITE= 0.000

QUARTZ(IF CORUNDUM IS USED)= 36.282
QUARTZ(IF SILLIMANITE IS USED)= 36.282
DIFF. SIO2= 0.000 TOTAL =100.000

%AN IN PLAGIOCLASE=22.4
FELDSPAR RATIO :%OR= 53.9 %AB= 35.8 %AN= 10.3
RESIDUA:OR= 35.3 AB= 23.4 QZ= 41.4
MUSCOVITE FACT. 0.0
DE LA ROCHE-VALUES : R1= 2840.0 R2= 376.3

APPENDIX VI

Pearce diagrams

LEGEND

---- : Lower TBQ / granite gneiss contact

⊗ : Hornblende - bearing granite gneiss

✖ : Biotite - bearing granite gneiss

• : Transition zone and granite gneiss lenses

● : TBQ

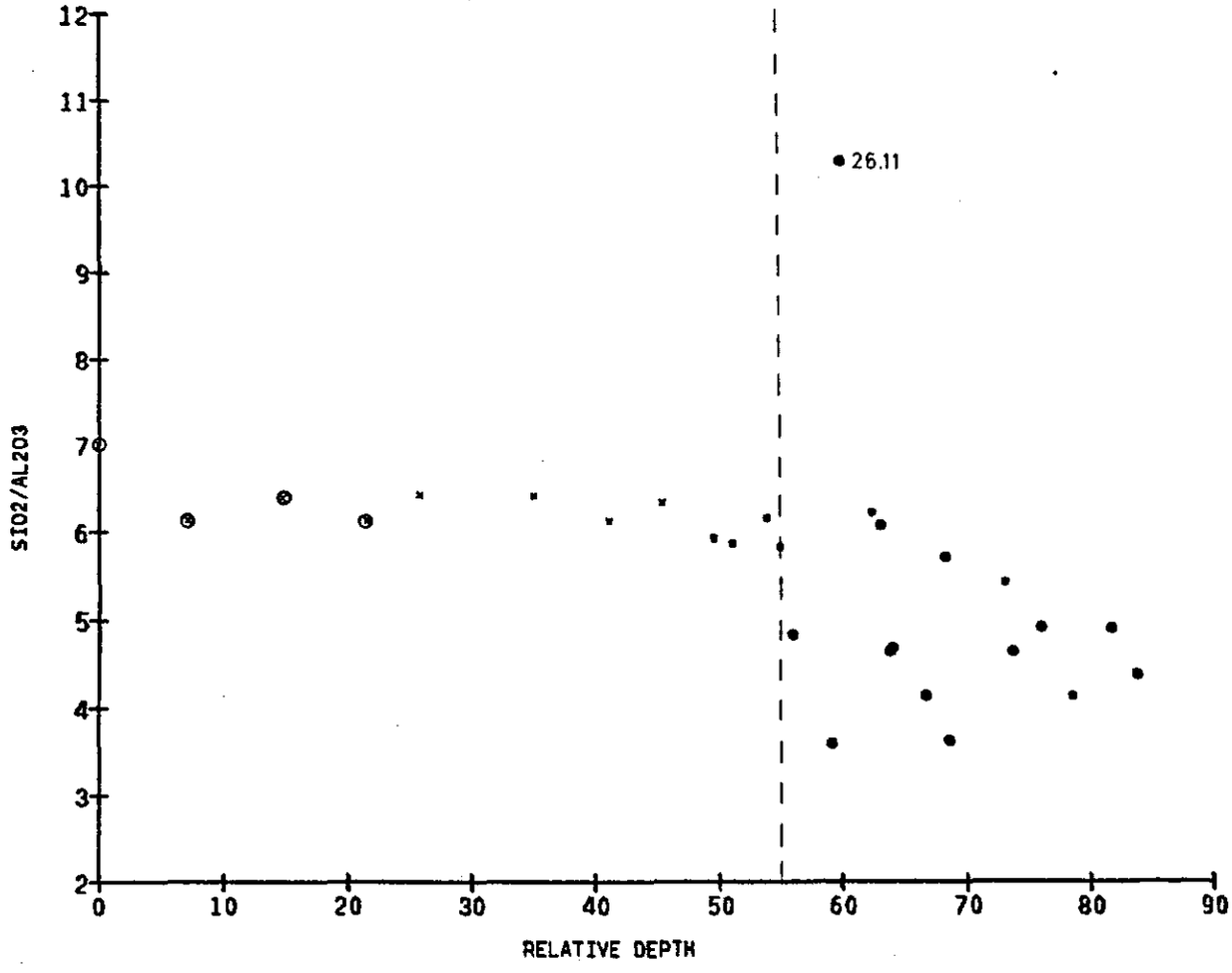
SIO2/AL203
RELATIVE DEPTH
26.11
12
11
10
9
8
7
6
5
4
3
2
0
10
20
30
40
50
60
70
80
90

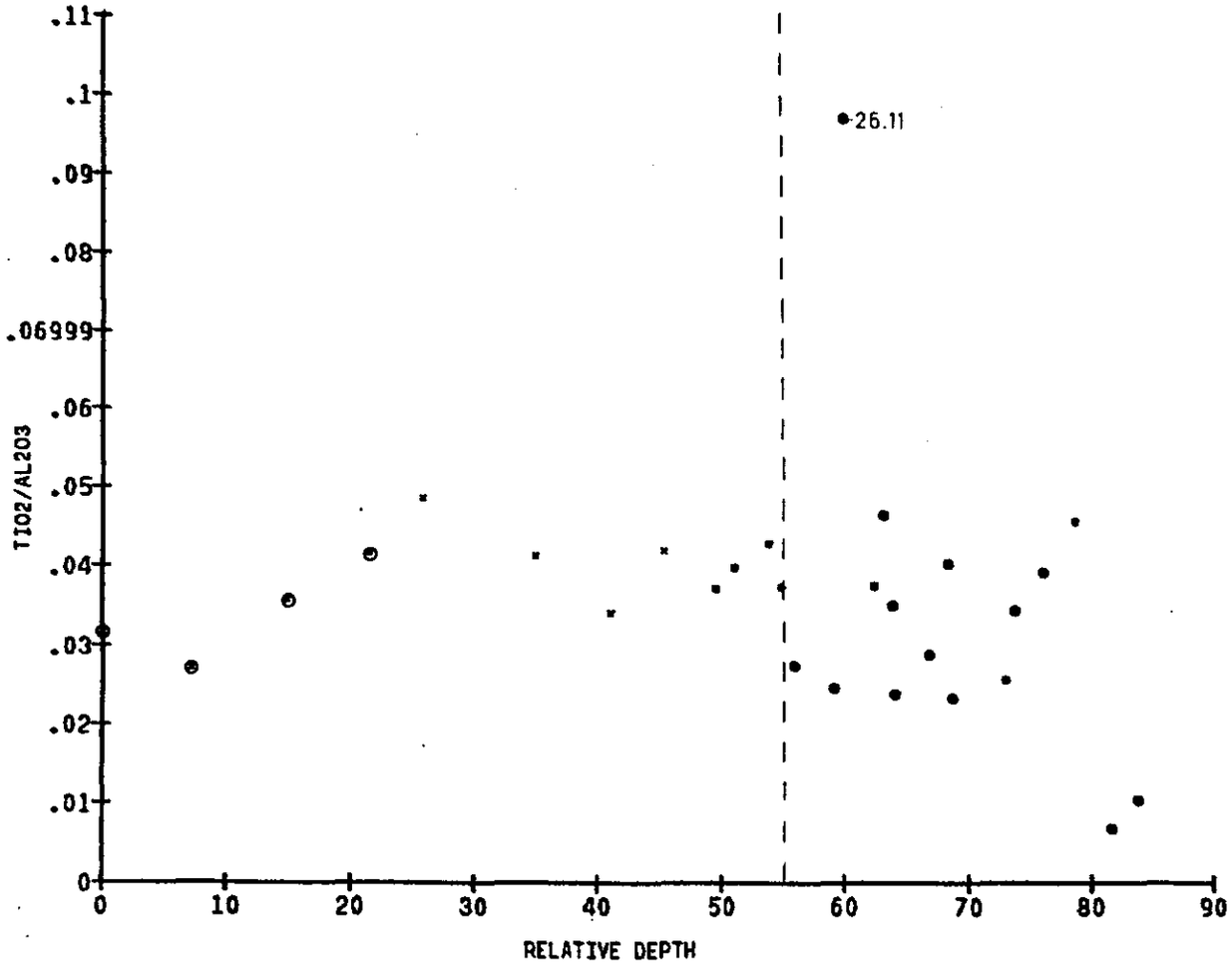
TIO2/AL203
RELATIVE DEPTH
26.11
.11
.1
.09
.08
.06999
.06
.05
.04
.03
.02
.01
0
0
10
20
30
40
50
60
70
80
90

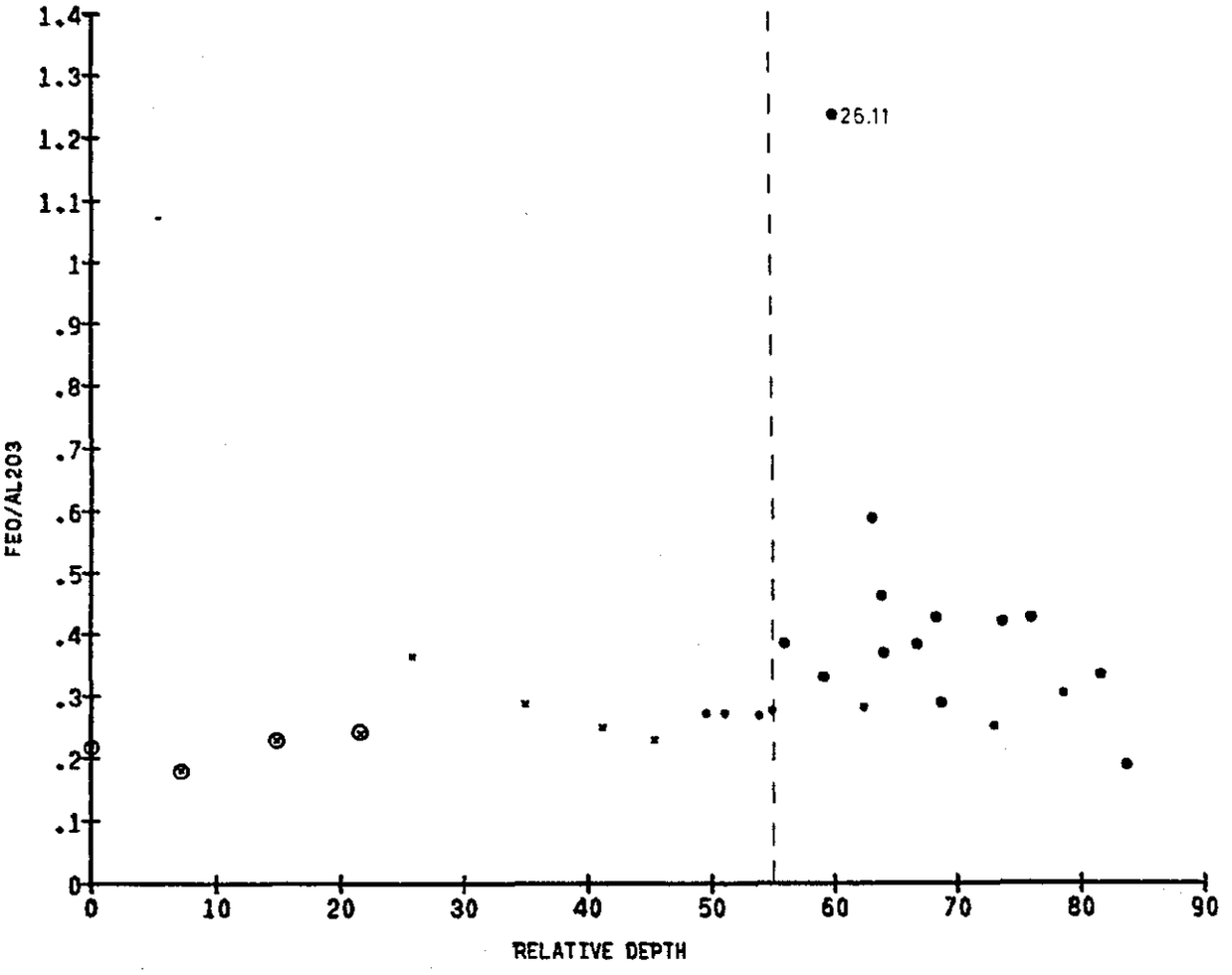
FEO/AL203
RELATIVE DEPTH
26.11

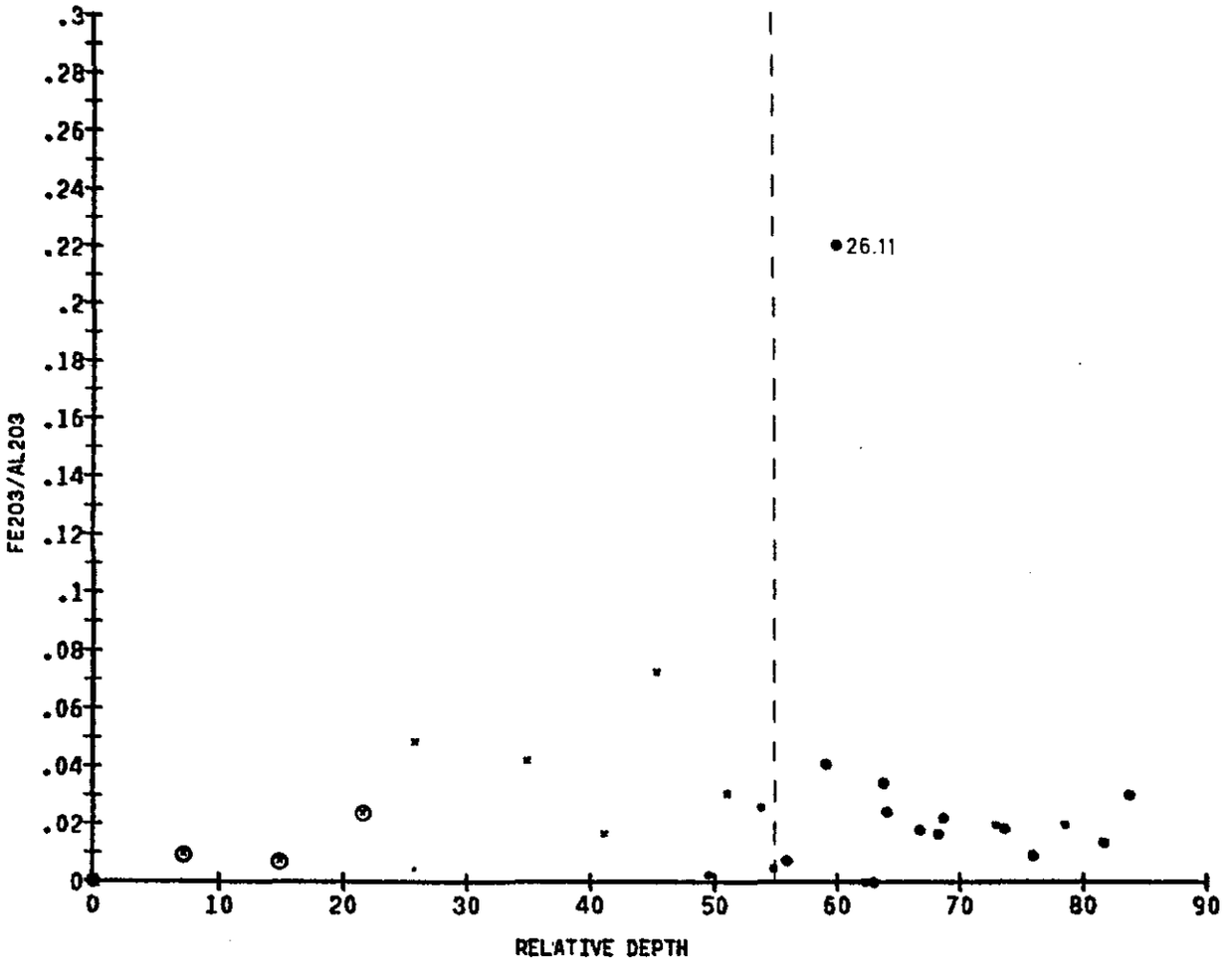
FE203/AL203
RELATIVE DEPTH
26.11

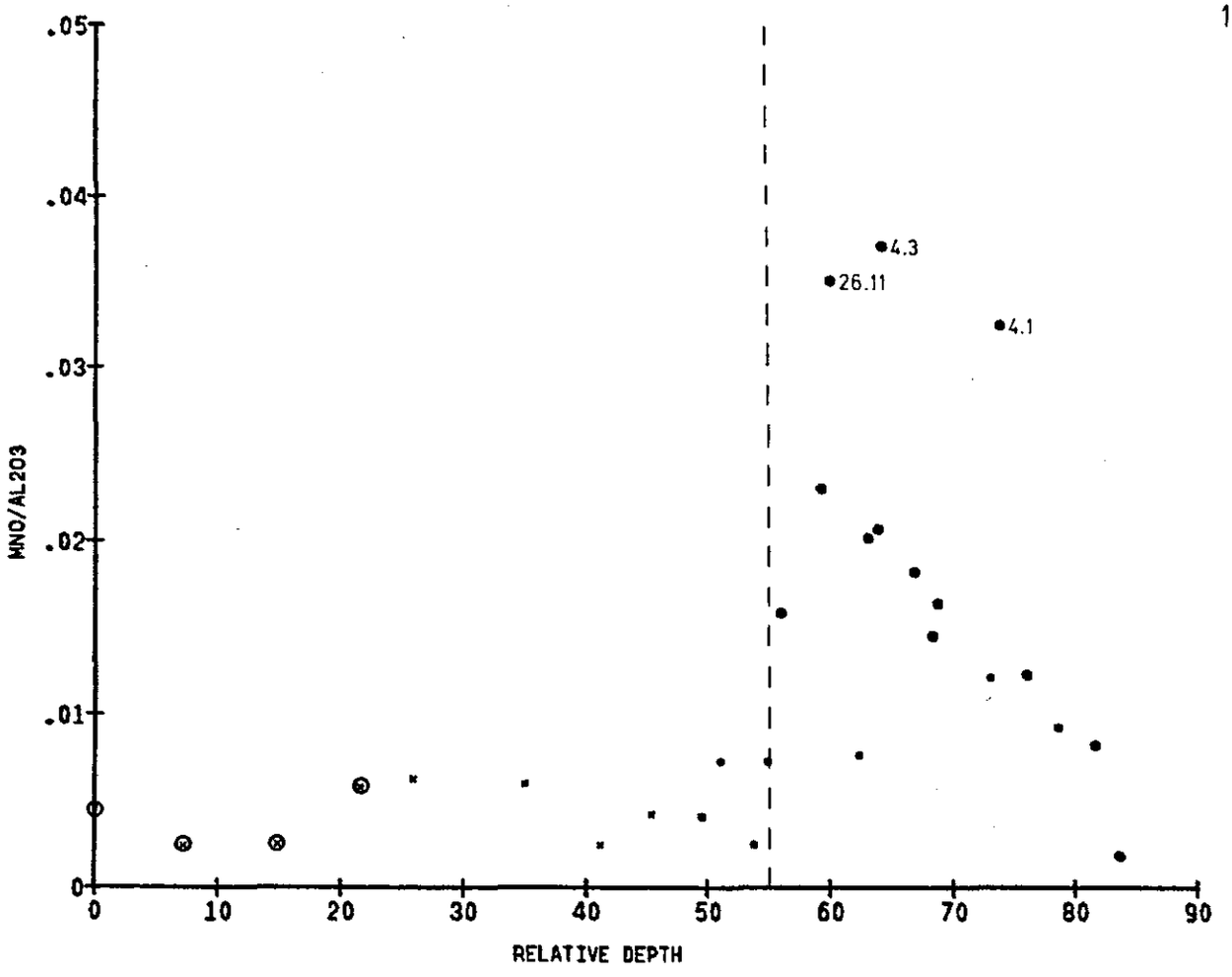
.05
.04
.03
.02
.01
0
MNO/AL203
4.3
26.11
4.1
0
10
20
30
40
50
60
70
80
90
RELATIVE DEPTH

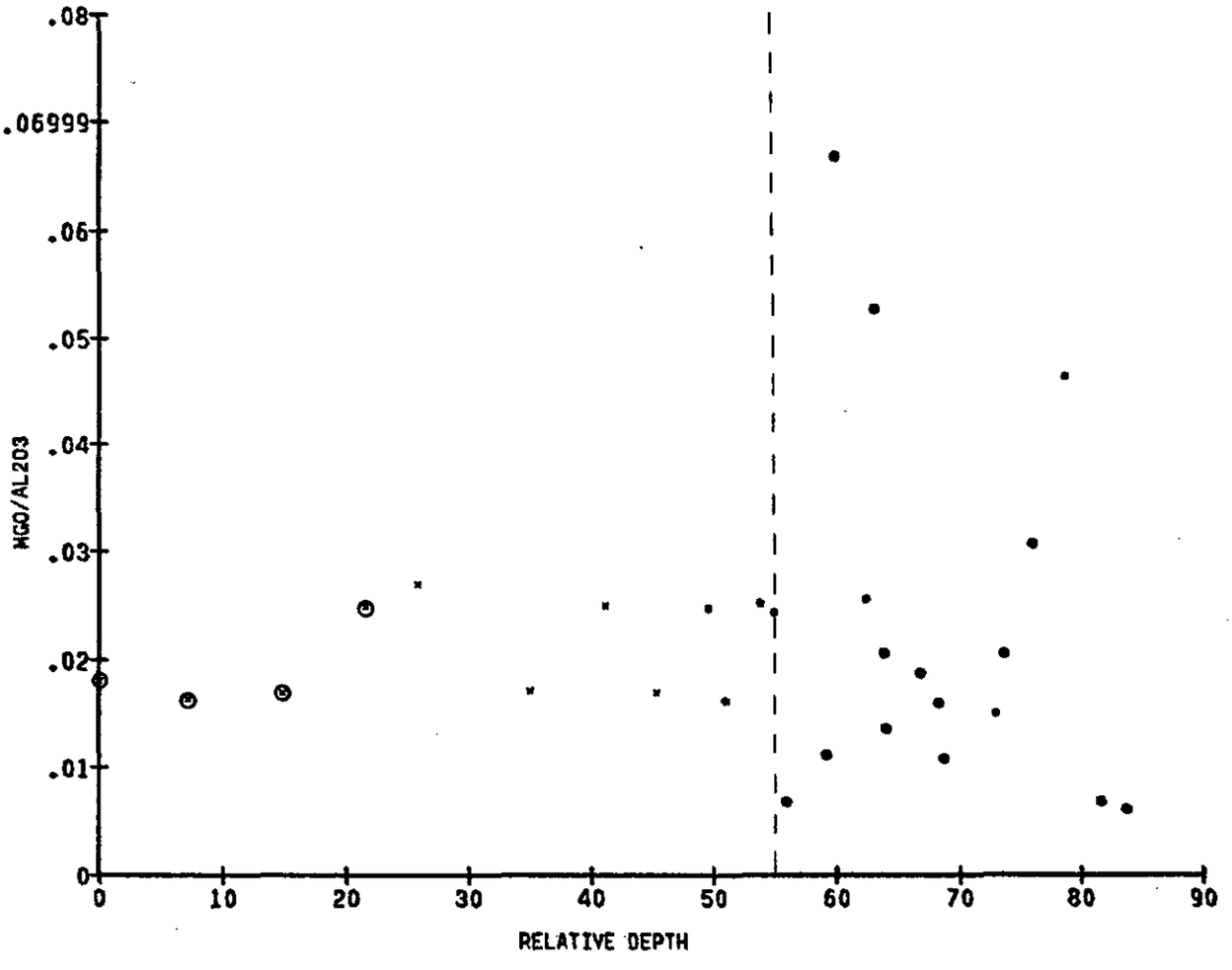
.08
.06999
.06
.05
.04
.03
.02
.01
0
MGO/AL203
0
10
20
30
40
50
60
70
80
90
RELATIVE DEPTH

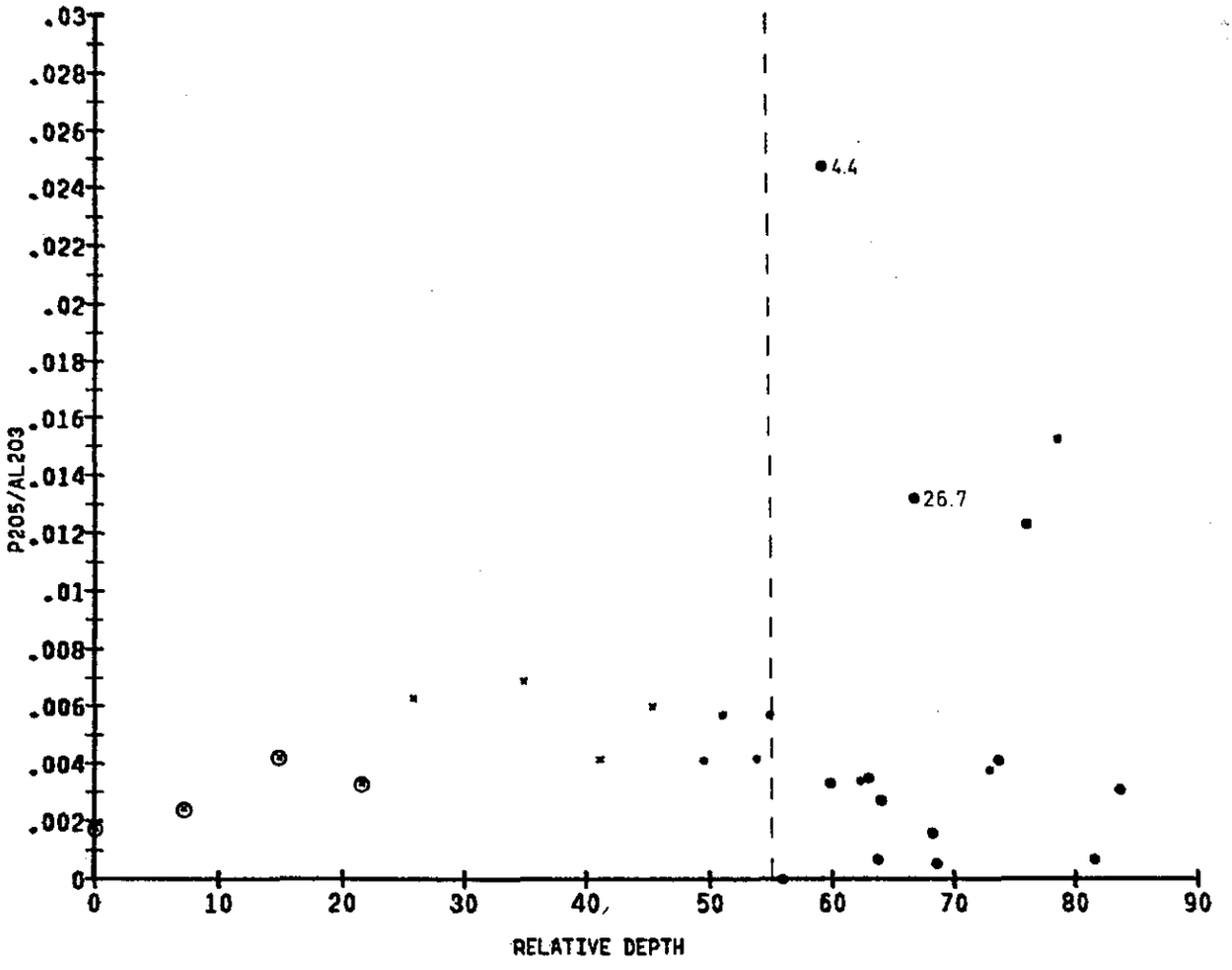
P2O5/AL2O3
.03
.028
.026
.024
.022
.02
.018
.016
.014
.012
.01
.008
.006
.004
.002
0
4.4
26.7
0
10
20
30
40
50
60
70
80
90
RELATIVE DEPTH

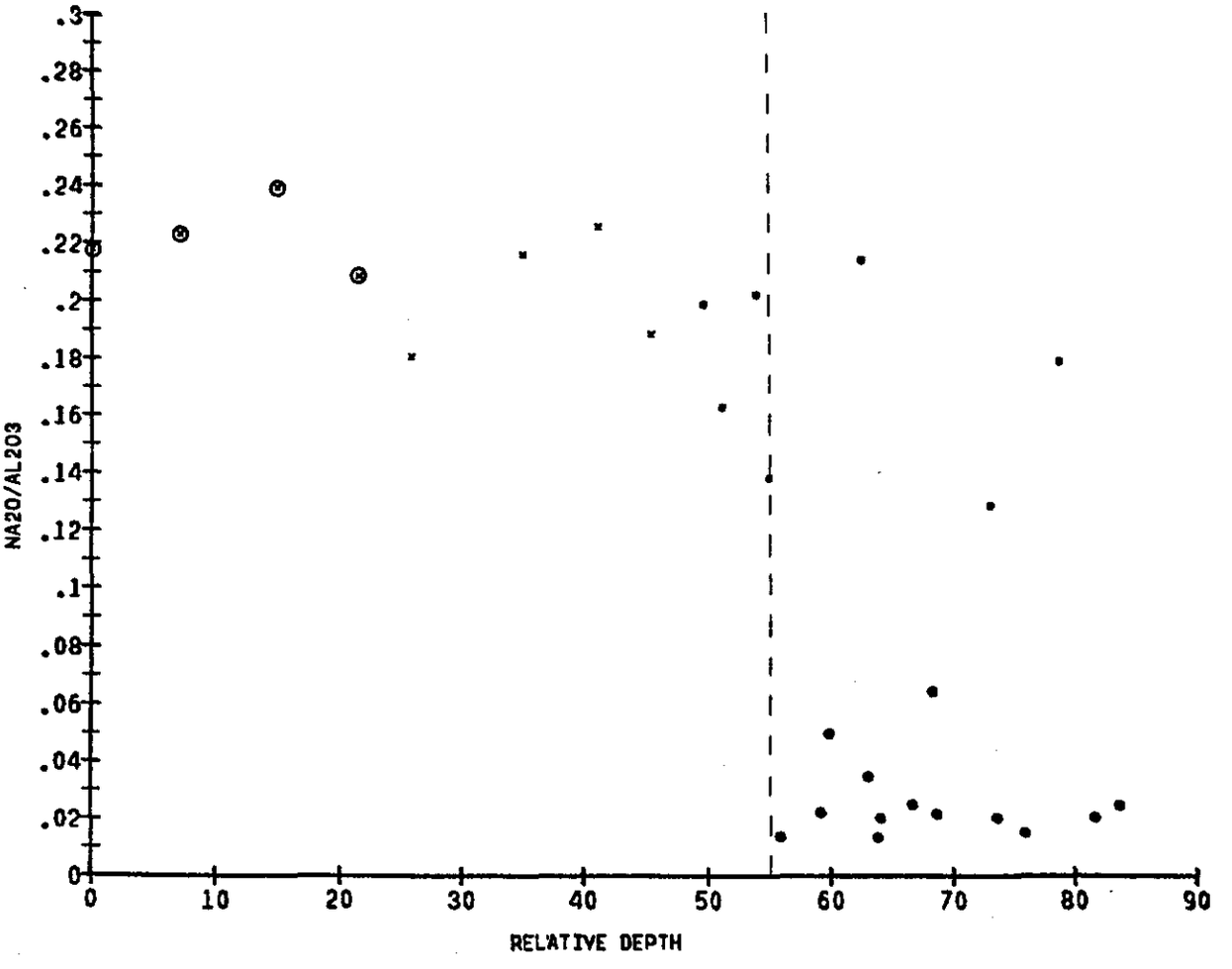
NA2O/AL2O3
.3
.28
.26
.24
.22
.2
.18
.16
.14
.12
.1
.08
.06
.04
.02
0
0
10
20
30
40
50
60
70
80
90
RELATIVE DEPTH

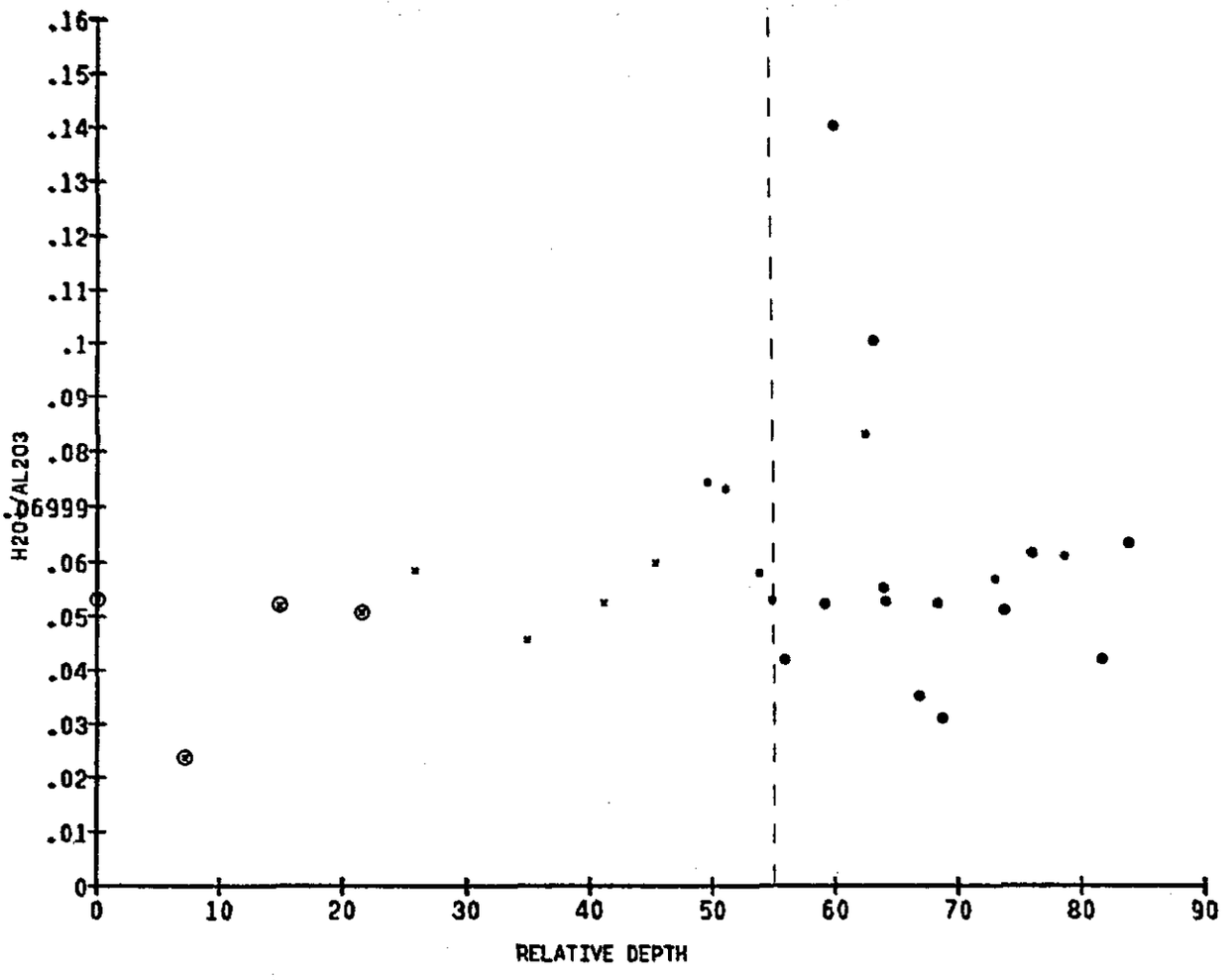
H2O/AL203
.16
.15
.14
.13
.12
.11
.1
.09
.08
.07
.06
.05
.04
.03
.02
.01
0
0
10
20
30
40
50
60
70
80
90
RELATIVE DEPTH

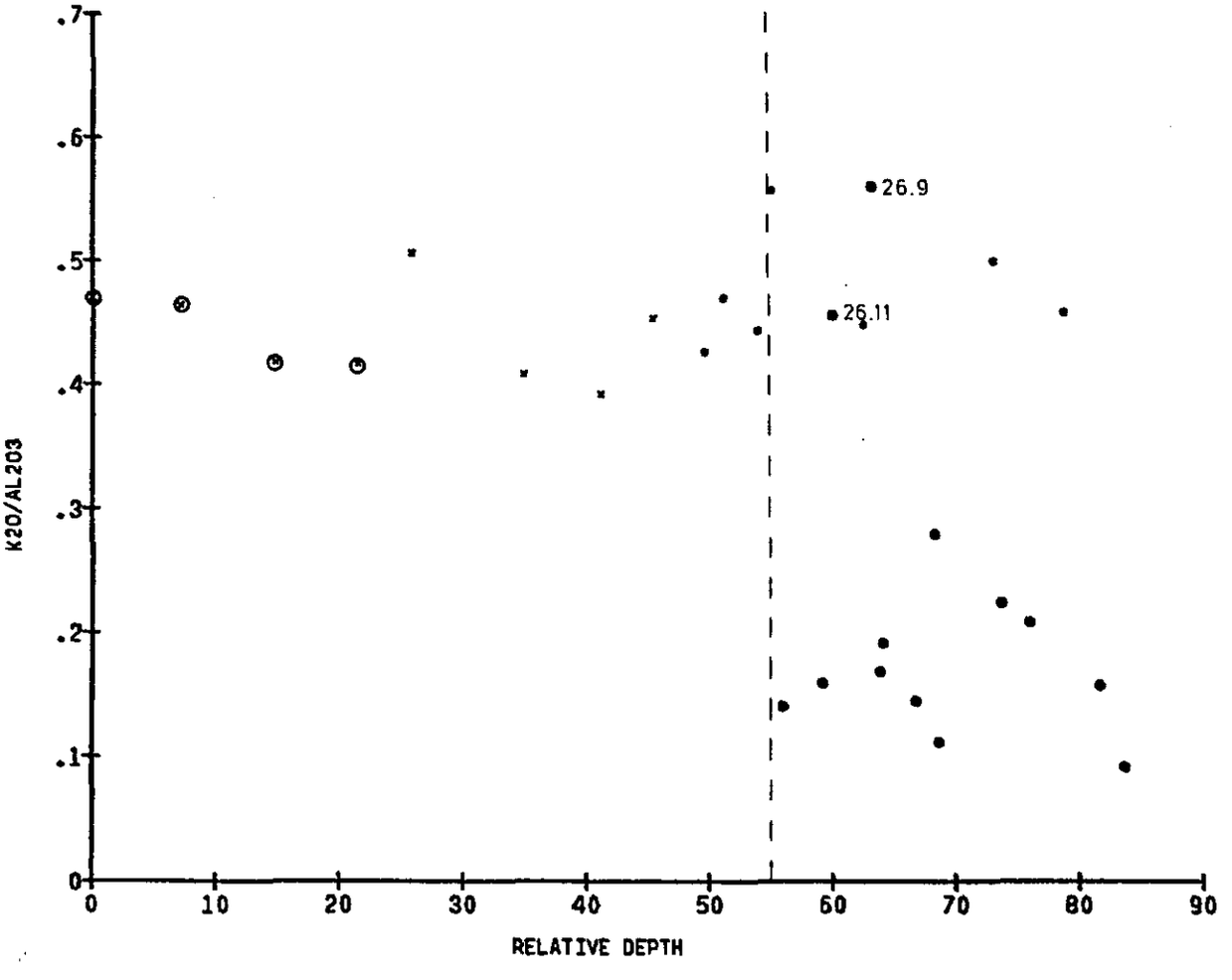
K2O/AL203
.7
.6
.5
.4
.3
.2
.1
0
26.9
26.11
0
10
20
30
40
50
60
70
80
90
RELATIVE DEPTH

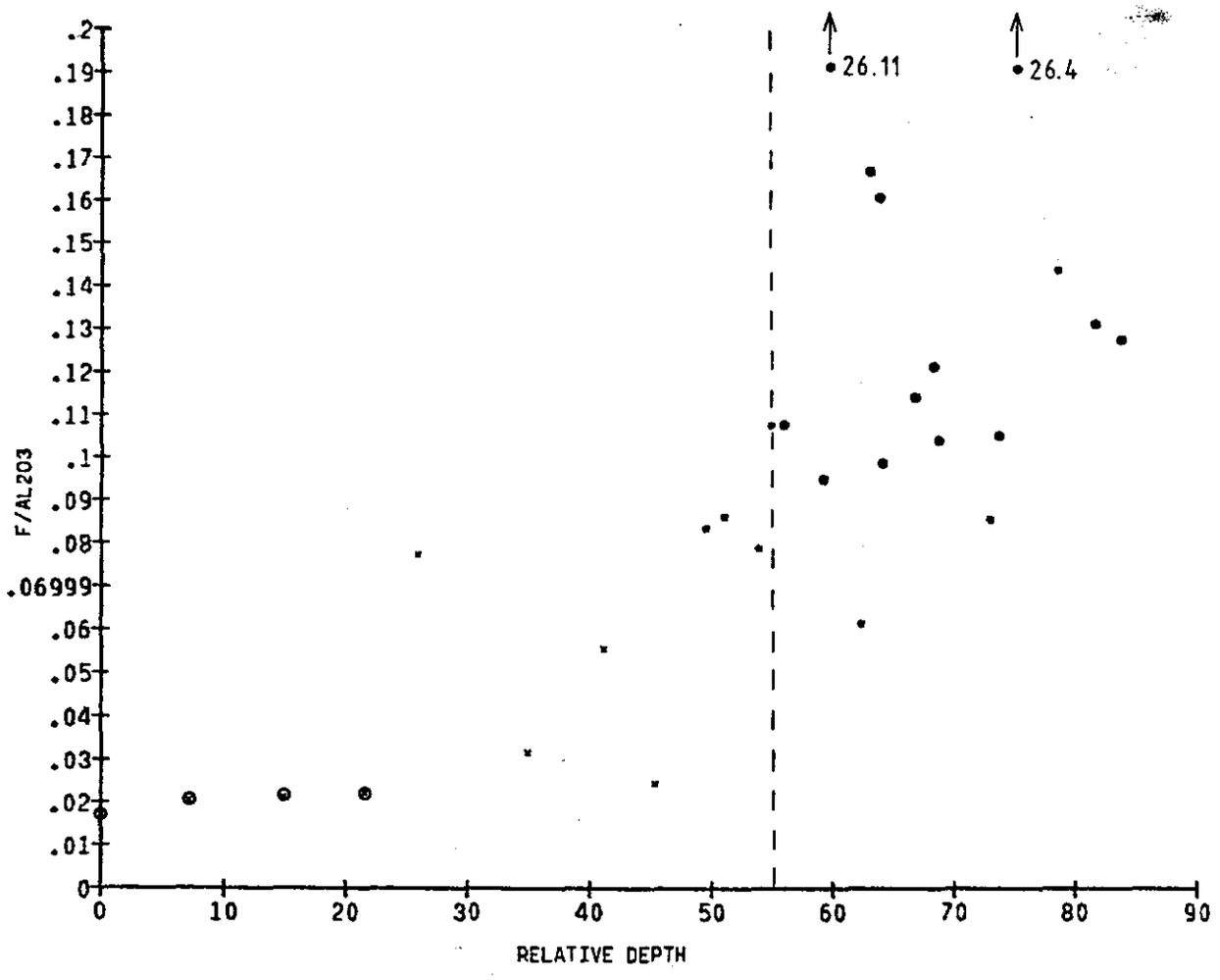
F/AL203
.2
.19
.18
.17
.16
.15
.14
.13
.12
.11
.1
.09
.08
.06999
.06
.05
.04
.03
.02
.01
0
0
10
20
30
40
50
60
70
80
90
RELATIVE DEPTH
26.11
26.4

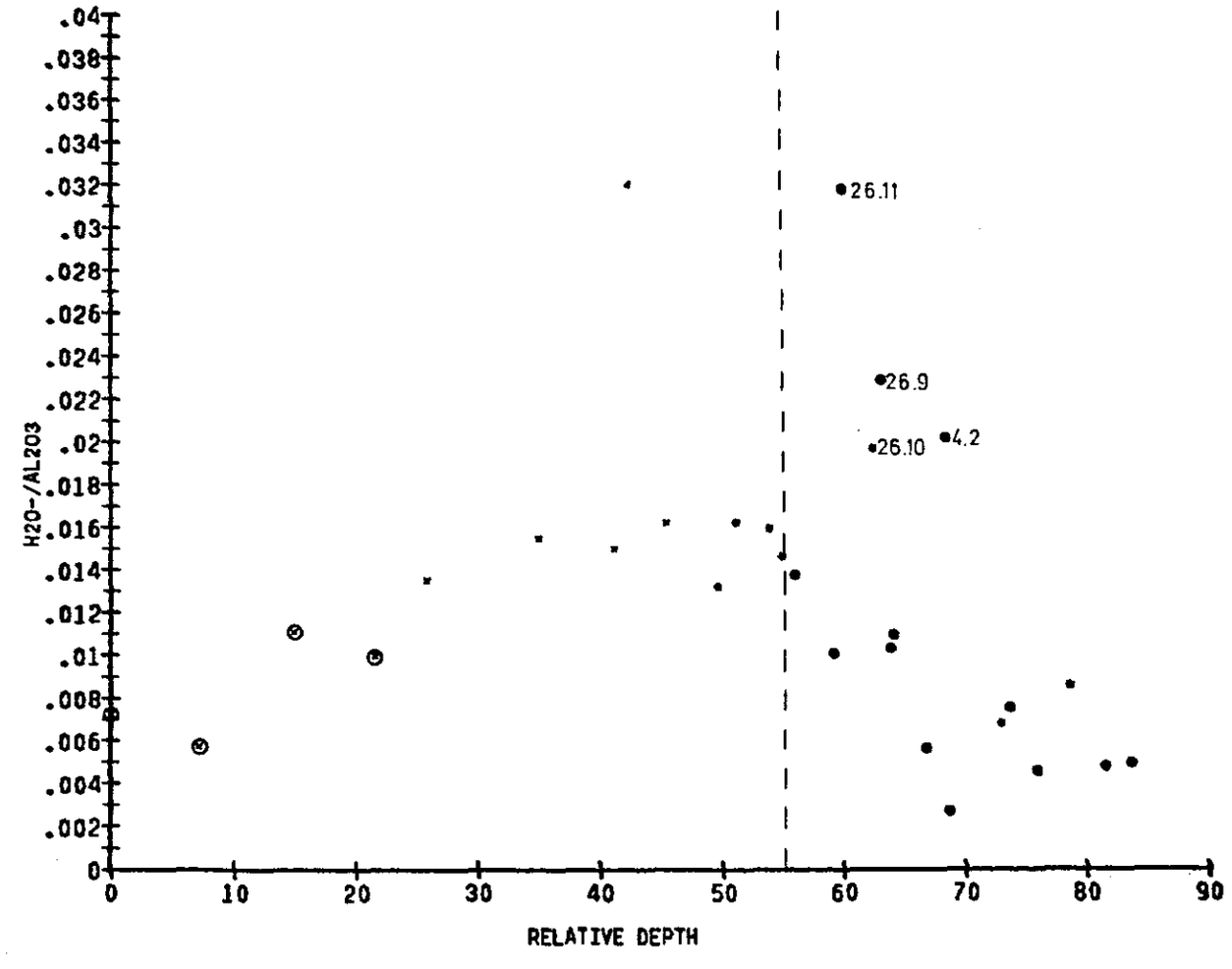
H2O-/AL203
.04
.038
.036
.034
.032
.03
.028
.026
.024
.022
.02
.018
.016
.014
.012
.01
.008
.006
.004
.002
0
0
10
20
30
40
50
60
70
80
90
RELATIVE DEPTH
26.11
26.9
26.10
4.2

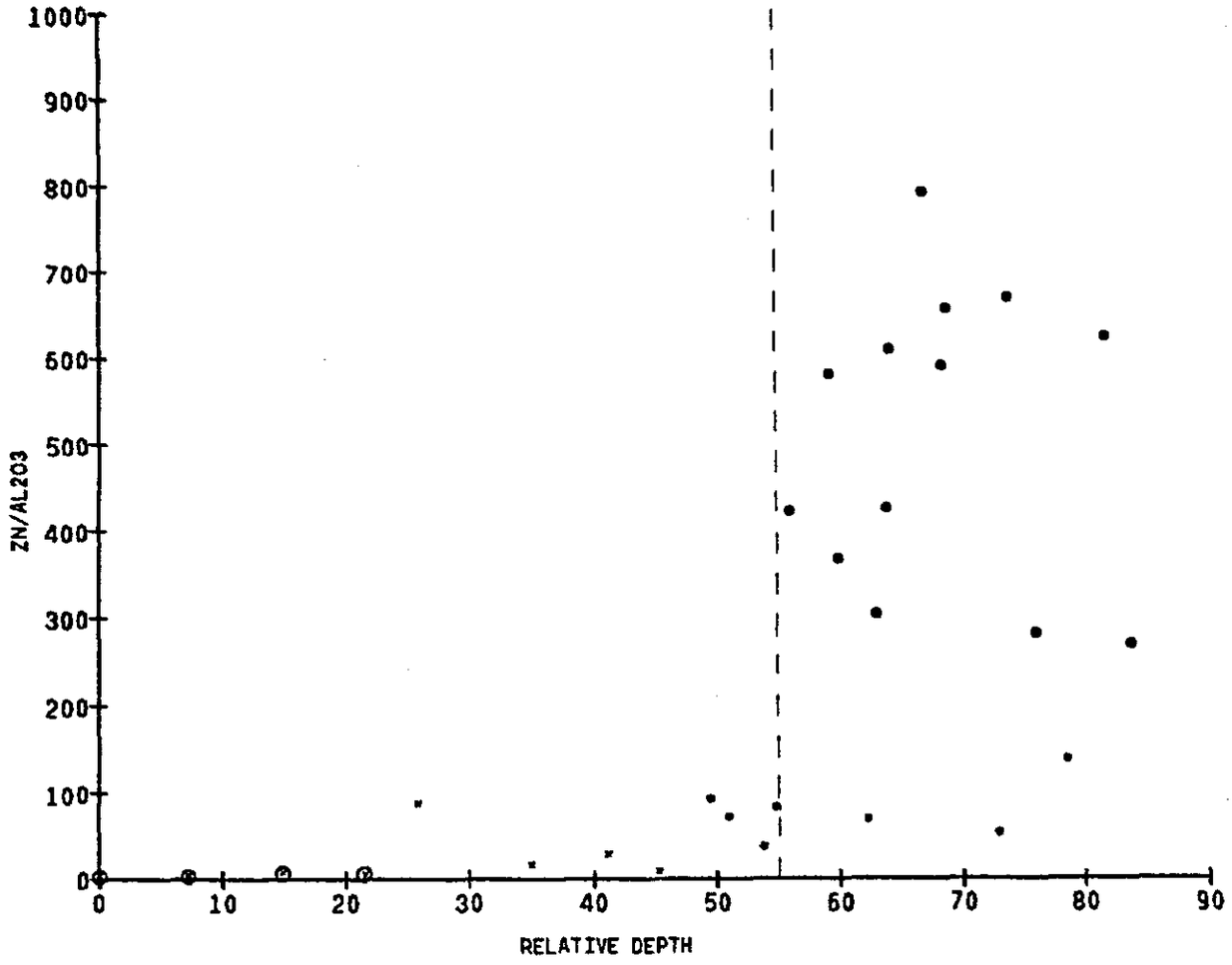
ZN/AL203
1000
900
800
700
600
500
400
300
200
100
0
0
10
20
30
40
50
60
70
80
90
RELATIVE DEPTH

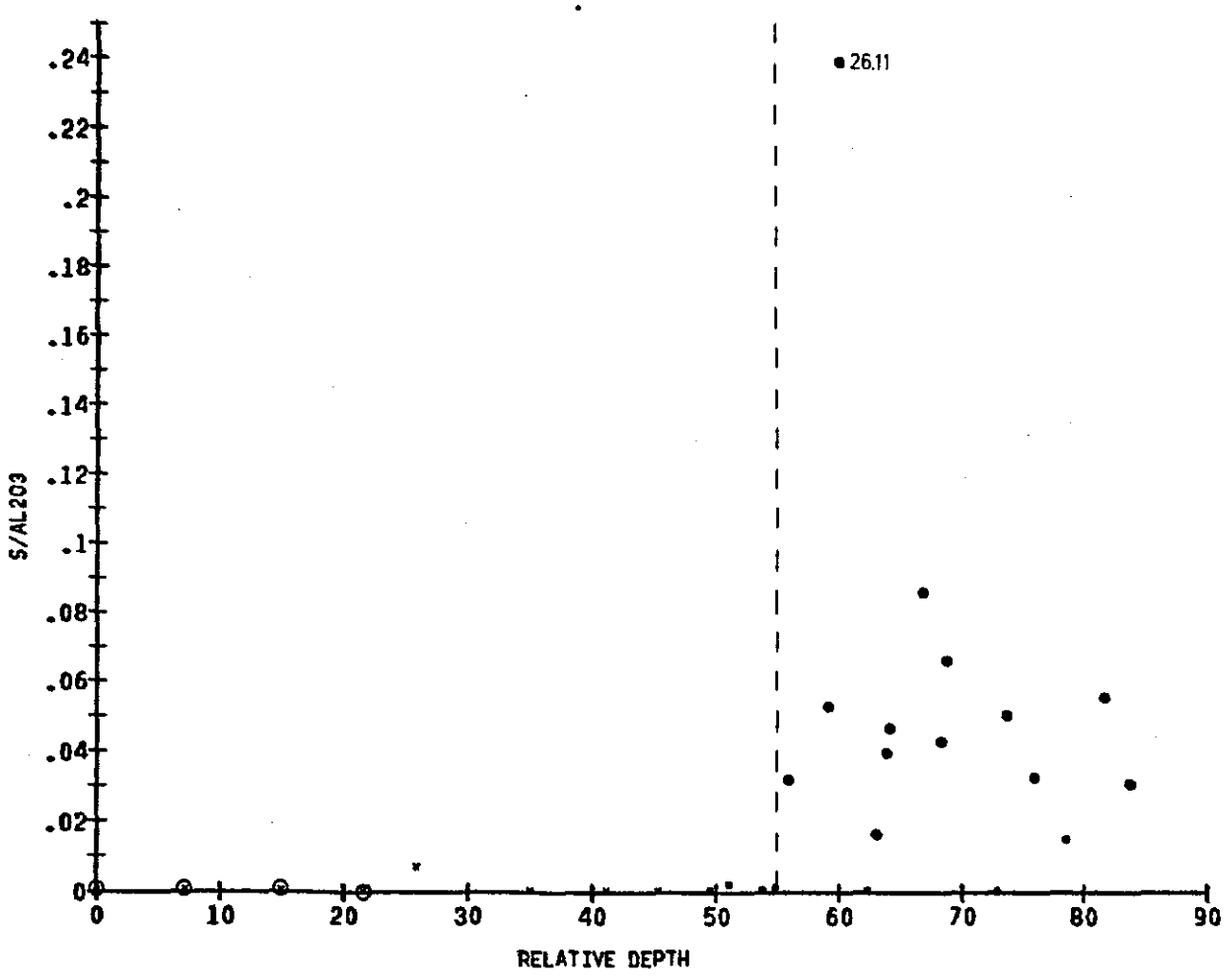
S/AL203
.24
.22
.2
.18
.16
.14
.12
.1
.08
.06
.04
.02
0
26.11
0
10
20
30
40
50
60
70
80
90
RELATIVE DEPTH

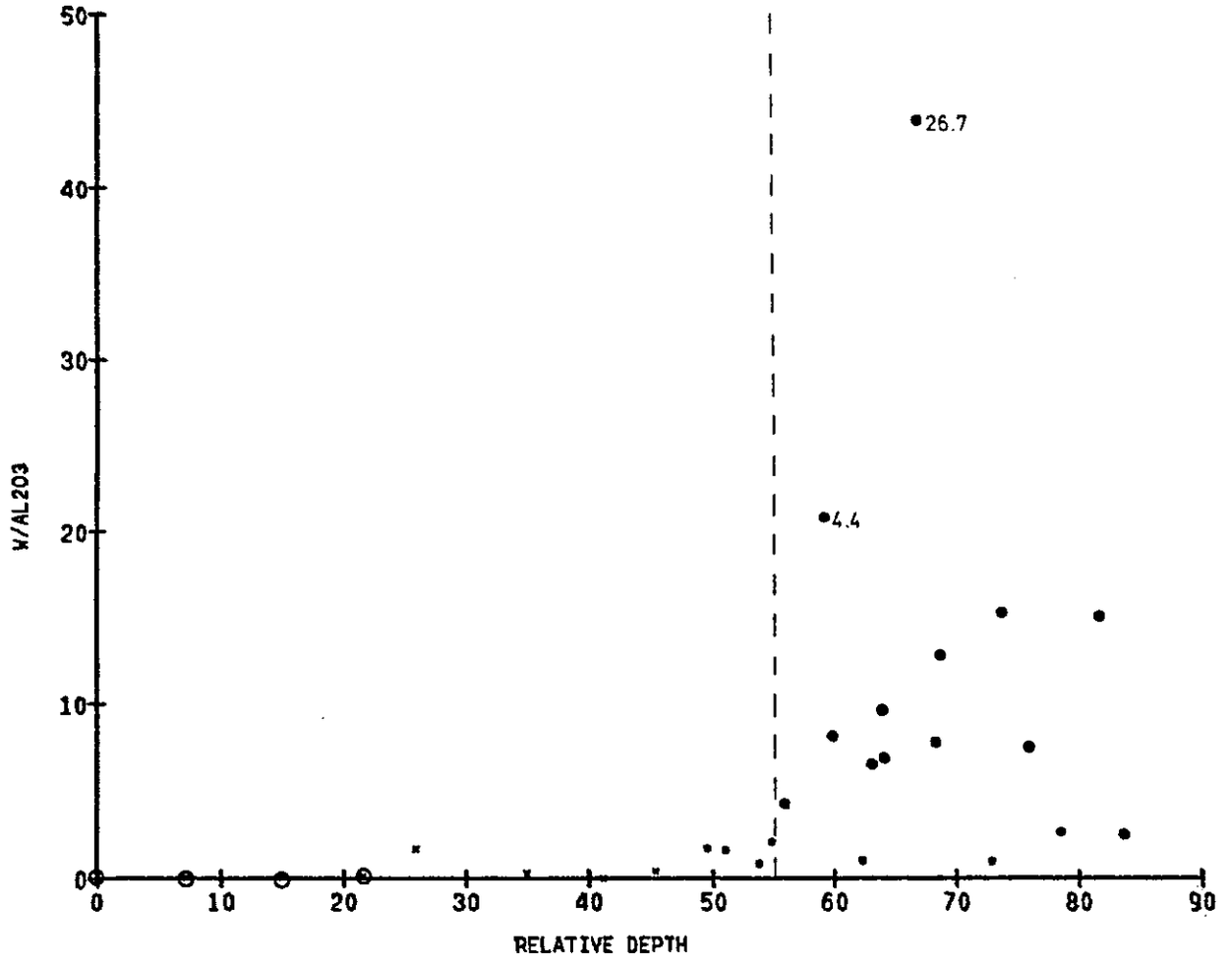
W/AL203
RELATIVE DEPTH
26.7
4.4
0
10
20
30
40
50
60
70
80
90

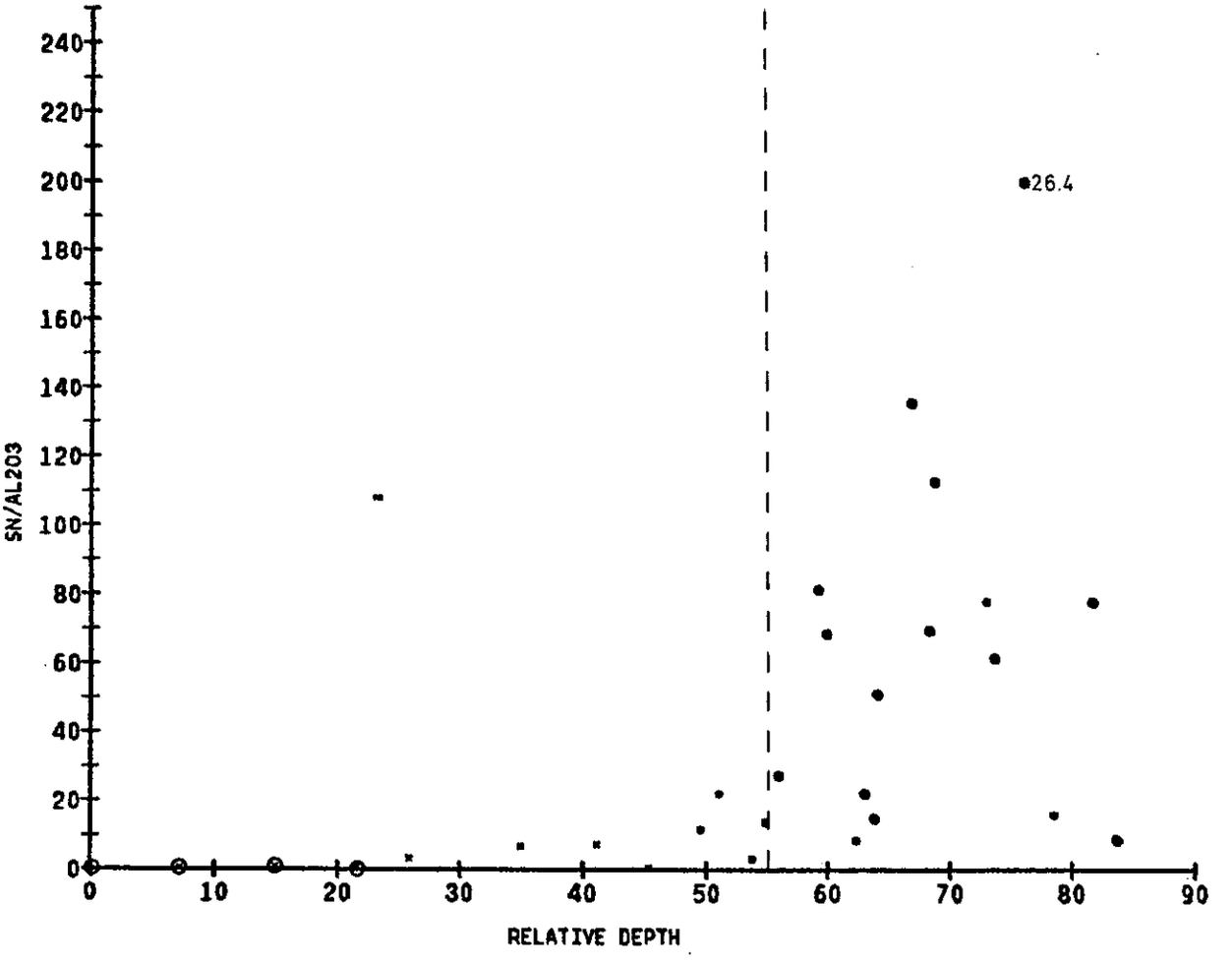
SN/AL203
RELATIVE DEPTH
26.4
0
20
40
60
80
100
120
140
160
180
200
220
240

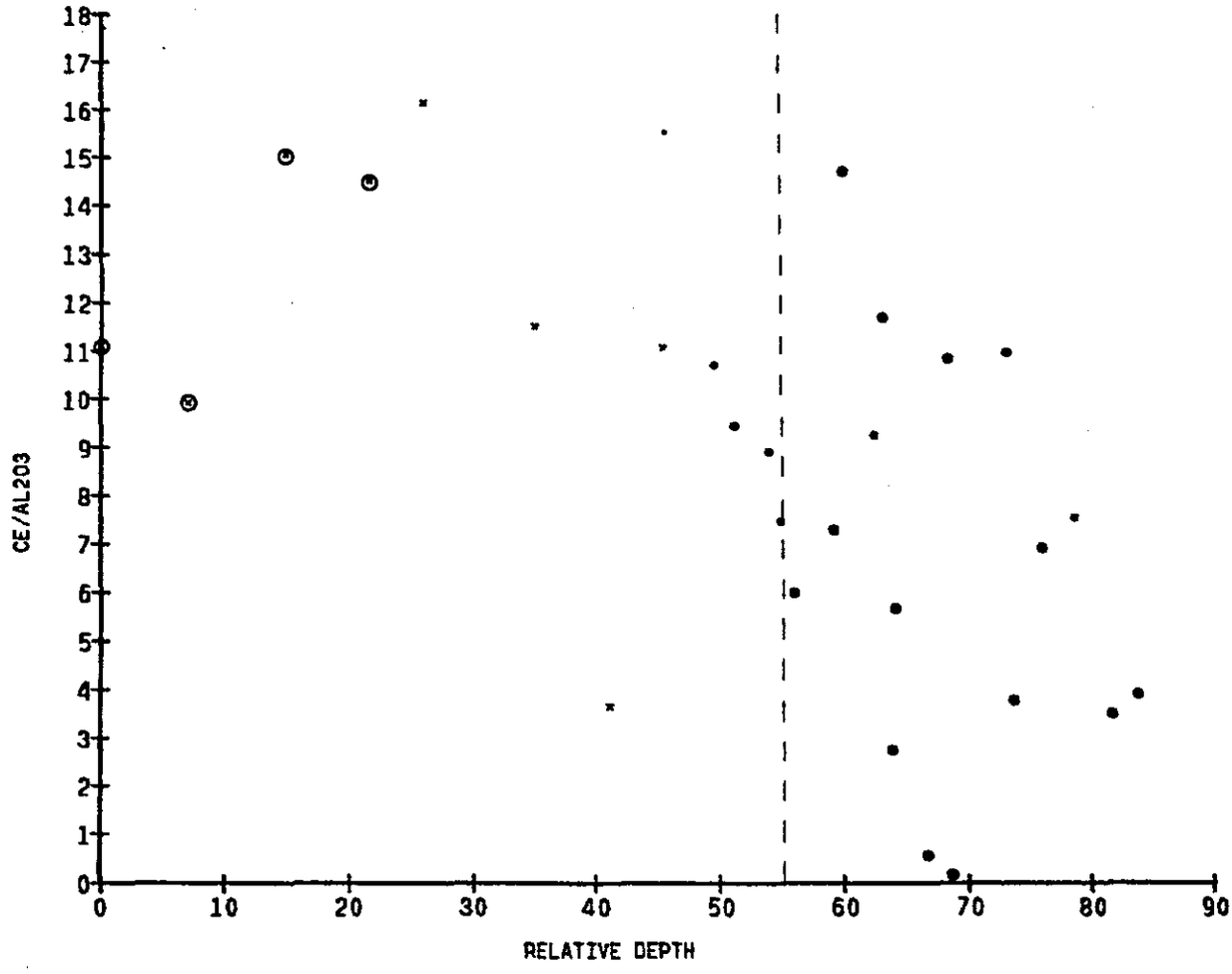
CE/AL203
RELATIVE DEPTH
0
10
20
30
40
50
60
70
80
90
1
2
3
4
5
6
7
8
9
10
11
12
13
14
15
16
17
18

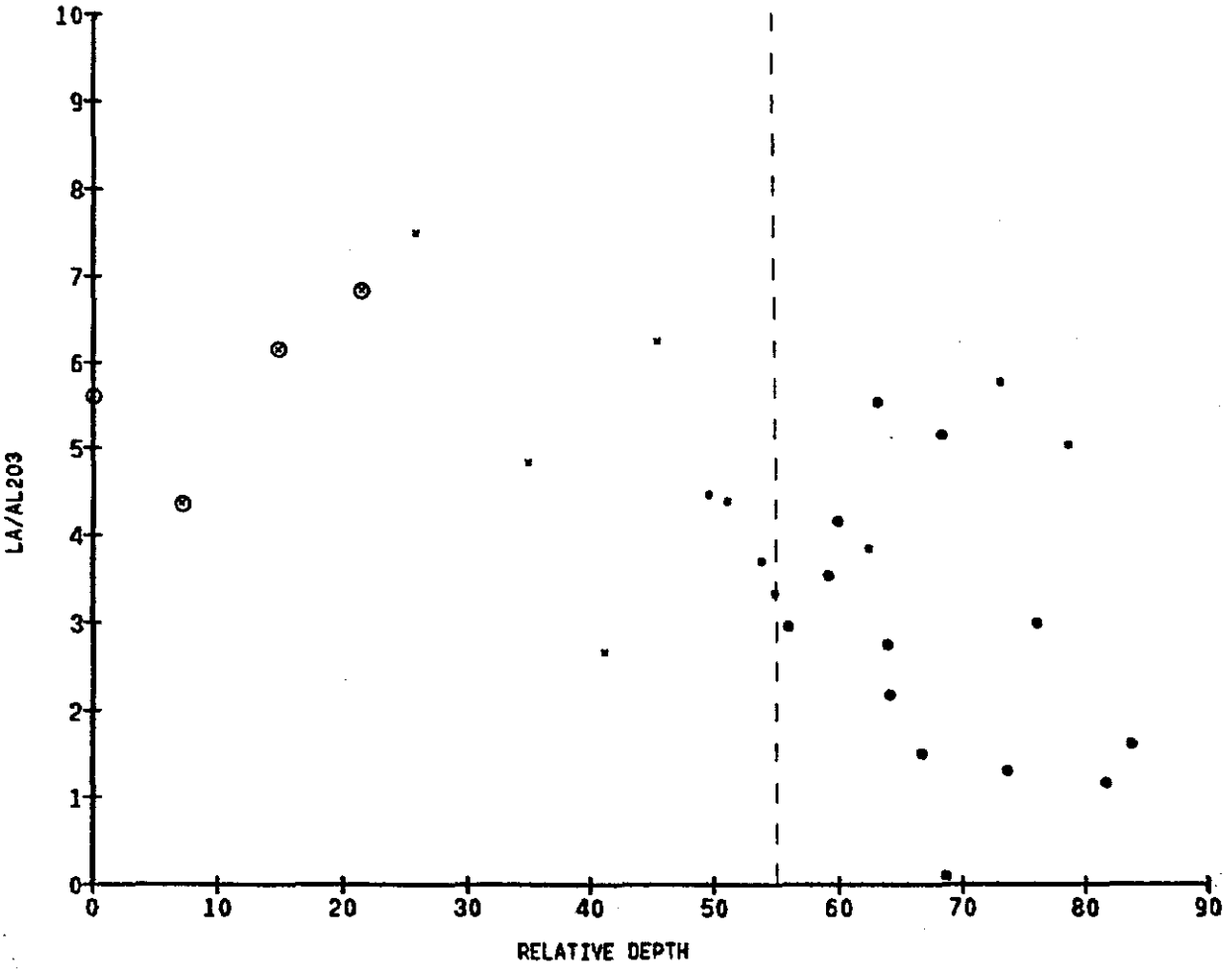
LA/AL203
RELATIVE DEPTH
0
10
20
30
40
50
60
70
80
90
1
2
3
4
5
6
7
8
9
10

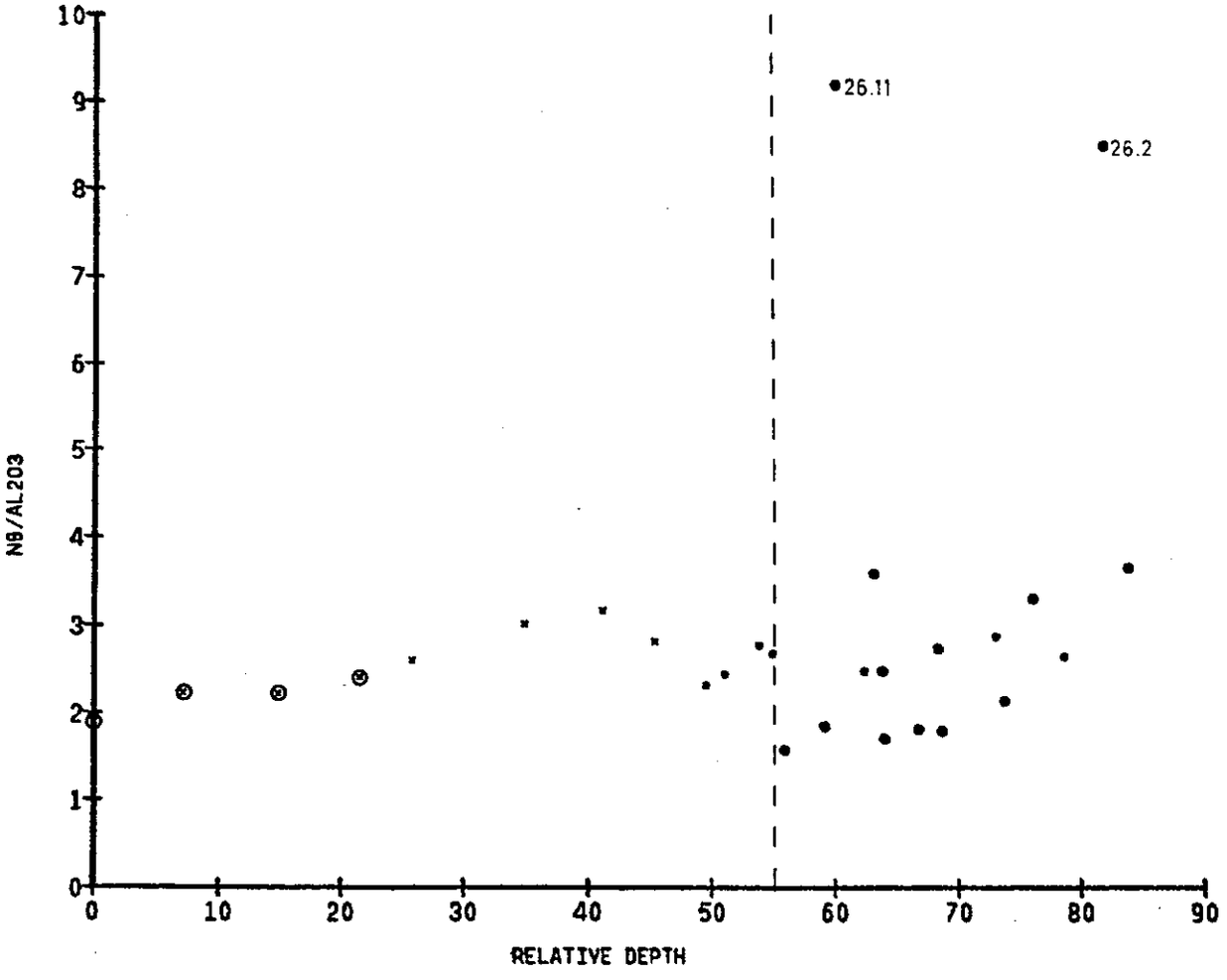
NB/AL203
RELATIVE DEPTH
26.11
26.2
0
10
20
30
40
50
60
70
80
90
1
2
3
4
5
6
7
8
9

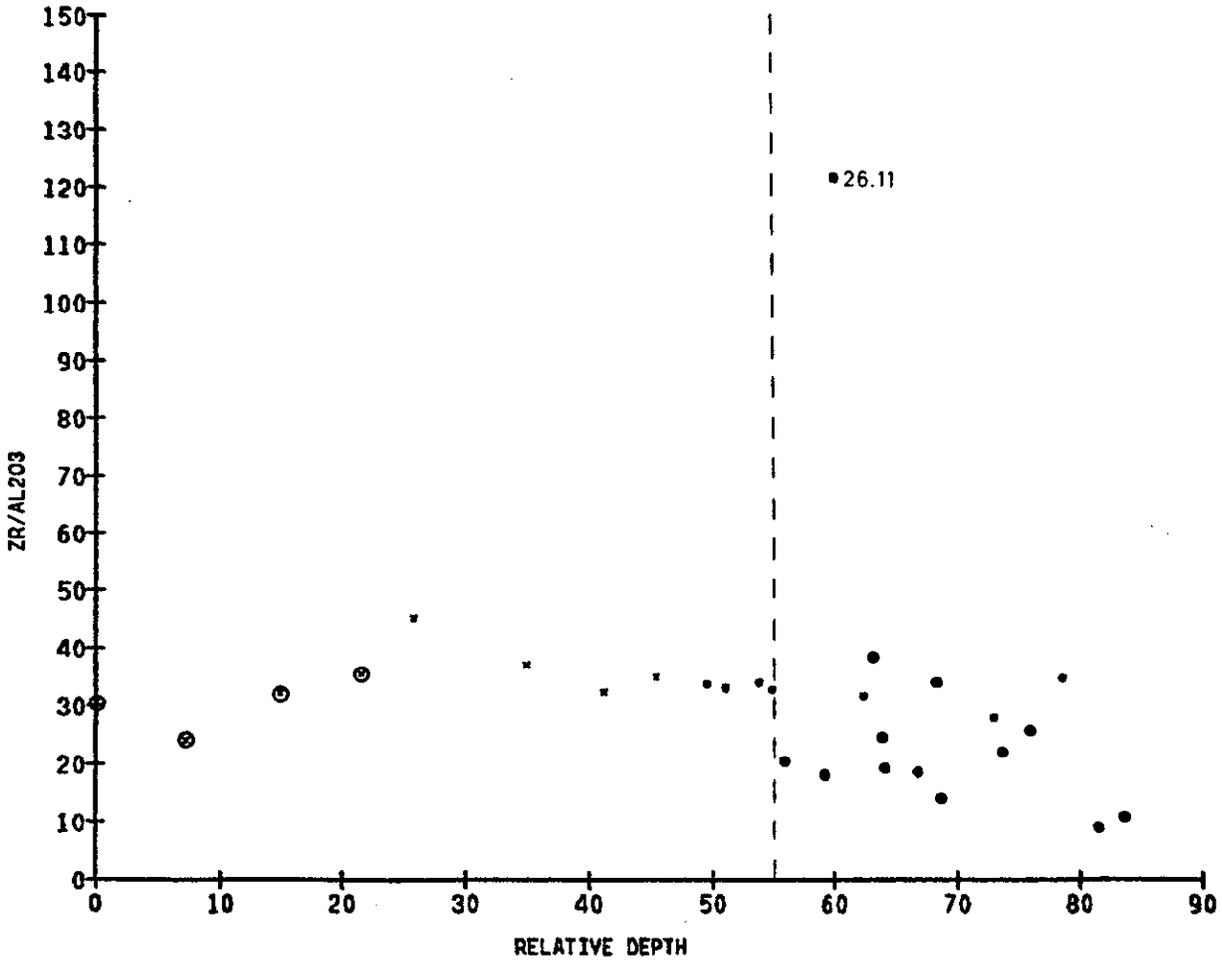
ZR/AL203
RELATIVE DEPTH
26.11
0
10
20
30
40
50
60
70
80
90
100
110
120
130
140
150

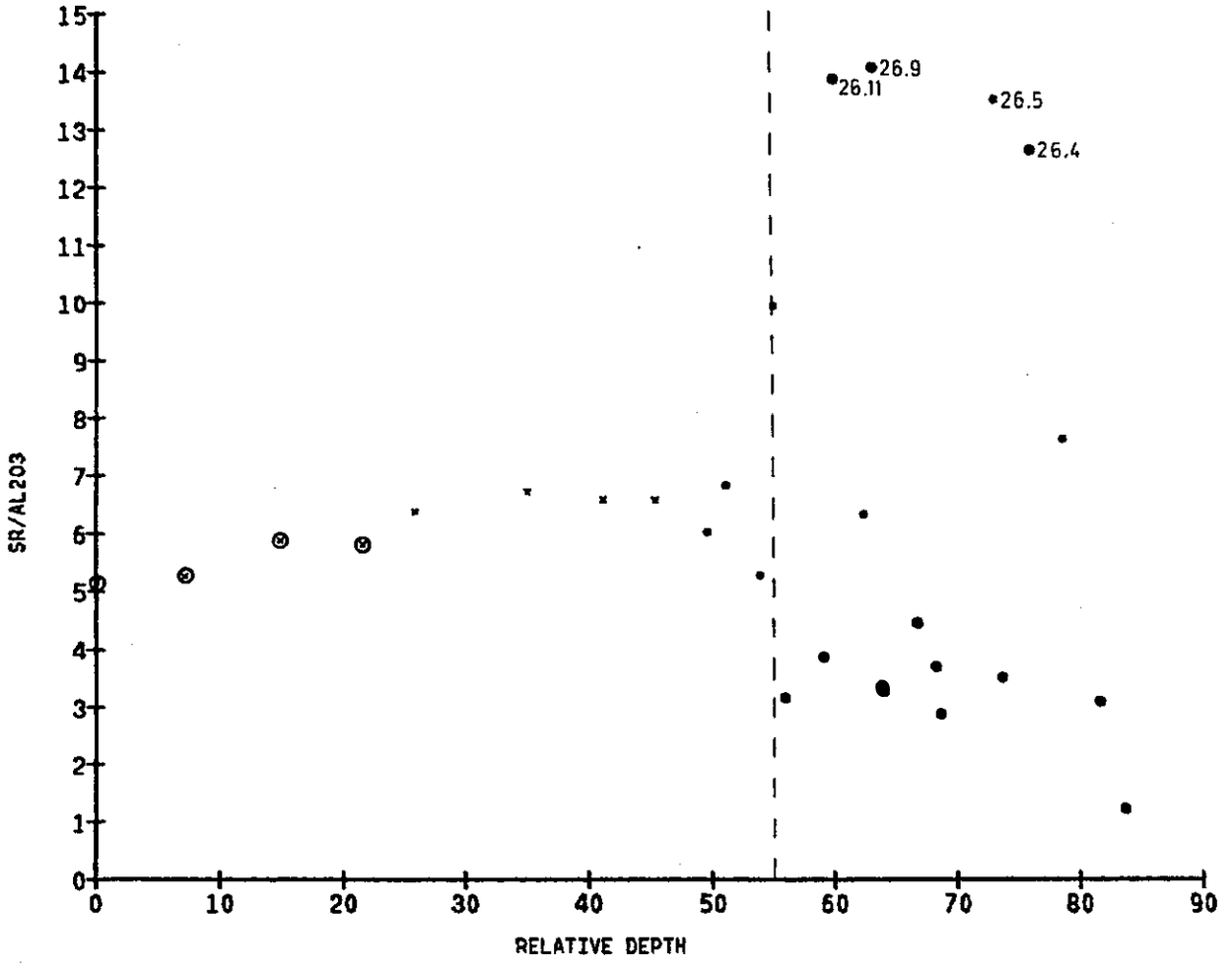
SR/AL203
RELATIVE DEPTH
26.9
26.11
26.5
26.4

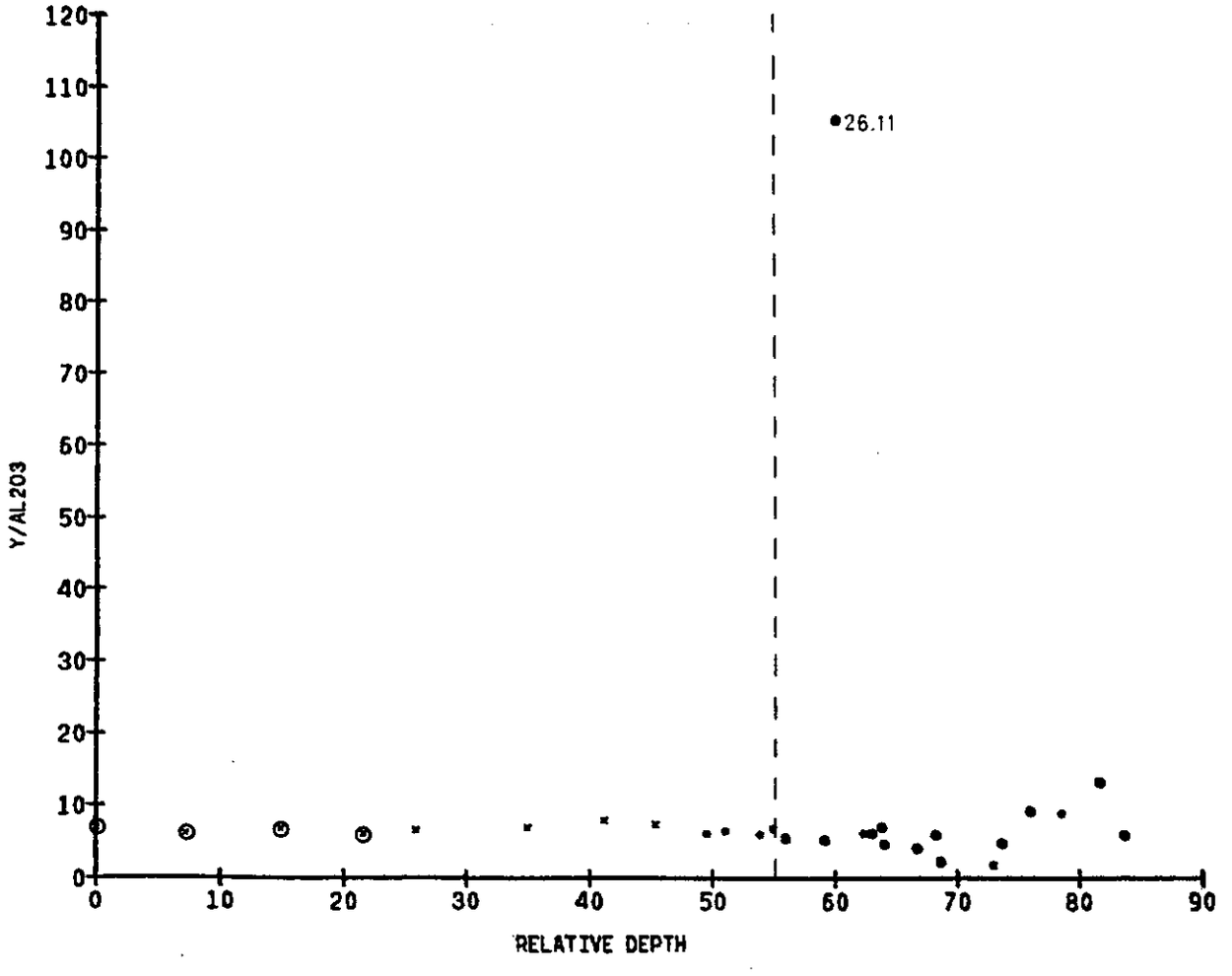
Y/AL203
RELATIVE DEPTH
26.11

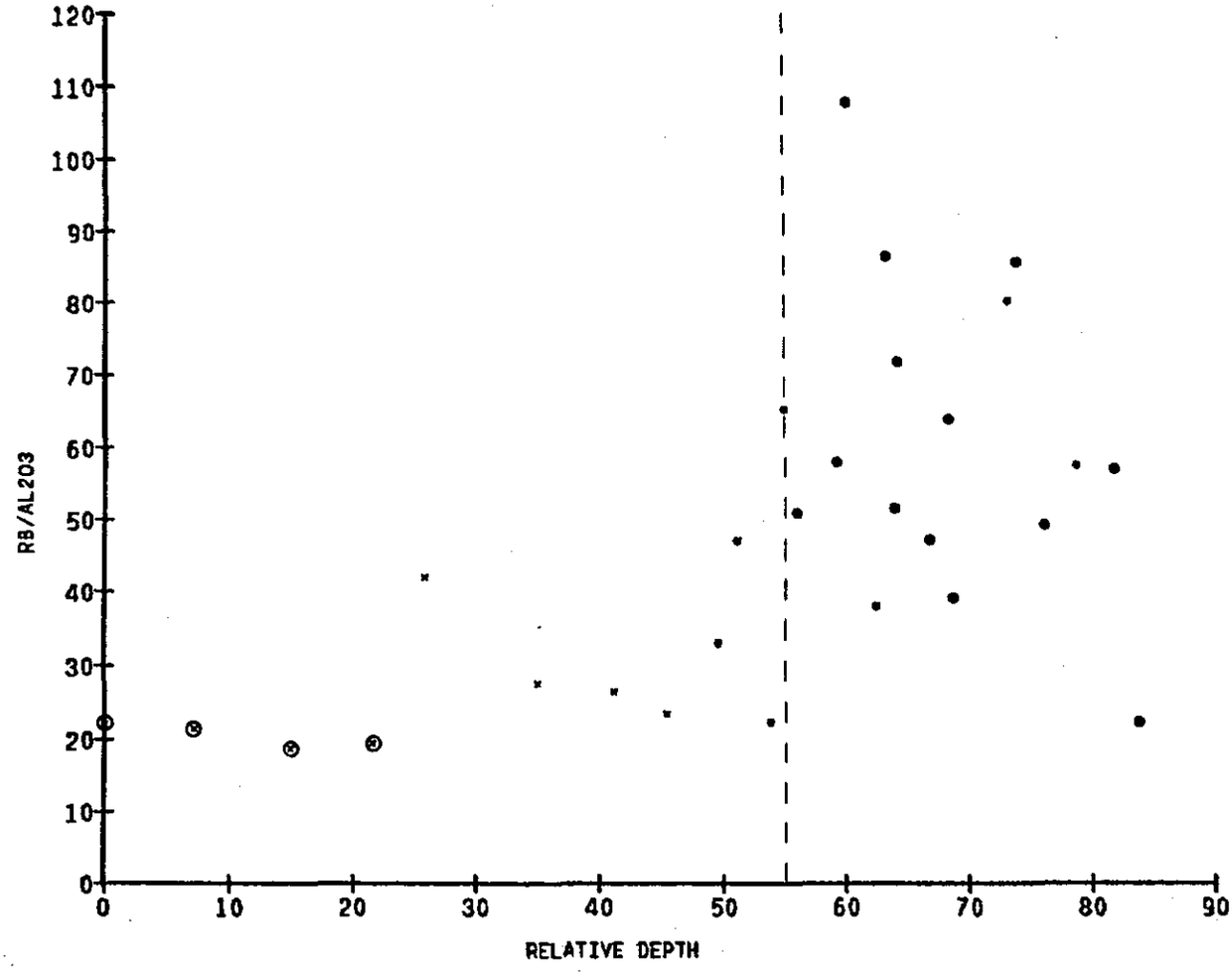
RB/AL203
RELATIVE DEPTH
0
10
20
30
40
50
60
70
80
90
100
110
120

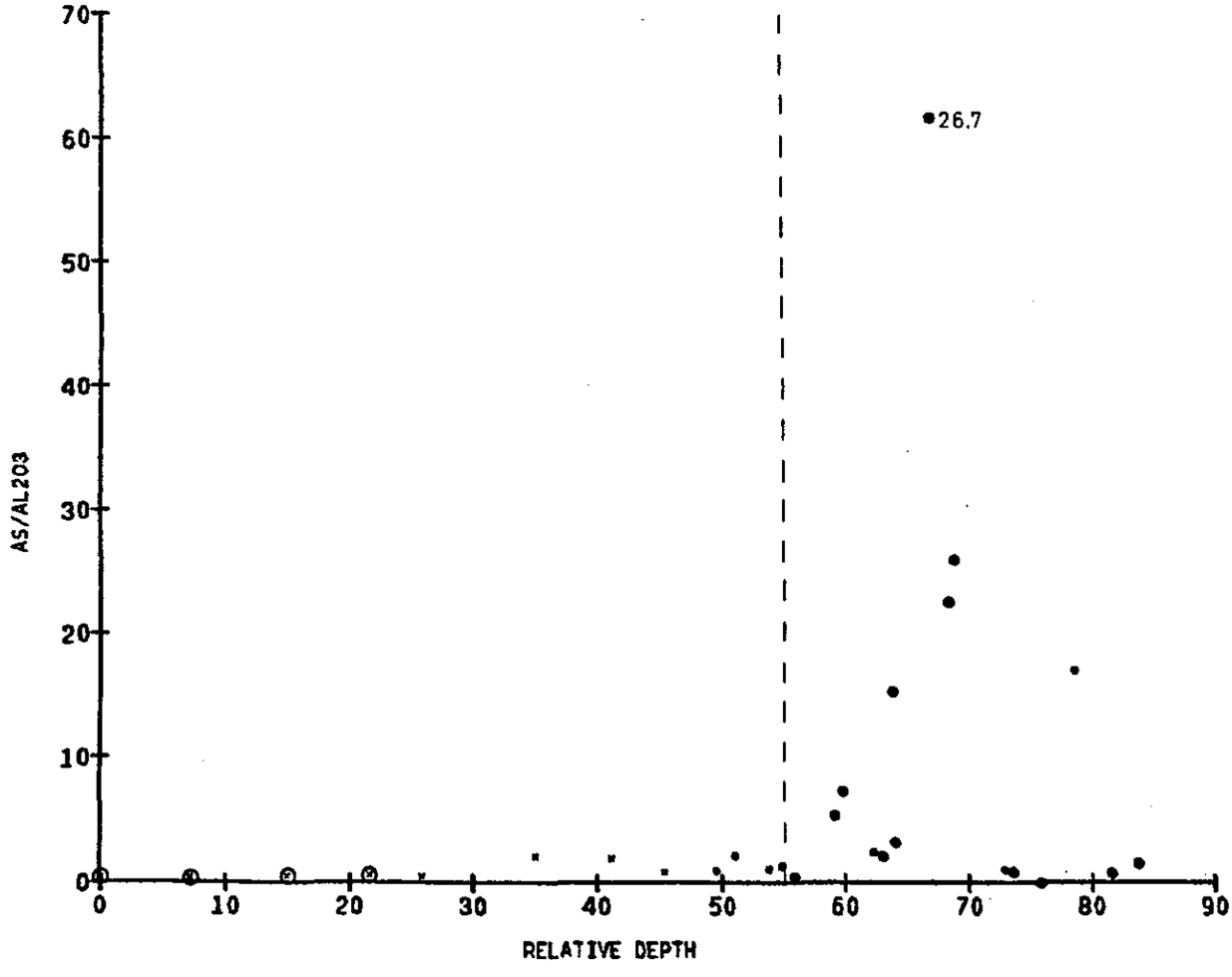
AS/AL203
RELATIVE DEPTH
26.7
0
10
20
30
40
50
60
70
80
90

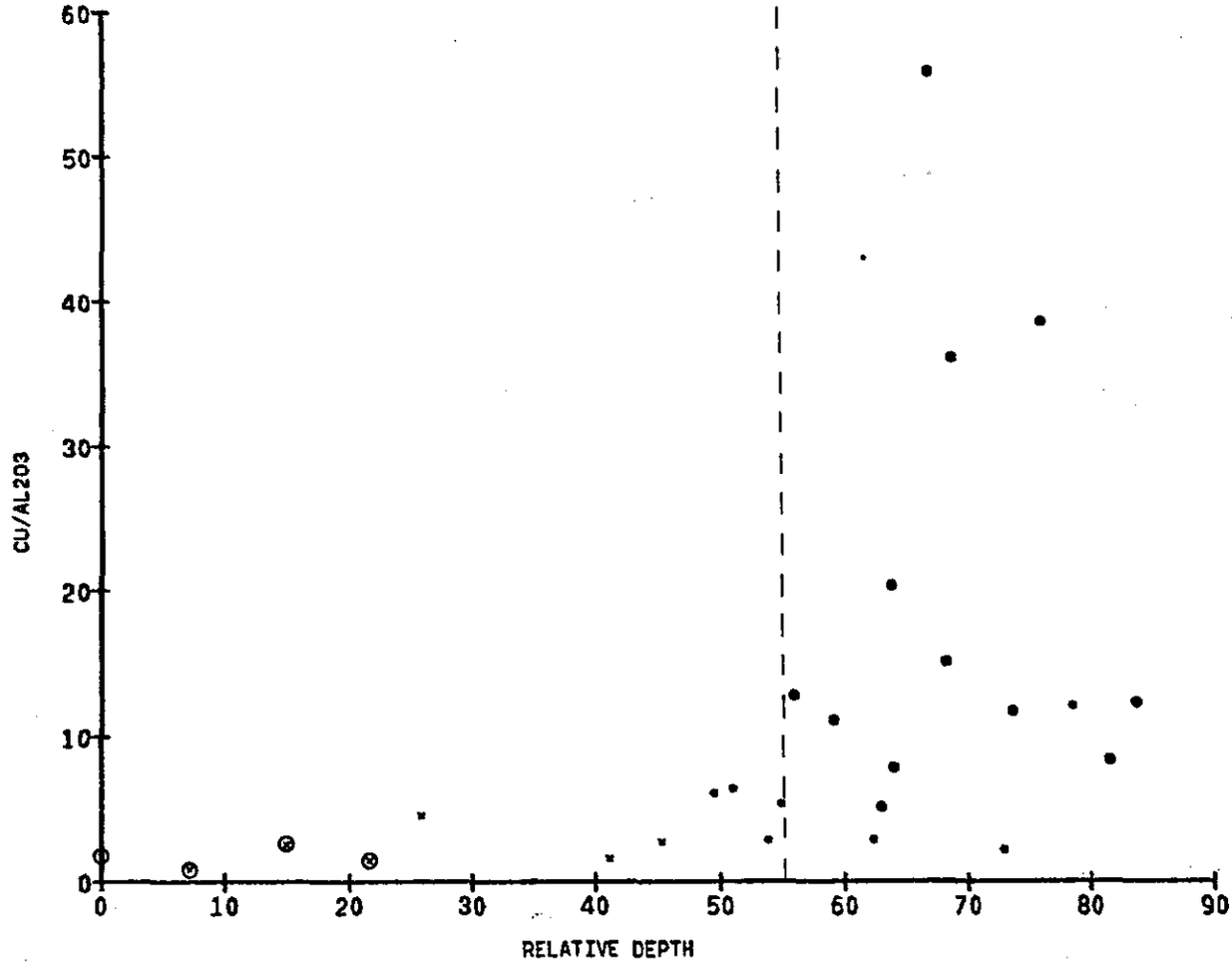
CU/AL203
RELATIVE DEPTH
0
10
20
30
40
50
60
70
80
90

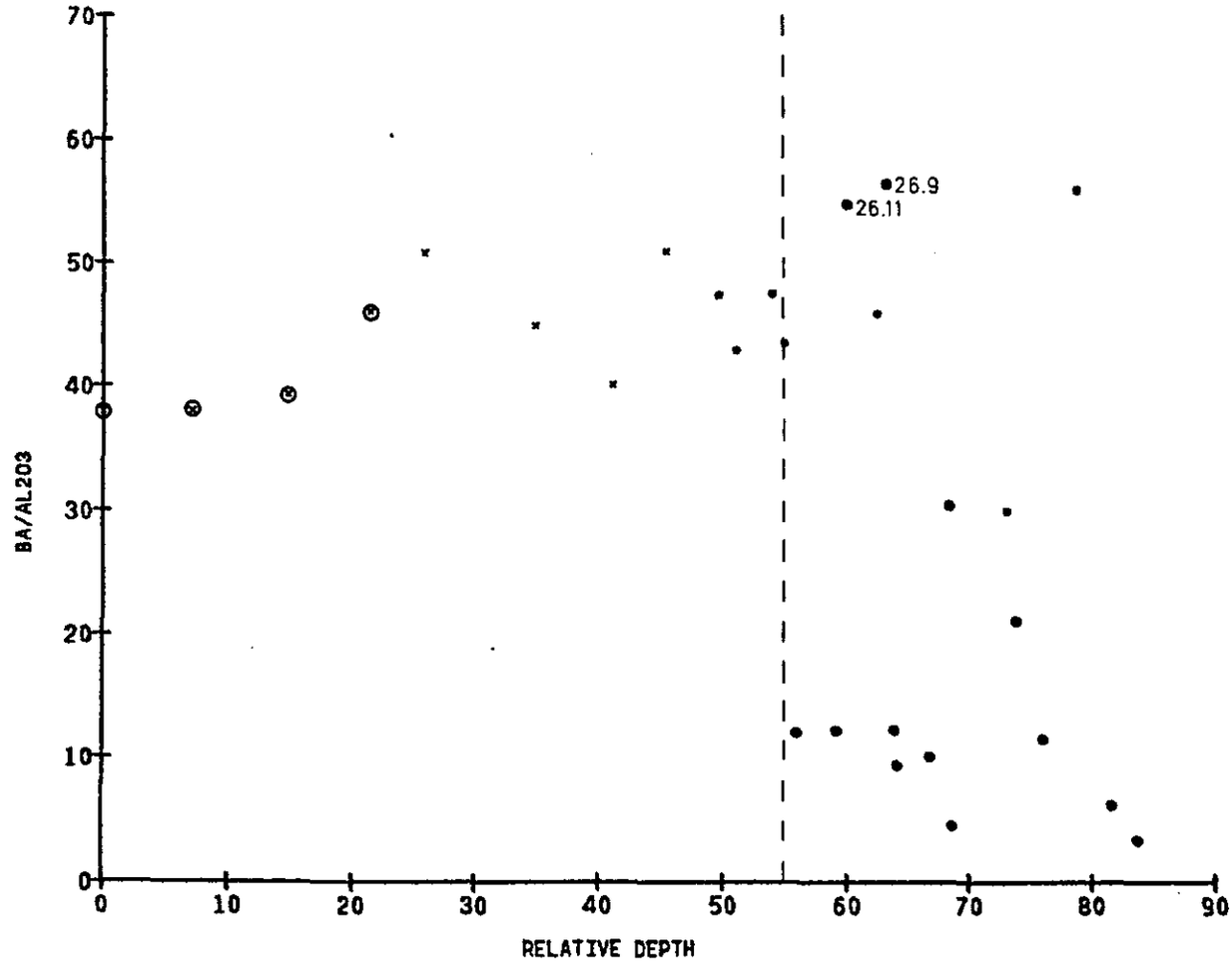
BA/AL203
RELATIVE DEPTH
26.9
26.11
0
10
20
30
40
50
60
70
80
90